AIRS/AMSU/HSB Version 7
Level 2 Product User Guide

Edited by:
Heidar Th. Thrastarson
Jet Propulsion Laboratory, California Institute of Technology

Contributions by:
Evan Manning, Brian Kahn, Eric J. Fetzer, Qing Yue, Sun Wong,
Peter Kalmus, Vivienne Payne, Edward T. Olsen,
Jet Propulsion Laboratory, California Institute of Technology
R. Chris Wilson, Raytheon Company
John Blaisdell, SAIC/GSFC, Lena Iredell, Adnet/GSFC
Joel Susskind, GSFC
Juying Warner, UMCP
Karen Cady-Pereira, AER

12 July 2020
Document Version 1.0.1

Jet Propulsion Laboratory
California Institute of Technology
Pasadena, CA

Submit Questions to:
https://airs.jpl.nasa.gov/data/support/ask-airs

Table of Contents

1 INTRODUCTION AND OVERVIEW 7

1.1 PRODUCT TYPES AND FLAVORS 8
1.2 DATA ACCESS 9
1.3 PRODUCT FILE NAMES 9
1.4 FILE FORMAT AND STRUCTURE 10
1.5 INVALID VALUES 10
1.6 DIMENSION, PRESSURE, GEOLOCATION, AND ANCILLARY FIELDS 11
1.7 QUALITY INDICATOR PRESSURE BOUNDARIES 11
1.8 DATA VALIDATION STATES 12

2 CLOUD CLEARED RADIANCES 14

2.1 DESCRIPTION 15
2.2 TYPE OF PRODUCT 15
2.3 QUALITY INDICATORS 15
2.4 VALIDATION 16
2.5 CAVEATS 16
2.6 SUGGESTIONS FOR RESEARCHERS 16
2.7 RECOMMENDED PAPERS 17
2.8 RECOMMENDED SUPPLEMENTAL USER DOCUMENTATION 17

3 MICROWAVE-ONLY PRODUCTS 18

3.1 DESCRIPTION 19
3.2 TYPE OF PRODUCT 20
3.3 QUALITY INDICATORS 20
3.4 VALIDATION 22
3.5 CAVEATS 22
3.6 SUGGESTIONS FOR RESEARCHERS 23
3.7 RECOMMENDED PAPERS 23
3.8 RECOMMENDED SUPPLEMENTAL USER DOCUMENTATION 24

4 SURFACE PROPERTIES 25

4.1 DESCRIPTION 26
4.2 TYPE OF PRODUCT 28
4.3 QUALITY INDICATORS 28
4.4 VALIDATION 29
4.5 CAVEATS 29
4.6 SUGGESTIONS FOR RESEARCHERS 29
4.7 RECOMMENDED PAPERS 29
4.8 RECOMMENDED SUPPLEMENTAL USER DOCUMENTATION 31

5 AIR TEMPERATURE RETRIEVALS 32

5.1 DESCRIPTION 32
5.1 TYPE OF PRODUCT 35
5.2 QUALITY INDICATORS 35
5.3 VALIDATION 36
5.4 CAVEATS 37
5.5 SUGGESTIONS FOR RESEARCHERS 38
5.6 RECOMMENDED PAPERS 38
5.7 RECOMMENDED SUPPLEMENTAL USER DOCUMENTATION 40

6 WATER VAPOR SATURATION QUANTITIES DERIVED FROM TEMPERATURE 41

6.1 DESCRIPTION 42
6.2 TYPE OF PRODUCT 43
6.3 QUALITY INDICATORS 43
6.4 CAVEATS 43
6.5 RECOMMENDED PAPERS 44
6.6 RECOMMENDED SUPPLEMENTAL USER DOCUMENTATION 44

7 TROPOPAUSE DERIVED FROM TEMPERATURE 45

7.1 DESCRIPTION 45
7.2 VALIDATION 46
7.3 RECOMMENDED SUPPLEMENTAL USER DOCUMENTATION 46

8 WATER VAPOR RETRIEVALS 47

8.1 DESCRIPTION 48
8.2 TYPE OF PRODUCT 49
8.3 QUALITY INDICATORS 49
8.4 VALIDATION 50
8.5 CAVEATS 52
8.6 SUGGESTIONS FOR RESEARCHERS 52
8.7 RECOMMENDED PAPERS 52
8.8 RECOMMENDED SUPPLEMENTAL USER DOCUMENTATION 56

9 RELATIVE HUMIDITY DERIVED FROM TEMPERATURE AND WATER VAPOR 57

9.1 DESCRIPTION 57
9.2 TYPE OF PRODUCT 57
9.3 QUALITY INDICATORS 57
9.4 VALIDATION 58
9.5 CAVEATS 58
9.6 RECOMMENDED PAPERS 58
9.7 RECOMMENDED SUPPLEMENTAL USER DOCUMENTATION 59

10 GEOPOTENTIAL HEIGHT DERIVED FROM TEMPERATURE AND WATER VAPOR 60

10.1 DESCRIPTION 60
10.2 TYPE OF PRODUCT 60
10.3 QUALITY INDICATORS 60
10.4 CAVEATS 60
10.5 RECOMMENDED SUPPLEMENTAL USER DOCUMENTATION 60

11 PRESSURE AT THE TOP OF THE PBL 61

11.1 DESCRIPTION 61
11.2 QUALITY INDICATORS 61
11.3 VALIDATION 61
11.4 RECOMMENDED PAPERS 61
11.5 RECOMMENDED SUPPLEMENTAL USER DOCUMENTATION 62

12 CLOUD RETRIEVALS ON 3X3 AIRS FIELD OF VIEW 63

12.1 DESCRIPTION 64
12.2 TYPE OF PRODUCT 65
12.3 QUALITY INDICATORS 65

12.4 VALIDATION 65
12.5 CAVEATS 65
12.6 SUGGESTIONS FOR RESEARCHERS 66
12.7 RECOMMENDED PAPERS 67
12.8 RECOMMENDED SUPPLEMENTAL USER DOCUMENTATION 69

13 CLOUD PHASE AND ICE CLOUD PROPERTIES 70

13.1 DESCRIPTION 71
13.2 QUALITY INDICATORS 71
13.3 VALIDATION 72
13.4 SUGGESTIONS FOR RESEARCHERS 72
13.5 RECOMMENDED PAPERS 72
13.6 RECOMMENDED SUPPLEMENTAL USER DOCUMENTATION 73

14 OZONE RETRIEVALS 74

14.1 DESCRIPTION 75
14.2 TYPE OF PRODUCT 79
14.3 QUALITY INDICATORS 79
14.4 VALIDATION 79
14.5 CAVEATS 79
14.6 SUGGESTIONS FOR RESEARCHERS 80
14.7 RECOMMENDED PAPERS 80
14.8 RECOMMENDED SUPPLEMENTAL USER DOCUMENTATION 82

15 CARBON MONOXIDE RETRIEVALS 83

15.1 DESCRIPTION 84
15.1 TYPE OF PRODUCT 86
15.2 QUALITY INDICATORS 86
15.3 VALIDATION 87
15.4 CAVEATS 87
15.5 SUGGESTIONS FOR RESEARCHERS 90
15.6 RECOMMENDED PAPERS 90
15.7 RECOMMENDED SUPPLEMENTAL USER DOCUMENTATION 92

16 METHANE RETRIEVALS 93

16.1 DESCRIPTION 94
16.2 TYPE OF PRODUCT 96
16.3 QUALITY INDICATORS 96
16.4 VALIDATION 97
16.5 CAVEATS 98
16.6 SUGGESTIONS FOR RESEARCHERS 98
16.7 RECOMMENDED PAPERS 98
16.8 RECOMMENDED SUPPLEMENTAL USER DOCUMENTATION 99

17 DUST AND SO2 FLAGS 101

17.1 DESCRIPTION 101
17.2 TYPE OF PRODUCT 102
17.3 QUALITY INDICATORS 102
17.4 VALIDATION 103
17.5 CAVEATS 103
17.6 RECOMMENDED PAPERS 104
17.7 RECOMMENDED SUPPLEMENTAL USER DOCUMENTATION 106

18 OUTGOING LONGWAVE RADIATION RETRIEVALS 107

18.1 DESCRIPTION 107
18.2 TYPE OF PRODUCT 108
18.3 QUALITY INDICATORS 108
18.4 VALIDATION 109
18.5 CAVEATS 109
18.6 SUGGESTIONS FOR RESEARCHERS 109
18.7 RECOMMENDED PAPERS 109
18.8 RECOMMENDED SUPPLEMENTAL USER DOCUMENTATION 110

APPENDIX A. LEVEL 2 PRODUCT INTERFACE SPECIFICATIONS 111

A1: L2 STANDARD ATMOSPHERIC/SURFACE PRODUCT INTERFACE SPECIFICATION 113
Dimensions 113
Geolocation Fields 114
Attributes 114
Per-Granule Data Fields 117
Along-Track Data Fields 117
Full Swath Data Fields 120
A2: L2 SUPPORT ATMOSPHERIC/SURFACE PRODUCT INTERFACE SPECIFICATION 135
Dimensions 135
Geolocation Fields 137
Attributes 137
Per-Granule Data Fields 141
Along-Track Data Fields 142
Full Swath Data Fields 145
A3: L2 STANDARD CLOUD CLEARED RADIANCE PRODUCT INTERFACE SPECIFICATION 183
Dimensions 183
Geolocation Fields 183
Attributes 184
Per-Granule Data Fields 187
Along-Track Data Fields 188
Full Swath Data Fields 191

The research was carried out at the Jet Propulsion Laboratory, California Institute of Technology, under a contract with the National Aeronautics and Space Administration (80NM0018D0004).
Copyright 2020. All rights reserved.

Table of Figures

Figure 1: Validation of temperature and water vapor profiles. *37*
Figure 2: Global water vapor statistics of AIRS retrievals compared to collocated ECMWF. *51*
Figure 3: Total Ozone Retrieval for August 31, 2018 and August 16, 2019 with comparison to OMPS total ozone. *78*
Figure 4: The 9 CO trapezoids. *86*
Figure 5: Comparison of the V6 and V7 global distribution of CO VMR at 500 hPa. *88*
Figure 6: DOFS for AIRS CO V6. ..... *89*
Figure 7: Comparison of AIRS V6 and V7 CH_4 VMRs at 400 hPa (ppbv) and CH_4 column averaged total column (ppbv) on April 3, 2016. ..... *97*
Figure 9: AIRS V6 SO_2 flags compared with Aura/OMI SO_2 total column on 27 May 2011 ..... *103*

1 Introduction and Overview

The AIRS suite of instruments on NASA's Aqua satellite includes the hyperspectral Atmospheric Infrared Sounder (AIRS), and two microwave instruments, the Advanced Microwave Sounding Unit (AMSU) and the Humidity Sounder for Brazil (HSB). The polar sun-synchronous orbit results in overpasses at around 1:30 am and 1:30 pm local time, with the instruments scanning across-track with footprints of about 45 km at nadir for AMSU and about 15 km at nadir for AIRS. Level 2 (L2) products from the AIRS suite of instruments are retrieved from Level 1B radiances, and include geophysical variables for temperature, water vapor, clouds and trace gases.

The purpose of the document is to give users of the Version 7 (V7) L2 products from the AIRS suite of instruments a summary of the key information they require to properly use the products in their research. This is not a complete characterization of the L2 products. An overview of the AIRS mission, including the AIRS suite of instruments, the data processing algorithms, data products and their organization, and the organization of the AIRS documentation, is given in

Overview_of_the_AIRS_Mission.pdf.

Changes from the previous data release Version 6 are summarized in

V7_Changes_from_V6.pdf.

And testing and validation of Version 7 is described in

V7_L2_Performance_Test_and_Validation_Report.pdf.

All AIRS documents, which are referred to throughout this document by file name, can be accessed through the Goddard Earth Sciences Data and Information Services Center (GES DISC) at the following webpage:

https://disc.gsfc.nasa.gov/information/documents?title=AIRS%20Documentation

In this document, each class of Level 2 product is presented. For example, a user pursuing research on the distribution and transport of carbon monoxide will find much of interest in that section and can ignore most of the other sections. **All users, however, must read the sections describing the *Air Temperature Retrievals* and the *Water Vapor Retrievals*. Information appearing in these two sections is critically important to proper understanding and use of the other Level 2 products in research.**

In Appendix A, all fields available in the Level 2 product files are listed with short descriptions. This includes dimensions, geolocation and other ancillary fields that are common to many of the geophysical variables and are not listed in the subsections for each variable. For previous AIRS version releases this information was contained in a separate Released Processing Files Description document.

1.1 Product Types and Flavors

The AIRS Level 2 retrieval uses layer mean quantities for water vapor, ozone, carbon monoxide, and methane. Versions of AIRS products prior to V6 reported only column totals and layer quantities for these gases. As in V6, the primary products in V7 Level 2 Standard and Support Products for all gases are now level products (values at the specific pressure level upon which they are reported) instead of layer products (slab values reported on the bounding pressure level nearest to the surface). The level quantities are derived from the internal 100-layer quantities by a smoothing spline, tuned to reflect information content and atmospheric variability. The procedure is further described in the following document:

V7_L2_Levels_Layers_Trapezoids.pdf

The derivation of level quantities from layer quantities is essentially done by interpolation with smoothing kernels. This mathematical transformation leads to occasional strange results for water vapor profiles with inversions, typically near the surface.

We include the Level 2 Support Products in this document, which contain profiles reported on 100 levels, whereas profiles in the Standard Product are reported on either 28 or 15 levels. However, users interested in the potential higher resolution of the Support Products should familiarize themselves with the verticality functions that properly convey that resolution when applied to these products. This approach is more complex than using the Standard Products, and the resulting resolution will be only slightly higher than that of the Standard Products. The true resolution is considerably coarser than 100 levels would imply. Users are also advised to make use of quality control (QC) flags provided with all variables, and avoid using results flagged with QC=2 even when physically plausible values are present. The major utility of the Support Products is for forward calculation of radiances via the AIRS rapid transmission algorithm (RTA), the calculation of level quantities from layer quantities, beta testing future products and for investigating the operation of the retrieval algorithm. The averaging kernel matrices for various products are stored here as well to avoid swelling the size of the Level 2 Standard Product files to a point that would be inconvenient for most users.

Users who do access the Level 2 Support Products should take note that the indices of the levels and layers of profiles are reversed from those in the Level 2 Standard Products. The numbering of profile indices for the Support Product starts from top of the atmosphere and increases in index number downward toward the surface; and the index numbering scheme is opposite in the Standard Product. Thus, index 20 is at a lower altitude than index 21 in the Level 2 Standard Product but index 20 is at a higher altitude than index 21 in the Level 2 Support Product. The Level 2 Standard Product pressure levels and Level 2 Support Product pressure levels are given in the documents:

V7_L2_Standard_Pressure_Levels.pdf
V7_L2_Support_Pressure_Levels.pdf

There are three Version 7 processing streams of Level 2 data that differ based on the combination of instrument radiances from the AIRS Suite of instruments used in the

retrieval process. We refer to each of these processing streams as a different "flavor" of V7 products. The main flavor of the Level 2 retrieval product files results from the retrieval using only the AIRS infrared radiances. This product spans the period from beginning of mission (August 30, 2002) until the present. We will refer to the product files by their "shortnames" in this document when necessary to avoid confusion. The AIRS-Only Level 2 Standard Product Physical Retrieval has shortname "**AIRS2RET**". The shortnames for the corresponding Level 2 Support Product and Level 2 Cloud Cleared Product are "**AIRS2SUP**" and "**AIRS2CCF**".

A second flavor of Level 2 retrieval product files results from the retrieval using the combined AIRS infrared and AMSU microwave radiances. This product spans the period from beginning of mission (August 30, 2002) until September 24, 2016, when AMSU-A2 failed. The combined AMSU+AIRS Level 2 Standard Product Physical Retrieval has shortname "**AIRX2RET**". The shortnames for the corresponding Level 2 Support Product and Level 2 Cloud Cleared Product are "**AIRX2SUP**" and "**AIRI2CCF**".

Another combined IR/MW Level 2 retrieval product spans the period from beginning of mission to February 5, 2003. On that date, the Humidity Sounder for Brazil (HSB) failed. Level 2 Standard Product files resulting from the retrieval using AIRS infrared, AMSU microwave and HSB microwave radiances (AMSU+HSB+AIRS) have shortname "**AIRH2RET**". The corresponding shortnames for the Level 2 Support Product and Level 2 Cloud Cleared Product are "**AIRH2SUP**" and "**AIRH2CCF**".

1.2 Data Access

AIRS Level 2 products are available to the user community via the Goddard Earth Sciences Data and Information Services Center (GES DISC). The GES DISC provides additional information and documentation about the AIRS L2 products and other products of interest, as well as ordering and data sub-setting tools and services:

https://disc.gsfc.nasa.gov

The shortnames referred to above are used as collection names in the GES DISC system and can be used in keyword searches for datasets on the GES DISC web page, which also provides various filters to locate datasets of interest. For convenience, the table in the following subsection has links to the GES DISC landing pages for the datasets described above, along with file name examples. Typical file sizes are as follows:

Level 2 Data Set	Granule Size
Standard Product	3.5 MB
Support Product	25 MB
Cloud-cleared radiances	14 MB

1.3 Product File Names

The following are examples of Level 2 product files for granule 120 for an example date (January 1, 2019 or September 6, 2002). Recall that there are 240 daily data granules for each Level 2 product. In each file name, the "AIRS" string is followed by date, granule number, processing level, a string identifying the product type, version number, a string

containing a letter for the processing facility ("G" for GES DISC) and a run tag with local processing time, and finally the filetype extension.

The general form for file names is: AIRS.yyyy.mm.dd.granule.L2.type.vx.timestamp.hdf

The processing timestamp has the general form 'yydddhhmmss'.

Product Flavor	Shortname	Standard Product File Name
AIRS	AIRS2RET	AIRS.2019.01.28.120.L2.RetStd_IR.v7.0.1.0.G20071160428.hdf
AIRS/AMSU	AIRX2RET	AIRS.2002.09.06.120.L2.RetStd.v7.0.1.0.G20057185843.hdf
AIRS/AMSU/HSB	AIRH2RET	AIRS.2002.09.06.120.L2.RetStd_H.v7.0.1.0.G20058153833.hdf
		Support Product File Name
AIRS	AIRS2SUP	AIRS.2019.01.28.120.L2.RetSup_IR.v7.0.1.0.G20071160428.hdf
AIRS/AMSU	AIRX2SUP	AIRS.2002.09.06.120.L2.RetSup.v7.0.1.0.G20057185843.hdf
AIRS/AMSU/HSB	AIRH2SUP	AIRS.2002.09.06.120.L2.RetSup_H.v7.0.1.0.G20058153833.hdf
		Cloud Cleared Radiance Product File Name
AIRS	AIRSCCF	AIRS.2002.09.06.120.L2.CC_IR.v7.0.2.0.Gyydddhhmmss.hdf
AIRS/AMSU	AIRICCF	AIRS.2002.09.06.120.L2.CC.v7.0.1.0.G20057185843.hdf
AIRS/AMSU/HSB	AIRHCCF	AIRS.2002.09.06.120.L2.CC_H.v7.0.2.0.G20058153833.hdf

1.4 File Format and Structure

Hierarchical Data Format (HDF) has been common for NASA Earth Observing System (EOS) data products. AIRS Level 2 product files are provided in the HDF-EOS swath format. The version used is HDF-EOS2, which is based on HDF4. Each file contains all observations of a given type made during a period of exactly 6 minutes. For each day there are 240 six-minute granules, numbered 1-240. Over the course of 6 minutes the EOS-Aqua platform travels approximately 1500 km, and the AIRS-suite instruments scan a swath approximately 1500 km wide. The products have exactly one swath per file. Further descriptions of file structure and contents, with a list of all fields provided, are given in Appendix A: Level 2 Product Interface Specifications.

Maps showing the location of each available granule can be accessed at the following URL (Level 1 granules are the same as for Level 2):

https://disc.gsfc.nasa.gov/datasets/AIRXAMAP_005/summary

1.5 Invalid Values

On occasion, there will be data that is missing for various reasons. In the situation where there are incomplete granules within the 6-minute product granule, the missing data will be filled with 'Fill Values'. The fill value will exist in the same location the missing data would exist. This will preserve the shape of the 6-minute granule. With this in mind, it is advised to check the data for fill values before use. Invalid or missing data will have the following fill value:

-9999 for floating-point and 16-bit and 32-bit integers
-1 or 255 for 8-bit fields.

1.6 Dimension, Pressure, Geolocation, and Ancillary Fields

The fields that provide the dimensions of the various arrays in the Physical Retrieval Level 2 Standard Product data files, are listed with short descriptions in Appendix A1, along with pressure arrays, geolocation fields, and other ancillary fields. The horizontal dimension fields are **GeoXTrack** (30) and **AIRSXTrack** (3) in the cross-track direction, and **GeoTrack** (nominally 45) and **AIRSTrack** (3) in the along-track direction. Vertical dimension fields include **StdPressureLev** and **StdPressureLay** (both 28). The values of the standard pressure array are given in **pressStd** and **pressH2O** is the water vapor pressure array. Pressure arrays are presented in the following documents:

V7_L2_Standard_Pressure_Levels.pdf
V7_L2_Support_Pressure_Levels.pdf

Note that the **pressH2O** values are identical to the first 15 entries in **pressStd**.

Geolocation fields are provided for all retrievals and include **Latitude**, **Longitude**, and **Time**. With a solid angle width of about 1.1 degrees in diameter, the Field of View (FOV) for the AIRS instrument corresponds to a footprint of about 15 km in the nadir. With an angular width of about 3.3 degrees, the AMSU footprint is around 45 km at nadir. Retrievals of most geophysical parameters are performed within a 3x3 array of AIRS FOVs, contained within an AMSU footprint, referred to as an AIRS Field of Regard (FOR). **Latitude** and **Longitude** apply to the FOR, while **latAIRS** and **lonAIRS** apply to each AIRS spot within a FOR. Other fields are provided for all retrievals that specify spacecraft and solar angles. Surface ancillary fields include **landFrac,** which gives the fraction of a footprint that is land, **topog,** which defines mean topography, the surface pressure first guess, **PSurfStd**, and **nSurfStd,** which gives the index of the first pressure level above mean surface.

1.7 Quality Indicator Pressure Boundaries

The overall Quality Assurance (QA) fields listed in the table below are provided for all retrievals, and are set as a result of QA determinations in the retrieval algorithm. They are very useful for deciding which retrievals should be excluded from a sample. For example, a study of the lower troposphere should not use retrievals for which **PBest** < 700 hPa.

NOTE: Level Indices Are 1-Based.

All parameters that are level numbers, such as **nSurfStd, nBestStd and nGoodStd** are 1-based. Those who work in FORTRAN and MATLAB will be unaffected. However, those who work in C, IDL and Python must take care when using **nSurfStd** and other parameters that are level numbers. The following two expressions yield the same value for mypress:

FORTRAN and MATLAB: mypress = **pressStd**(**nBestStd**)
C, IDL and Python: mypress = **pressStd**[**nBestStd**-1]

Field Name	Dimension per FOV	Description
PBest	1	Maximum value of pressure for which atmospheric temperature profile QC=0 (hPa)
PGood	1	Maximum value of pressure for which atmospheric temperature profile QC=0 or 1 (hPa)
nBestStd	1	Standard level index (1-based) of highest pressure (i.e., lowest altitude) for which atmospheric temperature profile QC=0. A value of 29 (there are only 28 standard pressure levels) indicates that no part of the profile satisfies QC=0 (1 → 29)
nGoodStd	1	Standard level index (1-based) of highest pressure (i.e., lowest altitude) for which atmospheric temperature profile QC=0 or 1. A value of 29 (there are only 28 standard pressure levels) indicates that no part of the profile satisfies QC=0 or 1 (1 → 29)

1.8 Data Validation States

The validation states for Level 2 Data Products in the Version 7 release are given in the table below, along with uncertainty estimates and vertical coverage, where applicable. This table is only intended to give a general idea about the products. For more details on validation, uncertainties and coverage, the reader is referred to the product-specific sections in this document and references therein to validation reports and relevant journal papers. The AIRS webpage also has a frequently updated searchable database for AIRS-related publications:

https://airs.jpl.nasa.gov/sounding-science/publications/

AIRS product validation states have traditionally been categorized as "**Provisional**" and "**Validated: Stages 1-3**". The state of product validation depends upon surface type, latitude and product type.

Prov = Provisional: Product quality is sufficient for use by the general research community, but users are urged to contact the AIRS science team before using the data in publications

Val1 = Stage 1 Validation: Product accuracy has been estimated using a small number of independent measurements obtained from selected locations and time periods and ground-truth/field program efforts.

Val2 = Stage 2 Validation: Product accuracy has been assessed over a widely distributed set of locations and time periods via several ground-truth and validation efforts.

Val3 = Stage 3 Validation: Product accuracy has been assessed and the uncertainties in the product well established via independent measurements in a systematic and statistically robust way representing global conditions

The validation state for the Level 3 Gridded Data Product matches that of the corresponding Level 1B or Level 2 Data Product from which it is generated.

Standard Geophysical Product	Uncertainty Estimate	Vertical Coverage	Val Status
Cloud Cleared IR Radiance	Accuracy ~1 K Precision 0.3-8 K	N/A	Val2
Sea Surface Temperature	1 K	N/A	Val3
Land Surface Temperature	2-3 K	N/A	Val2
Surface Emissivity	-	N/A	Val2
Temperature Profile	Tropo: 1-2 K/km Above: 2-3 K/km	Surface to 1 hPa	Val3
Water Vapor Profile	Tropo: 15%/2km Sensitivity thresh: ~30 ppmv	Surface to 200 hPa or tropopause	Val3
Total Precipitable Water	~5%	N/A	Val3
Effective Cloud Fraction	-	900 to 100 hPa	Val3
Cloud Top Height	-	900 to 100 hPa	Val3
Cloud Top Temperature	-	900 to 100 hPa	Val3
Total O_3 Column	5%	N/A	Val3
O_3 Profile	20%	250 to 70 hPa	Val2
CO Amount	15%	~400-600 hPa	Val2
CH_4 Amount	20%	From ~850 hPa to lower stratosphere	Val1
SO_2 Flag	–	N/A	Prov
Dust/Aerosol Flag	-	N/A	Val1
CO_2	~2 ppmv	300-500 hPa layer	Val2
Cloud Thermodynamic Phase and Ice Cloud Properties	-	-	Val3

2 Cloud Cleared Radiances

There are three Level 2 Cloud-Cleared Radiance Product data streams:

- **AIRSCCF** produced by AIRS retrieval processing (available 2002-08-30 to present)
- **AIRICCF** produced by AIRS+AMSU retrieval processing (available 2002-08-30 to 2016-09-24)
- **AIRHCCF** produced by AIRS+AMSU+HSB retrieval processing (available 2002-08-30 to 2003-02-05)

All data are available in the Level 2 Standard Cloud-Cleared Radiance Product, a series of HDF-EOS2 (HDF4-based) Swath format files for each 6-minute AIRS retrieval granule similar to the Level 2 Standard Product and Level 2 Support Product.

In Appendix A3, all the fields contained in the Cloud-Cleared Radiance Product files are listed with short descriptions. A subset of the fields is provided in the table below for convenience. These data fields are provided for each Field of Regard (i.e., retrieval footprint). The full table in Appendix A3 includes available informative fields, for example viewing geometry, so that it will not be necessary for users to open the associated Level 2 Physical Retrieval product granules to access that information. Also included in Appendix A3, are the fields that provide the dimensions of the various arrays in the Cloud Cleared Radiances Standard Product data files, along with geolocation fields, channel information fields and other ancillary fields. The dimension fields include the horizontal dimension fields **GeoXTrack** (with a value of 30), for the cross-track direction, and **GeoTrack** (nominally 45), for the along-track direction, as well as **Channel**, **AIRSXTrack**, **AIRSTrack**, and **Module**. The geolocation fields include **Latitude**, **Longitude**, and **Time**. Channel information fields that are given once per granule include **nominal_freq**, **CalChanSummary**, **ExcludedChans**, **NeN_L1B**, and **NeN_L1B_Static**. The along-track data fields **CalFlag** and **CalScanSummary** may also be of immediate interest to users, as well as **CalGranSummary**, which is listed as an attribute.

Researchers using the cloud cleared radiance product should read the document

V7_L2_Cloud_Cleared_Radiances.pdf,

which contains a more detailed description of the cloud cleared radiances and associated brightness temperature, error estimates and quality control.

Field Name	Dimension per FOV	Description
radiances	Channel = 2378	Cloud-cleared radiances for each channel (milliWatts/m^2/cm^{-1}/steradian)
radiances_QC	Channel = 2378	Quality flag array (0,1,2)
radiance_err	Channel = 2378	Error estimate for radiances (milliWatts/m^2/cm^{-1}/steradian)

CldClearParam	AIRTrack *AIRSXTrack =3x3	Cloud clearing parameter Eta. Positive values are cloudier than average for the FOR, negative values are clearer.
landFrac	1	Fraction of spot that is land (0.0 → 1.0)
landFrac_err	1	Error estimate for landFrac
CCfinal_Noise_Amp	1	Internal retrieval quality indicator -- noise amplification factor from cloud clearing because of extrapolation, dimensionless. Note: the name is misleading: this is the value after the second cloud clearing iteration, not the last.
scanang	1	Scanning angle of the central AIRS instrument field-of-view with respect to the spacecraft (-180.0 → 180.0, negative at start of scan, 0 at nadir)
solzen	1	Solar zenith angle (0.0 → 180.0) degrees from zenith (measured relative to the geodetic vertical on the reference (WGS84) spheroid and including corrections outlined in EOS SDP toolkit for normal accuracy.)
sun_glint_distance	1	Distance (km) from footprint center to location of the sun glint (-9999 for unknown, 30000 for no glint visible because spacecraft is in Earth's shadow)

2.1 Description

The AIRS Level 2 Cloud Cleared Radiances are the clear column radiances due to the atmospheric column resulting from the physical retrieval, i.e. the radiances that the instrument would have observed in the absence of clouds.

2.2 Type of Product

The radiances are reported for all 2378 AIRS infrared channels for each Field of Regard retrieval footprint (50km spatial resolution at nadir) in the units of mW/m^2-sr-cm^{-1}. There are 1350 possible retrievals in each AIRS 6-minute granule. The AIRS Level 2 Cloud Cleared Radiance Product is reported in the same HDF-EOS swath format as the accompanying AIRS Level 2 Standard Product and AIRS Level 2 Support Product.

2.3 Quality Indicators

In all Quality Control (QC) fields:

0→Highest Quality, 1→Good Quality, 2→ Do Not Use

Fields of View in which **radiances_QC** = 1 may be sufficiently accurate for statistical studies, but results should be carefully checked

The channel-by-channel quality flags were introduced in V6 and are in the same form in V7. The error estimates for each channel (**radiance_err**) are converted to brightness temperature error estimates (ΔT), and **radiances_QC** values are then set as follows:

= 0 if $\Delta T < 1.0$ K
= 1 if $1.0 <= \Delta T < 2.5$ K
= 2 otherwise

Studies of test data have identified retrievals for which the cloud cleared radiances in the window regions

750 cm^{-1} to 1137 cm^{-1} and 2400 cm^{-1} to 2665 cm^{-1}

exhibit large biases and standard deviations while thought to be clear scenes. It was found that under some conditions with extensive stratus cloud cover, window channel observations "thought to be clear" were awarded very low noise amplification factors. Users can remove these cases by applying the following additional filter:

Do not use (i.e., set radiances_QC = 2) for channels in the window regions if:

0.3333 < **CCfinal_Noise_Amp** < 0.3334

and

TSurfStd_QC = 2

Please study the last several pages discussing Figures 4 and 5 of

V7_L2_Cloud_Cleared_Radiances.pdf

2.4 Validation

After the loss of AMSU-A2 the AIRS team compared AIRS-only Cloud Cleared Radiances to AIRS+AMSU for V6 and found the only significant difference was that the amount of level 0 and 1 cases was greater for AIRS+AMSU. The quality control for both data products performed similarly in describing the fidelity of their own data. Comparison between V6 and V7 (both AIRS-only and AIRS+AMSU) as well as with clear MODIS radiances is described in the following document:

V7_L2_Performance_Test_and_Validation_Report.pdf

2.5 Caveats

This section will be updated over time as V7 data products are analyzed and validated.

2.6 Suggestions for Researchers

This section will be updated over time as V7 data products are analyzed and validated.

Aside from being an integral part of the retrieval process, the cloud cleared radiance products can also be potentially used in data assimilation experiments and also for process studies.

The most important channels for radiance assimilation purposes are in the longwave temperature sounding spectral region 650 cm^{-1} – 740 cm^{-1}, and the error estimate methodology was designed primarily for use in this spectral region.

Clear column radiances in channels with QC=0 for a given retrieval case are considered to have the highest accuracy, and are recommended for potential use in data assimilation experiments. Clear column radiances in channels with QC=1 are considered to be of good quality and are recommended for inclusion in other applications, such as process studies. Clear column radiances in channels with QC=2 are not recommended for scientific use.

Guidelines in the **L1B_Product_User_Guide.pdf** may be useful for evaluation of candidate channels to use.

2.7 Recommended Papers

This section will be updated over time as research with V7 data products are published.

Chahine, M.T. (1977), Remote Sounding of cloudy atmospheres. II. Multiple cloud formations, J. Atmos Sci, 34, 744-757.

Susskind, J, C.D. Barnet, and J. Blaisdell (1998), Determination of atmospheric and surface parameters from simulated AIRS/AMSU sounding data: Retrieval methodology and cloud clearing methodology, Adv. Space Res, 21, 369-384.

Susskind, J., C.D. Barnet, J.M. Blaisdell (2003), Retrieval of Atmospheric and Surface Parameters from AIRS/AMSU/HSB Data in the Presence of Clouds, IEEE Trans. Geoscience and Remote Sensing, 41, 390-409, doi:10.1109/TGRS.2002.808236.

Susskind J., C. Barnet, J. Blaisdell, L. Iredell, F. Keita, L. Kouvaris, G. Molnar, M. Chahine (2006), Accuracy of geophysical parameters derived from Atmospheric Infrared Sounder/Advanced Microwave Sounding Unit as a function of fractional cloud cover, J. Geophys, Res., 111, D09S17, doi:10.1029/02005JD006272.

Susskind, Joel, John M. Blaisdell, and Lena Iredell. "Improved methodology for surface and atmospheric soundings, error estimates, and quality control procedures: the atmospheric infrared sounder science team version-6 retrieval algorithm." Journal of Applied Remote Sensing 8, no. 1 (2014): 084994-084994.

2.8 Recommended Supplemental User Documentation

Overview_of_the_AIRS_Mission.pdf
V7_L2_Cloud_Cleared_Radiances.pdf
V7_L2_Performance_Test_and_Validation_Report.pdf
V7_L2_Quality_Control_and_Error_Estimation.pdf
V7_Retrieval_Channel_Sets.pdf
V7_Retrieval_Flow.pdf
L1B_Product_User_Guide.pdf
L1B_Calibration_Properties_Files (series of ASCII files)
V7_L2_Channel_Properties_Files (series of ASCII files)

3 Microwave-Only Products

The Microwave-Only (MW-Only) standard products are retrieved by the MW retrieval stage of the AIRS algorithm using AMSU radiances in the **AIRX2RET** product and AMSU+HSB radiances in the **AIRH2RET** product. No IR data are used to retrieve these products. All other products described later in this document are retrieved employing the AMSU+AIRS (**AIRX2RET**) or AIRS-Only (**AIRS2RET**) retrieval stages of the AIRS algorithm, providing greater vertical resolution of temperature and water vapor fields, improved surface emissivity and retrievals of atmospheric constituents. The spatial footprint for all retrievals is the field-of-view (FOV) of the Advanced Microwave Sounding Unit (AMSU), which is 40.5 km at nadir. Note that MW-Only products are absent from the mainline Version 7 AIRS-Only (**AIRS2RET**) products.

The **AIRH2RET** Microwave-Only Support Products contain useful (at altitudes below the 300 hPa level) retrieved moisture profiles as well as rain rate, cloud liquid water and a cloud/ice flag. This is not the case for the **AIRX2RET** Microwave-Only Support Products.

Standard Product

Field Name	Dimension per FOV	Description
TAirMWOnlyStd	StdPressureLev =28	Atmospheric Temperature retrieved using only MW information (no IR) at StdPressLev in Kelvins.
TAirMWOnlyStd_QC	StdPressureLev =28	Quality flag profile for TAirMWOnlyStd (0,1,2)
GP_Height_MWOnly	StdPressureLev =28	Geopotential Heights from MW-Only retrieval (No IR information used) at StdPressureLev (m above mean sea level)
GP_Height_MWOnly_QC	StdPressureLev =28	Quality flag array for GP_Height_MWOnly (0,1,2)
sfcTbMWStd	MWHingeSurf=7	Microwave surface brightness (Kelvins) (Emitted radiance only, reflected radiance not included.)
sfcTbMWStd_QC	MWHingeSurf=7	Quality flag array (0,1,2)
EmisMWStd	MWHingeSurf=7	Spectral MW emissivity at the 7 MW frequencies listed for dimension MWHingeSurf
EmisMWStdErr	MWHingeSurf=7	Error estimate (unitless)
EmisMWStd_QC	MWHingeSurf=7	Quality flag array (0,1,2)
MW_ret_used	1	MW-Only final retrieval used
MWSurfClass	1	Surface class from microwave (MW) information:; 0 → coastline (Liquid water covers 50-99% of area); 1 → land (Liquid water covers < 50% of area); 2 → ocean (Liquid water covers > 99% of area); 3 → sea ice (High MW emissivity); 4 → sea ice (Low MW emissivity); 5 → snow (Higher-frequency MW scattering); 6 → glacier/snow (Very low-frequency MW scattering); 7 → snow (Lower-frequency MW scattering); -1 → unknown (not attempted) (unitless)

totH2OMWOnlyStd	1	Total precipitable water vapor from MW-only retrieval (no IR information used) (kg/m2)
totH2OMWOnlyStd_QC	1	Quality flag (0,1,2)
totCldH2OStd	1	Total cloud liquid water (kg/m2)
totCldH2OStdErr	1	Error estimate (kg/m2)
totCldH2OStd_QC	1	Quality flag (0,1,2)

Support Product (full list available in Appendix A2)

Field Name	Dimension per FOV	Description
TAirMWOnly	XtraPressureLev=100	Retrieved Atmospheric Temperature Profile. Value below index nSurfSup may be an unphysical extrapolated value for a pressure level below the surface (K)
TAirMWOnly_QC	XtraPressureLev=100	Quality Control for TAirMWOnly.; 0: Highest Quality; 1: Good Quality; 2: Do Not Use
TAirMWOnlyErr	XtraPressureLev=100	Error estimate (K), only located in the Level 2 Support Product
H2OCDMWOnly	XtraPressureLay=100	Layer column water vapor (molecules/cm2)
H2OCDMWOnly_QC	XtraPressureLay=100	Quality flag (0,1,2)

Parameters in Support Product if HSB Radiances Available (AIRH2SUP)

Field Name	Dimension per FOV	Description
rain_rate_50km	1	Rain rate (mm/hr)
rain_rate_15km	AIRSTrack*AIRSXTrack =3x3	Rain rate for HSB 15km spots (mm/hr)
lwCDSup	XtraPressureLay=100	Layer molecular column density of cloud liquid water (molecules/cm2)
lwCDSup_QC	XtraPressureLay=100	Quality flag (0,1,2)
lwCDSupErr	XtraPressureLay=100	Error estimate (molecules/cm2)
cIWSup	XtraPressureLay=100	Cloud Ice/Water flag liquid = 0 ice = 1

3.1 Description

The 28 Level 2 Standard pressure levels (**pressStd**) are arranged in order of decreasing pressure, from 1100 hPa to 0.1 hPa. A table of their values is provided in the document, **V7_L2_Standard_Pressure_Levels.pdf**. The index of the lowest altitude pressure level for which a reported **TAirMWOnlyStd** is valid is **nSurfStd**, which may be 1→15 depending upon topography. The surface pressure, interpolated from the NCEP GFS forecast and the local DEM topography, is **PSurfStd**.

totCldH2OStd is the integral of the cloud liquid water profile. The estimated error, **totCldH2OStdErr**, is set according to surface type with values ranging from 0.02 kg/m2 to 0.15 kg/m2 if **totH2OMWOnlyStd_QC** = 0 or 1. In the event that **totH2OMWOnlyStd_QC** = 2, it is set to 1.00 kg/m2.

MWSurfClass is produced by a classification algorithm employing AMSU-A data and the **landFrac** parameter (i.e., the fraction of the surface of the FOV covered by land). The possible values are:

MWSurfClass	Description
-1	unknown (not attempted)
0	coastline (liquid water covers 50% to 99% of FOV)
1	land (liquid water covers less than 50% of FOV)
2	ocean (liquid water covers more than 99% of FOV)
3	sea ice (high MW emissivity)
4	sea ice (low MW emissivity)
5	snow (higher-frequency MW scattering)
6	glacier/snow (very low-frequency MW scattering)
7	snow (lower-frequency MW scattering)

The difference between **MWSurfClass** = 3 and 4, or among **MWSurfClass** = 5, 6, 7 is in the microwave signature of the ice and/or snow. There are complex physical reasons for the differences, including age. Users may collapse the **MWSurfClass** values present here into NOAA's AMSU-product classes by combining 3 and 4 for sea ice and 5, 6 and 7 for land snow/ice.

sfcTbMWStd is the surface brightness temperature retrieved at the seven frequencies: 23.8, 31.4, 50.3, 52.8, 89.0, 150.0, 183.31 GHz. **EmisMWStd** is derived as the ratio of **sfcTbMWStd** to an estimated MW-Only surface skin temperature. The estimated error, **EmisMWStdErr**, is frequency dependent and varies between 0.015 and 0.034, based on simulations. If the retrieved values are rejected, **EmisMWStdErr** values are set ≥ 1.0 and **EmisMWStd_QC** values are set to 2. The effective MW-Only surface skin temperature may be calculated by dividing an element of **sfcTbMWStd** by the corresponding element of **EmisMWStd**, but we advise users doing so that the values resulting from this calculation are not supported and are not validated as a product.

3.2 Type of Product

MW-Only Standard Product profiles for temperatures and heights are **level** quantities, i.e. the values are reported at fixed pressure levels. This differs from layer quantities (in the Support Product), which are reported on the fixed pressure levels but represent the layer bounded by the level on which they are reported and the next higher (in altitude) level. Users may calculate the approximate effective layer pressure by taking the geometric mean of the level pressures bounding the layer. Thus the effective layer pressure for a layer quantity reported on the 700 hPa level is SQRT(600.0*700.0) = 648 hPa.
For more detail, see **V7_L2_Levels_Layers_Trapezoids.pdf** for a full discussion of level and layer quantities. See also **V7_L2_Standard_Pressure_Levels.pdf**.

3.3 Quality Indicators

In all QC fields: 0→Highest Quality, 1→Good Quality, 2→ Do Not Use

The user is encouraged to read the QC and error estimation document:

V7_L2_Quality_Control_and_Error_Estimation.pdf

The MW-Only retrieval stage sets bits in **MW_ret_code** (located in the Level 2 Support Product) upon encountering errors:

MW_ret_code	Explanation
1	moisture variables rejected by residual test
2	tropospheric temperature profile rejected by residual test
4	excessive liquid water (> 0.5 kg/m2)
8	insufficient valid channels
16	numerical error
32	emissivity > 1 for any AMSU-A channel
64	stratospheric temperature profile rejected by residual test
128 or -128	microwave retrieval not attempted

The part of the **TAirMWOnlyStd** profile at pressures equal to or greater than 201 hPa is set by examining the bits in **MW_ret_code** corresponding to the microwave retrieval in that portion of the atmospheric column.

If any of the first six bits (bits 1→6) are set, then **TAirMWOnlyStd_QC** for those levels is set to Quality = 2; otherwise it is set to Quality = 0. **sfcTbMWStd_QC** and **EmisMWStd_QC** are also set by this check.

The part of the **TAirMWOnlyStd** profile at pressures less than 201 hPa is set by examining the bits in **MW_ret_code** corresponding to the microwave retrieval in that portion of the atmospheric column.

If any of three bits (bits 4, 5 or 7) are set, then **TAirMWOnlyStd_QC** for those levels is set to 2; otherwise it is set to 0.

The failure of HSB on February 5, 2003 degraded various moisture research products, and the quality flags **totH2OMWOnlyStd_QC** and **totcldH2OStd_QC** are set in part by the availability of HSB data. If any of the first six bits (bits 1→6) of **MW_ret_code** are set then these two quality flags are set to Quality = 2. If the test on **MW_ret_code** yields no fault, an additional test is performed. If HSB data are present these quality flags are set to 0. If HSB data are not present and **MWSurfClass** = 0 or 2, these quality flags are set to Quality = 1, and they are set to Quality = 2 for all other surface types. **Note that Quality = 1 constitutes the best level of quality that can be achieved for totH2OMWOnlyStd and totcldH2OStd when HSB data are not available (i.e., the AIRX2RET product).**

The failure of HSB also impacts **sfcTbMWStd** and **EmisMWStd**. In the absence of HSB, array elements 6 and 7 (corresponding to 150 GHz and 183.31 GHz) are marked Quality = 2 and contain fill values (-9999.).

The degradation and ultimate failure of AMSU channels 4 and 5, impacts array element 4 (corresponding to 52.8 GHz) of **sfcTbMWStd, EmisMWStd, sfcTbMWStd_QC** and **EmisMWStd_QC**. Array element 4 of **sfcTbMWStd** and **EmisMWStd** contain values derived by regression, but array element 4 of **sfcTbMWStd_QC** and **EmisMWStd_QC** are set to Quality = 2 to reflect the absence of an actual measurement.

To ensure continuity throughout the entire mission, the V7 retrieval algorithm for MW-Only products provided by the AMSU+AIRS processing does not use AMSU channels 4 and 5, even in the earlier stage of the mission when those channels were good.

To maximize the quality of the retrieval (of moisture product in particular), the V7 retrieval algorithm for MW-Only products provided by the AMSU+HSB+AIRS processing does use AMSU channels 4 and 5.

The quantity **GP_Height_MWOnly** depends on both temperature and moisture, working upward from the surface. **GP_Height_MWOnly_QC** for the entire profile is set to the higher value of **TAirMWOnly_QC** (at the surface, i.e. first array element) or **H2OCDMWOnly_QC** (at the surface).

3.4 Validation

Testing of MW-only products is summarized in the following V6 report:

V6_L2 Performance_and_Test_Report.pdf

Further validation for V7 has not been performed at this point.

3.5 Caveats

This section will be updated over time as V7 data products are analyzed and validated.

There is no retrieval of MW-Only water vapor for altitudes above the 300 hPa pressure level in the AIRS+AMSU+HSB (**AIRH2RET**) product. There is no retrieval of MW-Only water vapor profile at any altitude in the AIRS+AMSU (**AIRX2RET**) product; there is only a constraint on the total burden of moisture for the **AIRX2RET** product. We do not recommend the use of the MW-Only water vapor profile in the **AIRX2RET** product.

Note that there are values for **EmisMWStd** and **sfcTbMWStd** for the 150 GHz and 183 GHz channels only if HSB data are available, otherwise the values will be set to -9999.0. The AIRS Level 2 Standard Product in which HSB data are available is the **AIRH2RET** version. The **AIRX2RET** version does not ingest HSB data.

Note also that with the failure of AMSU channels 4 and 5 and thus their exclusion in V7 AMSU+AIRS processing, we have no independent value for **sfcTbMWStd** and **EmisMWStd** at 52.8 GHz.

In brief, the user should filter MW-Only moisture retrievals as follows:

If HSB data are used in the retrieval (**AIRH2RET**), then users may use both the column totals and profiles of the MW-Only moisture products, subject to their individual QC values.
If HSB data are not used in the retrieval (**AIRX2RET**), then users may only use the column totals of the MW-Only moisture products, subject to their individual QC values. Rejected moisture retrievals (Quality = 2) should be avoided.

All parameters that are level numbers, such as **nSurfStd**, are 1-based. Those who work in FORTRAN and MATLAB will be unaffected. However, those who work in C, IDL and Python must take care when using **nSurfStd** and other parameters that are level numbers. The following two expressions yield the same value:

FORTRAN and MATLAB: **TAirMWOnlyStd**(**nSurfStd**)
C, IDL and Python: **TAirMWOnlyStd**[**nSurfStd**-1]

The value of **TAirMWOnlyStd** at index **nSurfStd** (in FORTRAN and MATLAB) or index **nSurfStd**-1 (in C, IDL and Python) may be an unphysical extrapolated value for a pressure level below the surface. The user must also compare **PSurfStd** to the associated **pressStd** element. If (for IDL) **PSurfStd** < **pressStd**[**nSurfStd**-1] then the level falls below the local surface and **TAirMWOnlyStd**[**nSurfStd**-1] is not physical.

3.6 Suggestions for Researchers

This section will be updated over time as V7 data products are analyzed and validated.

We caution users to avoid combining MW-only retrieval products with products retrieved via the combined IR/MW algorithm (AMSU+AIRS or AMSU+HSB+AIRS) or the AIRS-Only algorithm in their analyses. The three products are quite different in character, sampling and quality.

3.7 Recommended Papers

This section will be updated over time as research with V7 data products are published.

Cadeddu et al, 2007, “Measurements and retrievals from a new 183 GHz water vapor radiometer in the Arctic, IEEE Trans. Geosci. Rem. Sens. v.45, pp.2207-2215, doi: 10.1109/TGRS.2006.888970

Fetzer, E.; McMillin, L.M.; Tobin, D.; Aumann, H.H.; Gunson, M.R.; McMillan, W.W.; Hagan, D.E.; Hofstadter, M.D.; Yoe, J.; Whiteman, D.N.; Barnes, J.E.; Bennartz, R.; Vomel, H.; Walden, V.; Newchurch, M.; Minnett, P.J.; Atlas, R.; Schmidlin, F.; Olsen, E.T.; Goldberg, M.D.; Sisong Zhou; HanJung Ding; Smith, W.L.; Revercomb, H., "AIRS/AMSU/HSB validation," Geoscience and Remote Sensing, IEEE Transactions on , vol.41, no.2, pp. 418-431, Feb. 2003

Fetzer, E. J., W. G. Read, D. Waliser, B. H. Kahn, B. Tian, H. Vömel, F. W. Irion, H. Su, A. Eldering, M. de la Torre Juarez, J. Jiang and V. Dang (2008), Comparison of upper tropospheric water vapor observations from the Microwave Limb Sounder and Atmospheric Infrared Sounder, J. Geophys. Res., 113, D22110, doi:10.1029/2008JD010000.

Gettelman,A., Weinstock,E. M., Fetzer,E. J., Irion,F. W., Eldering,A., Richard,E. C., Rosenlof,K. H., Thompson,T. L., Pittman,J. V., Webster,C. R., Herman,R. L. (2004), Validation of Aqua satellite data in the upper troposphere and lower stratosphere with in situ aircraft instruments, Geophys. Res. Lett., 31, L22107, doi:10.1029/2004GL020730.

Grody, F.Weng, and R. Ferraro (2000), "Application of AMSU for obtaining hydrological parameters," in Microwave Radiometry and Remote Sensing of the Earth's Surface and Atmosphere, edited by P. Pampaloni and S. Paloscia, pp. 339–352, Brill Acad., Leiden, Netherlands.

Hagan D. E., C. R. Webster, C. B. Farmer, R. D. May, R. L. Herman, E. M. Weinstock, L. E. Christensen, L. R. Lait, P. A. Newman (2004), Validating AIRS upper atmosphere water vapor retrievals using aircraft and balloon in situ measurements, Geophys. Res. Lett., 31, L21103, doi:10.1029/2004GL020302.N.

Lambrigtsen, B.H., "Calibration of the AIRS microwave instruments," Geoscience and Remote Sensing, IEEE Transactions on Geoscience and Remote Sensing, vol.41, no.2, pp. 369-378, Feb. 2003.

Lambrigtsen, B.H.; Calheiros, R.V., "The Humidity Sounder for Brazil - an international partnership," Geoscience and Remote Sensing, IEEE Transactions on Geoscience and Remote Sensing, vol.41, no.2, pp. 352-361, Feb. 2003.

Read, W. G., A. Lambert, J. Bacmeister, R. E. Cofield, L. E. Christensen, D. T. Cuddy, W. H. Daffer, B. J. Drouin, E. Fetzer, L. Froidevaux, et al. (2007), Aura Microwave Limb Sounder upper tropospheric and lower stratospheric H2O and relative humidity with respect to ice validation, J. Geophys. Res., 112, D24S35, doi:10.1029/2007JD008752.

Rosenkranz, P.W. (2001), "Retrieval of temperature and moisture profiles from AMSU-A and AMSU-B measurements", IEEE Trans. Geosci. Rem. Sens. v.39, pp.2429-2435.

Rosenkranz, P.W. (2003), "Rapid radiative transfer model for AMSU/HSB channels," IEEE Trans. Geosci. Rem. Sens., v.41, pp.362-368.

Rosenkranz, P.W. (2006), "Cloud liquid-water profile retrieval algorithm and validation," J. Geophys. Res., v.111, D09S08, doi:10.1029/2005JD00583.

Rosenkranz, P.W. and C. D. Barnet (2006), "Microwave radiative transfer model validation," J. Geophys. Res., v.111, D09S07, doi:10.1029/2005JD006008.

Tretyakov et al., 2005, "60 GHz Oxygen Band: precise broadening and central frequencies of fine structure lines, absolute absorption profile at atmospheric pressure and revision of mixing coefficients," J. Mol. Spectros. v.231, pp.1-14, doi: 10.1016/j.j,s.2004.11.011

3.8 Recommended Supplemental User Documentation

Overview_of_the_AIRS_Mission.pdf
V7_L2_Quality_Control_and_Error_Estimation.pdf
V7_L2_Standard_Pressure_Levels.pdf
V7_L2_Levels_Layers_Trapezoids.pdf
V7_Retrieval_Flow.pdf

4 Surface Properties

Retrieved surface quantities are listed and described below, along with surface properties that are not retrieved (surface class, forecast snow depth and sea ice fraction). Near-surface air temperature and water vapor products are covered in the temperature and water vapor retrieval sections (Sections 5 and 8).

Standard Product

Field Name	Dimension per FOV	Description
TSurfStd	1	Surface skin temperature (K)
TSurfStdErr	1	Error estimate for TSurfStd (K)
TSurfStd_QC	1	Quality flag (0,1,2)
numHingeSurf	1	Number of IR hinge points for surface emissivity and reflectance (unitless)
freqEmis	HingeSurf=100	Frequencies for surface emissivity and reflectance in order of increasing frequency. Only the first numHingeSurf elements are valid. (cm-1)
emisIRStd	HingeSurf=100	Spectral IR surface emissivities in order of increasing frequency from 649 to 2666 cm-1 by a series of "hinge points" that differ between land and ocean. Only the first numHingeSurf elements are valid. (unitless)
emisIRStdErr	HingeSurf=100	Error estimate (unitless)
emisIRStd_QC	HingeSurf=100	Quality flag array (0,1,2)
SurfClass	1	Surface class used in physical retrieval, from microwave (MW) and/or infrared (IR). Identical to MWSurfClass when MW is used; 0 for coastline (Liquid water covers 50-99% of area); 1 for land (Liquid water covers < 50% of area); 2 for ocean (Liquid water covers > 99% of area); 3 for sea ice (Indicates high MW emissivity when MW information is used); 4 for sea ice (Indicates low MW emissivity. This value is only produced when MW information is used.); 5 for snow (Indicates higher-frequency MW scattering when MW information is used); 6 for glacier/snow (Indicates very low-frequency MW scattering. This value is only produced when MW information is used.); 7 for snow (Indicates lower-frequency MW scattering. This value is only produced when MW information is used.); -1 for unknown When MW data is not available (mainline AIRS-only system, only types 0, 1, 2, 3, and 5 are generated, based on the land fraction and the Water Equivalent Accumulated Snow Depth and Ice Fraction from the forecast

Support Product

Field Name	Dimension per FOV	Description
Effective_Solar_Reflectance	HingeSurf =100	Spectral IR effective surface reflectances (unitless) in order of increasing frequency from 649 to 2666 cm^{-1} by a series of "hinge points" that differ between land and ocean. Only the first numHingeSurf elements are valid. The reflectances are "effective" because they include the effect of attenuation of the incoming solar radiation by clouds.
Effective_Solar_Reflectance_QC	HingeSurf =100	Quality flag array (0,1,2)
fcast_surf_snow_amnt	1	Forecast water equivalent accumulated snow depth (kg/m^2) (not a retrieved quantity)
fcast_sea_ice_frac	1	Forecast sea ice fraction (unitless) (not a retrieved quantity)

NOTE: Effective Solar Reflectance is used internally to represent the amount of solar radiation reflected from the surface as compared to unobstructed solar radiation falling on the surface. By its nature it includes the bidirectional reflectance coefficient multiplied by an attenuation factor due to incoming clouds. As these factors cannot be separated, we see no physical utility to this product and it cannot be readily validated. It is included in the product only for completion.

4.1 Description

The AIRS standard surface product is the result of the combined IR/MW retrieval or of the IR-Only retrieval (AIRS-Only) when AMSU is not used. The AIRS-Only Level 2 Standard Product has shortname **AIRS2RET**; the AIRS+AMSU Level 2 Standard Product has shortname **AIRX2RET**; the AIRS+AMSU+HSB Level 2 Standard Product has shortname **AIRH2RET**. The record of the IR/MW retrieval runs from August 30th in 2002 until September 25th in 2016. There are no data after the failure of AMSU channels 1 and 2. The record of IR-only retrievals runs to the present. See the MW-Only product (Section 3) for surface products derived solely from the microwave radiance data, which is absent from **AIRS2RET**.

SurfClass is a surface classification derived from MW and/or IR radiance tests and used in the physical retrieval. It is present in the Level 2 Standard Product as well as the Level 2 Support Product. It is identical to **MWSurfClass** when MW radiances are used. In the case of the AIRS-Only retrieval, **landFrac, fcast_surf_snow_amnt,** and **fcast_sea_ice_frac** are available and are used to determine if the surface is land or ocean and frozen or not. The use of **fcast_surf_snow_amnt** and **fcast_sea_ice_frac** is new for Version 7 and has made significant improvements in sea ice margins.

The initial surface emissivity over non-frozen ocean (**landFrac**<0.01, **MWSurfClass**=2) follows the shape of the Masuda model as updated by Wu and Smith (1997) and recomputed at higher spectral resolution by van Delst and Wu[2]. Their adjustable parameter is set for a wind speed of 5 m/s.

[2] http://library.ssec.wisc.edu/research_Resources/publications/pdfs/ITSC11/vandelst01_ITSC11_2000.pdf

In V5 the initial surface emissivity over all other surface classes (e.g., land and ice), was set using a NOAA surface regression. In V6, the first guess emissivity was set using the UW-Madison global MODIS IR baseline-fit emissivity product (**UWIREMIS**[3]). This approach is continued in V7. The **UWIREMIS** is based on the MODIS **MYD11C3** v4.1 product and extends the original 6 MODIS IR emissivity bands to 10 'hinge-points' in the infrared domain (3.6-12 µm). The MODIS-derived starting emissivity is available in support product fields as **MODIS_emis**, **MODIS_emis_spots** (6 hinge points, AMSU and AIRS spot size respectively), and **MODIS_emis_10hinge** (10 hinge points, AMSU spot size). This makes **UWIREMIS** applicable to any given sensor's spectral resolution (e.g. AIRS, IASI). Using **UWIREMIS** greatly improved shortwave emissivity spectral shape compared to V5, where shortwave emissivity was regressed from the longwave emissivity shape. Once the Land Surface Temperature (LST) has been solved for, the longwave spectral emissivity is solved for in a separate step, assuming that values of Ts, T(p) an q(p) are already known. The logic for the emissivity guess based on **UWIREMIS** for different surface classes (Table 4.1) is shown in Table 4.2.

Table 4.1: Surface class type and associated logic

n	Surface Class	Logic
0	Coastline	Liquid water covers 50-99% of area
1	Land	Liquid water covers <50% of area
2	Ocean	Liquid water covers >99% of area
3	Sea ice	High microwave emissivity
4	Sea ice	Low microwave emissivity
5	Snow	Higher-frequency microwave scattering
6	Glacier/snow	Very low-frequency microwave scattering
7	Snow	Lower-frequency microwave scattering

Table 4.2: MODIS emissivity first guess logic based on surface type and topography

Surface Type	Logic	Emissivity Guess	Reasoning
Ocean	(n=2) and (topog=0) and no MODIS guess	Masuda water	Definitely Ocean
	(n=2) and MODIS provides guess	(MODIS + Masuda water)/2	MODIS provides guess indicating land or inland water possible
	(n=2) and topog>0 and no MODIS guess	Masuda water	Probably Ocean
Sea ice	(n=3) or (n=4)	MODIS ice (UCSB Library spectra from Mammoth Lakes)	Definitely sea ice
Non-frozen land	(n=0) or (n=1)	f*MODIS+(f-1)*Masuda f = land fraction	Mixed land and water based on land fraction
Frozen land	(n=5, 6, 7) and MODIS provides guess	(MODIS + MODIS ice)/2	Could be bare or frozen surface
	(n=5, 6, 7) and no MODIS guess	MODIS ice	Sea ice or glacier most likely

There has been considerable confusion over the years about the use of "hinge points" to define the emissivity and reflectance spectrum. Different retrievals may use different sets of hinge points. There is no physical meaning to the choice of hinge points. They are

[3] http://cimss.ssec.wisc.edu/iremis/

purely a method of describing a piecewise linear (in frequency) curve in spectral space. To compute a surface emissivity at a particular frequency, the researcher should interpolate in frequency between the emissivities provided at adjacent hinge points. Nothing philosophical should be read into the choice of hinge points or why they vary among profiles.

For modeling the upwelling radiance surfaces are assumed Lambertian, except for the short-wave component of the reflected solar component. In this case, the reflectance is modeled to take into account the reflected incoming solar component that may not be Lambertian.

4.2 Type of Product

The AIRS surface products are all level quantities, describing the state at **PSurfStd**.

NOTE: **PSurfStd** is not an AIRS product. It is interpolated from the Global Forecast System (GFS) forecasts and corrected using the local digital elevation model (DEM) topography of the retrieval field-of-view (FOV) and is used as an input to the AIRS processing.

4.3 Quality Indicators

The user is encouraged to read the QC and error estimation document:

V7_L2_Quality_Control_and_Error_Estimation.pdf

The surface quality **Qual_Surf** is set by testing the surface temperature error estimate, **TSurfStdErr** against a threshold.

Over Ocean:

- **Qual_Surf** = 0 if **TSurfStdErr** < 1.1 K (1.2 K in AIRS-only)
- **Qual_Surf** = 1
  if Lat > -40° and **TSurfStdErr** < 1.4 K
  if Lat < -60° and **TSurfStdErr** < 2.0 K
  if -60° ≤ Lat ≤ -40°
  and **TSurfStdErr** < 2.0 – (0.3)(60+Lat)
- **Qual_Surf** = 2 if **TSurfStdErr** fails test

Over Land and Frozen Cases:

- **Qual_Surf** = 1 if **PGood** = **PSurfStd** and **TSurfStdErr** < 7 K
- **Qual_Surf** = 2 otherwise

Qual_Surf is not reported separately, but is used to set **TSurfStd_QC** and the other surface QC flags.

The philosophy for quality control over ocean differs from that of all other cases. Over ocean the quality control attempts to identify quite good cases because we think that is what researchers require. If the yield is not appropriate for a particular application, users

are encouraged to use **TSurfStdErr** as a more precise filter. Over land, other data sources are not as readily available and we have chosen to mark few cases as "best" pending further refinement and validation of the emissivity products, but mark a large selection of cases as "good" to ensure adequate coverage for production of monthly means for climate studies.

4.4 Validation

The AIRS surface products have been validated for V6, with results described in

V6_L2_Performance_and_Test_Report.pdf

Further validation for V7 surface products has not been performed at this point.

4.5 Caveats

This section will be updated over time as V7 data products are analyzed and validated.

emisIRstd represents the emissivity from 649 cm^{-1} to 2666 cm^{-1} by a series of "hinge points" which may differ between land and ocean because of the internal processing paths and assumptions. The user must read **freqEmis** to know the values of the **numHingeSurf** hinge points for each profile, and then interpolate linearly in wavelength to find the emissivity at a particular frequency. In V7, all profiles define the same 39 hinge points. However, this is not guaranteed for future versions if we develop better land spectra, so the user is well-advised to continue to read **numHingeSurf** and **freqEmis** for each profile to be certain of consistency.

4.6 Suggestions for Researchers

This section will be updated over time as V7 data products are analyzed and validated.

The surface emissivity retrieval is set to have minimum limits of 0.65 (shortwave band 2564 cm^{-1}) and 0.92 (longwave band 909 cm^{-1}). Emissivity retrievals with values that fall below these limits are generally considered unphysical at AIRS spatial resolution (50km). However, on occasion emissivity values below these limits will be reported for Q0 (best) and Q1 (good) quality flags when there is a valid first guess emissivity (from MODIS **MYD11C3** climatology) that is unusually low, most likely due to cloud contamination. **TSurfStd** values should be used with due caution for these causes.

4.7 Recommended Papers

This section will be updated over time as research with V7 data products are published.

Chen, Francis, Miller (2002), Surface temperature of the Arctic: Comparison of TOVS satellite retrievals with surface observations, J. Climate, 15, 3698–3708. DOI: 10.1175/1520-0442(2002)015<3698:STOTAC>2.0.CH4;2

Ferguson, Craig R., Eric F. Wood, 2010: An Evaluation of Satellite Remote Sensing Data Products for Land Surface Hydrology: Atmospheric Infrared Sounder*. J. Hydrometeor, 11, 1234–1262. doi: 10.1175/2010JHM1217.

Hulley, G. C., S. J. Hook, E. Manning, S-Y Lee, and E. Fetzer, 2009. Validation of the Atmospheric Infrared Sounder (AIRS) Version 5 Land Surface Emissivity Product over the Namib and Kalahari Deserts, J. Geophys. Res, 114, D19104

Hulley, G. C., and S. J. Hook (2012), A radiance-based method for estimating uncertainties in the Atmospheric Infrared Sounder (AIRS) land surface temperature product, J. Geophys. Res., 117, D20117, doi:10.1029/2012JD018102.

Heilliette,S., Chedin,A., Scott,N. A., Armante,R. (2004), Parametrization of the effect of surface reflection on spectral infrared radiance measurements. Application to IASI, Journal of Quantitative Spectroscopy & Radiative Transfer, 86, 201-214. doi:10.1016/j.jqsrt.2003.08.002

Knuteson et al (2003), Aircraft measurements for validation of AIRS land surface temperature and emissivity products at the Southern Great Plains validation site, Fourier Transform Spectroscopy (Trends in Optics and Photonics Series Vol.84). 138.

Maddy, E. S. and C. D. Barnet (2008), Vertical Resolution Estimates in Version 5 of AIRS Operational Retrievals, IEEE Trans. Geosci. Remote Sens., 46(8), 2375-2384.

Nalli,N. R. and Smith,W. L. (2003), Retrieval of ocean and lake surface temperatures from hyperspectral radiance observations, Journal of Atmospheric and Oceanic Technology, 20, 810-1825. doi: 10.1175/1520-0426(2003)020<1810:ROOALS>2.0.CH4;2

Ruzmaikin A., H.H Aumann, J.N. Lee, and J. Susskind (2017), Diurnal Cycle Variability of Surface Temperature Inferred from AIRS data, J. Geophys. Res., 122, doi:10.1002/2016JD026265.

Seemann, Suzanne W., Eva E. Borbas, Robert O. Knuteson, Gordon R. Stephenson, Hung-Lung Huang, 2008: Development of a Global Infrared Land Surface Emissivity Database for Application to Clear Sky Sounding Retrievals from Multispectral Satellite Radiance Measurements. J. Appl. Meteor. Climatol., 47, 108–123, doi: http://dx.doi.org/10.1175/2007JAMC1590.1

Susskind, J., C. D. Barnet, and J. Blaisdell (2003), Retrieval of atmospheric and surface parameters from AIRS/AMSU/HSB data in the presence of clouds, IEEE Trans. Geosci. Remote Sens., 41(2), 390–409.

Susskind, J. and J. Blaisdell (2008), Improved surface parameter retrievals using AIRS/AMSU data, Proc. SPIE Int. Soc. Opt. Eng., 6966, 696610, doi:10.1117/12.774759.

Susskind, J., Schmidt, G. A., Lee, J. N. & Iredell, L. (2019), Recent global warming as confirmed by AIRS, Environ. Res. Lett., 14 (4). https://doi.org/10.1088%2F1748-9326%2Faafd4e

Wu and Smith (1997), Emissivity of rough sea surface for 8-13 μm: modeling and verification," Appl. Opt. 36, 2609-2619

Yao, Zhigang, Jun Li, Jinlong Li, Hong Zhang, 2011: Surface Emissivity Impact on Temperature and Moisture Soundings from Hyperspectral Infrared Radiance Measurements. J. Appl. Meteor. Climatol., 50, 1225–1235. doi: 10.1175/2010JAMC2587.

Zhou, L., M. Goldberg, C. Barnet, Z. Cheng, F. Sun, W. Wolf, T. King, X. Liu, H. Sun, and M. Divakarla (2008), Regression of surface spectral emissivity from hyperspectural instruments, IEEE Trans. Geosci. Remote Sens., 46(2), 328–333, doi:10.1109/TGRS.2007.912712

4.8 Recommended Supplemental User Documentation

Overview_of_the_AIRS_Mission.pdf
V7_L2_Performance_Test_and_Validation_Report.pdf
V7_L2_Quality_Control_and_Error_Estimation.pdf
V7_Retrieval_Channel_Sets.pdf
V7_Retrieval_Flow.pdf

5 Air Temperature Retrievals

Standard Product

Field Name	Dimension per FOV	Description
TAirStd	StdPressureLev=28	Retrieved Atmospheric Temperature Profile at StdPressLev (K)
TAirStdErr	StdPressureLev=28	Error estimate for TAirStd (K)
TAirStd_QC	StdPressureLev=28	Quality flag array (0,1,2)
TSurfAir	1	Retrieved Surface Air Temperature (K)
TSurfAirErr	1	Error Estimate for TSurfAir (K)
TSurfAir_QC	1	Quality flag (0,1,2)
Temp_dof	1	Degrees of freedom, a measure of the amount of information in temperature profile retrieval (dimensionless)

Support Product (full list in Appendix A2)

Field Name	Dimension per FOV	Description
TAirSup	XtraPressureLev=100	Atmospheric Temperature at XtraPressLev in Kelvins. Value at 1-based index of nSurfSup may be an unphysical extrapolated value for a pressure level below the surface. Use TSurfAir for the surface air temperature
TAirSup_QC	XtraPressureLev=100	Quality flag array (0,1,2)
TAirSupErr	XtraPressureLev=100	Error estimate for TAIRSup (K)
num_Temp_Func	1	Number of valid entries in each dimension of Temp_ave_kern_30func
Temp_ave_kern_30func	TempFunc*TempFunc =30x30	Averaging kernel for temperature retrieval*
Temp_verticality_30func	TempFunc = 30	Sum of the rows of Temp_Ave_kern_30func*
Temp_eff_press_30func	TempFunc = 30	Temperature effective pressure for the center of each trapezoid*
Temp_trapezoid_layers_30func	TempFunc = 30	Layers on which the Temperature variables are defined.*

*NOTE: For V7, 30func has been added to the variable name so that user's V6 analysis software will not inadvertently use the new, differently dimensioned output.

5.1 Description

The AIRS-only standard temperature product is the result of the IR-only retrieval, while the AIRS/AMSU product is the result of the combined IR/MW retrieval. The record of the IR/MW retrieval runs from August 30th in 2002 until September 25th in 2016. There are no data after the failure of AMSU channels 1 and 2. The record of IR-only retrievals runs to the present. See the MW-Only product (Section 3) for temperature products derived solely from the microwave data.

The atmospheric temperature profile (**TAirStd**) is reported on the standard pressure levels (**pressStd**) that are above the altitude of the highest topography in the retrieval field-of-view (FOV). The surface air temperature (**TSurfAir**) and **TAirStd** are obtained from the 100-level support product air temperature profile (**TAirSup**) using interpolation that is linear in the logarithm of the support pressure (**pressSup**). Note that **TSurfAir**

will equal **TAirStd**(**nSurfStd**) only if **pressStd**(**nSurfStd**) is equal to **PSurfStd**. This will seldom be the case.

The 28 Level 2 Standard pressure levels (**pressStd**) are arranged in order of decreasing pressure. The highest altitude pressure level is pressStd(28) = 0.1 hPa. The index of the lowest altitude pressure level for which a reported **TAirStd** is valid is **nSurfStd**, which may be 1, 2, …, 15 depending upon topography. The surface pressure, **PSurfStd**, is interpolated from the NCEP GFS forecast and the local DEM topography.

The 100 Level 2 Support pressure levels (**pressSup**) are arranged in order of increasing pressure. The highest altitude pressure level is pressSup(1) = 0.0161 hPa. Use **TSurfAir** for the surface air temperature at the index of the surface pressure level **nSurfSup**.

Several changes for the temperature retrieval have been introduced in Version 7, as compared to the previous Version 6. In the retrieval, trapezoidal layers are used which have associated averaging kernels, verticality and degrees of freedom (see below and **V7_L2_Levels_Layers_Trapezoids.pdf**). In Version 7, the number of temperature retrieval trapezoids was increased in the boundary layer and they were made more uniform vertically, which led to a better representation of the boundary layer and of the tropopause. Longwave channels with cloud clearing corrections larger than 5K for a given profile are now excluded from the temperature retrieval for that profile. In Version 6, the surface temperature was modified in the temperature retrieval step. This feature was removed for Version 7. Finally, seven additional 4μm channels were added to the temperature retrieval to increase information at the top of the atmosphere, which also affects the ozone retrieval.

Temp_verticality_30func is a 30-point vector computed by summing the rows of the 30x30 temperature averaging kernel, **Temp_avg_kern_30func**, both of which are stored in the AIRS Level 2 Support Product. The associated 30-point pressure array is provided in **Temp_eff_press_30func** in the AIRS Level 2 Support Product. The peak value of **Temp_verticality_30func** indicates the vertical location of the maximum sensitivity of the Temperature product and the width of this peaked function qualitatively describes the vertical resolution of the retrieval. The magnitudes of **Temp_verticality_30func** are a rough measure of the fraction of the retrieval determined from the data as opposed to the first guess. A value near unity indicates the retrieval is highly determined by the radiance measurements and thus has high information content. A smaller value indicates the retrieval contains a large fraction of the first guess. **Temp_dof** is the number of degrees of freedom (a measure of the amount of information in the retrieval), and is the trace of **Temp_ave_kern_30func**.

NOTE: **num_Temp_Func** provides the number of valid entries in each dimension of **Temp_ave_kern_30func**. Topography limits the number of valid temperature averaging kernel trapezoids.

The effective pressures of the temperature trapezoids may be calculated from the minimum pressure level boundaries and maximum pressure level boundaries tabulated in

V7_L2_Levels_Layers_Trapezoids.pdf (in the subsection for the first and last trapezoid hinge points). But there are two modifications to the pressures in that table. The first is that the minimum pressure level for the top of the atmosphere is 0.005 hPa, because the RTA assumes that as the TOA minimum pressure. The second is that the maximum pressure level can be no greater than **PSurfStd**. This will reduce the number of trapezoids over land due to topography. The algorithm to calculate the **Temp_eff_press_30func** array is:

Temp_eff_press_30func(1) = (press(2) – 0.005)/log(press(2)/0.005)
Temp_eff_press_30func(i) = (press(i+1)-press(i))/log(press(i+1)/press(i))
For first occurrence of press(i+1) > PSurfStd,
Temp_eff_press_30func(i_last)
= (PSurfStd-press(i_last))/log(PSurfStd/press(i_last))
And all trapezoids below this one are null and void.

The result of this calculation is shown in Table 5.1.

Table 5.1: Example of 30 effective pressures for temperature trapezoidal averaging kernels

Trapezoid Number	Temp_eff_press (hPa)
1	0.05768
2	0.51105
3	1.69410
4	4.08545
5	8.17456
6	14.46466
7	23.45983
8	35.65499
9	51.52827
10	71.53490
11	96.10223
12	125.62588
13	160.46672
14	195.58664
15	229.26326
16	266.36298
17	306.98032
18	351.19669
19	399.08032
20	*450.68631
21	*506.05643
22	*565.21936
23	*628.19073
24	*694.97308
25	*765.55670
26	*827.32367
27	*878.56976
28	*931.47028
29	*990.39478
30	*variable

*Over land, may be variable or null and void
(pressure at summit of Mt Everest is approximately 300 hPa)

5.1 Type of Product

All standard temperature products are level quantities, which means that the values are reported at fixed pressure levels. This differs from layer quantities, which are reported on the fixed pressure levels but represent the layer bounded by the level on which they are reported and the next higher level (in altitude). For more detail, see the document **V7_L2_Levels_Layers_Trapezoids.pdf** for a full discussion of level and layer quantities.

5.2 Quality Indicators

The user is encouraged to read the QC and error estimation document:

V7_L2_Quality_Control_and_Error_Estimation.pdf

The temperature profile (**TAirStd**) has associated error and QC profiles (**TAirStdErr** and **TAirStd_QC**), providing estimates of error and the QC at each pressure level. QC=0 indicates the highest quality retrieval; QC=1 indicates good quality retrievals; and QC=2 indicates the use of such data is not recommended.

Several modifications have been made to the temperature and water vapor quality control in V7:

- The error estimate used as the decision point for atmospheric temperature and water profile QCs is moved from 6 layers above the surface in V6 to 2 layers above the surface over frozen and land surfaces in V7. This effectively uses the entire profile error estimate information and allows the algorithm to make finer distinctions of quality over land and frozen areas near the surface.
- The numerical threshold points for marking profile levels with QC=2 is tightened over land from the mid to lower atmosphere, and for frozen cases in the middle atmosphere, while the numerical threshold for frozen cases near the surface is slightly loosened which increases the yield over frozen surfaces.

The V5 legacy QC parameters **PBest** and **PGood** are still provided in V7 and facilitate the filtering of data. The V4 legacy quality factors that were carried forward in V5 have been removed from the V6 and V7 products as they are no longer consistent with the current complexity of quality flagging.

PBest, nBestStd and nBestSup:

PBest indicates **TAirStd** is “best” from the top of the atmosphere (TOA) downward to the level of **PBest**, i.e. **TAIRStd_QC** = 0 for the profile for levels at altitudes above and including **PBest**. “Best” data products individually meet our accuracy requirements and may be used for comparison with in situ measurements, data assimilation and statistical climate studies.

nBestStd is the index of the lowest altitude level of the **pressStd** and **TAirStd** profiles for which the quality is “best”. Levels whose indices are in the range i = **nBestStd**, **nBestStd** + 1, …, 28 are therefore marked quality = 0. It is set to a value

of 29 to indicate that none are "best". Take note that **nBestStd** is 1-based (as are arrays in FORTRAN and MATLAB) rather than 0-based (as are arrays in C, IDL and Python). **nBestSup** is the equivalent index for the Support product.

PGood, nGoodStd and nGoodSup:

PGood indicates **TAirStd** is "good" from the level below **PBest** to the level of **PGood**, i.e. **TAIRStd_QC** ≤ 1 for the portion of the **TAirStd** profile above and including the level of **PGood**. If **PBest** is less than **PGood**, then the levels below that of **PBest** and above and including that of **PGood** are flagged as quality = 1 ("good"). If **PBest** = **PGood**, then all levels above and including the common pressure level are flagged quality = 0. "Good" data products may be used for statistical climate studies, as they meet the accuracy requirements only when temporally and/or spatially averaged.

nGoodStd is the index of the lowest altitude level of the **pressStd** and **TAirStd** profiles for which the quality is "good". Levels whose indices are in the range i = **nGoodStd**., **nGoodStd** + 1, …, **nBestStd**-1 are therefore marked quality = 1. It is set to a value of 29 to indicate that none are "good". Take note that **nGoodStd** is 1-based (as are arrays in FORTRAN and MATLAB) rather than 0-based (as are arrays in C, IDL and Python). **nGoodSup** is the equivalent index for the Support product.

Note that it is possible that **PBest** = **PGood** and **nBestStd** = **nGoodStd**. The **TAirStd** profile below **PGood** is rejected and its quality set = 2 ("do not use").

If the entire temperature profile is rejected, **PBest** = **PGood** = 0 and **nBestStd** = **nGoodStd** = 29. There may, however, still be values in the **TAirStd** profile if some stage of the retrieval was successful. The flagged profile may be an excessively noisy full retrieval or the output from an intermediate stage of the retrieval process.

5.3 Validation

For detailed analysis on retrieval yield and bias characteristics of the AIRS V7 temperature retrievals, readers may refer to Section 5.1 for results on vertical profile and Section 5.3 for results on near surface air temperature in:

V7_L2_Performance_Test_and_Validation_Report.pdf

Figure 1 shows example results for both temperature and water vapor profiles, with AIRS V7 compared to IGRA radiosondes in terms of bias and root-mean-square error.

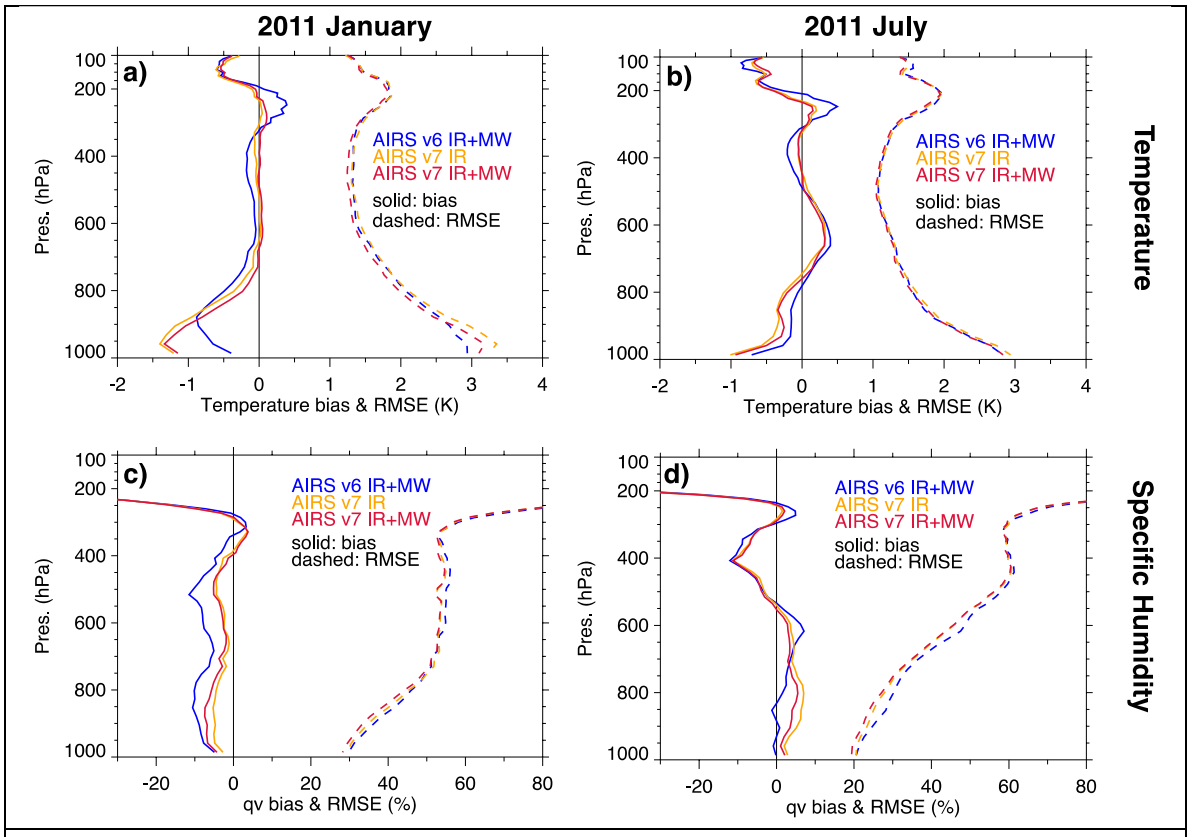

Figure 1: Validation of temperature and water vapor profiles.

Biases (solid lines) and RMSE (dashed lines) of AIRS level 2 temperature (a, b) and specific humidity (c, d) vertical profiles compared to the collocated IGRA radiosondes for 2011 January (left column) and 2011 July (right column).

5.4 Caveats

This section will be updated over time as V7 data products are analyzed and validated.

All parameters that are level numbers, such as **nSurfStd**, **nBestStd**, **nGoodStd**, **nBestSup**, and **nGoodSup**, are 1-based. Those who work in FORTRAN and MATLAB will be unaffected. However, those who work in C, IDL and Python must take care when using **nSurfStd** and other parameters that are level numbers. The following two expressions yield the same value:

FORTRAN and MATLAB: **pressStd**(**nBestStd**)
C, IDL and Python: **pressStd**[**nBestStd**-1]

The quality indicator is based on the empirical error estimate **TAirStdErr.** The output error estimate may not be consistent with the atmospheric temperature error estimate used by the physical retrieval algorithm. The latter is not written to the output.
V7 uses an improved neural network first guess to provide the first guess in difficult cases. Compared with V6, the number of Quality = 0 cases has increased and the number

of Quality = 2 cases have been reduced in V7 except over certainty difficult to retrieve cases such as overcast conditions over snow/ice covered surfaces.

In response to the desire of researchers to use retrievals near to tropical storms, we have revised the algorithm to report the stratospheric portion of the temperature retrieval above 30 hPa as Quality = 0 in all cases where the retrieval successfully completed. In these difficult cases, **PBest** is set to a relatively low value. At pressures greater than **PBest**, Quality = 1. This continues toward the surface until the pressure **PGood**. Beyond that pressure Quality = 2. In these cases, retrieval values are provided where possible. Less than 1 % of cases are now marked Quality = 2 for the entire profile, and these rare cases indicate difficulties in the IR/MW retrieval that makes them very suspect.

TSurfAir sometimes differs by more than 2.5 K from the interval defined by the values of **TAirStd** for the levels immediately above and below the surface.

The temperature profile is estimated at fixed pressure levels, and **TSurfAir** is derived by extrapolating from the nearest of those pressure levels to the actual surface pressure. However, it is important to note that the vertical resolution of AIRS is on the order of 1-2 km in the lower atmosphere, and it is therefore not possible to distinguish between, say, 2 m and 10 m above the surface. Instead, **TSurfAir** should be viewed as a mean value for a range of heights "near the surface".

5.5 Suggestions for Researchers

This section will be updated over time as V7 data products are analyzed and validated.

We strongly recommend using the "_QC" or **PBest** and **PGood** quality indicators. The values that are set for subsetting data should be carefully chosen, and depend upon how the data are to be used. At the very least, **PGood** should exceed the maximum pressure of interest (QC=0 or 1). If the thrust of the research is comparison with in situ measurements (e.g., radiosondes), then **PBest** should exceed the maximum pressure of interest (QC=0). The portions of profiles nearer to the surface than PGood should be discarded and those at pressures greater than **PSurfStd** are invalid. The level-by-level quality factors are consistent with the definitions of **PGood** and **PBest**.

5.6 Recommended Papers

This section will be updated over time as research with V7 data products are published.

Behrangi, A., E. J. Fetzer, and S. L. Granger (2016), Early detection of drought onset using near surface temperature and humidity observed from space, Int.J.Remote Sens., 37(16), 3911-3923. https://dx.doi.org/10.1080/01431161.2016.1204478

Bisht, J. S. H., P. K. Thapliyal, M. V. Shukla, and R. Kumar. "A comparative study of different AIRS products for the detection of near-surface temperature inversion: a case study over New Delhi." Remote Sensing Letters 4, no. 1 (2013): 94-103.

Boisvert, L. N., J. N. Lee, J. T. M. Lenaerts, B. Noël, M. R. van den Broeke, and A. W. Nolin (2016), Using remotely sensed data from AIRS to estimate the vapor flux on the

Greenland ice sheet: Comparisons with observations and a regional climate model, J. Geophys. Res. Atmos., 122, doi:10.1002/2016JD025674.

Divakarla, M., C. D. Barnet, M. D. Goldberg, L. M. McMillin, E. Maddy, W. Wolf and L. Zhow (2006), Validation of AIRS temperature and water vapor retrievals with matched radiosonde measurements and forecasts, J. Geophys. Res., 111, D09S15, doi:10.1029/2005JD006116

Devasthale, A., J. Sedlar, T. Koenigk, and E. J. Fetzer. "The thermodynamic state of the Arctic atmosphere observed by AIRS: comparisons during the record minimum sea ice extents of 2007 and 2012." Atmospheric Chemistry and Physics 13, no. 15 (2013): 7441-7450.

Dwivedi, S., Narayanan, M. S., Venkat Ratnam, M., and Narayana Rao, D.: Characteristics of monsoon inversions over the Arabian Sea observed by satellite sounder and reanalysis data sets, Atmos. Chem. Phys., 16, 4497-4509, doi:10.5194/acp-16-4497-2016, 2016

Fetzer E. J., J. Teixeira, E. T. Olsen, E. F. Fishbein (2004), Satellite remote sounding of atmospheric boundary layer temperature inversions over the subtropical eastern Pacific, Geophys. Res. Lett., 31, L17102, doi:10.1029/2004GL020174.

Gao, W., Zhao, F. Gai, C. (2006), Validation of AIRS retrieval temperature and moisture products and their application in numerical models, Acta Metorol. Sinica, Acta Meteorologica Sinica, 64, 271-280.

Gao, W.H., Zhao, F.S., Xu, Y.F., Feng, X., "Validation of the Surface Air Temperature Products Retrieved From the Atmospheric Infrared Sounder Over China," Geoscience and Remote Sensing, IEEE Transactions on Geoscience and Remote Sensing, vol.46, no.6, pp.1783-1789, June 2008

Guan, B., D. E. Waliser, F. M. Ralph, E. J. Fetzer, and P. J. Neiman (2016), Hydrometeorological characteristics of rain-on-snow events associated with atmospheric rivers, Geophys. Res. Lett., 43, 2964–2973, doi:10.1002/2016GL067978.

Gupta, A., S. K. Dhaka, V. Panwar, R. Bhatnagar, V. Kumar, Savita M. Datta, and S. K. Dash. "AIRS observations of seasonal variability in meridional temperature gradient over Indian region at 100 hPa." Journal of Earth System Science 122, no. 1 (2013): 201-213.

Hearty, T. J., A. Savtchenko, B. Tian, E. Fetzer, Y. L. Yung, M. Theobald, B. Vollmer, E. Fishbein, and Y.-I. Won (2014), Estimating sampling biases and measurement uncertainties of AIRS/AMSU-A temperature and water vapor observations using MERRA reanalysis, J. Geophys. Res. Atmos., 119, 2725–2741, doi:10.1002/2013JD021205.

Kalmus, P., S. Wong, and J. Teixeira (2015), The Pacific Subtropical Cloud Transition: A MAGIC Assessment of AIRS and ECMWF Thermodynamic Structure, IEEE Geoscience and Remote Sensing Letters, Article in Press, doi: http://dx.doi.org/10.1109/LGRS.2015.2413771.

Milstein, A. B., and W. J. Blackwell (2016), Neural network temperature and moisture retrieval algorithm validation for AIRS/AMSU and CrIS/ATMS, J. Geophys. Res. Atmos., 121, 1414–1430, doi:10.1002/2015JD024008.

Naud, C. M., J. F. Booth, and A. D. Del Genio (2016), The Relationship between Boundary Layer Stability and Cloud Cover in the Post-Cold-Frontal Region, Journal of Climate, 29(22), 8129-8149. http://dx.doi.org/10.1175/jcli-d-15-0700.1

Ricaud, P., F. Carminati, Y. Courcoux, A. Pellegrini, J.-L. Attié, L. El Amraoui, R. Abida, C. Genthon, T. August and J. Warner (2014). Statistical analyses and correlation between tropospheric temperature and humidity at Dome C, Antarctica. Antarctic Science, 26, pp 290-308. doi:10.1017/S0954102013000564.

Susskind, J., J. Blaisdell, L. Iredell, and F. Keita (2011), "Improved Temperature Sounding and Quality Control Methodology Using AIRS/AMSU Data: The AIRS Science Team Version-5 Retrieval Algorithm", IEEE Transactions on Geoscience and Remote Sensing, 49, 3, doi:10.1109/TGRS.2010.2070508.

Susskind J., C. Barnet, J. Blaisdell, L. Iredell, F. Keita, L. Kouvaris, G. Molnar, M. Chahine (2006), Accuracy of geophysical parameters derived from Atmospheric Infrared Sounder/Advanced Microwave Sounding Unit as a function of fractional cloud cover, J. Geophys. Res., 111, D09S17, doi:10.1029/2005JD006272.

Tobin D. C., H. E. Revercomb, R. O. Knuteson, B. M. Lesht, L. L. Strow, S. E. Hannon, W. F. Feltz, L. A. Moy, E. J. Fetzer, T. S. Cress (2006), Atmospheric Radiation Measurement site atmospheric state best estimates for Atmospheric Infrared Sounder temperature and water vapor retrieval validation, J. Geophys. Res., 111, D09S14, doi:10.1029/2005JD006103.

Wong, Sun, Eric J. Fetzer, Mathias Schreier, Gerald Manipon, Evan F. Fishbein, Brian H. Kahn, Qing Yue, and Fredrick W. Irion. "Cloud-induced uncertainties in AIRS and ECMWF temperature and specific humidity." Journal of Geophysical Research: Atmospheres (2015).

Wu,X. B., Li,J., Zhang,W. J., Wang,F. (2005), Atmospheric profile retrieval with AIRS data and validation at the ARM CART site.

Yue, Q., E.J. Fetzer, B.H. Kahn, S. Wong, G. Manipon, A. Guillaume, and B. Wilson, 2013: Cloud-State-Dependent Sampling in AIRS Observations Based on CloudSat Cloud Classification. *J. Climate*, **26**, 8357–8377, https://doi.org/10.1175/JCLI-D-13-00065.1.

Zhang, J., Z. Li, J. Li, and J. Li (2014), Ensemble retrieval of atmospheric temperature profiles from AIRS, Adv. Atmos. Sci., 31(3), 559-569, http://dx.doi.org/10.1007/s00376-013-3094-z.

5.7 Recommended Supplemental User Documentation

Overview_of_the_AIRS_Mission.pdf
V7_L2_Performance_Test_and_Validation_Report.pdf
V7_L2_Quality_Control_and_Error_Estimation.pdf
V7_L2_Standard_Pressure_Levels.pdf
V7_L2_Support_Pressure_Levels.pdf
V7_L2_Levels_Layers_Trapezoids.pdf
V7_Retrieval_Channel_Sets.pdf
V7_Retrieval_Flow.pdf

6 Water Vapor Saturation Quantities Derived from Temperature

Standard Product

Field Name	Dimension per FOV	Description
H2OMMRSat	H2OPressureLay=14	Layer Water vapor saturation mass mixing ratio (gm/kg dry air) over equilibrium phase (set to -9999 when saturation pressure exceeds 1% of ambient pressure.)
H2OMMRSat_QC	H2OPressureLay=14	Quality flag array (0,1,2)
H2OMMRSatLevStd	H2OPressureLev=15	Level Water vapor saturation mass mixing ratio (gm/kg dry air) over equilibrium phase (set to -9999 when saturation pressure exceeds 1% of ambient pressure.)
H2OMMRSatLevStd_QC	H2OPressureLev=15	Quality flag array (0,1,2)
H2OMMRSatSurf	1	Water vapor saturation Mass Mixing Ratio at the surface (gm/kg dry air) over equilibrium phase
H2OMMRSatSurf_QC	1	Quality flag (0,1,2)
H2OMMRSat_liquid	H2OPressureLay=14	Layer Water vapor saturation mass mixing ratio (gm/kg dry air) over liquid phase (set to -9999 when saturation pressure exceeds 1% of ambient pressure.)
H2OMMRSat_liquid_QC	H2OPressureLay=14	Quality flag array (0,1,2)
H2OMMRSatLevStd_liquid	H2OPressureLev=15	Level Water vapor saturation mass mixing ratio (gm/kg dry air) over liquid phase (set to -9999 when saturation pressure exceeds 1% of ambient pressure.)
H2OMMRSatLevStd_liquid_QC	H2OPressureLev=15	Quality flag array (0,1,2)
H2OMMRSatSurf_liquid	1	Water Vapor saturation Mass Mixing Ratio at the surface (gm/kg dry air) over liquid phase
H2OMMRSatSurf_liquid_QC	1	Quality flag (0,1,2)

Support Product (full list in Appendix A2)

Field Name	Dimension per FOV	Description
H2OMMRSatLevSup	XtraPressureLev=100	Level Water vapor saturation mass mixing ratio (gm/kg dry air) over equilibrium phase (set to -9999 when saturation pressure exceeds 1% of ambient pressure.)
H2OMMRSatLevSup_QC	XtraPressureLev=100	Quality flag array (0,1,2)
H2OMMRSatLevSup_liquid	XtraPressureLev=100	Level Water vapor saturation mass mixing ratio (gm/kg dry air) over liquid phase (set to -9999 when saturation pressure exceeds 1% of ambient pressure.)
H2OMMRSatLevSup_liquid_QC	XtraPressureLev=100	Quality flag array (0,1,2)

6.1 Description

H2OMMRSatLevStd_liquid and **H2OMMRSatLevStd** are **level** quantities, which represent the integrated mass of water vapor in saturated equilibrium divided by the mass of dry air at the **pressH2O** pressure levels upon which they are reported. Users found the layer quantities in V5 and earlier releases confusing, so these level quantities were introduced in V6 and retained in V7. The saturation equilibrium water vapor mass mixing ratio at the surface (**PSurfStd)** is provided by **H2OMMRSatSurf**.

Generally, the saturation mass mixing ratios are calculated as

$$X_{sat\ H2O} = \frac{M_{H_2O}}{M_{dry\ air}} \frac{P_{sat\ H2O}}{P - P_{sat\ H2O}}$$

where M is mass, P is ambient pressure and $P_{sat\ H2O}$ the saturation pressure. For cases in the stratosphere when saturation pressure exceeds the ambient pressure, a maximum saturation pressure is imposed in the code. **H2OMMRSatLevStd_liquid** assumes equilibrium with liquid water. **H2OMMRSatLevStd** is in equilibrium with liquid so long as the **TAirSup** (100 level profile) exceeds 273.15 K. If **TAirSup** drops below that threshold, the saturation calculation shifts to that over water ice. Near the surface the two saturation profiles are identical, but they will diverge in the case that the temperature profile crosses the threshold. In the saturation pressure calculation, the constituent relationship employed is that of Murphy and Koop (2005).

Level quantities are calculated from layer quantities by the procedure described in

V7_L2_Levels_Layers_Trapezoids.pdf

The derivation of level quantities from layer quantities is essentially done by interpolation with smoothing kernels. This mathematical transformation leads to occasional strange results for water vapor profiles with inversions, typically near the surface.

For backward compatibility, we retain the **layer** profiles, **H2OMMRSat_liquid** and **H2OMMRSat**. Both provide profiles of the integrated mass of water vapor in saturated equilibrium between **pressH2O** levels divided by the integrated mass of dry air in layers. **H2OMMRSat_liquid** assumes equilibrium with liquid water. **H2OMMRSat** is in equilibrium with liquid so long as the **TAirSup** (100 level profile) exceeds 273.15 K. If **TAirSup** drops below that threshold, the saturation calculation shifts to that over water ice. Thus, within a layer in which the temperature crosses 273.15 K, the calculation will shift between saturation over liquid to that over ice to derive its integrated mass of water vapor. Near the surface the two saturation profiles are identical, but they will diverge in the case that the temperature profile crosses the threshold. As for the level quantities, the constituent relationship employed is that of Murphy and Koop (2005).

6.2 Type of Product

The equilibrium saturation specific moisture is provided both as **layer** profiles and as **level** profiles. Layer quantities are reported on the fixed pressure levels but represent the layer bounded by the level on which they are reported and the next higher level (in altitude). Level quantities are values reported at fixed pressure levels and represent the product at each level. For more detail, see

V7_L2_Levels_Layers_Trapezoids.pdf

for a full discussion of level and layer quantities.

6.3 Quality Indicators

The user is encouraged to read the Quality Control (QC) and error estimation document:

V7_L2_Quality_Control_and_Error_Estimation.pdf

All the profiles for saturation quantities and the temperature profiles they are derived from have associated error and QC profiles, providing estimates of error and the QC at each pressure level. The users will find that the parameters **PBest** and **PGood** will facilitate their filtering of data.

6.4 Caveats

This section will be updated over time as V7 data products are analyzed and validated.

To ensure the best continuity throughout the entire mission, the physical retrieval uses no AMSU channels in the mainline "AIRS-Only" flavor. AMSU channels 3 and 8-13 are used in the neural network startup. To provide continuity from 2002 to 2016, the products from the V7 AIRS/AMSU retrieval flavor do not use AMSU channels 4 and 5, even in the earlier stage of the mission when those channels were good.

To maximize the quality of the retrieval (of moisture product in particular), the V7 retrieval algorithm for products provided by the AMSU+HSB+AIRS processing does use AMSU channels 4 and 5.

H2OMMRSatLevStd and **H2OMMRSatLevStd_liquid** both provide level profiles of the integrated mass of water vapor in saturated equilibrium at the **pressH2O** levels on which they are reported. **H2OMMRSatSurf** provides a level quantity at the surface pressure, **PSurfStd**.

H2OMMRSat_liquid and **H2OMMRSat** both provide layer profiles of the integrated mass of water vapor in saturated equilibrium between **pressH2O** levels divided by the integrated mass of dry air. **H2OMMRSat_liquid** assumes equilibrium with liquid water. **H2OMMRSat** is in equilibrium with the physically correct equilibrium phase: liquid or ice. The physically correct equilibrium phase is ice from the point at which **TAirSup** (100 level profile) falls below 273.15 K; otherwise the equilibrium phase is liquid water.

6.5 Recommended Papers

Buck, A. L. (1981), New equations for computing vapor pressure and enhancement factor, J. Appl. Meteorol., 20, 1527-1532.

Murphy, D. M. and T. Koop (2005), Review of the vapour pressures of ice and supercooled water for atmospheric applications, Quart. J. Royal Met. Soc, 608 Part B, 1539-1565.

6.6 Recommended Supplemental User Documentation

Overview_of_the_AIRS_Mission.pdf
V7_L2_Quality_Control_and_Error_Estimation.pdf
V7_L2_Levels_Layers_Trapezoids.pdf

7 Tropopause Derived from Temperature

Field Name	Dimension per FOV	Description
PTropopause	1	Tropopause height (hPa)
PTropopause_QC	1	Quality flag (0,1,2)
T_Tropopause	1	Tropopause temperature (K)
T_Tropopause_QC	1	Quality flag (0,1,2)

7.1 Description

The tropopause height, **PTropopause** is determined by testing the lapse rate of the higher vertical resolution air temperature profile (**TAirSup**) against the WMO (1992) criteria:

1. The first tropopause (i.e., the conventional tropopause) is defined as the lowest level at which
    a. the lapse rate decreases to 2 K/km or less, and
    b. the average lapse rate from this level to any level within the next higher 2 km does not exceed 2 K/km.
2. If above the first tropopause the average lapse rate between any level and all higher levels within 1 km exceed 3 K/km, then a second tropopause is defined by the same criterion as under the statement above. This tropopause may be either within or above the 1 km layer.
3. A level otherwise satisfying the definition of tropopause, but occurring at an altitude below that of the 500 hPa level will not be designated a tropopause unless it is the only level satisfying the definition and the average lapse rate fails to exceed 3 K/km over at least 1 km in any higher layer.

The Version 7 (V7) code evaluates the lapse rate by taking the derivative of the cubic spline interpolation of the Level 2 Support Product profiles of **TAirSup** versus **pressSup**. Between the 100 support levels, the lapse rate is linearly interpolated between values at the support levels to determine where condition (1a) is satisfied. Linear interpolation is used rather than evaluating the derivative of the spline (a quadratic function) to filter oscillation from the interpolation. Average lapse rates to test against conditions (1b), (2), and (3) are evaluated in the same fashion, except that the averages are evaluated over the thickness obtained by approximating altitude thicknesses by the first term of the Taylor series expansion of altitude in temperature. The equation for altitude thickness can be written as

$$\Delta z = H_0 \frac{\Delta P\, T}{P\, T_0}$$

where z is altitude, P is pressure, $H_0 = RT_0/g$ is the scale height and R is the gas constant for dry air. **T_Tropopause** is thus determined as well. The V7 algorithm interpolates between the levels of the support profile in order to obtain a better estimate of the temperature minimum and a continuous range of pressure.

7.2 Validation

The Tropopause product has been validated for Version 6 (V6), with results described in

V6_L2_Performance_and_Test_Report.pdf

but further validation for V7 has not been performed at this point. No algorithm changes were done for the tropopause product specifically between V6 and V7, although it may be affected by other changes in the retrieval, described in

V7_L2_Performance_Test_and_Validation_Report.pdf

7.3 Recommended Supplemental User Documentation

Overview_of_the AIRS_Mission.pdf
V7_L2_Quality_Control_and_Error_Estimation.pdf

8 Water Vapor Retrievals

The AIRS water vapor retrievals include the results of the IR-Only retrieval algorithm and the combined IR/MW retrieval algorithm. The record of IR-only retrievals runs to the present. The record of the IR/MW retrieval runs from August 30th in 2002 until September 25th in 2016. There are no data after the failure of AMSU channels 1 and 2. See the MW-Only product (above) for moisture products derived solely from MW data.

As in Version 6 (V6), Version 7 (V7) reports **level** profiles in addition to the layer profiles common to Version 5. A **layer** profile value is the mass mixing ratio (integrated over log of pressure) of a layer bounded by the pressure level on which it is reported and the next higher (in altitude) pressure level. A level profile value is the mass mixing ratio at the pressure level upon which it is reported. The procedure to calculate level quantities from layer quantities is described in

V7_L2_Levels_Layers_Trapezoids.pdf

The derivation of level quantities from layer quantities is essentially done by interpolation with smoothing kernels. This mathematical transformation leads to occasional strange results for water vapor profiles with inversions, typically near the surface. Be sure to filter the level profile by means of **H2OMMRLevStd_QC**.

The IR-Only and IR/MW products share the same variable names and they are listed in the following tables.

Standard Product

Field Name	Dimension per FOV	Description
totH2OStd	1	Total precipitable water vapor (kg/m2)
totH2OStd_QC	1	Quality flag (0,1,2)
totH2OStdErr	1	Error estimate for totH2OStd (kg/m2)
H2OMMRStd	H2OPressureLay=14	Layer Water Vapor Mass Mixing Ratio (g/kg dry air)
H2OMMRStd_QC	H2OPressureLay=14	Quality flag array (0,1,2)
H2OMMRStdErr	H2OPressureLay=14	Error estimate for H2OMMRStd (g/kg dry air)
H2OMMRLevStd	H2OPressureLev=15	Level Water Vapor Mass Mixing Ratio (g/kg dry air)
H2OMMRLevStd_QC	H2OPressureLev=15	Quality flag array (0,1,2)
H2OMMRLevStdErr	H2OPressureLev=15	Error estimate for H2OMMRLevStd (g/kg dry air)
H2OMMRSurf	1	Water Vapor Mass Mixing Ratio at the surface (g/kg dry air)
H2OMMRSurf_QC	1	Quality flag (0,1,2)
H2OMMRSurfErr	1	Error estimate for H2OMMRSurf
num_H2O_Func	1	Number of valid entries in each dimension of H2O_ave_kern_21func (in the support products).
H2O_verticality_21func	H2OFunc=21	Sum of the rows of H2O_ave_kern.
H2O_dof	1	Measure of the amount of information in H2O retrieval (degrees of freedom).

Support Product (full list in Appendix A2)

The variables listed in the Standard Product table above all exist in the Support Product, except that the layer profiles are given in molecules/cm2 instead of mass mixing ratio. Some additional variables, including averaging kernels, are listed in the following table.

Field Name	Dimension per FOV	Description
H2OCDSup	XtraPressureLay =100	Layer column water vapor (molecules/cm2)
H2OCDSup_QC	XtraPressureLay =100	Quality flag array (0,1,2)
H2OCDSupErr	XtraPressureLay =100	Error estimate for H2OCDSup (molecules/cm2)
H2OMMRLevSup	XtraPressureLay =100	Level Water Vapor Mass Mixing Ratio (g/kg dry air)
H2OMMRLevSup_QC	XtraPressureLay =100	Quality flag array (0,1,2)
H2OMMRLevSupErr	XtraPressureLay =100	Error estimate for H2OMMRLevSup (g/kg dry air)
H2O_trapezoid_layers_21func	H2OFunc=21	Trapezoid layer numbers*
H2O_eff_press_21func	H2OFunc=21	Effective pressure for the center of each H2O trapezoid (hPa)*
H2O_VMR_eff_21func	H2OFunc=21	Effective H2O volume mixing ratio for each trapezoid (vmr) (unitless)*
H2O_VMR_eff_21func _QC	H2OFunc=21	Quality flag array (0,1,2)*
H2O_VMR_eff_21func _err	H2OFunc=21	Error estimate for H2O_VMR_eff (unitless)*
H2O_ave_kern_21func	H2OFunc *H2OFunc=21x21	Averaging kernel for water vapor retrieval (unitless)*

*NOTE: For V7, 21func has been added to the variable name so that user's V6 analysis software will not inadvertently use the new, differently dimensioned output.

8.1 Description

The **level** atmospheric precipitable water vapor profile (**H2OMMRLevStd**) is the retrieved mean mass mixing ratio at the pressure level upon which it is reported; the **layer** atmospheric precipitable water vapor profile (**H2OMMRStd**) is the retrieved mean mass mixing ratio between two **pressH2O** levels and is reported on the lower altitude bounding pressure level bounding the layer. Standard pressure levels are arranged in order of decreasing pressure. The pressure levels on which moisture products are reported, **pressH2O**, are the same as the first 15 levels of the 28 available (i.e. for **PressStd** ≥ 50mb). The **H2OMMRStd** quoted on the lowest altitude pressure level above the surface (index = **nSurfStd**, which may be 1, 2, …, 15) is the mean mass mixing ratio in the layer bounded by the next higher level and the surface, i.e. the pressure of the lower boundary of that layer is actually **PSurfStd**.

totH2OStd is the total column moisture burden from top of atmosphere (TOA) to the surface. It is impossible for a user to integrate **H2OMMRStd** to compare the result to **totH2OStd**. The standard product moisture profile does not have sufficient vertical resolution, and the intrusion of topography into the final layer over land further complicates the calculation.

H2O_verticality_21func is a 21-point vector computed by summing the rows of the 21x21 H_2O averaging kernel, **H2O_ave_kern_21func**, stored in the AIRS Level 2 Support Product. The associated 21-point pressure array is provided in **H2O_eff_press_21func**. The peak value of **H2O_verticality_21func** indicates the vertical location of the maximum sensitivity of the H_2O product and the width of this peaked function qualitatively describes the vertical resolution of the retrieval. The magnitudes of **H2O_verticality_21func** are a rough measure of the fraction of the retrieval determined from the data as opposed to the first guess. A value near unity indicates the retrieval is highly determined by the radiance measurements and thus has high information content. A smaller value indicates the retrieval contains a large fraction of the first guess. **H2O_dof** is the number of degrees of freedom (a measure of the amount of information in the retrieval), and is the trace of **H2O_ave_kern_21func**.

NOTE: **num_H2O_Func** provides the number of valid entries in each dimension of **H2O_ave_kern_21func**. Topography limits the number of valid H_2O averaging kernel trapezoids.

NOTE: the problem with associating the verticality with a total column averaging kernel is that it neglects the fact that the retrieval can only move as superpositions of the trapezoids. Convolution using the verticality alone will not account for the possibility that the "independent H_2O profile" contains structure that the trapezoids can or cannot resolve.

8.2 Type of Product

As in V6, V7 provides standard moisture product profiles as layer quantities and level quantities. See

V7_L2_Levels_Layers_Trapezoids.pdf

for a full discussion of level and layer quantities.

8.3 Quality Indicators

The user is encouraged to read the Quality Control (QC) and error estimation document:

V7_L2_Quality_Control_and_Error_Estimation.pdf

The quality flags for profile values (**H2OMMRStd_QC** and **H2OMMRLevStd_QC**) should be used as filters for inclusion/exclusion of moisture profiles. QC=0 indicates the highest quality retrieval; QC=1 indicates good quality retrievals; and QC=2 indicates the use of such data is not recommended. The profile QC arrays are set according to **PBest** and **PGood**, with the exception that **H2OMMRLevStd_QC** may differ if the algorithm that derived the level quantity from the layer quantity encountered difficulty. The safest path is to use the two moisture QC arrays. **totH2OStd_QC** and **H2OMMRSurf_QC** depend on the entire water profile being of acceptable quality, since a large fraction of the water is near the surface.

Several modifications have been made to the temperature and water vapor quality control in V7:

- The error estimate used as the decision point for atmospheric temperature and water profile QCs is moved from 6 layers above the surface in V6 to 2 layers above the surface over frozen and land surfaces in V7. This effectively uses the entire profile error estimate information and allows the algorithm to make finer distinctions of quality over land and frozen areas near the surface.
- The numerical threshold points for marking profile levels with QC=2 is tightened over land from the mid to lower atmosphere, and for frozen cases in the middle atmosphere, while the numerical threshold for frozen cases near the surface is slightly loosened which increases the yield over frozen surfaces.

8.4 Validation

Validation results for Version 7 are described in

V7_L2_Performance_Test_and_Validation_Report.pdf

Figure 1 in Section 5 (Temperature Retrievals) shows example validation results from this report for both temperature and water vapor profiles, with AIRS V7 compared to IGRA radiosondes in terms of bias and root-mean-square error. Figure 2 gives another example from the report, showing statistics for AIRS water vapor retrievals compared to ECMWF profiles.

8.5 Caveats

This section will be updated over time as V7 data products are analyzed and validated.

There is no retrieval of water vapor for altitudes at or above the 100 hPa pressure level. The profile of water vapor at 100 hPa and higher altitudes is set equal to the first guess. The quality of AIRS+AMSU (**AIRX2RET**) and AIRS_AMSU+HSB (**AIRH2RET**) and AIRS-Only (**AIRS2RET**) water vapor retrievals begins to degrade for altitudes above the 300 hPa pressure level. AIRS is insensitive to water vapor at mixing ratios of less than 15-20 ppm. This is extensively documented against in situ data by Gettelman et al. (2004) and against MLS in Read et al. (2007) and Fetzer et al. (2008).

V7 water vapor retrievals have smaller water vapor RMSEs than V6 except during anomalous condition such as heatwaves. In the heatwave condition, V7 water vapor retrievals have larger RMSEs than V6 in the boundary layer (below 700 hPa). In the middle troposphere, V7 water vapor retrievals are not influenced by heatwaves and have smaller RMSEs than V6 retrievals. For details, please see our testing report:

V7_L2_Performance_Test_and_Validation_Report.pdf

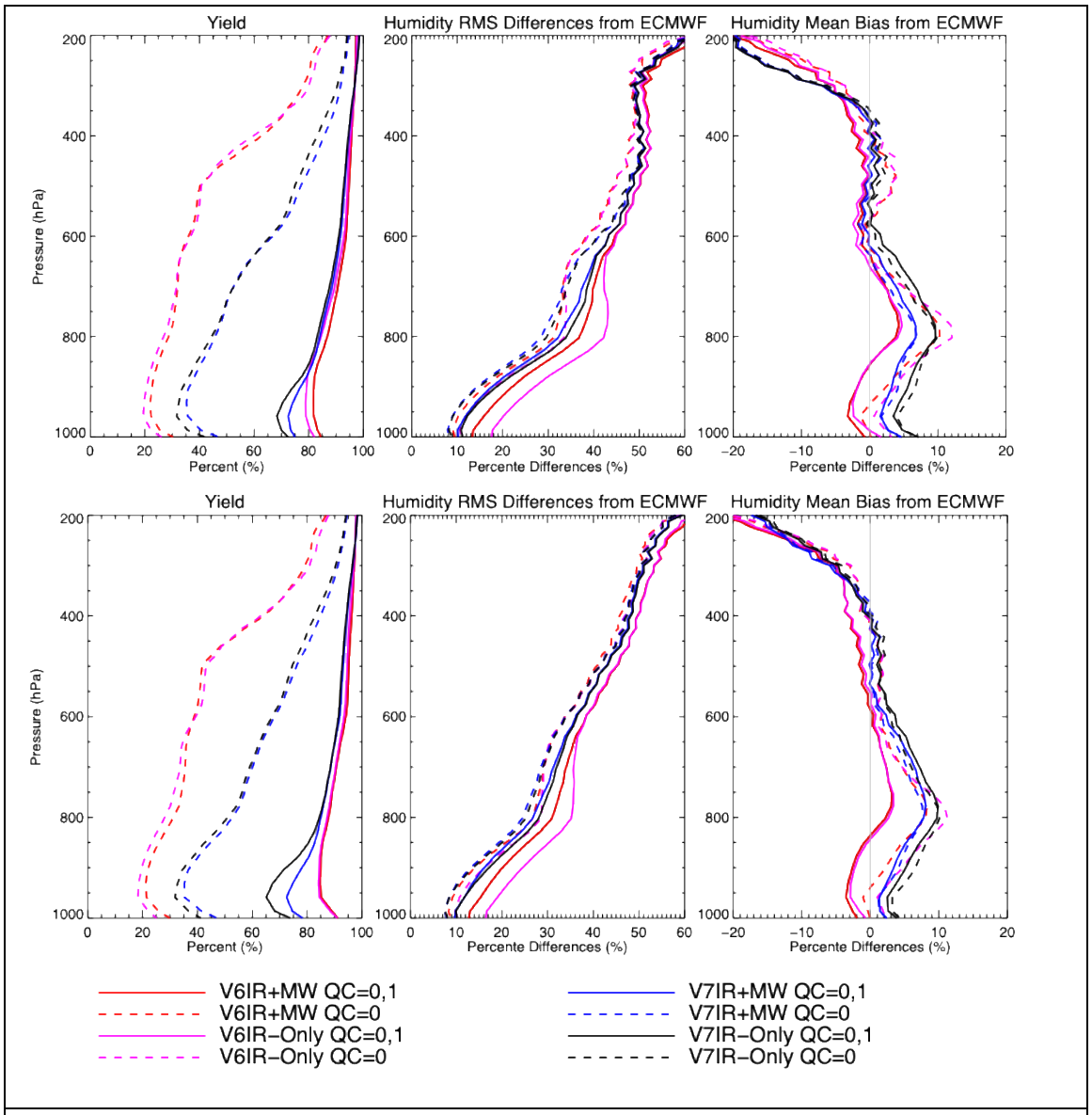

Figure 2: Global water vapor statistics of AIRS retrievals compared to collocated ECMWF.

Results are generated with seven days' worth of global data (all surface types) in January 2003 (top row) and July 2003 (bottom row). Bias and RMSE are calculated at the support pressure levels. Left column shows % of QC'd retrievals accepted as a function of pressure; Central column shows the % RMS difference w.r.t. ECMWF; Right column shows the % bias w.r.t. ECMWF.

8.6 Suggestions for Researchers

This section will be updated over time as V7 data products are analyzed and validated.

Researchers must use the values of **PBest** and **PGood** to identify the portion of the moisture profile which is suitable for assimilation and which is of somewhat lesser quality but is suitable for statistical climate studies.

- **pressH2O** ≤ **PBest** is suitable for assimilation
- **pressH2O** ≤ **Good** is suitable for statistical climate studies
- **pressH2O** > **Good** must be discarded

These pressure values are reflected in the level-by-level quality flags for the water vapor variables. The levels and/or layers whose *_QC values equal 0 are suitable for assimilation, whereas those whose *_QC values equal 1 are suitable for statistical climate studies. Do not use levels/layers whose *_QC values equal 2.

We recommend that researchers also employ the estimated error, **H2OMMRStdErr**, as an additional filter to excise those profiles in which the estimated error is negative or greater than 50% of **H2OMMRStd**.

8.7 Recommended Papers

This section will be updated over time as research with V7 data products are published.

Behrangi, Ali, Sun Wong, Kaniska Mallick, and Joshua B. Fisher (2014), "On the net surface water exchange rate estimated from remote-sensing observation and reanalysis." International Journal of Remote Sensing 35, no. 6: 2170-2185.

Behrangi, A., E. J. Fetzer, and S. L. Granger (2016), Early detection of drought onset using near surface temperature and humidity observed from space, Int.J.Remote Sens., 37(16), 3911-3923. https://dx.doi.org/10.1080/01431161.2016.1204478

Bloch, Magdalena, and Grzegorz Karasiński. "Water vapour mixing ratio profiles over Hornsund, Arctic. Intercomparison of lidar and AIRS results." Acta Geophysica 62, no. 2 (2014): 290-301.

Boisvert, L. N., J. N. Lee, J. T. M. Lenaerts, B. Noël, M. R. van den Broeke, and A. W. Nolin (2016), Using remotely sensed data from AIRS to estimate the vapor flux on the Greenland ice sheet: Comparisons with observations and a regional climate model, J. Geophys. Res. Atmos., 122, doi:10.1002/2016JD025674.

Buck, A. L. (1981), New equations for computing vapor pressure and enhancement factor, J. Appl. Meteorol., 20, 1527-1532.

Chung, E.-S., B. J. Soden, X. Huang, L. Shi, and V. O. John (2016), An assessment of the consistency between satellite measurements of upper tropospheric water vapor, J. Geophys. Res. Atmos., 121, doi:10.1002/2015JD024496

Divakarla, M., C. D. Barnet, M. D. Goldberg, L. M. McMillin, E. Maddy, W. Wolf and L. Zhow (2006), Validation of AIRS temperature and water vapor retrievals with matched radiosonde measurements and forecasts, J. Geophys. Res., 111, D09S15, doi:10.1029/2005JD006116

Du, J., F. Cooper, and S. Fueglistaler (2012), Statistical analysis of global variations of atmospheric relative humidity as observed by AIRS, J. Geophys. Res., 117, D12315, doi:10.1029/2012JD017550

Dwivedi, S., Narayanan, M. S., Venkat Ratnam, M., and Narayana Rao, D. (2016): Characteristics of monsoon inversions over the Arabian Sea observed by satellite sounder and reanalysis data sets, Atmos. Chem. Phys., 16, 4497, doi:10.5194/acp-16-4497-2016

Fetzer E. J., B. H. Lambrigtsen, A. Eldering, H. H. Aumann, M. T. Chahine (2006), Biases in total precipitable water vapor climatologies from Atmospheric Infrared Sounder and Advanced Microwave Scanning Radiometer, J. Geophys. Res., 111, D09S16, doi:10.1029/2005JD006598.

Fetzer, E. J., W. G. Read, D. Waliser, B. H. Kahn, B. Tian, H. Vömel, F. W. Irion, H. Su, A. Eldering, M. de la Torre Juarez, J. Jiang and V. Dang (2008), Comparison of upper tropospheric water vapor observations from the Microwave Limb Sounder and Atmospheric Infrared Sounder, J. Geophys. Res., 113, D22110, doi:10.1029/2008JD010000.

Froidevaux, L, N. J., Livesey, W. G. Read, Y. B. Jiang, C C. Jimenez, M. J. Filipiak, M. J. Schwartz, M. L. Santee, H. C. Pumphrey, J. H. Jiang, D. L. Wu, G. L. Manney, B. J. Drouin, J. W. Waters, E. J. Fetzer, P. F. Bernath, C. D. Boone, K. A. Walker, K. W. Jucks, G. C. Toon, J. J. Margitan, B. Sen, C. R. Webster, L. E. Christensen, J. W. Elkins, E. Atlas, R. A. Lueb, and R. Hendershot (2006), Early validation analyses of atmospheric profiles from EOS MLS on the Aura satellite, IEEE Transactions Geosciences and Remote Sensing, 44(5), 1106-1121.

Fu X., B. Wang, L. Tao (2006), Satellite data reveal the 3-D moisture structure of Tropical Intraseasonal Oscillation and its coupling with underlying ocean, Geophys. Res. Lett., 33, L03705, doi:10.1029/2005GL025074.

Gettelman,A., Weinstock,E. M., Fetzer,E. J., Irion,F. W., Eldering,A., Richard,E. C., Rosenlof,K. H., Thompson,T. L., Pittman,J. V., Webster,C. R., Herman,R. L. (2004), Validation of Aqua satellite data in the upper troposphere and lower stratosphere with in situ aircraft instruments, Geophys. Res. Lett., 31, L22107, doi:10.1029/2004GL020730.

Gettelman A., V. P. Walden, L. M. Miloshevich, W. L. Roth, B. Halter (2006), Relative humidity over Antarctica from radiosondes, satellites, and a general circulation model, J. Geophys. Res., 111, D09S13, doi:10.1029/2005JD006636.

Gettelman, A., E.J. Fetzer, A. Eldering, W.F. Irion (2006), “The Global Distribution of Supersaturation in the Upper Troposphere from the Atmospheric Infrared Sounder”, J. Climate, 19, 6089-6103. DOI: 10.1175/JCLI3955.1

Gettelman, A., W.D. Collins, E.J. Fetzer, A. Eldering, W.F. Irion, P.B. Duffy, G. Bala (2006), Climatology of Upper-Tropospheric Relative Humidity from the Atmospheric Infrared Sounder and Implications for Climate, J. Climate, 19, 6104-6121. DOI: 10.1175/JCLI3956.1

Guan, B., D. E. Waliser, F. M. Ralph, E. J. Fetzer, and P. J. Neiman (2016), Hydrometeorological characteristics of rain-on-snow events associated with atmospheric rivers, Geophys. Res. Lett., 43, 2964–2973, doi:10.1002/2016GL067978.

Hagan D. E., C. R. Webster, C. B. Farmer, R. D. May, R. L. Herman, E. M. Weinstock, L. E. Christensen, L. R. Lait, P. A. Newman (2004), Validating AIRS upper atmosphere water vapor retrievals using aircraft and balloon in situ measurements, Geophys. Res. Lett., 31, L21103, doi:10.1029/2004GL020302.

Hearty, T. J., A. Savtchenko, B. Tian, E. Fetzer, Y. L. Yung, M. Theobald, B. Vollmer, E. Fishbein, and Y.-I. Won (2014), Estimating sampling biases and measurement uncertainties of AIRS/AMSU-A temperature and water vapor observations using MERRA reanalysis, J. Geophys. Res. Atmos., 119, 2725–2741, doi:10.1002/2013JD021205.

Kalmus, P., S. Wong, and J. Teixeira (2015), The Pacific Subtropical Cloud Transition: A MAGIC Assessment of AIRS and ECMWF Thermodynamic Structure, IEEE Geoscience and Remote Sensing Letters, 12(7), 1586-1590, doi: 10.1109/LGRS.2015.2413771.

Livingston, J., E.J. Fetzer et al. (2007), Comparison of water vapor measurements by airborne Sun photometer and near-coincident in situ and satellite sensors during INTEX/ITCT 2004, J. Geophys. Res., 112, D12S16, doi:10.1029/2006JD007733.

Miloshevich L. M., H. Vömel, D. N. Whiteman, B. M. Lesht, F. J. Schmidlin, F. Russo (2006), Absolute accuracy of water vapor measurements from six operational radiosonde types launched during AWEX-G and implications for AIRS validation, J. Geophys. Res., 111, D09S10, doi:10.1029/2005JD006083.

Moradizadeh, M., M. Momeni, and M. R. Saradjian (2014), Estimation and validation of atmospheric water vapor content using a MODIS NIR band ratio technique based on AIRS water vapor products, Arabian Journal of Geosciences, 7(5), 1891-1897, http://dx.doi.org/10.1007/s12517-013-0828-2.

Murphy, D. M. and T. Koop (2005), Review of the vapour pressures of ice and supercooled water for atmospheric applications, Quart. J. Royal Met. Soc, 608 Part B, 1539-1565.

Milstein, A. B., and W. J. Blackwell (2016), Neural network temperature and moisture retrieval algorithm validation for AIRS/AMSU and CrIS/ATMS, J. Geophys. Res. Atmos., 121, 1414–1430, doi:10.1002/2015JD024008.

Pierce D. W., T. P. Barnett, E. J. Fetzer, P. J. Gleckler (2006), Three-dimensional tropospheric water vapor in coupled climate models compared with observations from the AIRS satellite system, Geophys. Res. Lett., 33, L21701, doi:10.1029/2006GL027060.

Pressel, Kyle G., William D. Collins, 2012: First-Order Structure Function Analysis of Statistical Scale Invariance in the AIRS-Observed Water Vapor Field. J. Climate, 25, 5538-5555. doi: http://dx.doi.org/10.1175/JCLI-D-11-00374.1

Qin, J., K. Yang, T. Koike, H. Lu, Y. Ma, and X. Xu (2012), Evaluation of AIRS Precipitable Water Vapor against Ground-based GPS Measurements over the Tibetan Plateau and Its Surroundings, Journal of the Meteorological Society of Japan, 90C, 87-98, http://dx.doi.org/10.2151/jmsj.2012-C06.

Read, W.G., A. Lambert, J. Backmeister, R.E. Cofield, L.E. Christensen, D.T. Cuddy, W.H. Daffer, B.J. Drouin, E. Fetzer, L. Froidevaux, R. Fuller, R. Herman, R.F. Jarnot, J.H. Jiang, Y.B. Jiang, K. Kelly, B.W. Knosp, H.C. Pumphrey, K.H. Rosenlof, X. Sabounchi, M.L. Santee, M.J. Schwartz, W.V. Snyder, P.C. Stek, H. Su, L.L. Takacs, R.P. Thurstans, H. Vomel, P.A. Wagner, J.W. Waters, C.R. Webster, E.M. Weinstock, and D.L. Wu (2007), "Aura Microwave Limb Sounder Upper Tropospheric and Lower Stratospheric H2O and RHi Validation," J. Geophys. Res., 112, D24S35, doi:10.1029/2007JD008752.

Ricaud, P., F. Carminati, Y. Courcoux, A. Pellegrini, J.-L. Attié, L. El Amraoui, R. Abida, C. Genthon, T. August and J. Warner (2014). Statistical analyses and correlation between tropospheric temperature and humidity at Dome C, Antarctica. Antarctic Science, 26, pp 290-308. doi:10.1017/S0954102013000564.

Roman, J., R. Knuteson, T. August, T. Hultberg, S. Ackerman, and H. Revercomb (2016), A global assessment of NASA AIRS v6 and EUMETSAT IASI v6 precipitable water vapor using ground-based GPS SuomiNet stations, J. Geophys. Res. Atmos., 121, 8925–8948, doi:10.1002/2016JD024806.

Ruzmaikin, Alexander, Hartmut H. Aumann, Evan M. Manning, 2014: Relative Humidity in the Troposphere with AIRS. J. Atmos. Sci., 71, 2516–2533. doi: http://dx.doi.org/10.1175/JAS-D-13-0363.1

Tobin D. C., H. E. Revercomb, R. O. Knuteson, B. M. Lesht, L. L. Strow, S. E. Hannon, W. F. Feltz, L. A. Moy, E. J. Fetzer, T. S. Cress (2006), Atmospheric Radiation Measurement site atmospheric state best estimates for Atmospheric Infrared Sounder temperature and water vapor retrieval validation, J. Geophys. Res., 111, D09S14, doi:10.1029/2005JD006103.

Wong, Sun, Eric J. Fetzer, Brian H. Kahn, Baijun Tian, Bjorn H. Lambrigtsen, Hengchun Ye, 2011: Closing the Global Water Vapor Budget with AIRS Water Vapor, MERRA Reanalysis, TRMM and GPCP Precipitation, and GSSTF Surface Evaporation. J. Climate, 24, 6307-6321. http://dx.doi.org/10.1175/2011JCLI4154.1

Wong, Sun, Eric J. Fetzer, Mathias Schreier, Gerald Manipon, Evan F. Fishbein, Brian H. Kahn, Qing Yue, and Fredrick W. Irion (2015). "Cloud-induced uncertainties in AIRS and ECMWF temperature and specific humidity." J. Geophys. Res.: Atmospheres.

Ye, H., E. J. Fetzer, S. Wong, A. Behrangi, E. T. Olsen, J. Cohen, B. H. Lambrigtsen, and L. Chen (2014), Impact of increased water vapor on precipitation efficiency over northern Eurasia, Geophys. Res. Lett., 41, 2941–2947, doi:10.1002/2014GL059830.

Zhang, Y., D. Wang, P. Zhai, and G. Gu (2012), Applicability of AIRS Monthly Mean Atmospheric Water Vapor Profiles over the Tibetan Plateau Region, J. Atmos. Ocean. Technol., 29(11), 1617-1628, http://dx.doi.org/10.1175/JTECH-D-11-00207.1

8.8 Recommended Supplemental User Documentation

Overview_of_the_AIRS_Mission.pdf
V7_L2_Performance_Test_and_Validation_Report.pdf
V7_L2_Quality_Control_and_Error_Estimation.pdf
V7_L2_Standard_Pressure_Levels.pdf
V7_L2_Support_Pressure_Levels.pdf
V7_L2_Levels_Layers_Trapezoids.pdf
V7_Retrieval_Channel_Sets.pdf
V7_Retrieval_Flow.pdf

9 Relative Humidity Derived from Temperature and Water Vapor

Field Name	Dimension per FOV	Description
RelHum	H2OPressureLev=15	Relative humidity over equilibrium phase (%)
RelHum_QC	H2OPressureLev=15	Quality flag array (0,1,2)
RelHumSurf	1	Relative humidity at the surface over equilibrium phase (%)
RelHumSurf_QC	1	Quality flag (0,1,2)
RelHum_liquid	H2OPressureLev=15	Relative humidity over liquid phase (%)
RelHum_liquid_QC	H2OPressureLev=15	Quality flag array (0,1,2)
RelHumSurf_liquid	1	Relative humidity at the surface over liquid phase (%)
RelHumSurf_liquid_QC	1	Quality flag (0,1,2)

9.1 Description

The relative humidity quantities are calculated as ratios of the retrieved specific humidity mixing ratios from section 8 and the temperature-dependent saturation mixing ratios in section 6.

RelHum takes into account the possibility of a phase change from liquid to ice whereas **RelHumid_liquid** does not. The pressure levels on which these products are reported, **pressH2O**, are the same as the first 15 levels of the 28 available standard levels (i.e. for **pressStd** ≥ 50mb). **RelHumSurf** is the relative humidity at the surface pressure, **PSurfStd**.

9.2 Type of Product

The Level 2 Standard Product relative humidity products are all level quantities.

9.3 Quality Indicators

The user is encouraged to read the Quality Control (QC) and error estimation document:

V7_L2_Quality_Control_and_Error_Estimation.pdf

The QC of the relative humidity profiles is set by the QC of temperature/specific humidity profiles, and the QC of the relative humidity at the surface is set by the QC of the surface air parameters.

For version 7, one relative humidity quality check was modified from version 6. In V6, cases with unrealistic relative humidity and low cloud fractions were identified and the profiles were marked as QC=2 up to 100hPa. In V7 this test is revised to address the uncertainty associated with the cloud top pressure in a less restrictive way by moving **PGood** and **PBest** only a few levels instead of to 100hPa.

9.4 Validation

Validation results for relative humidity are summarized in

V7_L2_Performance_Test_and_Validation_Report.pdf

9.5 Caveats

This section will be updated over time as V7 data products are analyzed and validated.

There is no retrieval of water vapor for altitudes at or above the 100 hPa pressure level. The profile of water vapor at 100 hPa and higher altitudes is set equal to the first guess. The quality of AIRS water vapor retrievals begins to degrade for altitudes above the 300 hPa pressure level. AIRS is insensitive to water vapor at mixing ratios of less than 15-20 ppm.

High Relative Humidity in Regions and Levels Where Specific Humidity is Very Low:

Most values of the atmospheric relative humidity (**RelHum**) are between 0 and 100%. But supersaturation with relative humidity greater than 100% is also common, especially in the upper troposphere and lower stratosphere (UTLS). Thus, the range of AIRS V7 L2 **RelHum** is usually 0 to ~200%. However, some **RelHum** values can exceed 200% or be as large as 500%. These values are typically associated with very low specific humidity or cold temperature and the AIRS instruments have trouble accurately retrieving humidity in these cases. Therefore, these high **RelHum** values are unrealistic and should be excluded in research. Specific examples and figures are shown for Level 3 **RelHum**, which is just a gridded average of Level 2 **RelHum,** in the Level 3 user guide:

V7_L3_Product_User_Guide.pdf.

For example, over Canada between the Great Lakes and Hudson Bay, on January 22, 2011, at 925 hPa the **RelHum** is over 200% when the temperature is around 245 K (very cold) and the specific humidity is around 0.1 g/kg (very dry).

9.6 Recommended Papers

Gettelman, A., et al. (2004), Validation of Aqua satellite data in the upper troposphere and lower stratosphere with in situ aircraft instruments, *Geophys. Res. Lett.*, 31, L22107, doi:10.1029/2004GL020730.

Gettelman, A., W.D. Collins, E.J. Fetzer, A. Eldering, F.W. Irion, P.B. Duffy, and G. Bala, 2006: Climatology of Upper-Tropospheric Relative Humidity from the Atmospheric Infrared Sounder and Implications for Climate. *J. Climate*, **19**, 6104–6121, https://doi.org/10.1175/JCLI3956.1

Wu, L., Braun, S. A., Qu, J. J., and Hao, X. (2006), Simulating the formation of Hurricane Isabel (2003) with AIRS data, *Geophys. Res. Lett.*, 33, L04804, doi:10.1029/2005GL024665.

Wu, L. (2007), Impact of Saharan air layer on hurricane peak intensity, *Geophys. Res. Lett.*, 34, L09802, doi:10.1029/2007GL029564.

Casey, S.P., A.E. Dessler, and C. Schumacher, 2009: Five-Year Climatology of Midtroposphere Dry Air Layers in Warm Tropical Ocean Regions as Viewed by AIRS/Aqua. *J. Appl. Meteor. Climatol.*, **48**, 1831-1842, https://doi.org/10.1175/2009JAMC2099.1

Milz, M., Buehler, S. A., and John, V. O. (2009), Comparison of AIRS and AMSU-B monthly mean estimates of upper tropospheric humidity, *Geophys. Res. Lett.*, 36, L10804, doi:10.1029/2008GL037068.

Shu, S., and Wu, L. (2009), Analysis of the influence of Saharan air layer on tropical cyclone intensity using AIRS/Aqua data, *Geophys. Res. Lett.*, 36, L09809, doi:10.1029/2009GL037634.

Wu, L. (2009), Comparison of atmospheric infrared sounder temperature and relative humidity profiles with NASA African Monsoon Multidisciplinary Analyses (NAMMA) dropsonde observations, *J. Geophys. Res.*, 114, D19205, doi:10.1029/2009JD012083.

Gettelman, A., W.D. Collins, E.J. Fetzer, A. Eldering, F.W. Irion, P.B. Duffy, and G. Bala, 2006: Climatology of Upper-Tropospheric Relative Humidity from the Atmospheric Infrared Sounder and Implications for Climate. *J. Climate*, **19**, 6104–6121, https://doi.org/10.1175/JCLI3956.1

9.7 Recommended Supplemental User Documentation

Overview_of_the_AIRS_Mission.pdf
V7_L2_Performance_Test_and_Validation_Report.pdf
V7_L2_Quality_Control_and_Error_Estimation.pdf
V7_L2_Standard_Pressure_Levels.pdf
V7_L2_Support_Pressure_Levels.pdf
V7_L2_Levels_Layers_Trapezoids.pdf
V7_Retrieval_Channel_Sets.pdf
V7_Retrieval_Flow.pdf
V7_L3_Product_User_Guide.pdf

10 Geopotential Height Derived from Temperature and Water Vapor

Field Name	Dimension per FOV	Description
GP_Tropopause	1	Geopotential height at tropopause (m above mean sea level)
GP_Tropopause_QC	1	Quality flag (0,1,2)
GP_Height	StdPressureLev =28	Geopotential Heights at StdPressureLev (m above mean sea level)
GP_Height_QC	StdPressureLev =28	Quality flag array (0,1,2)
GP_Surface	1	Geopotential Height of surface (m above mean sea level)
GP_Surface_QC	1	Quality flag (0,1,2)

10.1 Description

AIRS profiles and tropopause height are generally provided on a pressure grid. Geopotential heights provide the information users need to translate between this pressure grid and physical altitude.

10.2 Type of Product

GP_Height and **GP_Height_QC** are level products.

10.3 Quality Indicators

The user is encouraged to read the QC and error estimation document:

V7_L2_Quality_Control_and_Error_Estimation.pdf

10.4 Caveats

Geopotential heights are derived by integrating up through the atmosphere from the surface, therefore the quality at all levels of the atmosphere is only good when the quality of both temperature and water vapor is good near the surface.

10.5 Recommended Supplemental User Documentation

Overview_of_the_AIRS_Mission.pdf
V7_L2_Quality_Control_and_Error_Estimation.pdf

11 Pressure at the Top of the PBL

11.1 Description

A provisional product, **bndry_lyr_top**, the pressure at the top of the planetary boundary layer and its associated quality control are reported in the Level 2 Support Product at the resolution of the Field of Regard (AMSU Field of View), since the vertical positioning of thermodynamic profile gradients is used to locate the top of the Planetary Boundary Layer (PBL). This height is reported in units of pressure (hPa). The boundary layer top height is the pressure of the level with the largest gradient of a relative humidity (relative to liquid phase of water) layer profile calculated on the support pressure layer grid. As a result, the boundary layer top height may derive from a strong gradient in either temperature or water vapor mixing ratio. This product is considered a derived rather than a retrieved parameter, and so no error estimate is provided. See Martins et al. (2010).

11.2 Quality Indicators

The user is encouraged to read the QC and error estimation document:

V7_L2_Quality_Control_and_Error_Estimation.pdf

bndry_lyr_top_QC is set to 0 unless:

1. If **SurfClass** $\neq$ 2 (i.e., not nonfrozen ocean) then **bndry_lyr_top_QC** = 2
2. If a noncontiguous layer has a gradient over 97% of the value of the gradient for the chosen layer then **bndry_lyr_top_QC** = 1
3. If the relative humidity input to the calculation is < 0 or > 3 then **bndry_lyr_top_QC** = 1.
4. **bndry_lyr_top_QC** is set never to be lower (better) than **TSurfAir_QC**.
5. If RelHumSurf > 100% then **bndry_lyr_top_QC** = 2.

11.3 Validation

The PBL top height product has been validated for Version 6, with results described in **V6_L2_Performance_and_Test_Report.pdf**, but further validation for Version 7 has not been performed at this point.

No algorithm changes were done for the PBL top height product specifically between V6 and V7, although it may be affected by other changes in the retrieval, described in

V7_L2_Performance_Test_and_Validation_Report.pdf

11.4 Recommended Papers

This section will be updated over time as research with V7 data products are published.

Kahn, B. H., G. Matheou, Q. Yue, T. Fauchez, E. J. Fetzer, M. Lebsock, J. Martins, M. M. Schreier, K. Suzuki, and J. Teixeira (2017), A satellite and reanalysis view of cloud organization, thermodynamic, and dynamic variability within the subtropical marine boundary layer, Atmos. Chem. Phys. Discuss., doi:10.5194/acp-2017-59

Kalmus, P., S. Wong, and J. Teixeira (2015), The Pacific Subtropical Cloud Transition: A MAGIC Assessment of AIRS and ECMWF Thermodynamic Structure, IEEE Geoscience and Remote Sensing Letters, 12(7), 1586-1590, http://dx.doi.org/10.1109/LGRS.2015.2413771.

Luo, T., Z. Wang, D. M. Zhang, and B. Chen (2016), Marine boundary layer structure as observed by A-train satellites, Atmospheric Chemistry and Physics, 16(9), 5891-5903. https://dx.doi.org/10.5194/acp-16-5891-2016.

Martins, J. P. A., J. Teixeira, P. M. M. Soares, P. M. A. Miranda, B. H. Kahn, V. T. Dang, F. W. Irion, E. J. Fetzer, and E. Fishbein (2010), Infrared sounding of the trade-wind boundary layer: AIRS and the RICO experiment, Geophys. Res. Lett., 37, L24806, doi:10.1029/2010GL045902

Yue, Qing, Brian H. Kahn, Eric J. Fetzer, and João Teixeira. "Relationship between marine boundary layer clouds and lower tropospheric stability observed by AIRS, CloudSat, and CALIOP." Journal of Geophysical Research: Atmospheres (1984–2012) 116, no. D18 (2011).

Yue, Qing, Brian H. Kahn, Heng Xiao, Mathias M. Schreier, Eric J. Fetzer, João Teixeira, and Kay Sušelj. "Transitions of cloud-topped marine boundary layers characterized by AIRS, MODIS, and a large eddy simulation model." Journal of Geophysical Research: Atmospheres 118, no. 15 (2013): 8598-8611.

11.5 Recommended Supplemental User Documentation

Overview_of_the_AIRS_Mission.pdf
V6_L2_Performance_and_Test_Report.pdf
V7_L2_Performance_Test_and_Validation_Report.pdf
V7_L2_Quality_Control_and_Error_Estimation.pdf
V7_L2_Standard_Pressure_Levels.pdf
V7_L2_Support_Pressure_Levels.pdf
V7_Retrieval_Flow.pdf

12 Cloud Retrievals on 3x3 AIRS Field of View

Field Name	Dimension per FOV	Description
CldFrcTot	1	Total effective cloud fraction over all cloud layers and all 9 spots (0.0 → 1.0) assuming unit cloud top emissivity.
CldFrcTot_QC	1	Quality flag (0,1,2)
CldFrcStd	AIRSTrack *AIRSXTrack *Cloud =3x3x2	Effective cloud fraction (0.0 → 1.0) assuming unit cloud top emissivity in order of increasing pressure. Only first nCld elements are valid. Caution: For CldFrcStd = 1, only the average cloud fraction over the nine spots is reported (duplicated nine times) for each level
CldFrcStd_QC	AIRSTrack *AIRSXTrack *Cloud =3x3x2	Quality flag array (0,1,2)
CldFrcStdErr	AIRSTrack *AIRSXTrack *Cloud =3x3x2	Error estimate for CldFrcStd (0.0 → 1.0)
PCldTop	AIRSTrack *AIRSXTrack *Cloud =3x3x2	Cloud top pressure (hPa) in each of the 9 AIRS FOVs within the Field of Regard (AMSU retrieval FOV) in order of increasing pressure. Only first nCld elements are valid.
PCldTop_QC	AIRSTrack *AIRSXTrack *Cloud =3x3x2	Quality flag array (0,1,2)
PCldTopErr	AIRSTrack *AIRSXTrack *Cloud =3x3x2	Error estimate for PCldTop (hPa).
TCldTop	AIRSTrack *AIRSXTrack *Cloud =3x3x2	Cloud top temperature (K) in order of increasing pressure in each of the 9 AIRS FOVs within the Field of Regard (AMSU retrieval FOV). Only first nCld elements are valid.
TCldTop_QC	AIRSTrack *AIRSXTrack *Cloud =3x3x2	Quality flag array (0,1,2)
TCldTopErr	AIRSTrack *AIRSXTrack *Cloud =3x3x2	Error estimate for TCldTop (K) in each of the 9 AIRS FOVs within the Field of Regard (AMSU retrieval FOV).
nCld	AIRSTrack *AIRSXTrack *Cloud =3x3x2	Number of retrieved cloud layers in each of the 9 AIRS FOVs within the Field of Regard (can be 0,1, or 2)

12.1 Description

PCldTop, **TCldTop** and **nCld** are reported for the 3x3 (14 km at nadir) AIRS spots within the (50 km at nadir) Field of Regard (FOR = AMSU FOV).

NOTE: The effective cloud fraction is given by the product of the fraction of the FOV covered by clouds and the cloud emissivity at 11 μm.

The combined IR/MW algorithm retrieves up to two amounts of clouds at distinct pressure levels, each having its own effective cloud fraction as seen from above for each AIRS FOV (geospatial extent is ~14 km at nadir). If there are two reported layers, the first is the one at the higher altitude. AIRS radiances at a given frequency are affected by the product of the cloud fraction and the cloud emissivity as well as the geophysical state. We currently solve for the best fit cloud solution across a wide range of frequencies assuming that the cloud emissivity is frequency independent. The cloud retrieval minimizes the radiance residuals given the retrieved geophysical state. (Note: cloud formations occur in cloud clearing and are not necessarily flat. Cloud layers occur in cloud retrieval and are pancakes.)

PCldTop is the retrieved cloud top pressure for each reported cloud height at the AIRS resolution, **PCldTopStd** (in the support product) the retrieved cloud top pressure averaged to the AMSU resolution. Each has an associated error and quality flag at the same resolution. In addition, the cloud top temperature and its associated error and QC flag at each resolution are reported as **TCldTop** and **TCldTopStd** for the same cloud formations. These are interpolated from the AIRS **TAirSup** and **TAirSupErr** fields.

The effective cloud fraction **CldFrcStd** and its error **CldFrcStdErr** are derived from the radiances in the 9 AIRS spots (each of geospatial extent ~14 km at nadir) within the FOR (AMSU FOV). The values in both range between 0.0 and 1.0. In the event that two cloud heights are reported, the sum over both layers of **CldFrcStd** does not exceed 1.0. Under some conditions the final nine spot cloud parameter retrieval fails. If the final cloud retrieval fails, then the retrieval is marked Quality = 2 and the **CldFrcStd** array is set to the value of an earlier single FOV cloud retrieval step within the AMSU FOV which is more stable. Under this condition, we report nine sets of cloud parameters that are all identical. This occurs in less than one percent of the retrievals and we do not think these values will be useful.

For a full discussion on how these products are obtained and simple comparisons and validation assessments, please consult the following papers:

- Kahn et al. (2014), “The Atmospheric Infrared Sounder Version 6 Cloud Products”
- Susskind et al. (2011), “Improved Temperature Sounding and Quality Control Methodology using AIRS/AMSU Data: The AIRS Science Team Version 5 Retrieval Algorithm”

- Susskind et al. (2014), "Improved methodology for surface and atmospheric soundings, error estimates, and quality control procedures: the atmospheric infrared sounder science team version-6 retrieval algorithm"

The cloud products are functionally the same between Version 6 and Version 7.

12.2 Type of Product

The cloud formation products are level quantities, thus that the values are reported at discrete pressure levels.

12.3 Quality Indicators

The user is encouraged to read the Quality Control (QC) and error estimation document and the cloud product section of the performance and test report:

V7_L2_Quality_Control_and_Error_Estimation.pdf
V7_Retrieval_Performance _and_Test_Report.pdf

QC for cloud products is set as follows:

- If the final retrieval is accepted, Quality = 0
- If the final retrieval is accepted, but the final retrieved surface temperature differs from the neural net (prior) surface temperature by more than 5 K, the clouds are calculated from the retrieval with the neural net surface substituted, Quality = 1
- If the cloud retrieval does not complete, Quality = 2

12.4 Validation

Test results on V7 cloud products are summarized in

V7_L2_Performance_Test_and_Validation_Report.pdf

12.5 Caveats

This section will be updated over time as V7 data products are analyzed and validated.

The user is cautioned that all reported cloud fraction values are "effective cloud fractions" calculated assuming opaque black clouds. If the actual emissivity is less than 1.0 or the cloud is partially transmissive, the actual cloud fraction is correspondingly larger than what we report, but radiatively equivalent.

The tendency for clouds to settle at round numbers was corrected in V6. We now allow clouds to within 10 hPa of the surface.

It has been shown that the higher quality retrievals for **TAirStd** and **H2OMMRStd** do not correspond to higher quality retrievals of cloud fields [Kahn et al. 2007a]: in fact, these product accuracies have opposite tendencies. This is expected as a stronger cloud radiative signature is associated with a more accurate cloud temperature, pressure, and amount. Thus, scenes in which it is more difficult to retrieve **TAirStd** and

H2OMMRStd contain more accurate cloud retrievals and are associated with smaller uncertainties [see Kahn et al. 2007a,b].

The cloud retrievals assume spectral unit emissivity and only two layers are considered in the retrieval. Furthermore, if a cloud top pressure is retrieved above the tropopause it is readjusted to the tropopause level. There are additional caveats, further discussed in Kahn et al. [2007a,b]. Validation efforts and scientific applications may be found in the references. Please refer to these publications for detailed discussion.

12.6 Suggestions for Researchers

This section will be updated over time as V7 data products are analyzed and validated.

Please refer to the publications below for validation and application of AIRS cloud fields in scientific analyses. In *Kahn et al*. [2007a] AIRS cloud top height (derived from cloud top pressure and TAirStd) is compared to Atmospheric Radiation Measurement (ARM) program millimeter-wave cloud radar and micropulse lidar observations of clouds coincident with EOS Aqua, as well as the Microwave Limb Sounder observations of thin tropopause-level cirrus clouds. *Kahn et al.* [2007b] comprehensively compare MODIS and AIRS operational cloud retrievals, including cloud top temperature and effective cloud fraction as a function of cloud and scene type. It is shown that AIRS is better able to capture thin cirrus clouds than the operational MODIS algorithm, although there are other instances in which MODIS may outperform AIRS.

Kahn et al. [2008a] validates the AIRS cloud fields as a function of cloud type as determined by CloudSat and CALIPSO. AIRS agrees somewhat better in these cases than with the ARM measurements, which highlights respective sensitivities to cloud tops between surface- and space-based measurements. In *Kahn et al*. [2008b] we demonstrate the application of AIRS cloud fields in deriving optical and microphysical properties of thin cirrus. The thin cirrus properties in turn are related to AIRS relative humidity fields and demonstrate the power of AIRS to observe multiple fields simultaneously. Lastly, the fast radiative transfer model used to derive cirrus properties from AIRS radiances is discussed in *Yue et al*. [2007]. Comparisons of these products are made with V6 in Kahn et al. (2014), and are used in studies of extratropical cyclones (Naud and Kahn, 2015), Arctic cloud trends (Boisvert and Stroeve, 2015; Devasthale et al., 2016), and the Southern Annular Mode (SAM) variations over Antarctica (Lubin et al., 2015).

The researcher is recommended to review these (and other) AIRS-related publications, and to contact any of the authors of these publications to answer further inquiries. Brian Kahn, who has headed the balance of the AIRS cloud validation efforts, can be contacted at **brian.h.kahn@jpl.nasa.gov**.

12.7 Recommended Papers

This section will be updated over time as research with V7 data products are published.

Aumann, H. H., and A. Ruzmaikin (2013), "Frequency of deep convective clouds in the tropical zone from 10 years of AIRS data." Atmospheric Chemistry and Physics 13, no. 21: 10795-10806.

Boisvert, L. N., and J. C. Stroeve (2015), The Arctic is becoming warmer and wetter as revealed by the Atmospheric Infrared Sounder, Geophys. Res. Lett., 42, 4439–4446, doi:10.1002/2015GL063775.

Chang, K.-W., T. S. L'Ecuyer, B. H. Kahn, and V. Natraj (2017), Information content of visible and midinfrared radiances for retrieving tropical ice cloud properties, Journal of Geophysical Research. Atmospheres, 122(9), 4944-4966. http://dx.doi.org/10.1002/2016JD026357

Cullather, R. I., Y.-K. Lim, L. N. Boisvert, L. Brucker, J. N. Lee, and S. M. J. Nowicki (2016), Analysis of the warmest Arctic winter, 2015–2016, Geophys. Res. Lett., 43, 10,808–10,816, doi:10.1002/ 2016GL071228.

Devasthale, A., J. Sedlar, B. H. Kahn, M. Tjernström, E. J. Fetzer, B. Tian, J. Teixeira, and T. S. Pagano (2016), A decade of spaceborne observations of the Arctic atmosphere: Novel insights from NASA's AIRS instrument, Bull. Amer. Met. Soc., 97, 2163–2176, doi:10.1175/BAMS-D-14-00202.1.

Jin, H., and S. L. Nasiri. "Evaluation of AIRS cloud thermodynamic phase determination with CALIPSO." Journal of Applied Meteorology and Climatology 2013 (2013).

Kahn, B. H., Eldering, A., Braverman, A.J., Fetzer, E.J., Jiang, J.H., Fishbein, E., and Wu, D.L. (2007a): Toward the characterization of upper tropospheric clouds using Atmospheric Infrared Sounder and Microwave Limb Sounder observations, J. Geophys. Res., 112, D05202, doi:10.1029/2006JD007336.

Kahn, B. H., E. Fishbein, S. L. Nasiri, A. Eldering, E. J. Fetzer, M. J. Garay, and S.-Y. Lee (2007b), The radiative consistency of Atmospheric Infrared Sounder and Moderate Resolution Imaging Spectroradiometer cloud retrievals, J. Geophys. Res., 112, D09201, doi:10.1029/2006JD007486.

Kahn, B.H., Chahine, M.T., Stephens, G.L, Mace, G.C., Marhcand, R.T., Wang, Z., Barnet, C.D., Eldering, A., Holz, R.E., Kuehn, R.E., Vane, D.G. (2008a), Cloud type comparisons of AIRS, CloudSat and CALIPSO cloud height and amount Atmospheric Chemistry and Physics, 8, 5, 1231-1248

Kahn, B. H., Liang, C. K., Eldering, A., Gettelman, A., Yue, Q., and Liou, K. N., (2008b): Tropical thin cirrus and relative humidity observed by the Atmospheric Infrared Sounder, Atmos. Chem. Phys., 8, 1501-1518, 2008.

Kahn, B. H., F. W. Irion, V. T. Dang, E. M. Manning, S. L. Nasiri, C. M. Naud, J. M. Blaisdell et al. (2014), "The atmospheric infrared sounder version 6 cloud products." *Atmos. Chem. Phys* 14: 399-426.

Kahn, B. H., G. Matheou, Q. Yue, T. Fauchez, E. J. Fetzer, M. Lebsock, J. Martins, M. M. Schreier, K. Suzuki, and J. Teixeira (2017), An A-train and MERRA view of cloud, thermodynamic, and dynamic variability within the subtropical marine boundary layer, *Atmos. Chem. Phys.*, **17**, 9451–9468, https://doi.org/10.5194/acp-17-9451-2017.

Lubin, D., B. H. Kahn, M. A. Lazzara, P. Rowe, and V. P. Walden (2015), Variability in AIRS-retrieved cloud amount and thermodynamic phase over west versus east Antarctica influenced by the SAM, Geophys. Res. Lett., 42, doi:10.1002/2014GL062285.

McCoy, D. T., R. Eastman, D. L. Hartmann, and R. Wood (2017), The change in low cloud cover in a warmed climate inferred from AIRS, MODIS, and ERA-interim, Journal of Climate, 30(10), 3609-3620. https://dx.doi.org/10.1175/JCLI-D-15-0734.1.

Naud, C. M., and B. H. Kahn (2015), Thermodynamic phase and ice cloud properties in northern hemisphere winter extratropical cyclones observed by Aqua AIRS, J. Appl. Meteor. Climatol., 54, 2283–2303, doi:10.1175/JAMC-D-15-0045.1.

Naud, C. M., J. F. Booth, and A. D. Del Genio (2016), The Relationship between Boundary Layer Stability and Cloud Cover in the Post-Cold-Frontal Region, Journal of Climate, 29(22), 8129-8149. http://dx.doi.org/10.1175/jcli-d-15-0700.1

Ou, S. S. C., B. Kahn, K. Liou, Y. Takano, M. M. Schreier, and Q. Yue (2012), Retrieval of Cirrus Cloud Properties From the Atmospheric Infrared Sounder: The k-Coefficient Approach Using Cloud-Cleared Radiances as Input, IEEE Trans. Geosci. Remote Sens., Article in Press, doi: http://dx.doi.org/10.1109/TGRS.2012.2205261

Protopapadaki, S. E., C. J. Stubenrauch, and A. G. Feofilov (2017), Upper tropospheric cloud systems derived from IR sounders: properties of cirrus anvils in the tropics, Atmospheric Chemistry and Physics, 17(6), 3845-3859. http://dx.doi.org/10.5194/acp-17-3845-2017.

Schreier, M. M., Kahn, B. H., Sušelj, K., Karlsson, J., Ou, S. C., Yue, Q., and Nasiri, S. L.: Atmospheric parameters in a subtropical cloud regime transition derived by AIRS and MODIS: observed statistical variability compared to ERA-Interim, Atmos. Chem. Phys., 14, 3573-3587, doi:10.5194/acp-14-3573-2014, 2014.

Schreier, M., and K. Suselj (2016) Analysis of collocated AIRS and MODIS data: a global investigation of correlations between clouds and atmosphere in 2004–2012, International Journal of Remote Sensing, 37:11, 2524-2540, DOI: 10.1080/01431161.2016.1177244

Susskind, J., Blaisdell, J.M., Iredell, L., Keita, F.,Improved Temperature Sounding and Quality Control Methodology using AIRS/AMSU Data: The AIRS Science Team Version 5 Retrieval Algorithm, Geoscience and Remote Sensing, IEEE Transactions, March 2011, Volume 49, Issue 3, pages 883-907

Susskind, Joel, John M. Blaisdell, and Lena Iredell. "Improved methodology for surface and atmospheric soundings, error estimates, and quality control procedures: the atmospheric infrared sounder science team version-6 retrieval algorithm." Journal of Applied Remote Sensing 8, no. 1 (2014): 084994-084994.

Yue, Q., K.N. Liou, S.C. Ou, B.H. Kahn, P. Yang, and G.G. Mace, (2007), Interpretation of AIRS Data in Thin Cirrus Atmospheres Based on a Fast Radiative Transfer Model. J. Atmos. Sci., 64, 3827_x0013_3842.

Yue, Qing, Brian H. Kahn, Heng Xiao, Mathias M. Schreier, Eric J. Fetzer, João Teixeira, and Kay Sušelj, (2013), "Transitions of cloud-topped marine boundary layers characterized by AIRS, MODIS, and a large eddy simulation model." Journal of Geophysical Research: Atmospheres 118, no. 15: 8598-8611.

Yue, Q., B. H. Kahn, E. J. Fetzer, M. Schreier, S. Wong, X. Chen, and X. Huang (2016), Observation-based longwave cloud radiative kernels derived from the A-train, J. Climate, 29, 2023–2040, doi:10.1175/JCLI-D-15-0257.1

Zelinka, M. D., K. M. Grise, S. A. Klein, C, Zhou, A. M. DeAngelis, and M. W. Christensen (2018), Drivers of the low-cloud response to poleward jet shifts in the North Pacific in observations and models, J. Climate, 31, 7925-7947.

12.8 Recommended Supplemental User Documentation

Overview_of_the_AIRS_Mission.pdf
V7_L2_Performance_Test_and_Validation_Report.pdf
V7_L2_Quality_Control_and_Error_Estimation.pdf
V7_L2_Standard_Pressure_Levels.pdf
V7_L2_Support_Pressure_Levels.pdf
V7_L2_Levels_Layers_Trapezoids.pdf
V7_Retrieval_Channel_Sets.pdf
V7_Retrieval_Flow.pdf

13 Cloud Phase and Ice Cloud Properties

Support Product (see Appendix A2 for a complete list of fields)

Field Name	Dimension per FOV	Description
Cloud_Resid_Ratio3x3	AIRSTrack *AIRSXTrack =3x3	Internal retrieval quality indicator, ratio of residual of cloud channels to predicted uncertainty, per AIRS FOV. Located in Support Product. (unitless)
cloud_phase_3x3	AIRSTrack *AIRSXTrack =3x3	Flag indicating whether clouds are ice or liquid water; -9999: No cloud phase retrieval was possible; -2: Liquid water (high confidence); -1: Liquid water (low confidence); 0: Unknown; 1: Ice (low confidence); 2: Ice (higher confidence); 3: Ice (very high confidence); 4: Ice (very high confidence)
cloud_phase_bits	AIRSTrack *AIRSXTrack =3x3	Internal bit field of individual tests used in cloud phase determination; Bit 15: unused Bit 14: unused Bit 13: unused Bit 12: unused Bit 11: unused Bit 10: unused Bit 9: Warm test Bit 8: Liquid water test #2 Bit 7: Liquid water test #1 Bit 6: ice test #4 Bit 5: ice test #3 Bit 4: ice test #2 Bit 3: ice test #1 Bit 2: Cloud fraction test Bit 1: Desert test Bit 0: One or more tests could not be performed
ice_cld_opt_dpth	AIRSTrack *AIRSXTrack =3x3	Ice cloud optical thickness (only reported when cloud_phase_3x3 greater than or equal to 1)
ice_cld_eff_diam	AIRSTrack *AIRSXTrack =3x3	Ice cloud effective diameter (microns; only reported when cloud_phase_3x3 greater than or equal to 1)
ice_cld_temp_eff	AIRSTrack *AIRSXTrack =3x3	Ice cloud top temperature (K; only reported when cloud_phase_3x3 greater than or equal to 1)
ice_cld_opt_dpth_QC	AIRSTrack *AIRSXTrack =3x3	QC=0 (best), QC=1 (good), QC=2 (do not use) (see Kahn et al. 2014, ACP, Table 2 for further detail)

ice_cld_eff_diam_QC	AIRSTrack *AIRSXTrack =3x3	QC=1 (good), QC=2 (do not use) (see Kahn et al. 2014, ACP, Table 2 for further detail)
ice_cld_temp_eff_QC	AIRSTrack *AIRSXTrack =3x3	QC=0 (best), QC=1 (good), QC=2 (do not use) (see Kahn et al. 2014, ACP, Table 2 for further detail)
log_ice_cld_opt_dpth_prior_var	AIRSTrack *AIRSXTrack =3x3	A priori variance for ice_cld_opt_dpth, a fixed value of 0.111
log_ice_cld_opt_dpth_prior_var	AIRSTrack *AIRSXTrack =3x3	A priori variance for ice_cld_eff_diam, fixed value of 0.16
ice_cld_temp_eff_prior_var	AIRSTrack *AIRSXTrack =3x3	A priori variance for ice_cld_temp_eff, fixed value of 225
ice_cld_opt_dpth_ave_kern	AIRSTrack *AIRSXTrack =3x3	Scalar averaging kernel (AK) for ice_cld_opt_dpth, ranges from 0.0 to 1.0
ice_cld_eff_diam_ave_kern	AIRSTrack *AIRSXTrack =3x3	Scalar AK for ice_cld_ eff_diam, ranges from 0.0 to 1.0
ice_cld_temp_eff_ave_kern	AIRSTrack *AIRSXTrack =3x3	Scalar AK for ice_cld_temp_eff, ranges from 0.0 to 1.0
ice_cld_opt_dpth_first_guess	AIRSTrack *AIRSXTrack =3x3	First guess of ice_cld_opt_dpth, fixed to 3.0

13.1 Description

cloud_phase_3x3 – flag for each of the 3x3 AIRS spots in an AMSU FOV indicating the phase (liquid or ice) of the moisture in a cloud.

The tests by which **cloud_phase_3x3** is set are described in

V7_Retrieval_Channel_Sets.pdf

ice_cld_opt_depth, **ice_cld_eff_diam**, and **ice_cld_temp_eff** are the ice cloud optical depth, effective diameter (in microns), and effective cloud top temperature (in Kelvins), respectively. The various quality control, error estimates, averaging kernels, and prior guess fields associated with these three variables are described in great detail in Kahn et al. (2014), while spatial patterns and secular trends are described in Kahn et al. (2018).

13.2 Quality Indicators

The user is encouraged to read the QC and error estimation document:

V7_L2_Quality_Control_and_Error_Estimation.pdf

cloud_phase_3x3 is a derived parameter, rather than a retrieved parameter and therefore does not have a _QC field associated with it. Instead, whenever the cloud phase cannot be determined the value of cloud_phase_3x3 is set to -9999 and the low bit of

cloud_phase_bits is set. These are cases where QC indicates that required inputs were of low quality. The cloud_phase_3x3 is validated against CALIOP observations in Jin and Nasiri (2014) for the entire globe outside of the polar regions, while the Arctic is carefully evaluated against CALIOP and CloudSat observations in Peterson et al. (2020). Reasons for cloud_phase_3x3 to be set to -9999 are:

1) QC=2 for surface emissivity
2) QC=2 for cloud fraction
3) All radiances = -9999 for all channels in any band.

cloud_phase_bits are based on radiometric (and other) tests which are used to derive a value for **cloud_phase_3x3**.

ice_cld_opt_depth, **ice_cld_eff_diam**, and **ice_cld_temp_eff** are the ice cloud optical depth, effective diameter, and effective cloud top temperature, respectively. A full description of these quantities (including those listed in the field name list above) can be found in Kahn et al. (2014). The retrieved values and error estimates are compared against MODIS ice cloud property retrievals in Kahn et al. (2015) and are described as a function of cloud heterogeneity in Guillaume et al. (2019). Kahn et al. (2018) derives spatial patterns and trends of the ice cloud property retrievals over the lifetime of the AIRS mission.

13.3 Validation

AIRS V6 validation results for cloud phase and ice cloud properties are partially summarized in

V6_L2 Performance_and_Test_Report.pdf

The primary V6 paper is Kahn et al. (2014). There is no change for V7 so please refer to that paper for details.

13.4 Suggestions for Researchers

Published studies that detail either the use or validation of **cloud_phase_3x3** include (but are not limited to) Jin and Nasiri (2014), Naud and Kahn (2015), Kahn et al. (2015), Lubin et al. (2015), Kahn et al. (2017), Kahn et al. (2018), Thompson et al. (2018), Guillaume et al. (2019), McCoy et al. (2019), and Peterson et al. (2020).

Published studies that detail either the use or validation of **ice_cld_opt_depth**, **ice_cld_eff_diam**, and **ice_cld_eff_temp** — and their respective error estimates, averaging kernels, and prior guesses — include (but are not limited to) Kahn et al. (2015), Kahn et al. (2018), and Guillaume et al. (2019).

13.5 Recommended Papers

Guillaume, A., B. H. Kahn, E. J. Fetzer, Q. Yue, G. J. Manipon, B. D. Wilson, and H. Hua (2019), Footprint-scale cloud type mixtures and their impacts on Atmospheric Infrared Sounder cloud property retrievals, *Atmos. Meas. Tech.*, **12**, 4361–4377, https://doi.org/10.5194/amt-12-4361-2019.

Jin, H., and S. L. Nasiri. "Evaluation of AIRS cloud thermodynamic phase determination with CALIPSO." Journal of Applied Meteorology and Climatology (2013).

Kahn, B. H., F. W. Irion, V. T. Dang, E. M. Manning, S. L. Nasiri, C. M. Naud, J. M. Blaisdell et al. (2014), "The atmospheric infrared sounder version 6 cloud products." *Atmos. Chem. Phys* 14: 399-426.

Kahn, B. H., M. M. Schreier, Q. Yue, E. J. Fetzer, F. W. Irion, S. Platnick, C. Wang, S. L. Nasiri, and T. S. L'Ecuyer (2015), Pixel-scale assessment and uncertainty analysis of AIRS and MODIS ice cloud optical thickness and effective radius, *J. Geophys. Res.*, **120**, doi:10.1002/2015JD023950.

Kahn, B. H., G. Matheou, Q. Yue, T. Fauchez, E. J. Fetzer, M. Lebsock, J. Martins, M. M. Schreier, K. Suzuki, and J. Teixeira (2017), An A-train and MERRA view of cloud, thermodynamic, and dynamic variability within the subtropical marine boundary layer, *Atmos. Chem. Phys.*, **17**, 9451–9468, https://doi.org/10.5194/acp-17-9451-2017.

Kahn, B. H., H. Takahashi, G. L. Stephens, Q. Yue, J. Delanoë, G. Manipon, E. M. Manning, and A. J. Heymsfield (2018), Ice cloud microphysical trends observed by the Atmospheric Infrared Sounder, *Atmos. Chem. Phys.*, 1**8**, 10715–10739, https://doi.org/10.5194/acp-18-10715-2018.

Lubin, D., B. H. Kahn, M. A. Lazzara, P. Rowe, and V. P. Walden (2015), Variability in AIRS-retrieved cloud amount and thermodynamic phase over west versus east Antarctica influenced by the SAM, Geophys. Res. Lett., 42, doi:10.1002/2014GL062285.

McCoy, D. T., and Colleagues (2019), Cloud feedbacks in extratropical cyclones: insight from long-term satellite data and high-resolution global simulations, *Atmos. Chem. Phys*., **19**, 1147–1172, https://doi.org/10.5194/acp-19-1147-2019.

Naud, C. M., and B. H. Kahn (2015), Thermodynamic phase and ice cloud properties in northern hemisphere winter extratropical cyclones observed by Aqua AIRS, J. Appl. Meteor. Climatol., 54, 2283–2303, doi:10.1175/JAMC-D-15-0045.1.

Peterson, C. A.., Q. Yue, B. H. Kahn, E. J. Fetzer, and X. Huang (2020), Evaluation of AIRS Arctic Cloud Phase Classification against Combined CloudSat-CALIPSO Observations, *J. Appl. Meteor. Climatol.* (submitted)

Thompson, D. R., B. H. Kahn, R. O. Green, S. A. Chien, E. M. Middleton, and D. Q. Tran (2018), Global spectroscopic survey of cloud thermodynamic phase at high spatial resolution, 2005-2015, *Atmos. Meas. Tech.*, **11**, 1019–1030, https://doi.org/10.5194/amt-11-1019-2018.

13.6 Recommended Supplemental User Documentation

Overview_of_the_AIRS_Mission.pdf
V7_L2_Performance_Test_and_Validation_Report.pdf
V7_L2_Quality_Control_and_Error_Estimation.pdf
V7_L2_Standard_Pressure_Levels.pdf
V7_L2_Support_Pressure_Levels.pdf
V7_L2_Levels_Layers_Trapezoids.pdf
V7_Retrieval_Channel_Sets.pdf
V7_Retrieval_Flow.pdf

14 Ozone Retrievals

Standard product

Field Name	Dimension per FOV	Description
totO3Std	1	Retrieved Total Ozone Burden, (DU)
totO3StdErr	1	Error estimate, (DU)
totO3Std_QC	1	Quality flag (0,1,2)
O3VMRStd	StdPressureLay=28	Layer retrieved Ozone Volume Mixing Ratio Profile (vmr), (unitless)
O3VMRStdErr	StdPressureLay=28	Error estimate (vmr), (unitless)
O3VMRStd_QC	StdPressureLay=28	Quality flag array (0,1,2)
O3VMRLevStd	StdPressureLev=28	Level retrieved Ozone Volume Mixing Ratio Profile (vmr), (unitless)
O3VMRLevStdErr	StdPressureLev=28	Error estimate (vmr), (unitless)
O3VMRLevStd_QC	StdPressureLev=28	Quality flag array (0,1,2)
num_O3_Func	1	Number of valid entries in each dimension of O3_ave_kern
O3_verticality_20func	O3Func=20	Sum of rows of O3_ave_kern, (unitless)*
O3_dof	1	Degrees of freedom, measure of amount of information in O3 retrieval, (unitless)

Support Product (see Appendix A2 for a complete list of fields)

Field Name	Dimension per FOV	Description
O3CDSup	XtraPressureLay=100	Layer column ozone, (molecules/cm2)
O3CDSup_QC	XtraPressureLay=100	Quality flag array (0,1,2)
O3CDSupErr	XtraPressureLay=100	Error estimate for O3CDSup, (molecules/cm2)
O3VMRLevSup	XtraPressureLay=100	Ozone volume mixing ratio (vmr), (unitless)
O3VMRLevSup_QC	XtraPressureLay=100	Quality flag array (0,1,2)
O3VMRLevSupErr	XtraPressureLay=100	Error estimate for O3VMRLevSup
O3VMRSurf	1	Ozone Volume Mixing Ratio at the surface (vmr), (unitless) DO NOT USE FOR RESEARCH. Retrieval has no sensitivity at surface. Value is from the initial guess adjusted as higher levels are adjusted by the retrieval
O3VMRSurfErr	1	Error estimate (vmr), (unitless)
O3VMRSurf_QC	1	Quality flag (0,1,2)
O3_eff_press_20func	O3Func=20	Ozone effective pressure for the center of each trapezoid*
O3_VMR_eff_20func	O3Func=20	Effective ozone volume mixing ratio (vmr) for each trapezoid, (unitless)*
O3_VMR_eff_20func_QC	O3Func=20	Quality flag (0,1,2)*
O3_VMR_eff_20func_err	O3Func=20	Error estimate for O3_VMR_eff_20func (vmr) (unitless)*
O3_ave_kern_20func	O3Func*O3Func =20x20	Averaging kernel for ozone retrieval, located in the support product*
O3_trapezoid_layers_20func	O3Func=20	Layers on which the O3 variables are defined.

O3_Resid_Ratio	1	Internal retrieval quality indicator; residuals of O3 channels as compared to predicted uncertainty, located in support product (unitless)
O3CDInit	XtraPressureLay=100	Prior for ozone column density (molecules/cm2)

*NOTE: For V7, 20func has been added to the variable name so that user's V6 analysis software will not inadvertently use the new, differently dimensioned output.

14.1 Description

The AIRS ozone product is a product of the IR stage of the combined IR/MW retrieval. The **level** atmospheric ozone profile (**O3VMRLevStd**) is the retrieved mean volume mixing ratio at the pressure level upon which it is reported. For backward compatibility with V5, we also provide the **layer** atmospheric ozone profile (**O3VMRStd**), the retrieved mean volume mixing ratio (ratio of number of O_3 molecules to the number of molecules of air in a unit volume) between two **pressStd** levels, reported on the lower altitude pressure level bounding the layer. Standard pressure levels are arranged in order of decreasing pressure.

Level quantities are calculated from layer quantities by the procedure described in

V7_L2_Levels_Layers_Trapezoids.pdf

The derivation of level quantities from layer quantities is essentially done by interpolation with smoothing kernels.

The ozone products are reported on all levels and layers above the surface. The **O3VMRStd** quoted on the lowest altitude pressure level above the surface (index = **nSurfStd**, which may be 1, 2, …, 15) is the mean volume mixing ratio in the layer bounded by the next higher level and the surface, i.e. the layer will be slightly thicker or thinner than the pressure on which it is quoted indicates and the lower bound pressure is actually **PSurfStd**.

totO3Std is the integrated column amount of O_3 from the top of the atmosphere (TOA = 0.005 hPa) to the surface. This quantity is computed by summing the 100 column density values, **O3CDSup,** contained in the AIRS Level 2 Support Products file with the appropriate weighting applied to the bottom layer which contains the surface. Layers below the surface are not included in this sum.

In the retrievals, trapezoidal layers are used, which have associated averaging kernels, verticality and degrees of freedom. In Version 7, 20 vertical trapezoids are used, allowing more shape in the O_3 retrieval as compared to the 9 vertical trapezoids used in Version 6. In addition, the profile is fixed above 1 mb to the first guess values as we have little sensitivity there and Version 6 products were observed to automatically follow the ozone changes at other levels. Variables whose dimensions are sensitive to this change from 9 to 20 functions have been renamed by inserting "20func" as part of the name to reduce the possibility of interpreting them with the wrong dimension.

O3_verticality_20func is a 20-point vector computed by summing the columns of the 20x20 O_3 averaging kernel, **O3_avg_kern_20func**, stored in the AIRS Level 2 Support Product. The associated 20-point pressure array is provided in **O3_eff_press_20func**. The peak value of **O3_verticality_20func** indicates the vertical location of the maximum sensitivity of the O_3 product and the width of this peaked function qualitatively describes the vertical resolution of the retrieval. The magnitudes of **O3_verticality_20func** are a rough measure of the fraction of the retrieval determined from the data as opposed to the first guess. A value near unity indicates the retrieval is highly determined by the radiance measurements and thus has high information content. A smaller value indicates the retrieval contains a large fraction of the first guess.

O3_dof is the number of degrees of freedom which is also a measure of the amount of information in the retrieval. It is computed as the sum of the diagonal elements (trace) of the 20x20 O_3 averaging kernel, **O3_avg_kern_20func**

NOTE: the problem with associating the verticality with a total column averaging kernel is that it neglects the fact that the retrieval can only move as superpositions of the trapezoids. Convolution using the verticality alone will not account for the possibility that the "independent O_3 profile" contains structure that the trapezoids cannot resolve.

O3CDSup provides the retrieved O_3 column density on 100 pressure levels used internally in the physical retrieval. **O3VMRLevSup** provides a smoothed version of this profile but in units of VMR and on 100 levels.

O3_VMR_eff is contained in the AIRS Level 2 Support Products file and is the retrieved volume mixing ratio (ratio of number of O_3 molecules to the number of molecules of air in a unit volume) for a layer defined by the faces of an O_3 trapezoidal retrieval function. The boundaries of faces of these layers are specified in **O3_trapezoid_layers** in which is an array of 1-based **pressSup** level indices. **O3_eff_press_20func** provides the effective pressure for each trapezoid. There are 20 such trapezoidal layers corresponding to the 20 trapezoidal retrieval functions utilized for O_3.

NOTE: **num_O3_Func** provides the number of valid entries in each dimension of **O3_ave_kern_20func**. Topography limits the number of valid O_3 averaging kernel trapezoids.

Please see the following documents for more details on various aspects of the vertical representation of ozone and other AIRS products:

V7_L2_Standard_Pressure_Levels.pdf
V7_L2_Support_Pressure_Levels.pdf
V7_L2_Levels_Layers_Trapezoids.pdf

The ozone first guess is an observationally-based climatology analogous to that developed for Version 8 TOMS and SBUV [McPeters et al., 2007], but updated to include data through 2011, categorized into ozone hole and non-hole profiles. The updated climatology data can be found at:

https://acd-ext.gsfc.nasa.gov/anonftp/toms/Labow_climatology

A detailed discussion of the methodology used in this climatology is contained in McPeters & Labow (2012). On a profile-by-profile basis, we select which of the two profile shapes (ozone hole or non-hole) to begin the retrieval based on the 50 hPa temperature given by the neural network guess. The cutoff temperature for selecting which ozone vertical profile to use rises during the austral spring. While this is only a first guess to the retrieval process, the new profile shape is significantly better in many cases and carries over into improved retrieved ozone profiles because we do not have sufficient vertical resolution to resolve the vertical discontinuities in an ozone hole profile. The climatology is month-by-month on 10° latitude bins from 85S to 85N. The ozone first guess for V7 is thus updated from that used for V6. This newer climatology was generated on the 100 pressure layers in the Level 2 Support Pressure array.

The climatology is then interpolated in latitude and time to the particular profile. (Version 6 did not do a time interpolation.) An adjustment is then made to align the tropopause of the guess to the tropopause of the neural network temperature profile. This adjusted guess, which is the prior for the retrieval, is contained in **O3CDInit**.

In addition to changes to the trapezoids described above, several other changes have been made for the ozone retrievals in Version 7, as compared to the previous Version 6. A total of 65 channels are used for Version 7, compared to 41 channels used in the Version 6 retrieval. Their selection includes the peak of the P-branch in the ozone 10 μm band. In cases where there is little contrast between the surface and the stratosphere, the peak channels are now omitted from the retrieval since their inclusion had led to spurious results requiring damping in Version 6. The "noise propagation threshold," DB_{max}, discussed in Susskind et al. [2003], has been significantly increased since Version 6, resulting in less damping of the final profile. An additional important update is that the ozone retrieval simultaneously solves for the surface emissivity in the ozone band at two hinge points. This primarily improves results over desert and ice.

The damping was decreased everywhere and was made spatially variable in a simple way, reducing the damping even further during summer months in mid-latitude and polar regions, recognizing that very large excursions from the first guess are normal in propagating waves during those months. This enabled a much better match to OMPS data, although we still do not reach the OMPS values in the most extreme cases.

Surface emissivity noise covariance contribution was removed from the ozone retrieval, since emissivity is now part of the solution space. The water noise covariance contribution was also removed because it was found that this reduced the overdamping present in all previous versions. We believe we have a reasonable balance now between the climatological prior and the radiances.

Figure 3 shows the total ozone retrieved for an August day in two recent years, compared to the OMPS results, as a representation of extending knowledge of the ozone hole southwards.

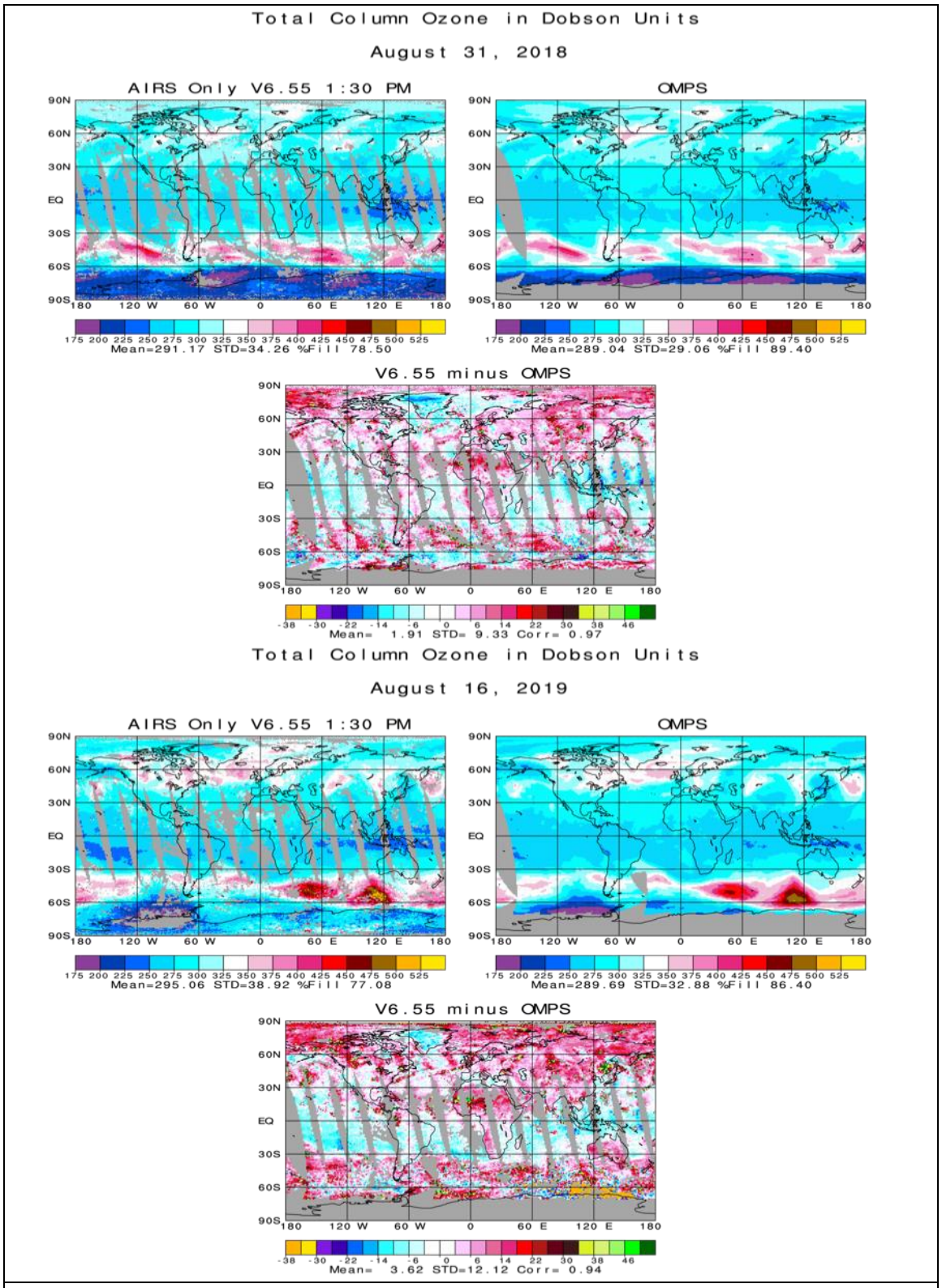

Figure 3: Total Ozone Retrieval for August 31, 2018 and August 16, 2019 with comparison to OMPS total ozone.

AIRS Version 6.55 was the developmental version chosen to become Version 7.

14.2 Type of Product

O3VMRLevStd is a **level** quantity and so values represent the concentration at the pressure level upon which they are reported. **O3VMRStd** is a **layer** quantity, i.e., the values are reported on the fixed pressure levels but represent the layer bounded by the level on which they are reported and the next higher level (in altitude).

For more detail, see **V7_L2_Levels_Layers_Trapezoids.pdf** for a full discussion of level and layer quantities.

14.3 Quality Indicators

The user is encouraged to read the QC and error estimation document:

V7_L2_Quality_Control_and_Error_Estimation.pdf

The ozone quality control has been completely revised for version 7, recognizing that small inaccuracies in the lower troposphere do not necessarily contribute to inaccuracies in the total ozone column.

Quality control specific to ozone was added. We reject the ozone retrieval for the following four reasons, which reduces the overall Level 2 yield by 10-15%, but only rarely results in noticeable gaps in the Level 3 gridded product.

a) If the attempted change on the first iteration is too large. The temperature or water profiles may be in error, and the ozone retrieval may try to fix it with the ozone profile
b) If radiative closure is not achieved in the ozone channels. This usually happens because the surface temperature is grossly in error, and off-diagonal elements in the noise covariance matrix correctly reflect this, but the ozone retrieval is still poor in these cases.
c) If the UMBC dust test indicates the presence of significant dust. Over both land and ocean these retrievals can be erroneous.
d) If the change in emissivity from the first guess is very different in the ozone spectral region and the adjacent spectral regions. This test identified some spurious retrievals missed by the dust test.

14.4 Validation

V7 validation results are partially summarized in

V7_L2_Performance_Test_and_Validation_Report.pdf

14.5 Caveats

This section will be updated over time as V7 data products are analyzed and validated.

All **O3*_QC** flag are set to 0 if **PGood**=**PSurfStd**. We do not distinguish portions of the ozone profile as being of different qualities because all ozone channels sense the surface

as well atmospheric ozone and thus are sensitive to the entire profile's quality is compromised if the surface is not well characterized.

Errors in temperature profiles and water vapor mixing ratios will adversely affect the ozone retrieval. Significant biases (0 - 100%) may exist in the region between ~300 hPa and ~80 hPa; such biases currently being evaluated. Ozone mixing ratio data may not be reliable at pressures greater than 300 hPa or if the tropospheric mixing ratio is less 100 ppbv, however results may be qualitatively correct under conditions of high upper tropospheric ozone (such as in a tropopause fold). Mixing ratios and columns should not be considered reliable under conditions of very low skin temperatures (< 240 K).

The error fields, including **O3VMRLevStdErr**, **O3VMRStdErr, O3VMRLevSupErr, O3CDSupErr** and **totO3StdErr**, are fixed as a fraction of the ozone amount and should not be used.

The ozone first guess used to initialize the V5 retrieval is likely too high at pressures below ~0.5 hPa (altitudes above ~55 km) due to an error in extrapolation in its creation. This has a negligible effect on **totO3Std** and the portion of **O3VMRStd** profile at pressures greater than 0.5 hPa. At pressures lower than 0.5 hPa, biases in **O3VMRStd** are estimated to be between ~10% to ~50%. The extrapolation error occurs in the lowest 6 pressure levels of the support pressure level array (i.e., in the Level 2 Support Product **O3CDSup** array elements 1, 2, 3, 4, 5 and 6.

14.6 Suggestions for Researchers

This section will be updated over time as V7 data products are analyzed and validated.

V7 is a significant improvement over V6, but there are still problems under certain conditions, when the surface skin temperature does not compare well to AMSR-E or the scene has a significant cloud amount.

14.7 Recommended Papers

This section will be updated over time as research with V7 data products are published.

Bian J., A. Gettelman, H. Chen, L. L. Pan (2007), Validation of satellite ozone profile retrievals using Beijing ozonesonde data, J. Geophys. Res., 112, D06305, doi:10.1029/2006JD007502.

Brasseur, G. P., Hauglustaine, D. A., Walters, S., Rasch, P. J., Muller, J. F., Granier, C. and Tie, X. X.: MOZART, a global chemical transport model for ozone and related chemical trac- ers 1. Model description, J. Geophys. Res.-Atmos., 103(D21), 28 265–28 289, 1998.

Chen, Francis, Miller (2002), Surface temperature of the Arctic: Comparison of TOVS satellite retrievals with surface observations, J. Climate, 15, 3698–3708. DOI: 10.1175/1520-0442(2002)015<3698:STOTAC>2.0.CH4;2

Divakarla, M., C. Barnet, M. Goldberg, E. Maddy, F. Irion, M. Newchurch, XP. Liu, W. Wolf, L. Flynn, G. Labow, XZ. Xiong, J. Wei, LH. Zhou, LH (2008), Evaluation of Atmospheric Infrared Sounder ozone profiles and total ozone retrievals with matched ozonesonde measurements, ECMWF ozone data, and Ozone Monitoring Instrument retrievals, J. Geophys. Res., 113, D15308 DOI:10.1029/2007JD009317.

Goldberg, M. D., Y. Qu, L. M. McMillin, W. Wolf, L. Zhou and M. Divakarla (2003), AIRS near-real-time products and algorithms in support of operational numerical weather prediction, IEEE. Trans. Geosci. Remote Sens., 41 (2), 379-389.

Kim, B., and S. Sarkar (2017), Impact of wildfires on some greenhouse gases over continental USA: A study based on satellite data, Remote Sensing of Environment, 188, 118-126. http://dx.doi.org/10.1016/j.rse.2016.10.047.

Levelt, P. F., et al. (2006), Science objectives of the Ozone Monitoring Instrument, IEEE Trans. Geosci. Remote Sens., 44, 1199-1208.

McPeters, R. D., J. A. Logan, G. J. Labow (2007), Ozone Climatological Profiles for Satellite Retrieval Algorithms, J. Geophys. Res., 112, D05308, 10.1029/2005JD006823

Morris G. A., et al. (2006), Alaskan and Canadian forest fires exacerbate ozone pollution over Houston, Texas, on 19 and 20 July 2004, J. Geophys. Res., 111, D24S03, doi:10.1029/2006JD007090.

McPeters, R. D., and Labow, G. J. (2012), Climatology 2011: An MLS and sonde derived ozone climatology for satellite retrieval algorithms, J. Geophys. Res., 117, D10303, doi:10.1029/2011JD017006.

Pittman, J. V., L. L. Pan, J. C. Wei, F. W. Irion, X. Liu, E. S. Maddy, C. D. Barnet, K. Chance, R. S. Gao (2009), Evaluation of AIRS, IASI, and OMI ozone profile retrievals in the extratropical tropopause region using in situ aircraft measurements, J. Geophys. Res., 114, D24109, 10.1029/2009JD012493.

Sitnov, S. A., and I. I. Mokhov (2016), Satellite-derived peculiarities of total ozone field under atmospheric blocking conditions over the European part of Russia in summer 2010, Russian Meteorology and Hydrology 41.1: 28-36. doi: http://dx.doi.org/10.3103/S1068373916010040.

Susskind, J., C. D. Barnet, and J. M. Blaisdell (2003), Retrieval of atmospheric and surface parameters from AIRS/AMSU/HSB data in the presence of clouds, IEEE Trans. Geosci. Remote Sens., 41 (2), 390 – 409.

Tian B., Y. L. Yung, D. E. Waliser, T. Tyranowski, L. Kuai, E. J. Fetzer, F. W. Irion (2007), Intraseasonal variations of the tropical total ozone and their connection to the Madden-Julian Oscillation, Geophys. Res. Lett., 34, L08704, doi:10.1029/2007GL029451.

Wang, H., X. Zou, G. Li, 2012: An Improved Quality Control for AIRS Total Column Ozone Observations within and around Hurricanes. J. Atmos. Oceanic Technol., 29, 417-432. http://dx.doi.org/10.1175/JTECH-D-11-00108.1

Wei, Jennifer C., Laura L. Pan, Eric Maddy, Jasna V. Pittman, Murty Divarkarla, Xiaozhen Xiong, Chris Barnet, 2010: Ozone Profile Retrieval from an Advanced Infrared

Sounder: Experiments with Tropopause-Based Climatology and Optimal Estimation Approach. J. Atmos. Oceanic Technol., 27, 1123-1139. doi: http://dx.doi.org/10.1175/2010JTECHA1384.1

Ziemke, J. R., S. Chandra, and P. K. Bhartia (2001), "Cloud slicing": A new technique to derive upper tropospheric ozone from satellite measurements, J. Geophys. Res., 106 (D9), 9853-9867.

14.8 Recommended Supplemental User Documentation

Overview_of_the_AIRS_Mission.pdf
V7_L2_Performance_Test_and_Validation_Report.pdf
V7_L2_Quality_Control_and_Error_Estimation.pdf
V7_L2_Standard_Pressure_Levels.pdf
V7_L2_Support_Pressure_Levels.pdf
V7_L2_Levels_Layers_Trapezoids.pdf
V7_Retrieval_Channel_Sets.pdf
V7_Retrieval_Flow.pdf

15 Carbon Monoxide Retrievals

Standard Product

Field Name	Dimension per FOV	Description
CO_total_column	1	Retrieved total column CO, (molecules/cm2) DO NOT USE FOR RESEARCH
CO_total_column_QC	1	Quality flag (0,1,2)
COVMRLevStd	StdPressureLev=28	Level retrieved CO Volume Mixing Ratio Profile (vmr), (unitless)
COVMRLevStd_QC	StdPressureLev=28	Quality flag array (0,1,2)
COVMRLevStdErr	StdPressureLev=28	Error estimate for COVMRLevStd, Volume Mixing Ratio Profile (vmr), (unitless)
num_CO_Func	1	Number of valid entries in each dimension of CO_ave_kern
CO_verticality	COFunc=9	Sum of rows of CO_ave_kern, (unitless)
CO_dof	1	Degrees of freedom, measure of amount of information in CO retrieval, (unitless)

Support Product (see Appendix A2 for a complete list of fields)

Field Name	Dimension per FOV	Description
CO_trapezoid_layers	COFunc=9	1-based Index of **pressSup** array giving element defining lower altitude bound of trapezoid on which the CO variables are defined, located in support product (unitless)
CO_eff_press	COFunc=9	CO effective pressure for the center of each trapezoid, located in support product. These CO trapezoids were chosen to approximately match MOPITT standard levels, (hPa)
COCDSup	XtraPresureLev=100	Layer column carbon monoxide in molecules/cm2 (climatology when bad_co $\neq$ 0)
COCDSup_QC	XtraPresureLev=100	Quality flag array (0,1,2)
COCDSup_Err	XtraPresureLev=100	Error estimate for COCDSup
COVMRLevSup	XtraPresureLev=100	CO Volume Mixing Ratio at support levels (vmr) (unitless)
COVMRLevSup_QC	XtraPresureLev=100	Quality flag array (0,1,2)
COVMRLevSupErr	XtraPresureLev=100	Error estimate for COVMRLevSup
COVMRSurf	1	CO Volume Mixing Ratio at the surface (vmr) (unitless) DO NOT USE FOR RESEARCH. Retrieval has no sensitivity at surface. Value is from the initial guess
COVMRSurf_QC	1	Quality flag array (0,1,2)
COVMRSurfErr	1	Error estimate for COVMRSurf
CO_VMR_eff	COFunc=9	Effective CO Volume Mixing Ratio Profile (vmr) for each trapezoid, located in support product (unitless)
CO_VMR_eff_QC	COFunc=9	Quality flag array (0,1,2)
CO_VMR_eff_err	COFunc=9	Error estimate (vmr), located in support product (unitless)
CO_ave_kern	COFunc*COFunc =9x9	Averaging kernel for CO retrieval, located in support product

15.1 Description

The AIRS carbon monoxide product is a product of the IR stage of the combined IR/MW retrieval. A volume mixing ratio profile on the 28 standard pressure levels, **pressStd**, is provided in the Level 2 Standard Product. Level and layer profiles on the 100 support pressure levels, **pressSup**, are provided in the Level 2 Support Product.

The peak sensitivity of the AIRS retrieval to CO occurs at 500 hPa. The AIRS retrieval is not sensitive to this atmospheric constituent near the surface.

For the first guess profiles for the Version 7 CO retrieval, MOZART model profiles that are based on MOPITT observations are used. Separate monthly profiles for the northern and southern hemisphere are used, and an interpolation is made in the latitude transition region between 15N and 15S. A short description with the northern and southern hemisphere profiles is provided in the document:

V7_CO_Initial_Guess_Profiles.pdf

The northern and southern hemisphere profiles are monthly averages and a temporal interpolation is performed to obtain a value for any day of the year. The monthly average profile values are set to the middle day of the given month, and a linear interpolation between the monthly averages is used for any other days.

COVMRLevStd and **COVMRLevSup** are **level** quantities providing the retrieved carbon monoxide volume mixing ratio (ratio of number of CO molecules to the number of molecules of air in a unit volume) at the pressure levels upon which they are reported. The former is in the standard product and the latter is in the support product. Standard pressure levels are arranged in order of decreasing pressure and support pressure levels are arranged in order of increasing pressure.

COCDSup is a **layer** quantity in the support product providing the retrieved CO layer column density (number of CO molecules/cm^2) between two **pressSup** levels and is reported on the lower altitude pressure level bounding the layer.

Level quantities are calculated from layer quantities by the procedure described in

V7_L2_Levels_Layers_Trapezoids.pdf

The derivation of level quantities from layer quantities is essentially done by interpolation with smoothing kernels. The above document also contains a discussion of vertical representation in AIRS retrievals in terms of trapezoidal layers and associated averaging kernels, verticality and degrees of freedom.

CO_eff_press is defined as the pressure weighted center of the trapezoid layers, i.e.,

$$\text{CO_eff_press} = \frac{\left[P_{bottom} - P_{top}\right]}{\log\left(P_{bottom} / P_{top}\right)}$$

where P_{bottom} is the bottom pressure of a trapezoid face and P_{top} is the top pressure. These trapezoid layers were chosen so that the **CO_eff_press** match as closely as possible to the standard pressure levels used by MOPITT and to optimize the AIRS CO retrieval.

CO_VMR_eff is a **layer** quantity contained in the support product providing the retrieved volume mixing ratio (ratio of number of CO molecules to the number of molecules of air in a unit volume) for a layer defined by the faces of a CH4 trapezoidal retrieval function. The boundaries of faces of these layers are specified in **CO_trapezoid_layers** in which is an array of 1-based **pressSup** level indices. There are 9 such trapezoidal layers corresponding to the 9 trapezoidal retrieval functions utilized for CO (see Figure 4). **CO_VMR_eff** is reported at the effective trapezoid layer, **CO_eff_press**(**CO_trapezoid_layers**). It is computed from the integrated CO column density for the trapezoidal layer. Layers below the surface are filled with -9999. The value quoted on the lowest layer above the surface is the mean mixing ratio in the layer bounded by the next higher level and the surface. See

V7_L2_Support_Pressure_Levels.pdf
V7_L2_Levels_Layers_Trapezoids.pdf

CO_VMR_eff_err is the estimated error in CO mixing ratio due to the retrieved errors in temperature, water vapor and surface temperature as derived by Comer (2006) and McMillan (2011). This error is computed on the **pressSup** layers and then averaged to the CO trapezoids.

COVMRSurf is a **level** quantity in the support product providing the retrieved CO volume mixing ratio at the surface. Note that the AIRS retrieval primarily returns climatology in the lower troposphere and use of **COVMRSurf** in research is not recommended.

CO_total_column is the integrated column amount of CO from the top of the atmosphere (TOA = 0.005 hPa) to the surface. This quantity is computed by summing the 100 column density values, **COCDsup,** contained in the AIRS Level 2 Support Products file with the appropriate weighting applied to the bottom layer which contains the surface. Layers below the surface are not included in this sum. The reported total column is dominated by the initial guess and should not be used for research.

CO_verticality is a 9-point vector computed by summing the columns of the 9x9 CO averaging kernel, **CO_ave_kern**, stored in the AIRS Level 2 Support Product. The associated 9-point pressure array is provided in **CO_eff_press**. The peak value of **CO_verticality** indicates the vertical location of the maximum sensitivity of the CO product and the width of this peaked function qualitatively describes the vertical resolution of the retrieval. The magnitudes of **CO_verticality** are a rough measure of the fraction of the retrieval determined from the data as opposed to the first guess. A value near unity indicates the retrieval is highly determined by the radiance measurements and thus has high information content. A smaller value indicates the retrieval contains a large fraction of the first guess.

CO_dof is the number of degrees of freedom which is also a measure of the amount of information in the retrieval. It is computed as the sum of the diagonal elements (trace) of the 9x9 CO averaging kernel, **CO_avg_kern**. Version 5 validation and optimization studies (Comer, 2006) showed that **CO_dof** < 0.4 indicates little information in the retrieval comes from the measured radiances. Profiles for which 0.5 > **CO_dof** > 0.4 should be used with great caution.

NOTE: **num_CO_Func** provides the number of valid entries in each dimension of **CO_ave_kern**. Topography limits the number of valid CO averaging kernel trapezoids.

NOTE: the problem with associating the verticality with a total column averaging kernel is that it neglects the fact that the retrieval can only move as superpositions of the trapezoids. Convolution using the verticality alone will not account for the possibility that the "independent CO profile" contains structure that the trapezoids can or cannot resolve.

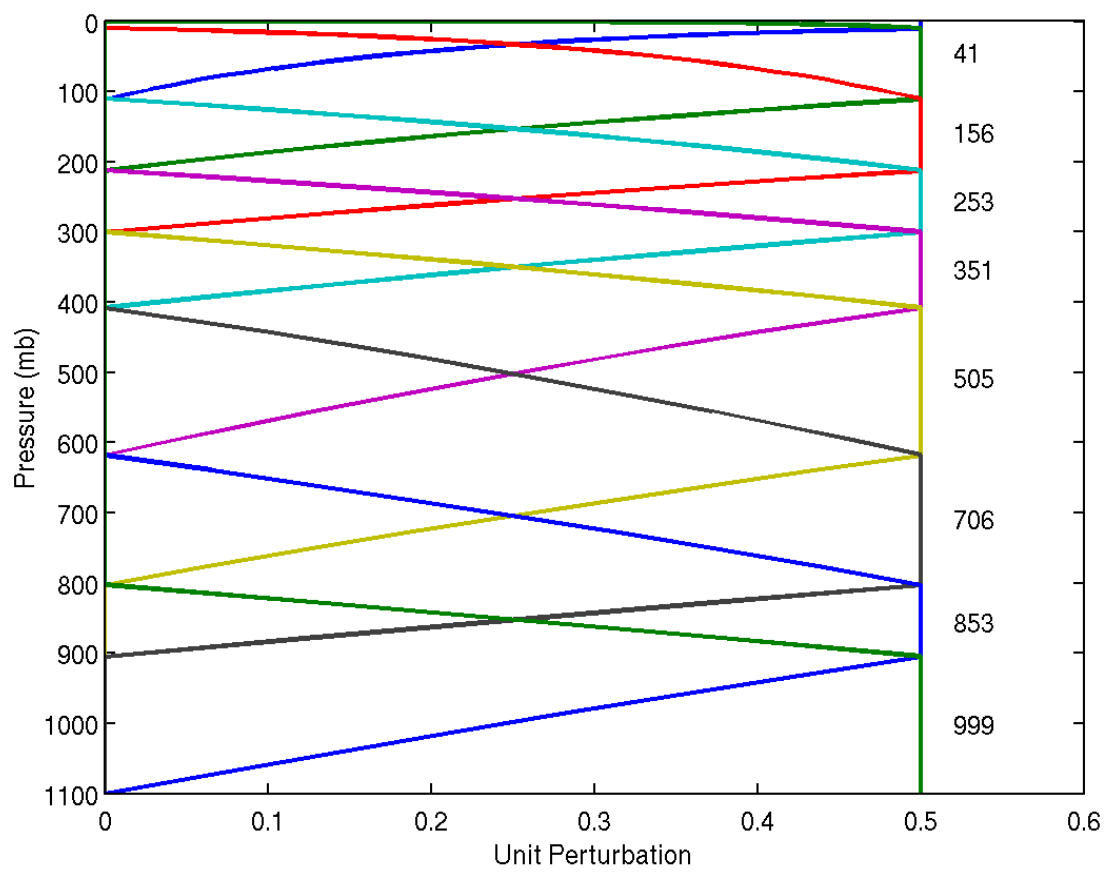

Figure 4: The 9 CO trapezoids.
Values at right are **CO_eff_press** for each. (Wallace McMillan)

15.2 Type of Product

The standard CO product profile is a level quantity, i.e. the values represent the volume mixing ratio at the pressure level on which they are reported.

15.3 Quality Indicators

The user is encouraged to read the QC and error estimation document:

V7_L2_Quality_Control_and_Error_Estimation.pdf

- If **PGood = PSurfStd**, and **CO_dof** > 0.5, then all CO products are marked Quality = 0.
- If **PGood = PSurfStd**, and 0.5 >= **CO_dof** > 0.4, then all CO products are marked Quality = 1.
- Otherwise, all CO products are marked Quality = 2.

15.4 Validation

The peak sensitivity of the AIRS retrieval to CO occurs at 500 hPa. The AIRS retrieval is not sensitive to this atmospheric constituent near the surface; therefore, we have chosen to evaluate Version 6 (V6) and Version 7 (V7) at 500 hPa. Figure 5 shows monthly mean AIRS CO VMR at 500 hPa for January and July. The spatial patterns and seasonal variability are very similar for V6 (Figure 5, top panels) and V7 (Figure 5, middle panels). Differences between V6 and V7 CO are minimal (Figure 5, bottom panel); any differences in the CO product are associated with differences that propagate through from updates to the temperature and water vapor retrieval, since no updates were made in V7 to the initial guess profile, or to CO absorption. (Note that there was a major change in V6 to the first guess CO profile compared to v5, where instead of a constant guess, different guesses were/are used in the northern and southern hemispheres, smoothly varying across the tropics. This guess is based on monthly climatologies.)
The AIRS CO retrieval has approximately 0.5 to 1.0 Degrees of Freedom for Signal (DOFS); the DOFS vary temporally and spatially, with the lowest values over high latitudes, and highest values over seasonally changing sections of Africa and the Middle East (Figure 6). There are fairly low DOFS (less than 0.5) over Amazonia in January and April, possibly due to greater cloud cover in the rainy season. There were insignificant changes in DOFS between V6 and V7.

Changes from V6 to V7 and validation of many V7 products, including for temperature and water vapor retrievals, are covered in

V7_L2_Performance_Test_and_Validation_Report.pdf

Further testing of V7 products, including for CO, will be published in a supplement to this report.

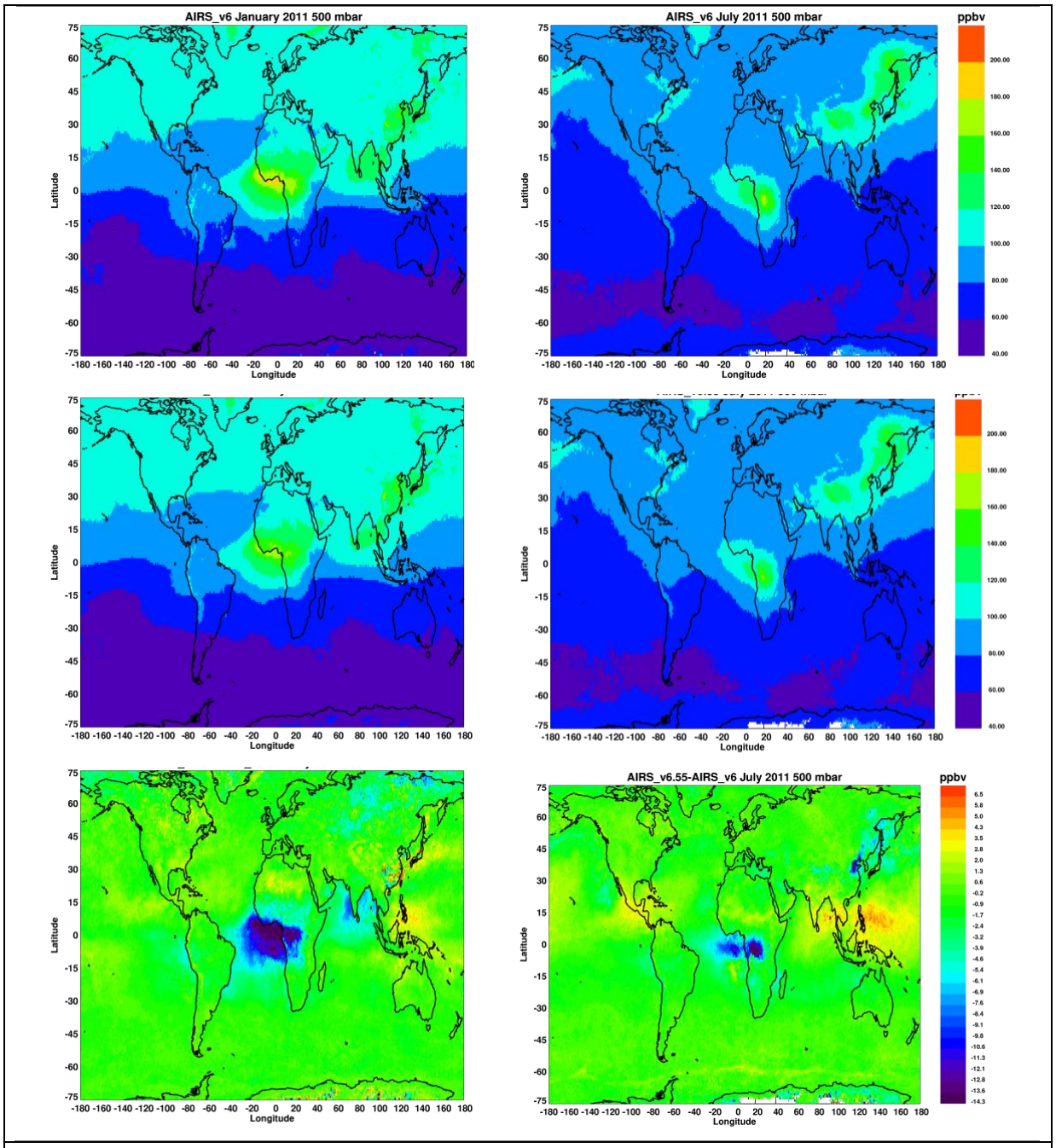

Figure 5: Comparison of the V6 and V7 global distribution of CO VMR at 500 hPa.
Left Column: January 2011; Right Column: July 2011
Top Row: V6; Middle Row: V7; Bottom Row: V7-V6
Note: Version 6.55 (in plot title) was the developmental version chosen to become Version 7.

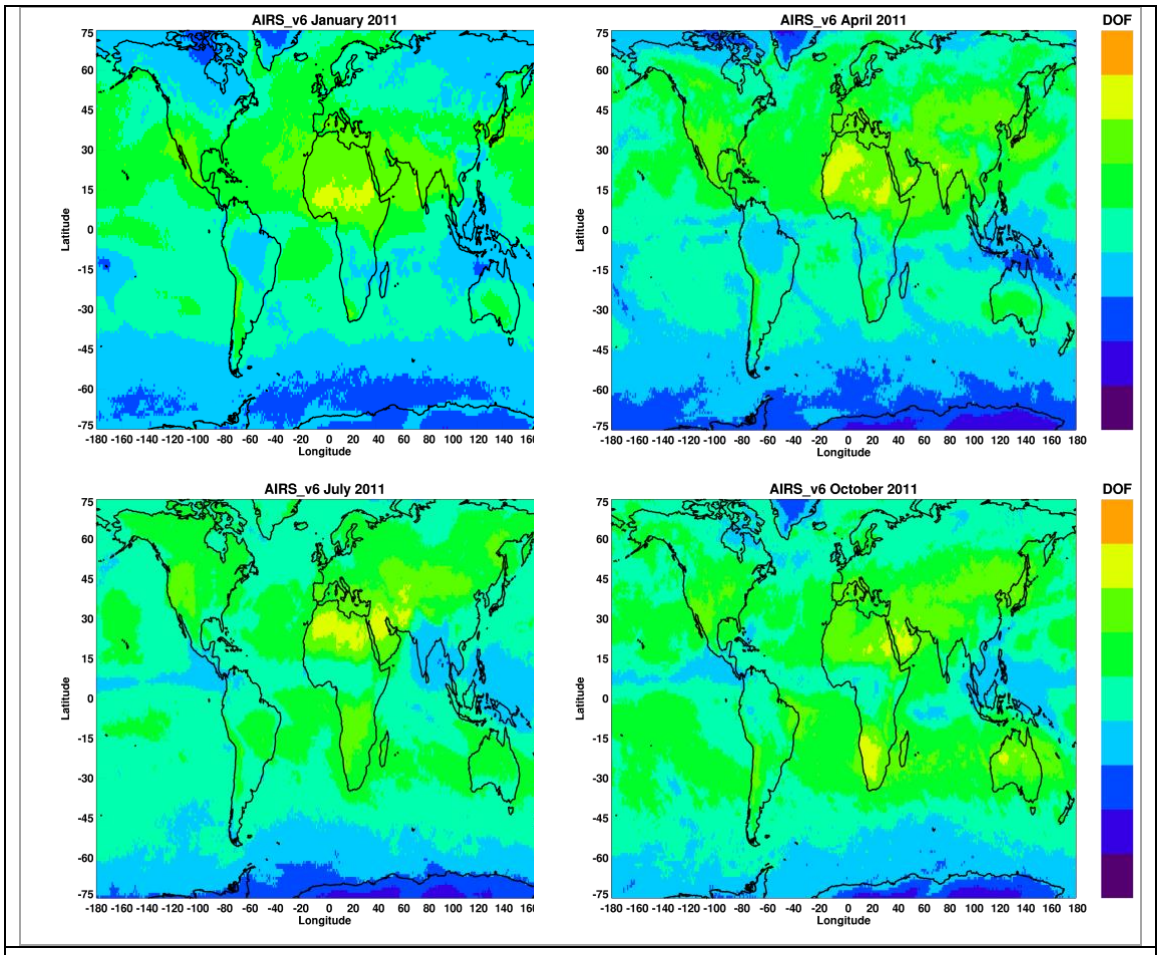

Figure 6: DOFS for AIRS CO V6.

15.5 Caveats

This section will be updated over time as V7 data products are analyzed and validated.

AIRS radiances provide little or no information about the vertical distribution of CO in the lower troposphere, and the AIRS retrieval algorithm primarily returns climatology. The AIRS project does not recommend doing science with the AIRS-derived lower-tropospheric CO.

The total column CO is dominated by the initial guess and thus should not be used for research.

Quality control is set to 0 if **PGood = PSurfStd** and the final IR retrieval is the atmospheric state of the reported products and **CO_dof** > 0.5.

15.6 Suggestions for Researchers

This section will be updated over time as V7 data products are analyzed and validated.

We are still assessing the derived error fields for quality control of V7 CO retrievals, but have erred on the conservative side to provide the best possible data.

We recommend that researchers pre-filter retrievals by requiring
(**PsurfStd** – **PBest**) < 200 hPa
and then filtering further by requiring Quality control = 0.

We strongly urge caution in using any retrievals for which Quality control > 0. We suggest that trapezoids for which **CO_VMR_eff_err** is negative or greater than 50% of **CO_VMR_eff** should be excised.

15.7 Recommended Papers

This section will be updated over time as research with V7 data products are published.

Brasseur, G. P., Hauglustaine, D. A., Walters, S., Rasch, P. J., Muller, J. F., Granier, C. and Tie, X. X. (1998), MOZART, a global chemical transport model for ozone and related chemical tracers 1. Model description, J. Geophys. Res.-Atmos., 103(D21), 28 265–28 289.

Comer, M.M. (2006), Retrieving Carbon Monoxide Abundances from the Atmospheric Infrared Sound, PhD dissertation, Department of Physics, University of Maryland Baltimore County.

Devasthale, A., M. A. Thomas (2012), An investigation of statistical link between inversion strength and carbon monoxide over Scandinavia in winter using AIRS data, Atmos. Environ., 56, 109-114, http://dx.doi.org/10.1016/j.atmosenv.2012.03.042.

Fisher, J. A., D. J. Jacob, M. T. Purdy, M. Kopacz, P. Le Sager, C. Carouge, C. D. Holmes et al. (2010), "Source attribution and interannual variability of Arctic pollution in spring constrained by aircraft (ARCTAS, ARCPAC) and satellite (AIRS) observations of carbon monoxide." Atmospheric Chemistry & Physics 10, pp 977-996.

Freitas S. R., K. M. Longo, M. O. Andreae (2006), Impact of including the plume rise of vegetation fires in numerical simulations of associated atmospheric pollutants, Geophys. Res. Lett., 33, L17808, doi:10.1029/2006GL026608.

Kopacz, Monika, D. J. Jacob, J. A. Fisher, J. A. Logan, Lin Zhang, I. A. Megretskaia, R. M. Yantosca et al. (2010), "Global estimates of CO sources with high resolution by adjoint inversion of multiple satellite datasets (MOPITT, AIRS, SCIAMACHY, TES)." Atmos. Chem. Phys 10, no. 3, pp 855-876.

Huang, M., et al. (2017), Impact of intercontinental pollution transport on North American ozone air pollution: an HTAP phase 2 multi-model study, Atmospheric Chemistry and Physics, 17(9), 5721-5750. http://dx.doi.org/10.5194/acp-17-5721-2017

Kim, P. S., D. J. Jacob, X. Liu, J. X. Warner, K. Yang, K. Chance, V. Thouret, and P. Nedelec. "Global ozone–CO correlations from OMI and AIRS: constraints on tropospheric ozone sources." Atmospheric Chemistry and Physics 13, no. 18 (2013): 9321-9335.

Kim, B., and S. Sarkar (2017), Impact of wildfires on some greenhouse gases over continental USA: A study based on satellite data, Remote Sensing of Environment, 188, 118-126. http://dx.doi.org/10.1016/j.rse.2016.10.047.

Kumar, A., Wu, S., Weise, M. F., Honrath, R., Owen, R. C., Helmig, D., Kramer, L., Val Martin, M., and Li, Q.: Free-troposphere ozone and carbon monoxide over the North Atlantic for 2001–2011, Atmos. Chem. Phys., 13, 12537-12547, doi:10.5194/acp-13-12537-2013, 2013.

McMillan W. W., C. Barnet, L. Strow, M. T. Chahine, M. L. McCourt, J. X. Warner, P. C. Novelli, S. Korontzi, E. S. Maddy, S. Datta (2005), "Daily global maps of carbon monoxide from NASA's Atmospheric Infrared Sounder", Geophys. Res. Lett., 32, L11801, doi:10.1029/2004GL021821.

McMillan, W. W., R. B. Pierce, L. C. Sparling, G. Osterman, K. McCann, M. L. Fischer, B. Rappenglueck et al. (2010), "An observational and modeling strategy to investigate the impact of remote sources on local air quality: A Houston, Texas, case study from the Second Texas Air Quality Study (TexAQS II)." Journal of Geophysical Research 115, no. D1, pp D01301.

McMillan, W. W., Keith D. Evans, Christopher D. Barnet, Eric S. Maddy, Glen W. Sachse, and Glenn S. Diskin (2011), Validating the AIRS Version 5 CO Retrieval With DACOM *In Situ* Measurements During INTEX-A and –B, IEEE Trans. on Geosci. Remote Sensing, 10.1109/TGRS.2011.2106505, 2011

Nara,Hideki; Tanimoto,Hiroshi; Nojiri,Yukihiro; Mukai,Hitoshi; Zeng,Jiye; Tohjima,Yasunori; Machida,Toshinobu, Emissions from biomass burning in South-east Asia in the 2006 El Nino year: shipboard and AIRS satellite observations, Environmental Chemistry, 2011, 8, 2, 213-223 http://dx.doi.org/10.1071/EN10113

Sachse, G. W., Hill, G. F., Wade, L. O., and Perry, M. G. (1987), Fast-response, high-precision carbon monoxide sensor using a tunable diode laser absorption technique, J. Geophys. Res., 92, 2071–2081.

Singh, H. B., Brune, W. H., Crawford, J. H., Flocke, F., and Jacob, D. J. (2009), Chemistry and transport of pollution over the Gulf of Mexico and the Pacific: Spring 2006 INTEX-B Campaign overview and first results, Atmos. Chem. Phys. Discuss., 9, 363-409.

Thonat, T., C. Crevoisier, N. A. Scott, A. Chedin, T. Schuck, R. Armante, and L. Crepeau (2012), Retrieval of tropospheric CO column from hyperspectral infrared sounders - application to four years of Aqua/AIRS and MetOp-A/IASI, Atmospheric Measurement Techniques, 5(10), 2413-2429, http://dx.doi.org/10.5194/amt-5-2413-2012.

Warner, J., M. M. Comer, C. D. Barnet, W. W. McMillan, W. Wolf, E. Maddy, and G. Sachse (2007), A comparison of satellite tropospheric carbon monoxide measurements from AIRS and MOPITT during INTEX-A, J. Geophys. Res., 112, D12S17, doi:10.1029/2006JD007925

Warner, J. X., Wei, Z., Strow, L. L., Barnet, C. D., Sparling, L. C., Diskin, G., and Sachse, G., 2010 (2010), Improved Agreement of AIRS Tropospheric Carbon Monoxide Products with other EOS Sensors Using Optimal Estimation Retrievals, Atmos. Chem. Phys., 10, 9521-9533, doi:10.5194/acp-10-9521-2010.

Warner, J., F. Carminati, Z. Wei, W. Lahoz, and J-L. Attié. "Tropospheric carbon monoxide variability from AIRS and IASI under clear and cloudy conditions." Atmospheric Chemistry and Physics Discussions 13, no. 6 (2013): 16337-16366.

Warner, J. X., R. Yang, Z. Wei, F. Carminati, A. Tangborn, Z. Sun, W. Lahoz, J-L. Attié, L. El Amraoui, and B. Duncan. "Global carbon monoxide products from combined AIRS, TES and MLS measurements on A-train satellites." Atmospheric Chemistry and Physics 14, no. 1 (2014): 103-114.

Zhang, L., H. Jiang, X. Lu, and J. Jin (2016), Comparison analysis of global carbon monoxide concentration derived from SCIAMACHY, AIRS, and MOPITT, Int.J.Remote Sens., 37(21), 5155-5175. https://dx.doi.org/10.1080/01431161.2016.1230282

15.8 Recommended Supplemental User Documentation

Overview_of_the_AIRS_Mission.pdf
V7_L2_Performance_Test_and_Validation_Report.pdf
V7_L2_Quality_Control_and_Error_Estimation.pdf
V7_L2_Standard_Pressure_Levels.pdf
V7_L2_Support_Pressure_Levels.pdf
V7_L2_Levels_Layers_Trapezoids.pdf
V7_Retrieval_Channel_Sets.pdf
V7_Retrieval_Flow.pdf
V7_CO_Initial_Guess_Profiles.pdf

16 Methane Retrievals

AIRS methane retrievals are broadly sensitive in the range between 850 hPa and the lower stratosphere, with peak sensitivity around 300-400 hPa, depending on surface and atmospheric conditions. The integrated total column value from CH_4 profiles reported for CH_4 is dominated by the initial guess and should not be used for research purposes.

No significant changes have been made to the methane retrieval in Version 7 (V7) compared to Version 6 (V6). Minimal differences in the methane arise from propagation of differences associated with updates to the V7 temperature and water vapor retrievals.

Note that there were previously significant changes in the V6 methane compared to V5 associated with:

- Modified first guess (see **V7_CH4_Initial_Guess_Profiles.pdf**)
- Number of retrieval functions increased from 7 to 10
- New tuning to the absorption coefficients in the peak CH_4 absorption channels
- Channel set and damping updated accordingly for the updated tuning
- Quality control was updated

Standard Product

Field Name	Dimension per FOR	Description
CH4_total_column	1	Retrieved total column CH_4, (molecules/cm^2) DO NOT USE FOR RESEARCH
CH4_total_column_QC	1	Quality flag (0,1,2)
CH4VMRLevStd	StdPressureLev=28	Level retrieved CH_4 Volume Mixing Ratio Profile (vmr), (ppbv)
CH4VMRLevStd_QC	StdPressureLev=28	Quality flag array (0,1,2)
CH4VMRLevStdErr	StdPressureLev=28	Error estimate for CH4VMRLevStd, Volume Mixing Ratio Profile (vmr), (unitless)
num_CH4_Func	1	Number of valid entries in each dimension of CH4_ave_kern
CH4_verticality_10func	CH4Func=10	Sum of rows of CH4_ave_kern, (unitless)
CH4_dof	1	Degrees of freedom, amount of information in CH_4 retrieval, (unitless)

Support Product (see Appendix A2 for a complete list of fields)

Field Name	Dimension per FOR	Description
CH4_trapezoid_layers_10func	CH4Func=10	1-based Index of **pressSup** array giving element defining lower altitude bound of trapezoid on which the CH_4 variables are defined, located in support product (unitless)
CH4_eff_press_10func	CH4Func=10	CH_4 effective pressure for the center of each trapezoid, located in support product.
CH4CDSup	XtraPresureLev=100	Layer column CH_4 in molecules/cm^2 (climatology when bad_co $\neq$ 0)
CH4CDSup_QC	XtraPresureLev=100	Quality flag array (0,1,2)
CH4CDSup_Err	XtraPresureLev=100	Error estimate for CH4CDSup
CH4VMRLevSup	XtraPresureLev=100	CH_4 Volume Mixing Ratio at support levels (vmr) (ppbv)
CH4VMRLevSup_QC	XtraPresureLev=100	Quality flag array (0,1,2)

CH4VMRLevSupErr	XtraPresureLev=100	Error estimate for CH4VMRLevSup
CH4VMRSurf	1	CH_4 Volume Mixing Ratio at the surface (vmr) (ppbv) DO NOT USE FOR RESEARCH. Retrieval has no sensitivity at surface. Value is from the initial guess
CH4VMRSurf_QC	1	Quality flag array (0,1,2)
CH4VMRSurfErr	1	Error estimate for CH4VMRSurf
CH4_VMR_eff_10func	CH4Func=10	Effective CH_4 Volume Mixing Ratio Profile (vmr) for each trapezoid, located in support product (unitless)
CH4_VMR_eff_10func_QC	CH4Func=10	Quality flag array (0,1,2)
CH4_VMR_eff_10func_err	CH4Func=10	Error estimate (vmr), located in support product (unitless)
CH4_ave_kern_10func	CH4Func*CH4Func =10x10	Averaging kernel for CH_4 retrieval, located in support product

16.1 Description

The AIRS methane product is a product of the IR stage of the combined IR/MW retrieval. A volume mixing ratio profile on the 28 standard pressure levels, **pressStd**, is provided in the Level 2 Standard Product. Level and layer profiles on the 100 support pressure levels, **pressSup**, are provided in the Level 2 Support Product.

Level quantities are calculated from layer quantities by the procedure described in

V7_L2_Levels_Layers_Trapezoids.pdf

The derivation of level quantities from layer quantities is essentially done by interpolation with smoothing kernels. The above document also contains a discussion of vertical representation in AIRS retrievals in terms of trapezoidal layers and associated averaging kernels, verticality and degrees of freedom.

The algorithm for computing first guess profiles for the V7 CH_4 retrieval and some example profiles are provided in the document:

V7_CH4_Initial_Guess_Profiles.pdf

CH4VMRLevStd and **CH4VMRLevSup** are **level** quantities providing the retrieved methane volume mixing ratio (ratio of number of CH_4 molecules to the number of molecules of air in a unit volume) at the pressure levels upon which they are reported. The former is in the standard product and the latter is in the support product. Standard pressure levels are arranged in order of decreasing pressure and support pressure levels are arranged in order of increasing pressure.

CH4CDSup is a **layer** quantity in the support product providing the retrieved CH_4 layer column density (number of CH_4 molecules/cm^2) between two **pressSup** levels and is reported on the lower altitude pressure level bounding the layer.

CH4_eff_press_10func is defined as the pressure weighted center of the trapezoid layers, i.e.,

$$CH4_eff_10func_press = \frac{\left[P_{bottom} - P_{top}\right]}{\log\left(P_{bottom}/P_{top}\right)}$$

where P_{bottom} is the bottom pressure of a trapezoid face and P_{top} is the top pressure.

CH4_VMR_eff_10func is a **layer** quantity contained in the support product providing the retrieved volume mixing ratio (ratio of number of CH_4 molecules to the number of molecules of air in a unit volume) for a layer defined by the faces of a CH_4 trapezoidal retrieval function. The boundaries of faces of these layers are specified in **CH4_trapezoid_layers_10func** in which is an array of 1-based **pressSup** level indices. There are 10 such trapezoidal layers corresponding to the 10 trapezoidal retrieval functions utilized for CH_4. **CH4_VMR_eff_10func** is reported at the effective trapezoid layer, **CH4_eff_press_10func**. It is computed from the integrated CH4 column density for the trapezoidal layer. Layers below the surface are filled with -9999. The value quoted on the lowest layer above the surface is the mean mixing ratio in the layer bounded by the next higher level and the surface. See

V7_L2_Support_Pressure_Levels.pdf
V7_L2_Levels_Layers_Trapezoids.pdf

CH4_VMR_eff_10func_err is the estimated error in CH_4 mixing ratio. This error is computed on the **pressSup** layers and then averaged to the CH_4 trapezoids.

CH4VMRSurf is a **level** quantity in the support product providing the retrieved CH_4 volume mixing ratio at the surface. It is not recommended for use in research as the retrieval has no sensitivity at the surface.

CH4_total_column is the integrated column amount of CH_4 from the top of the atmosphere (TOA = 0.005 hPa) to the surface. This quantity is computed by summing the 100 column density values, **CH4CDSup,** contained in the AIRS Level 2 Support Products file with the appropriate weighting applied to the bottom layer which contains the surface. Layers below the surface are not included in this sum. The reported total column is dominated by the initial guess and should not be used for research.

CH4_verticality_10func is a 10-point vector computed by summing the columns of the 10x10 CH_4 averaging kernel, **CH4_ave_kern_10func**, stored in the AIRS Level 2 Support Product. The associated 10-point pressure array is provided in **CH4_eff_press_10func**. The peak value of **CH4_verticality_10func** indicates the vertical location of the maximum sensitivity of the CH_4 product and the width of this peaked function qualitatively describes the vertical resolution of the retrieval. The magnitudes of **CH4_verticality_10func** are a rough measure of the fraction of the retrieval determined from the data as opposed to the first guess. A value near unity indicates the retrieval is highly determined by the radiance measurements and thus has high information content. A smaller value indicates the retrieval contains a large fraction of the first guess.

CH4_dof is the number of degrees of freedom which is also a measure of the amount of information in the retrieval. It is computed as the sum of the diagonal elements (trace) of the 10x10 CH_4 averaging kernel, **CH4_ave_kern_10func**, stored in the AIRS Support Product files.

NOTE: **num_CH4_Func** provides the number of valid entries in each dimension of **CH4_ave_kern**. Topography limits the number of valid CH_4 averaging kernel trapezoids.

NOTE: the problem with associating the verticality with a total column averaging kernel is that it neglects the fact that the retrieval can only move as superpositions of the trapezoids. Convolution using the verticality alone will not account for the possibility that the "independent CH_4 profile" contains structure that the trapezoids can or cannot resolve.

16.2 Type of Product

The standard CH_4 product profile is a level quantity, i.e. the values are reported on the standard pressure levels and provide the volume mixing ratios at the level on which they are reported.

16.3 Quality Indicators

The user is encouraged to read the QC and error estimation document:

V7_L2_Quality_Control_and_Error_Estimation.pdf

- If **PGood = PSurfStd** and **CH4_Resid_Ratio** < 1.5 and **CH4_dof** > 0.5, then all CH_4 products are marked Quality = 0.
- If **PGood = PSurfStd** and **CH4_Resid_Ratio** < 1.5 and 0.5 >= **CH4_dof** > 0.4, then all CH_4 products are marked Quality = 1.
- Otherwise, all CH_4 products are marked Quality = 2, and additional tests are then applied to lower the Quality if appropriate.

The CH_4 absorption band is within the water vapor absorption band near 7.6 μm, and thus the quality of the moisture product impacts that of the CH_4 product. Therefore, if **totH2OStd_QC** = 1, we set all CH_4 quality flags to 1 if:

- **CH4_Resid_Ratio** ≥ 1.0, or
- **PGood** ≤ 610 hPa

We found the contamination of CH_4 retrievals is mainly from low water clouds. Under the condition of **totH2OStd_QC** = 1, we set all CH_4 quality flags to 2 when the cloud fraction among the 9 AIRS spots within a retrieval FOV are mainly water clouds or they are very different. The test for water clouds uses **cloud_phase_3x3** (located in the Level 2 Support Product).

We recognize there remains a scan angle dependence of retrieved CH_4 at altitudes above the 200 hPa level in the tropics. To minimize its impact upon research, we set Quality=2

for the two most extreme scan angle retrievals at the beginning and end of each scan set (i.e., retrieval FOVs 1, 2, 29 and 30) whenever **PTropopause** ≤ 100 hPa.

16.4 Validation

A Validation Report for V7 data including for methane products is currently under preparation and will be published after the V7 data products become publicly available. Early V7 validation results are partially summarized in

V7_L2 Performance_and_Test_Report.pdf

Figure 7 shows a comparison of AIRS V6 (upper panels) against V7 (lower panels) CH_4 VMRs at 400 hPa (left panels) and the column averaged CH_4 (ppbv) (right panels). V7 shows better defined features and less noise. To quantify any improvement, thorough validation of both V6 and V7 is needed, and the work is ongoing.

The validation of the AIRS V7 CH_4 product will be made using the profiles from aircraft measurements obtained from different campaigns after the official V7 products become available.

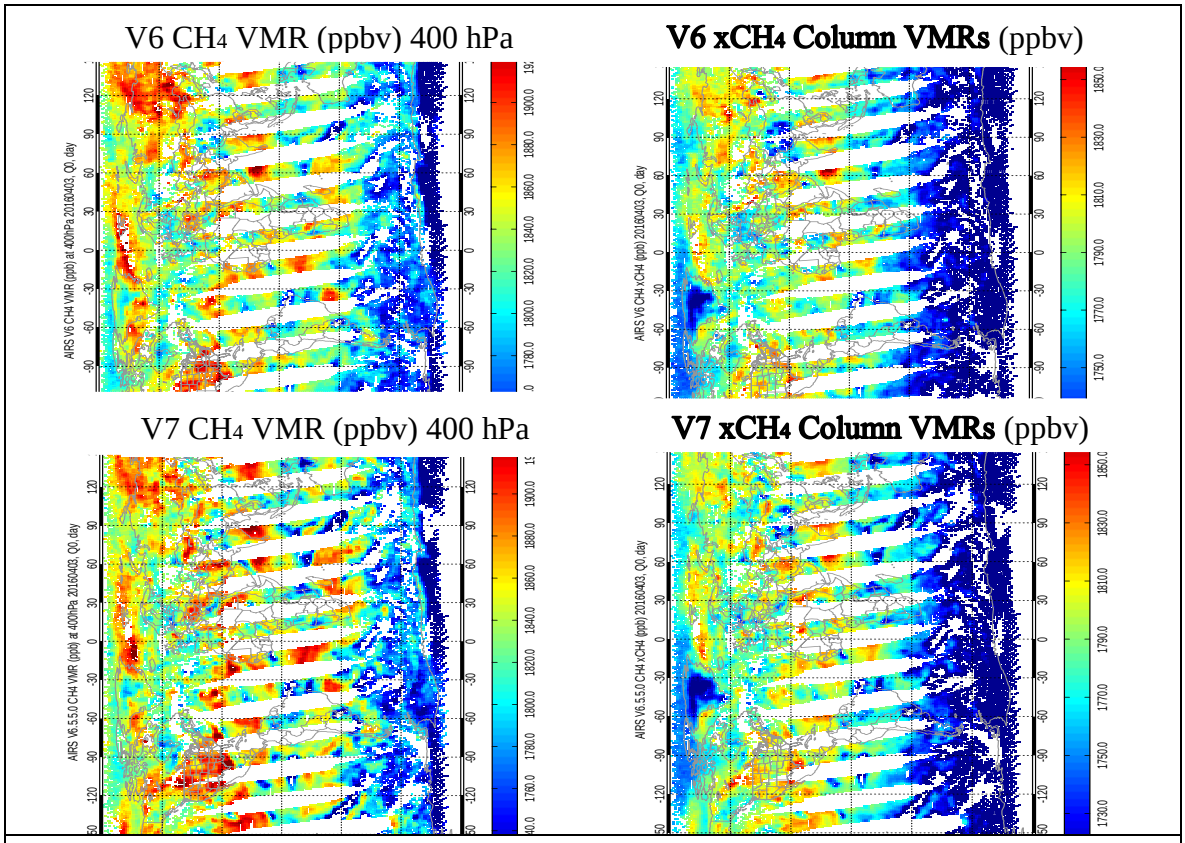

Figure 7: Comparison of AIRS V6 and V7 CH_4 VMRs at 400 hPa (ppbv) and CH_4 column averaged total column (ppbv) on April 3, 2016.
Top row: V6; Bottom row: V7;
Left Panels: VMRs at 400 hPa (ppbv);
Right panels: column averaged total column (ppbv).

16.5 Caveats

This section will be updated over time as V7 data products are analyzed and validated.

The AIRS retrieval is not sensitive to methane in the lower troposphere (below 850 hPa).

The total column CH_4 is dominated by the initial guess and thus should not be used for research.

Due to the uncertainty in CH_4 absorption spectrum, tuning of CH_4 channels in the Q-branch requires additional investigation. Current tuning for V7 is the same as for V6 and is based on HIAPER Pole-to-Pole Observations (HIPPO)-1, -2, -3 data, but is still limited due to the lack of aircraft data in the summer season.

16.6 Suggestions for Researchers

This section will be updated over time as V7 data products are analyzed and validated.

AIRS CH_4 measurements represent nearly two decades of global trends and variability from year 2002, and will be a good compliment to any future CH_4 sensors once inter-calibrated.

16.7 Recommended Papers

Kim, B., and S. Sarkar (2017), Impact of wildfires on some greenhouse gases over continental USA: A study based on satellite data, Remote Sensing of Environment, 188, 118-126. http://dx.doi.org/10.1016/j.rse.2016.10.047.

Peters, C. N., R. Bennartz, and G. M. Hornberger (2017), Satellite-derived methane emissions from inundation in Bangladesh, J. Geophys. Res. Biogeosci., 122, 1137–1155, doi:10.1002/2016JG003740.

Mahmood, I., M. F. Iqbal, M. I. Shahzad, A. Waqas, and L. Atique (2016), Spatiotemporal Monitoring of CO2 and CH4 over Pakistan Using Atmospheric Infrared Sounder (AIRS), Int. Lett. Nat. Sci., 58, 35-41. https://dx.doi.org/10.18052/www.scipress.com/ILNS.58.35.

Rajab, J.M., M.Z. MatJafri, H.S. Lim (2012), Methane Interannual Distribution over Peninsular Malaysia from Atmospheric Infrared Sounder Data: 2003-2009, *Aerosol and Air Quality Research*, **12**, 1459-1466, doi: 10.4209/aaqr.2012.02.0039

Streets, David G., Timothy Canty, Gregory R. Carmichael, Benjamin de Foy, Russell R. Dickerson, Bryan N. Duncan, David P. Edwards et al. "Emissions estimation from satellite retrievals: A review of current capability." Atmospheric Environment 77 (2013): 1011-1042.

Xiong, X., C. Barnet, E. Maddy, C. Sweeney, X. Liu, L. Zhou, and M. Goldberg, (2008), Characterization and validation of methane products from the Atmospheric Infrared Sounder (AIRS), *J. Geophys Res.*, **113**, G00A01, doi:10.1029/2007JG000500.

Xiong, X., C. Barnet, J. Wei, and E. Maddy. "Information-based mid-upper tropospheric methane derived from Atmospheric Infrared Sounder (AIRS) and its validation." Atmospheric Chemistry and Physics Discussions 9, no. 4 (2009): 16331-16360.

Xiong, X., S. Houweling, J. Wei, E. Maddy, F. Sun, C. D. Barnet (2009), Methane Plume over South Asia during the Monsoon Season: Satellite Observation and Model Simulation, *Atmos. Chem. Phys*., **9**, 783-794, 2009.

Xiong, X., Barnet, C. D., Maddy, E., Wei, J., Liu, X., Thomas.S.Pagano (2010), Seven Years' Observation of Mid-Upper Tropospheric Methane from Atmospheric Infrared Sounder, *Remote Sensing*, **2**, 2509-2530; doi:10.3390/rs2112509

Xiong, X., Barnet, C.; Zhuang, Q.; Machida, T.; Sweeney, C.; Patra, P.K. (2010), Mid-upper Tropospheric Methane in the High Northern Hemisphere: Space-borne Observations by AIRS, Aircraft Measurements and Model Simulations, *J. Geophys. Res*., **115**, D19309, doi:10.1029/2009JD013796.

Xiong, X. Z., Y. Han, Q. H. Liu, and F. Z. Weng (2016), Comparison of Atmospheric Methane Retrievals from AIRS and IASI, IEEE Journal of Selected Topics in Applied Earth Observations and Remote Sensing, 9(7), 3297-3303. http://dx.doi.org/10.1109/jstars.2016.2588279.

Xu, Y., J. Wang, J. Sun, Y. Xu, and W. Harris (2012), Spatial and Temporal Variations of Lower Tropospheric Methane During 2010-2011 in China, IEEE Journal of Selected Topics in Applied Earth Observations and Remote Sensing, 5(5), 1464-1473, http://dx.doi.org/10.1109/JSTARS.2012.2195640.

Zhang,XingYing, Bai,WenGuang, Zhang,Peng, Wang,WeiHe,(2011), Spatiotemporal variations in mid-upper tropospheric methane over China from satellite observations, Chin.Sci.Bull., 56, 31, 3321-3327

Zhang, Y., Chen, L., Tao, J., Su, L., Yu, C., and Fan, M., 2012, Retrieval of methane profiles from spaceborne hyperspectral infrared observations: Journal of Remote Sensing, v. 16, no. 2, p. 232-247

Zhang, Y., X. Xiong, J. Tao, C. Yu, M. Zou, L. Su, and L. Chen (2014), Methane retrieval from Atmospheric Infrared Sounder using EOF-based regression algorithm and its validation, Chinese Science Bulletin, 59(14), 1508-1518, http://dx.doi.org/10.1007/s11434-014-0232-7.

Zou, M., Xiong, X., Saitoh, N., Warner, J., Zhang, Y., Chen, L., Weng, F., and Fan, M.: Satellite observation of atmospheric methane: intercomparison between AIRS and GOSAT TANSO-FTS retrievals, Atmos. Meas. Tech., 9, 3567-3576, doi:10.5194/amt-9-3567-2016, 2016

16.8 Recommended Supplemental User Documentation

Overview_of_the_AIRS_Mission.pdf
V7_L2_Performance_Test_and_Validation_Report.pdf
V7_L2_Quality_Control_and_Error_Estimation.pdf
V7_L2_Standard_Pressure_Levels.pdf
V7_L2_Support_Pressure_Levels.pdf

V7_L2_Levels_Layers_Trapezoids.pdf
V7_Retrieval_Channel_Sets.pdf
V7_Retrieval_Flow.pdf
V7_CH4_Initial_Guess_Profiles.pdf

17 Dust and SO2 Flags

Standard Product

Field Name	Dimension per FOV	Description
dust_flag	AIRSTrack *AIRSXTrack =3x3	Flag indicating whether dust was detected in this scene; 1: Dust detected; 0: Dust not detected; -1: Dust test not valid because of land; -2: Dust test not valid because of high latitude; -3: Dust test not valid because of suspected cloud; -4: Dust test not valid because of bad input data

Support Product

Field Name	Dimension per FOV	Description
dust_score	AIRSTrack *AIRSXTrack =3x3	Each bit results from a different test comparing radiances. Higher scores indicate more certainty of dust present. Dust probable when dust_score>380. Not valid if dust_flag is negative.
BT_diff_SO2	AIRSTrack *AIRSXTrack =3x3	Tb(1433.06 cm-1) used as an indicator of SO2 release from volcanoes. Values under -6 K have likely volcanic SO2. (K)

17.1 Description

The dust and SO_2 flags are calculated directly from the L1B radiances and do not depend on other L2 products. Since the V7 L2 products are still based on the V5 L1B product, the user should see no changes in these flag values between V5, V6, and V7.

dust_flag – flag for each of the 3x3 AIRS spots in a Field of Regard (AMSU FOV) indicating whether dust was detected in the spot. Values are:

1 = dust detected

0 = dust not detected

-1 = dust test not valid because of land

-2 = dust test not valid because of high latitude

-3 = dust test not valid because of suspected cloud

-4 = dust test not valid because of bad input data

The flag is set based on **dust_score**, an array in the Level 2 Support Product that is dimensioned (1350,3,3) to provide information for each AIRS field of regard.

SO_2 detection - The detection of the presence of dust or volcanic SO_2 is made by comparison of radiances, and the flags originate in the AIRS Level 1B Product. They are propagated to the Level 2 Standard and Support Products. Each granule of Level 2 Standard Product has an attribute, **NumSO2FOVs**, which provides the number of retrieval FOVs (out of a nominal 1350 for a granule) with a significant SO_2 concentration based on the value of **BT_diff_SO2**. The support product also has a quality factor,

BT_diff_SO2_QC. These arrays are of dimension (1350,3,3), since they provide the information for each AIRS spot.

Data indicating which Fields of Regard (AMSU FOVs) and which AIRS spots within the AMSU FOVs indicate the presence of excessive SO_2 are located in the AIRS Level 2 Support Product. The entry is **BT_diff_SO2** and it is a 3x3 array of brightness temperature differences for each AMSU FOV. The temperature difference tested is:

$$\Delta T_b = T_b\left(1361.44\ cm^{-1}\right) - T_b\left(1433.06\ cm^{-1}\right)$$

If $\Delta T_b < -6\ K$ the presence of volcanic SO_2 is highly likely.

The tests by which **dust_flag** and **BT_diff_SO2** are set are described in

V7_Retrieval_Channel_Sets.pdf

17.1 Type of Product

The AIRS V7 SO_2 and Dust products are flags indicating the presence or absence of a detection of these constituents. The algorithm is unchanged from V5 and V6.

17.2 Quality Indicators

The user is encouraged to read the QC and error estimation document:

V7_L2_Quality_Control_and_Error_Estimation.pdf

BT_diff_SO2 is a simple difference between two Level 1B radiances so it will be good unless one of the detectors involved becomes bad. If it is bad it will be -9999.0.

Dust_flag and **dust_score** are derived parameters and therefore do not have QC fields. Negative values of **dust_flag** indicate when both are not trustworthy.

17.3 Validation

The AIRS sulfur dioxide products were validated for V6, with results described in

V6_L2 Performance_and_Test_Report.pdf

Further validation for V7 has not been performed at this point, but no algorithm changes were done for the sulfur dioxide or dust products specifically between V6 and V7.

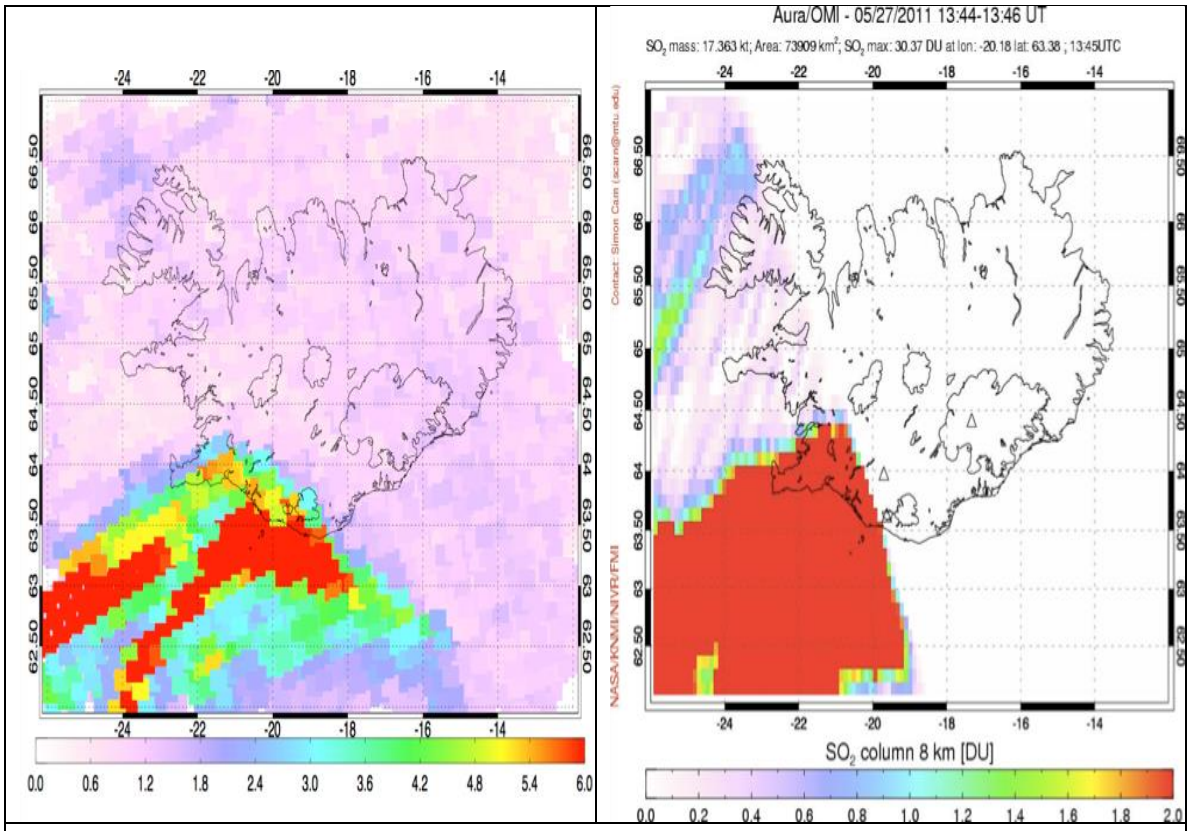

Figure 9: AIRS V6 SO_2 flags compared with Aura/OMI SO_2 total column on 27 May 2011
Left panel: AIRS V6 SO_2 flags color coded by ΔT_b
Right panel: Aura/OMI SO_2 total column (DU)

17.4 Caveats

This section will be updated over time as V7 data products are analyzed and validated.

The dust flag is valid **ONLY OVER OCEAN** and fails if thin cirrus or other clouds are present ABOVE the dust.

Physical retrievals can be seriously compromised if the AIRS field of regard is contaminated by dust and/or volcanic ash. Most dust-contaminated scenes are already marked as Quality = 2. However, cautious users should include the **dust_flag** and **dust_score** in their quality control filtering of data. Despite being valid only over ocean the dust detection algorithm should be useful for filtering data contaminated by dust in the Saharan Air Layer (SAL). **We recommend that users filtering to select high quality data over oceans should avoid AIRS Level 2 retrievals for which *dust_score ≥ 380 or dust_flag = 1, regardless of the values of other QA indicators*.**

We recommend that users filtering to select high quality data should also avoid AIRS Level 2 retrievals for which BT_diff_SO2 ≤ 6 K. Those retrievals may be contaminated by volcanic ash.

17.5 Recommended Papers

This section will be updated over time as research with V7 data products are published.

Brenot, H., Theys, N., Clarisse, L., van Geffen, J., van Gent, J., Van Roozendael, M., van der A, R., Hurtmans, D., Coheur, P.-F., Clerbaux, C., Valks, P., Hedelt, P., Prata, F., Rasson, O., Sievers, K., and Zehner, C.: Support to Aviation Control Service (SACS): an online service for near-real-time satellite monitoring of volcanic plumes, Nat. Hazards Earth Syst. Sci., 14, 1099-1123, doi:10.5194/nhess-14-1099-2014, 2014.

Carboni, E., Thomas, G.E., Sayer, A.M., Siddans, R., Poulsen, C.A., Grainger, R.G., Ahn, C., Antoine, D., Bevan, S., Braak, R., Brindley, H., DeSouza-Machado, S., Deuze, J.L., Diner, D., Ducos, F., Grey, W., Hsu, C., Kalashnikova, O.V., Kahn, R., North, P.R.J., Salustro, C., Smith, A., Tanre, D., Torres, O., and Veihelmann, B., 2012, Intercomparison of desert dust optical depth from satellite measurements: Atmospheric Measurement Techniques, v. 5, no. 8, p. 1973-2002. http://dx.doi.org/10.5194/amt-5-1973-2012

Carn S. A., L. L. Strow, S. de Souza-Machado, Y. Edmonds, S. Hannon (2005), Quantifying tropospheric volcanic emissions with AIRS: The 2002 eruption of Mt. Etna (Italy), Geophys. Res. Lett., 32, L02301, doi:10.1029/2004GL021034.

Carn, S. A., Arlin J. Krueger, Nickolay A. Krotkov, Kai Yang, and Keith Evans (2008), Tracking volcanic sulfur dioxide clouds for aviation hazard mitigation, Nat. Hazards, doi:10.1007/s11069-008-9228-4

Carn, Simon A., John S. Pallister, Luis Lara, John W. Ewert, Sebastian Watt, Alfred J. Prata, Ronald J. Thomas, and Gustavo Villarosa. "The unexpected awakening of Chaitén volcano, Chile." Eos, Transactions American Geophysical Union 90, no. 24 (2009): 205-206.

Corradini, S., L. Merucci, A. J. Prata, and A. Piscini (2010), Volcanic ash and SO2 in the 2008 Kasatochi eruption: Retrievals comparison from different IR satellite sensors, J. Geophys. Res., 115, D00L21, doi:10.1029/2009JD013634.

Davidi, A., A. B. Kostinski, I. Koren, and Y. Lehahn (2012), Observational bounds on atmospheric heating by aerosol absorption: Radiative signature of transatlantic dust, Geophys. Res. Lett., 39, L04803, doi:10.1029/2011GL050358

DeSouza-Machado, S. G., L. L. Strow, S. E. Hannon, and H. E. Motteler (2006), Infrared dust spectral signatures from AIRS, Geophys. Res. Lett., 33, L03801, doi:10.1029/2005GL024364.

DeSouza-Machado, S. G., et al. (2010), Infrared retrievals of dust using AIRS: Comparisons of optical depths and heights derived for a North African dust storm to other collocated EOS A-Train and surface observations, J. Geophys. Res., 115, D15201, doi:10.1029/2009JD012842.

Eckhardt, S., Prata, A. J., Seibert, P., Stebel, K., and Stohl, A.: Estimation of the vertical profile of sulfur dioxide injection into the atmosphere by a volcanic eruption using satellite column measurements and inverse transport modeling, Atmos. Chem. Phys., 8, 3881-3897, 2008.

Goldberg M. D., Y. Qu, L. McMillin, W. Wolf, L. Zhou, and M. Divakarla (2003), AIRS near-real-time products and algorithms in support of operational numerical weather prediction. IEEE Trans. Geosci. Remote Sens., 41(2), 379–399.

Griessbach, S., Hoffmann, L., Spang, R., von Hobe, M., Müller, R., and Riese, M.: Infrared limb emission measurements of aerosol in the troposphere and stratosphere, Atmos. Meas. Tech., 9, 4399-4423, doi:10.5194/amt-9-4399-2016, 2016.

Heng, Y., Hoffmann, L., Griessbach, S., Rößler, T., and Stein, O.: Inverse transport modeling of volcanic sulfur dioxide emissions using large-scale simulations, Geosci. Model Dev., 9, 1627-1645, doi:10.5194/gmd-9-1627-2016, 2016.

Hoffmann, L., T. Rößler, S. Griessbach, Y. Heng, and O. Stein (2016), Lagrangian transport simulations of volcanic sulfur dioxide emissions: Impact of meteorological data products, J. Geophys. Res. Atmos., 121, 4651–4673, doi:10.1002/2015JD023749.

Hsu, N. C., C. Li, N. A. Krotkov, Q. Liang, K. Yang, and S.-C. Tsay (2012), Rapid transpacific transport in autumn observed by the A-train satellites, J. Geophys. Res., 117, D06312, doi:10.1029/2011JD016626.

Krotkov, N.A., S.A. Carn, A.J. Krueger, P.K. Bhartia, and K. Yang (2006). Band residual difference algorithm for retrieval of SO2 from the Aura Ozone Monitoring Instrument (OMI). IEEE Trans.Geosci. Remote Sensing, AURA special issue, 44(5), 1259-1266, doi:10.1109/TGRS.2005.861932, 2006.

Maddy, E. S., et al. (2012), On the effect of dust aerosols on AIRS and IASI operational level 2 products, Geophys. Res. Lett., 39, L10809, doi:10.1029/2012GL052070

Mielonen, T., H. Portin, M. Komppula, A. Leskinen, J. Tamminen, I. Ialongo, J. Hakkarainen, K. E. J. Lehtinen, and A. Arola (2012), Biomass burning aerosols observed in Eastern Finland during the Russian wildfires in summer 2010 - Part 2: Remote sensing Atmospheric Environment, 47, 279-287, http://dx.doi.org/10.1016/j.atmosenv.2011.07.016.

Nalli N. R., et al. (2005), Profile observations of the Saharan air layer during AEROSE 2004, Geophys. Res. Lett., 32, L05815, doi:10.1029/2004GL022028.

Nalli N. R., et al. (2006), Ship-based measurements for infrared sensor validation during Aerosol and Ocean Science Expedition 2004, J. Geophys. Res., 111, D09S04, doi:10.1029/2005JD006385.

Pierangelo C., M. Mishchenko, Y. Balkanski, A. Chédin (2005), Retrieving the effective radius of Saharan dust coarse mode from AIRS, Geophys. Res. Lett., 32, L20813, doi:10.1029/2005GL023425.

Pan,Weiyu; Wu,Liguang; Shie,Chung-Lin, Influence of the Saharan Air Layer on Atlantic Tropical Cyclone Formation during the Period 1-12 September 2003, Adv.Atmos.Sci., 2011, 28, 1, 16-32,

Prata, A.J., Bernardo, C., Retrieval of volcanic SO2 column abundance from atmospheric infrared sounder data, Journal of Geophysical Research Atmospheres, 2007, 112, D20, D20204

Prata, A. J., G. Gangale, L. Clarisse, and F. Karagulian (2010), Ash and sulfur dioxide in the 2008 eruptions of Okmok and Kasatochi: Insights from high spectral resolution satellite measurements, J. Geophys. Res., 115, D00L18, doi:10.1029/2009JD013556.

Prata, A. J., and A. T. Prata (2012), Eyjafjallajökull volcanic ash concentrations determined using Spin Enhanced Visible and Infrared Imager measurements, J. Geophys. Res., 117, D00U23, doi:10.1029/2011JD016800.

Thomas, Helen E., I. Matthew Watson, Simon A. Carn, Alfredo J. Prata, and Vincent J. Realmuto. "A comparison of AIRS, MODIS and OMI sulphur dioxide retrievals in volcanic clouds." Geomatics, Natural Hazards and Risk 2, no. 3 (2011): 217-232.

Realmuto, V.J., Berk, A., Plume Tracker: Interactive mapping of volcanic sulfur dioxide emissions with high-performance radiative transfer modeling, J. Volcanol. Geotherm. Res. (2016), http://dx.doi.org/10.1016/j.jvolgeores.2016.07.001

Torres, O., C. Ahn, and Z. Chen. "Improvements to the OMI near-UV aerosol algorithm using A-train CALIOP and AIRS observations." Atmospheric Measurement Techniques 6, no. 11 (2013): 3257-3270.

Wong S., P. R. Colarco, A. E. Dessler (2006), Principal component analysis of the evolution of the Saharan air layer and dust transport: Comparisons between a model simulation and MODIS and AIRS retrievals, J. Geophys. Res., 111, D20109, doi:10.1029/2006JD007093.

Wright,R., Carn,S. A., Flynn,L. P. (2005), A satellite chronology of the May-June 2003 eruption of Anatahan volcano, Journal of Volcanology and Geothermal Research, 146, 102-116. doi: 10.1016/j.jvolgeores.2004.10.021

Yao, Z., J. Li, H. Han, A. Huang, B. J. Sohn, and P. Zhang (2012), Asian dust height and infrared optical depth retrievals over land from hyperspectral longwave infrared radiances, Journal of Geophysical Research-Atmospheres, 117, D19202, http://dx.doi.org/10.1029/2012JD017799.

17.6 Recommended Supplemental User Documentation

Overview_of_the_AIRS_Mission.pdf
V7_L2_Performance_Test_and_Validation_Report.pdf
V7_L2_Quality_Control_and_Error_Estimation.pdf
V7_L2_Standard_Pressure_Levels.pdf
V7_L2_Support_Pressure_Levels.pdf
V7_L2_Levels_Layers_Trapezoids.pdf
V7_Retrieval_Channel_Sets.pdf
V7_Retrieval_Flow.pdf

18 Outgoing Longwave Radiation Retrievals

Standard Product

Field Name	Dimension per FOV	Description
olr	1	Outgoing longwave radiation flux integrated over 100 to 3260 cm^{-1}, (W/m^2)
olr_err	1	Error estimate for olr, (W/m^2)
olr_QC	1	Quality flag (0,1,2)
olr3x3	AIRSTrack*AIRSXTrack=3x3	Outgoing longwave radiation flux integrated over 100 to 3260 cm^{-1}, per 15km AIRS FOV (W/m^2)
olr3x3_QC	AIRSTrack*AIRSXTrack=3x3	Quality flag array (0,1,2)
clrolr	1	Clear sky outgoing longwave radiation flux integrated over 100 to 3260 cm^{-1}, (W/m^2)
clrolr_err	1	Error estimate for clrolr, (W/m^2)
clrolr_QC	1	Quality flag (0,1,2)

Support Product (see Appendix A2 for a complete list of fields)

Field Name	Dimension per FOV	Description
spectralolr	OLRBand=16	Outgoing Longwave Radiation Flux integrated over 16 frequency bands (per 45 km AMSU-A FOV) (W/m^2)
spectralolr_QC	OLRBand=16	Quality flag (0,1,2)
spectralclrolr	OLRBand=16	Clear-sky Outgoing Longwave Radiation Flux integrated over 16 frequency bands (per 45 km AMSU-A FOV) (Watts/m^2)
spectralclrolr_QC	OLRBand=16	Quality flag (0,1,2)

18.1 Description

Outgoing longwave radiation (OLR) is the total longwave radiative flux (W/m^2) going to space, emitted by the earth-atmosphere system integrated over all angles and over all frequencies. OLR (**olr**) is not directly measured but is calculated from the retrieved state using an OLR RTA (the "AER" algorithm) due to Iacono et al. (2008). OLR at a given location is affected primarily by the earth's skin surface temperature, skin surface spectral emissivity, atmospheric vertical temperature and water vapor profile, as well as the heights, amounts, and spectral emissivities of multiple layers of cloud cover. OLR also depends on the vertical distributions of trace gases. V5 computed OLR according to Mehta and Susskind (1999) at the AMSU FOV resolution. V6 and V7 compute OLR according to Iacono et al (2008) at the AIRS spot resolution. Clear-sky outgoing longwave radiation (**clrolr**) is calculated using the same algorithm, setting the cloud fraction equal to zero.

The Iacono et al. (2008) algorithm computes spectral components of OLR in sixteen spectral bands covering the entire spectral range from 100 cm^{-1} to 3260 cm^{-1} and sums these up to give the total OLR. Because the OLR is computed from the retrieved solution, it is possible to compute the contribution from spectral regions not directly observed by AIRS. The contributions from each of the sixteen bands are output in the support product.

Contributions to clear sky and total OLR for a representative data period for the sixteen spectral bands are shown in Table 18.1, taken from Susskind et al., in preparation.

Table 18.1: Flux (W/m2) and Percentage Contributions of Spectral Band *m* to Total OLRCLR, OLR, and LWCRF

Band Number	Frequency Range	Clear Sky OLR		OLR		LWCRF	
m	cm-1	Flux	%	Flux	%	Flux	%
1	100-350	34.79	13.03	34.40	14.14	0.39	1.65
2	350-500	42.90	16.06	40.97	16.84	1.93	8.09
3	500-630	38.94	14.58	36.46	14.99	2.48	10.41
4	630-700	10.27	3.85	10.26	4.22	0.01	0.06
5	700-820	32.37	12.12	29.04	11.94	3.33	13.96
6	820-980	46.77	17.51	39.89	16.40	6.88	28.83
7	980-1080	16.88	6.32	14.50	5.96	2.37	9.96
8	1080-1180	17.69	6.62	14.73	6.05	2.97	12.44
9	1180-1390	17.13	6.41	14.70	6.04	2.43	10.20
10	1390-1480	2.43	0.91	2.26	0.93	0.17	0.72
11	1480-1800	2.95	1.10	2.78	1.14	0.17	0.70
12	1800-2080	2.37	0.89	2.01	0.83	0.36	1.53
13	2080-2250	0.79	0.30	0.63	0.26	0.16	0.69
14	2250-2380	0.05	0.02	0.05	0.02	0.00	0.00
15	2380-2600	0.44	0.16	0.34	0.14	0.10	0.44
16	2600-3260	0.34	0.13	0.25	0.10	0.08	0.34

18.2 Type of Product

The OLR products are integrated values for the radiances that would be observed at the top-of-atmosphere (TOA).

18.3 Quality Indicators

The user is encouraged to read the QC and error estimation document and the cloud product section of the performance and test report:

V7_L2_Quality_Control_and_Error_Estimation.pdf
V7_Retrieval_Performance _and_Test_Report.pdf

Quality of OLR (except for **clrolr**) is flagged as follows:

- If we accept a final retrieval, Quality = 0.
- If we accept a final retrieval, but the final retrieved surface temperature differs from the neural net surface temperature by > 5 K, the OLR is calculated from the neural net surface temperature, and Quality = 1.
- In the event that the cloud retrieval is not completed, Quality = 2.

The clear sky OLR products require an accurate retrieval to the surface, so their QC are set as follows. If the profile quality is good to the surface (**PGood = PSurfStd**), **clrolr_QC** (in the standard product) and **spectralclrolr_QC** (in the support product) are set to 0; otherwise they are both set to 2.

18.4 Validation

Early V7 validation results are partially summarized in

V7_L2_Performance_Test_and_Validation_Report.pdf

V6 validation results are reported in V6_L2_Performance_and_Test_Report.pdf and extensive V5 OLR validation is reported in Susskind et al. (2012).

18.5 Caveats

This section will be updated over time as V7 data products are analyzed and validated.

18.6 Suggestions for Researchers

This section will be updated over time as V7 data products are analyzed and validated.

OLR has been widely used as a proxy for convective activity in the tropics. Susskind et al. (2012) have used AIRS data to explain changes in OLR observed over the past decade in terms of the effects of El Niño/ La Niña oscillations over the time period on the distributions of tropical water vapor and cloud cover.

18.7 Recommended Papers

Aumann, Hartmut H., Alexander Ruzmaikin, Ali Behrangi, 2012: On the Surface Temperature Sensitivity of the Reflected Shortwave, Outgoing Longwave, and Net Incident Radiation. J. Climate, 25, 6585-6593. doi: http://dx.doi.org/10.1175/JCLI-D-11-00607.1

Chen, Xiuhong, Xianglei Huang, Norman G. Loeb, Heli Wei (2013), Comparisons of Clear-Sky Outgoing Far-IR Flux Inferred from Satellite Observations and Computed from the Three Most Recent Reanalysis Products. J. Climate, 26, 478–494, doi: 10.1175/JCLI-D-12-00212.1

Dessler, A. E., P. Yang, J. Lee, J. Solbrig, Z. Zhang, and K. Minschwaner (2008), An analysis of the dependence of clear-sky top-of-atmosphere outgoing longwave radiation on atmospheric temperature and water vapor, J. Geophys. Res., 113, D17102, doi:10.1029/2008JD010137.

Huang, X., N. G. Loeb, and W. Yang (2010), Spectrally resolved fluxes derived from collocated AIRS and CERES measurements and their application in model evaluation: 2. Cloudy sky and band-by-band cloud radiative forcing over the tropical oceans, J. Geophys. Res., 115, D21101, doi:10.1029/2010JD013932.

Huang, Xianglei, Jason N. S. Cole, Fei He, Gerald L. Potter, Lazaros Oreopoulos, Dongmin Lee, Max Suarez, Norman G. Loeb, 2013: Longwave Band-By-Band Cloud Radiative Effect and Its Application in GCM Evaluation. J. Climate, 26, 450–467,doi: 10.1175/JCLI-D-12-00112.1

Iacono, M.J., J.S. Delamere, E.J. Mlawer, M.W. Shephard, S.A. Clough, and W.D. Collins (2008), Radiative forcing by long-lived greenhouse gases, Calculations with the AER radiative transfer models, *J. Geophys*. Res., **113**, D13103, doi:10.1029/2008JD009944.

Kahn, B. H., X. Huang, G. L. Stephens, W. D. Collins, D. R. Feldman, H. Su, S. Wong, and Q. Yue (2016), ENSO regulation of far- and mid-infrared contributions to clear-sky OLR, Geophys. Res. Lett., 43, doi:10.1002/2016GL070263.

Loeb, N. G., S. Kato, W. Su, T. Wong, F. G. Rose, D. R. Doelling, J. R. Norris, and X. Huang (2012), Advances in Understanding Top-of-Atmosphere Radiation Variability from Satellite Observations, Surveys in Geophysics, 33(3-4), 359-385, http://dx.doi.org/10.1007/s10712-012-9175-1

Metha, A and J. Susskind (1999), Outgoing longwave radiation from the TOVS Pathfinder Path A data set, *J. Geophys. Res*., **104**, 12193 doi:10.1029/1999JD900059.

Moy, L. A., R. O. Knuteson, D. C. Tobin, H. E. Revercomb, L. A. Borg, and J. Susskind (2010), Comparison of measured and modeled outgoing longwave radiation for clear-sky ocean and land scenes using coincident CERES and AIRS observations, *J. Geophys. Res*., **115**, D15110, doi:10.1029/2009JD012758

Sedlar, J., and Devasthale, A., 2012, Clear-sky thermodynamic and radiative anomalies over a sea ice sensitive region of the Arctic: Journal of Geophysical Research-Atmospheres, v. 117, p. D19111. http://dx.doi.org/10.1029/2012JD017754

Stephens, G. L., B. H. Kahn, and M. Richardson (2016), The super greenhouse effect in a changing climate, J. Climate, 29, 5469–5482, doi:10.1175/JCLI-D-15-0234.1.

Sun, F., M. D. Goldberg, X. Liu, and J. J. Bates (2010), Estimation of outgoing longwave radiation from Atmospheric Infrared Sounder radiance measurements, J. Geophys. Res., 115, D09103, doi:10.1029/2009JD012799

Susskind, J., G. Molnar, L. Iredell, N. Loeb (2012), Interannual Variability of OLR as Observed by AIRS and CERES, *J. Geophys Res*., **117**, D23107, doi:10.1029/2012JD017997

18.8 Recommended Supplemental User Documentation

Overview_of_the_AIRS_Mission.pdf
V7_L2_Performance_Test_and_Validation_Report.pdf
V7_L2_Quality_Control_and_Error_Estimation.pdf
V7_L2_Standard_Pressure_Levels.pdf
V7_L2_Support_Pressure_Levels.pdf
V7_L2_Levels_Layers_Trapezoids.pdf
V7_Retrieval_Channel_Sets.pdf
V7_Retrieval_Flow.pdf

Appendix A. Level 2 Product Interface Specifications

In this appendix, all fields available in the Level 2 product files are listed with short descriptions. This includes dimensions, geolocation and other ancillary fields that are common to many of the geophysical variables and are not listed in the subsections for each variable. For previous AIRS version releases this information was contained in a separate Released Processing Files Description document.

Each file contains all observations of a given type made during a period of exactly 6 minutes. For each day there are 240 granules, numbered 1-240. Over the course of 6 minutes the EOS-Aqua platform travels approximately 1500 km, and the AIRS-suite instruments scan (whisk broom) a swath approximately 1500 km wide.

Start times of granules are keyed to the start of 1958. Because of leap seconds, they do not start at the same time as days do. For data from launch through 12-31-2005, granule 1 spans 00:05:26Z - 00:11:26Z and granule 240 starts at 23:59:26Z and ends at 00:05:26Z the next day. For data 12-31-2005 through the next leap second, granule 1 spans 00:05:25Z - 00:11:25Z and granule 240 starts at 23:59:25Z and ends at 00:05:25Z the next day.

These products have exactly one swath per file. The swath name is given in the interface specification.

The names of all dimensions, geolocation fields, fields and attributes are exactly as given in the "Name" column of the appropriate table, including underscores and capitalization.

The "Explanation" information, as provided in the product interface specifications, is a guide for users of the data and is not included the product files.

The contents of the "Type" column of the attribute and field tables can either specify a standard HDF type or a special AIRS type. The standard HDF types used by AIRS are:

String of 8-bit characters (Attributes only)
8-bit integer
8-bit unsigned integer
16-bit integer
16-bit unsigned integer
32-bit integer
32-bit unsigned integer
32-bit floating-point
64-bit floating-point

For all 16-bit or longer fields the value -9999 is used to flag bad or missing data. Special AIRS types are like structures, with the fields specified in tables as discussed below.

The first table of the interface specification lists "Dimensions" which are the HDF-EOS swath dimensions. The names "GeoTrack" and "GeoXTrack" have a special meaning for

this document: "GeoTrack" is understood to be the dimension along the path of the spacecraft, and "GeoXTrack" is the dimension across the spacecraft track, starting on the left looking forward along the spacecraft track. Some products also contain second across-track dimension "CalXTrack," equivalent to "GeoXTrack," except that "CalXTrack" refers to the number of calibration footprints per scanline.

"GeoTrack" is 45 for large-spot (FOR) products (AMSU-A, Level-2, cloud-cleared AIRS) and 135 for small-spot (FOV) products (AIRS, Vis/NIR, HSB).

These files contain no geolocation mappings or indexed mappings.

The second table specifies "geolocation fields." These are all 64-bit floating-point fields that give the location of the data in space and time. If the note before the table specifies that these fields appear once per scanline then they have the single dimension "GeoTrack." Otherwise, they appear once per footprint per scanline and have dimensions "GeoTrack,GeoXTrack."

The third table specifies "Attributes." These are scalar or string fields that appear only once per granule. They are attributes in the HDF-EOS Swath sense.

The fourth table specifies “Per-Granule Data Fields.” These are fields that are valid for the entire granule but that are not scalars because they have some additional dimension.

The fifth table specifies "Along-Track Data Fields." These are fields that occur once for every scanline. These fields have dimension "GeoTrack" before any "Extra Dimensions." So an "Along-Track Data Field" with "Extra Dimensions" of "None" has dimensions "GeoTrack"; whereas, if the "Extra Dimensions" is "SpaceXTrack (= 4)," then it has dimensions "GeoTrack,SpaceXTrack."

The sixth table specifies "Full Swath Data Fields." These are fields that occur once for every footprint of every scanline. These have dimensions "GeoTrack,GeoXTrack" before any "Extra Dimensions." So a "Full Swath Data Field" with "Extra Dimensions" of "None" has dimensions "GeoTrack,GeoXTrack"; whereas, if the "Extra Dimensions" is "Channel (= 2378)," then it has dimensions "GeoTrack,GeoXTrack,Channel."

A1: L2 Standard Atmospheric/Surface Product Interface Specification

Interface Specification Version 7.0.1.0
2019-12-04

ESDT ShortNames = "AIRX2RET", “AIRS2RET”, “AIRH2RET”’

Swath Name = "L2_Standard_atmospheric&surface_product"

Level = "Level2"

Footprints = 30

scanlines per scanset = 1

Dimensions

These fields define all dimensions that can be used for HDF-EOS swath fields.

The names "GeoTrack" and "GeoXTrack" have a special meaning for this document: "Cross-Track" data fields have a hidden dimension of "GeoXTrack"; "Along-Track" data fields have a hidden dimension of "GeoTrack"; "Full Swath Data Fields have hidden dimensions of both "GeoTrack" and "GeoXTrack".

Name	Value	Explanation
GeoXTrack	30	Dimension across track for footprint positions. Same as number of footprints per scanline. -- starting at the left and increasing towards the right as you look along the satellite's path
GeoTrack	# of scan lines in swath	Dimension along track for footprint positions. Same as number of scanlines in granule. Parallel to the satellite's path, increasing with time. (Nominally 45)
StdPressureLev	28	Number of standard pressure altitude levels (from bottom of the atmosphere up).
StdPressureLay	28	Number of standard pressure altitude layers (Always equal to StdPressureLev: last layer goes to the top of the atmosphere).
AIRSXTrack	3	The number of AIRS cross-track spots per AMSU-A spot. Direction is the same as GeoXTrack -- starting at the left and increasing towards the right as you look along the satellite's path
AIRSTrack	3	The number of AIRS along-track spots per AMSU-A spot. Direction is the same as GeoTrack -- parallel to the satellite's path, increasing with time
Cloud	2	Cloud layer dimension in order of increasing pressure. Only first nCld or numCloud elements are valid

MWHingeSurf	7	Number of standard frequency hinge points in Microwave surface emissivity and surface brightness. Frequencies are 23.8, 31.4, 50.3, 52.8, 89.0, 150.0, 183.31 GHz respectively.Values are also found in field MWHingeSurfFreqGHz.
H2OFunc	11	Functions on which water vapor retrieval is calculated
O3Func	9	Functions on which ozone retrieval is calculated
COFunc	9	Functions on which carbon monoxide retrieval is calculated
CH4Func	10	Functions on which methane retrieval is calculated
HingeSurf	100	Maximum number of frequency hinge points in IR surface emissivity
H2OPressureLev	15	Number of water vapor pressure altitude levels (from bottom of the atmosphere up).
H2OPressureLay	14	Number of standard pressure altitude layers (Always one less than H2OPressureLev).

Geolocation Fields

These fields appear for every footprint (GeoTrack * GeoXTrack times) and correspond to footprint center coordinates and "shutter" time.

Name	Explanation
Latitude	Footprint boresight geodetic Latitude in degrees North (-90.0 ... 90.0)
Longitude	Footprint boresight geodetic Longitude in degrees East (-180.0 ... 180.0)
Time	Footprint "shutter" TAI Time: floating-point elapsed seconds since Jan 1, 1993

Attributes

These fields appear only once per granule and use the HDF-EOS "Attribute" interface

Name	Type	Explanation
processing_level	string of 8-bit characters	Zero-terminated character string denoting processing level ("Level2")
instrument	string of 8-bit characters	Zero-terminated character string denoting instrument ("AIRS")
DayNightFlag	string of 8-bit characters	Zero-terminated character string set to "Night" when the subsatellite points at the beginning and end of a granule are both experiencing night according to the "civil twilight" standard (center of refracted sun is below the horizon). It is set to "Day" when both are experiencing day, and "Both" when one is experiencing day and the other night. "NA" is used when a determination cannot be made.
AutomaticQAFlag	string of 8-bit characters	Zero-terminated character string denoting granule data quality: (Always "Passed", "Failed", or "Suspect")
NumTotalData	32-bit integer	Total number of expected scene footprints
NumProcessData	32-bit integer	Number of scene footprints which are present and can be processed routinely (state = 0)
NumSpecialData	32-bit integer	Number of scene footprints which are present and can be processed only as a special test (state = 1)

NumBadData	32-bit integer	Number of scene footprints which are present but cannot be processed (state = 2)
NumMissingData	32-bit integer	Number of expected scene footprints which are not present (state = 3)
NumLandSurface	32-bit integer	Number of scene footprints for which the surface is more than 90% land
NumOceanSurface	32-bit integer	Number of scene footprints for which the surface is less than 10% land
node_type	string of 8-bit characters	Zero-terminated character string denoting whether granule is ascending, descending, or pole-crossing: ("Ascending" and "Descending" for entirely ascending or entirely descending granules, or "NorthPole" or "SouthPole" for pole-crossing granules. "NA" when determination cannot be made.)
start_year	32-bit integer	Year in which granule started, UTC (e.g. 1999)
start_month	32-bit integer	Month in which granule started, UTC (1 ... 12)
start_day	32-bit integer	Day of month in which granule started, UTC (1 ... 31)
start_hour	32-bit integer	Hour of day in which granule started, UTC (0 ... 23)
start_minute	32-bit integer	Minute of hour in which granule started, UTC (0 ... 59)
start_sec	32-bit floating-point	Second of minute in which granule started, UTC (0.0 ... 59.0)
start_orbit	32-bit integer	Orbit number of mission in which granule started
end_orbit	32-bit integer	Orbit number of mission in which granule ended
orbit_path	32-bit integer	Orbit path of start orbit (1 ... 233 as defined by EOS project)
start_orbit_row	32-bit integer	Orbit row at start of granule (1 ... 248 as defined by EOS project)
end_orbit_row	32-bit integer	Orbit row at end of granule (1 ... 248 as defined by EOS project)
granule_number	32-bit integer	Number of granule within day (1 ... 240)
num_scansets	32-bit integer	Number of scansets in granule (1 ... 45)
num_scanlines	32-bit integer	Number of scanlines in granule (1 * num_scansets)
start_Latitude	64-bit floating-point	Geodetic Latitude of spacecraft at start of granule (subsatellite location at midpoint of first scan) in degrees North (-90.0 ... 90.0)
start_Longitude	64-bit floating-point	Geodetic Longitude of spacecraft at start of granule (subsatellite location at midpoint of first scan) in degrees East (-180.0 ... 180.0)
start_Time	64-bit floating-point	TAI Time at start of granule (floating-point elapsed seconds since start of 1993)
end_Latitude	64-bit floating-point	Geodetic Latitude of spacecraft at end of granule (subsatellite location at midpoint of last scan) in degrees North (-90.0 ... 90.0)
end_Longitude	64-bit floating-point	Geodetic Longitude of spacecraft at end of granule (subsatellite location at midpoint of last scan) in degrees East (-180.0 ... 180.0)
end_Time	64-bit floating-point	TAI Time at end of granule (floating-point elapsed seconds since start of 1993)
eq_x_longitude	32-bit floating-point	Longitude of spacecraft at southward equator crossing nearest granule start in degrees East (-180.0 ... 180.0)
eq_x_tai	64-bit floating-point	Time of eq_x_longitude in TAI units (floating-point elapsed seconds since start of 1993)
LonGranuleCen	16-bit integer	Geodetic Longitude of the center of the granule in degrees East (-180 ... 180)
LatGranuleCen	16-bit integer	Geodetic Latitude of the center of the granule in degrees North (-90 ... 90)

LocTimeGranuleCen	16-bit integer	Local solar time at the center of the granule in minutes past midnight (0 ... 1439)
num_fpe	16-bit integer	Number of floating point errors
orbitgeoqa	32-bit unsigned integer	Orbit Geolocation QA:; Bit 0: (LSB, value 1) bad input value (last scanline); Bit 1: (value 2) bad input value (first scanline); Bit 2: (value 4) PGS_EPH_GetEphMet() gave PGSEPH_E_NO_SC_EPHEM_FILE; Bit 3: (value 8) PGS_EPH_GetEphMet() gave PGSEPH_E_BAD_ARRAY_SIZE; Bit 4: (value 16) PGS_EPH_GetEphMet() gave PGSTD_E_TIME_FMT_ERROR; Bit 5: (value 32) PGS_EPH_GetEphMet() gave PGSTD_E_TIME_VALUE_ERROR; Bit 6: (value 64) PGS_EPH_GetEphMet() gave PGSTD_E_SC_TAG_UNKNOWN; Bit 7: (value 128) PGS_EPH_GetEphMet() gave PGS_E_TOOLKIT; Bit 8: (value 256) PGS_TD_UTCtoTAI() gave PGSTD_E_NO_LEAP_SECS; Bit 9: (value 512) PGS_TD_UTCtoTAI() gave PGSTD_E_TIME_FMT_ERROR; Bit 10: (value 1024) PGS_TD_UTCtoTAI() gave PGSTD_E_TIME_VALUE_ERROR; Bit 11: (value 2048) PGS_TD_UTCtoTAI() gave PGS_E_TOOLKIT; Bit 12: (value 4096) PGS_CSC_DayNight() gave PGSTD_E_NO_LEAP_SECS; Bit 13: (value 8192) PGS_CSC_DayNight() gave PGSCSC_E_INVALID_LIMITTAG; Bit 14: (value 16384) PGS_CSC_DayNight() gave PGSCSC_E_BAD_ARRAY_SIZE; Bit 15: (value 32768) PGS_CSC_DayNight() gave PGSCSC_W_ERROR_IN_DAYNIGHT; Bit 16: (value 65536) PGS_CSC_DayNight() gave PGSCSC_W_BAD_TRANSFORM_VALUE; Bit 17: (value 131072) PGS_CSC_DayNight() gave PGSCSC_W_BELOW_HORIZON; Bit 18: (value 262144) PGS_CSC_DayNight() gave PGSCSC_W_PREDICTED_UT1 (This is expected except when reprocessing.); Bit 19: (value 524288) PGS_CSC_DayNight() gave PGSTD_E_NO_UT1_VALUE; Bit 20: (value 1048576) PGS_CSC_DayNight() gave PGSTD_E_BAD_INITIAL_TIME; Bit 21: (value 2097152) PGS_CSC_DayNight() gave PGSCBP_E_TIME_OUT_OF_RANGE; Bit 22: (value 4194304) PGS_CSC_DayNight() gave PGSCBP_E_UNABLE_TO_OPEN_FILE; Bit 23: (value 8388608) PGS_CSC_DayNight() gave PGSMEM_E_NO_MEMORY; Bit 24: (value 16777216) PGS_CSC_DayNight() gave PGS_E_TOOLKIT; Bit 25-31: not used
num_satgeoqa	16-bit integer	Number of scans with problems in satgeoqa
num_glintgeoqa	16-bit integer	Number of scans with problems in glintgeoqa

num_moongeoqa	16-bit integer	Number of scans with problems in moongeoqa
num_ftptgeoqa	16-bit integer	Number of footprints with problems in ftptgeoqa
num_zengeoqa	16-bit integer	Number of footprints with problems in zengeoqa
num_demgeoqa	16-bit integer	Number of footprints with problems in demgeoqa
CO_first_guess	string of 8-bit characters	Name of CO First Guess source.
CH4_first_guess	string of 8-bit characters	Name of CH4 First Guess source.
NumSO2FOVs	16-bit unsigned integer	Number of fields-of-view (out of a nominal 1350) with a signifcant SO2 concentration based on the value of BT_diff_SO2.

Per-Granule Data Fields

These fields appear only once per granule and use the HDF-EOS "Field" interface

Name	Type	Extra Dimensions	Explanation
pressStd	32-bit floating-point	StdPressureLev (= 28)	Standard pressures in hPa (bottom of the atmosphere first)
pressH2O	32-bit floating-point	H2OPressureLev (= 15)	Water vapor pressures in hPa (bottom of the atmosphere first)
MWHingeSurfFreqGHz	32-bit floating-point	MWHingeSurf (= 7)	Frequencies in GHz for MW surface parameters (SfcTbMWStd, EmisMWStd,...)

Along-Track Data Fields

These fields appear once per scanline (GeoTrack times)

Name	Type	Extra Dimensions	Explanation
satheight	32-bit floating-point	None	Satellite altitude at nadirTAI in km above reference ellipsoid (e.g. 725.2)
satroll	32-bit floating-point	None	Satellite attitude roll angle at nadirTAI (-180.0 ... 180.0 angle about the +x (roll) ORB axis, +x axis is positively oriented in the direction of orbital flight completing an orthogonal triad with y and z.)
satpitch	32-bit floating-point	None	Satellite attitude pitch angle at nadirTAI (-180.0 ... 180.0 angle about +y (pitch) ORB axis. +y axis is oriented normal to the orbit plane with the positive sense opposite to that of the orbit's angular momentum vector H.)
satyaw	32-bit floating-point	None	Satellite attitude yaw angle at nadirTAI (-180.0 ... 180.0 angle about +z (yaw) axis. +z axis is positively oriented Earthward parallel to the satellite radius vector R from the spacecraft center of mass to the center of the Earth.)
glintlat	32-bit floating-point	None	Solar glint geodetic latitude in degrees North at nadirTAI (-90.0 ... 90.0)
glintlon	32-bit floating-point	None	Solar glint geodetic longitude in degrees East at nadirTAI (-180.0 ... 180.0)
nadirTAI	64-bit floating-point	None	TAI time at which instrument is nominally looking directly down. (between footprints 15 & 16 for AMSU or between footprints 45 & 46 for AIRS/Vis & HSB) (floating-point elapsed seconds since start of 1993)

sat_lat	64-bit floating-point	None	Satellite geodetic latitude in degrees North (-90.0 ... 90.0)
sat_lon	64-bit floating-point	None	Satellite geodetic longitude in degrees East (-180.0 ... 180.0)
scan_node_type	8-bit integer	None	'A' for ascending, 'D' for descending, 'E' when an error is encountered in trying to determine a value.
satgeoqa	32-bit unsigned integer	None	Satellite Geolocation QA flags:; Bit 0: (LSB, value 1) bad input value; Bit 1: (value 2) PGS_TD_TAItoUTC() gave PGSTD_E_NO_LEAP_SECS; Bit 2: (value 4) PGS_TD_TAItoUTC() gave PGS_E_TOOLKIT; Bit 3: (value 8) PGS_EPH_EphemAttit() gave PGSEPH_W_BAD_EPHEM_VALUE; Bit 4: (value 16) PGS_EPH_EphemAttit() gave PGSEPH_E_BAD_EPHEM_FILE_HDR; Bit 5: (value 32) PGS_EPH_EphemAttit() gave PGSEPH_E_NO_SC_EPHEM_FILE; Bit 6: (value 64) PGS_EPH_EphemAttit() gave PGSEPH_E_NO_DATA_REQUESTED; Bit 7: (value 128) PGS_EPH_EphemAttit() gave PGSTD_E_SC_TAG_UNKNOWN; Bit 8: (value 256) PGS_EPH_EphemAttit() gave PGSEPH_E_BAD_ARRAY_SIZE; Bit 9: (value 512) PGS_EPH_EphemAttit() gave PGSTD_E_TIME_FMT_ERROR; Bit 10: (value 1024) PGS_EPH_EphemAttit() gave PGSTD_E_TIME_VALUE_ERROR; Bit 11: (value 2048) PGS_EPH_EphemAttit() gave PGSTD_E_NO_LEAP_SECS; Bit 12: (value 4096) PGS_EPH_EphemAttit() gave PGS_E_TOOLKIT; Bit 13: (value 8192) PGS_CSC_ECItoECR() gave PGSCSC_W_BAD_TRANSFORM_VALUE; Bit 14: (value 16384) PGS_CSC_ECItoECR() gave PGSCSC_E_BAD_ARRAY_SIZE; Bit 15: (value 32768) PGS_CSC_ECItoECR() gave PGSTD_E_NO_LEAP_SECS; Bit 16: (value 65536) PGS_CSC_ECItoECR() gave PGSTD_E_TIME_FMT_ERROR; Bit 17: (value 131072) PGS_CSC_ECItoECR() gave PGSTD_E_TIME_VALUE_ERROR; Bit 18: unused (set to zero); Bit 19: (value 524288) PGS_CSC_ECItoECR() gave PGSTD_E_NO_UT1_VALUE; Bit 20: (value 1048576) PGS_CSC_ECItoECR() gave PGS_E_TOOLKIT; Bit 21: (value 2097152) PGS_CSC_ECRtoGEO() gave PGSCSC_W_TOO_MANY_ITERS; Bit 22: (value 4194304) PGS_CSC_ECRtoGEO() gave PGSCSC_W_INVALID_ALTITUDE; Bit 23: (value 8388608) PGS_CSC_ECRtoGEO() gave PGSCSC_W_SPHERE_BODY; Bit 24: (value 16777216) PGS_CSC_ECRtoGEO() gave

			PGSCSC_W_LARGE_FLATTENING; Bit 25: (value 33554432) PGS_CSC_ECRtoGEO() gave PGSCSC_W_DEFAULT_EARTH_MODEL; Bit 26: (value 67108864) PGS_CSC_ECRtoGEO() gave PGSCSC_E_BAD_EARTH_MODEL; Bit 27: (value 134217728) PGS_CSC_ECRtoGEO() gave PGS_E_TOOLKIT; Bit 28-31: not used
glintgeoqa	16-bit unsigned integer	None	Glint Geolocation QA flags:; Bit 0: (LSB, value 1) bad input value; Bit 1: (value 2) glint location in Earth's shadow (Normal for night FOVs); Bit 2: (value 4) glint calculation not converging; Bit 3: (value 8) glint location sun vs. satellite zenith mismatch; Bit 4: (value 16) glint location sun vs. satellite azimuth mismatch; Bit 5: (value 32) bad glint location; Bit 6: (value 64) PGS_CSC_ZenithAzimuth() gave any 'W' class return code; Bit 7: (value 128) PGS_CSC_ZenithAzimuth() gave any 'E' class return code; Bit 8: (value 256) PGS_CBP_Earth_CB_Vector() gave any 'W' class return code; Bit 9: (value 512) PGS_CBP_Earth_CB_Vector() gave any 'E' class return code; Bit 10: (value 1024) PGS_CSC_ECItoECR() gave any 'W' class return code except PGSCSC_W_PREDICTED_UT1 (for Glint); Bit 11: (value 2048) PGS_CSC_ECItoECR() gave any 'E' class return code (for Glint); Bit 12: (value 4096) PGS_CSC_ECRtoGEO() gave any 'W' class return code (for Glint); Bit 13: (value 8192) PGS_CSC_ECRtoGEO() gave any 'E' class return code (for Glint); Bit 14: (value 16384) PGS_CSC_ECItoECR() gave any 'W' class return code except PGSCSC_W_PREDICTED_UT1 ; Bit 15: (value 32768) PGS_CSC_ECItoECR() gave any 'E' class return code
moongeoqa	16-bit unsigned integer	None	Moon Geolocation QA flags:; Bit 0: (LSB, value 1) bad input value; Bit 1: (value 2) PGS_TD_TAItoUTC() gave PGSTD_E_NO_LEAP_SECS; Bit 2: (value 4) PGS_TD_TAItoUTC() gave PGS_E_TOOLKIT; Bit 3: (value 8) PGS_CBP_Sat_CB_Vector() gave PGSCSC_W_BELOW_SURFACE; Bit 4: (value 16) PGS_CBP_Sat_CB_Vector() gave PGSCBP_W_BAD_CB_VECTOR; Bit 5: (value 32) PGS_CBP_Sat_CB_Vector() gave PGSCBP_E_BAD_ARRAY_SIZE; Bit 6: (value 64) PGS_CBP_Sat_CB_Vector() gave PGSCBP_E_INVALID_CB_ID; Bit 7: (value 128) PGS_CBP_Sat_CB_Vector() gave PGSMEM_E_NO_MEMORY;

			Bit 8: (value 256) PGS_CBP_Sat_CB_Vector() gave PGSCBP_E_UNABLE_TO_OPEN_FILE; Bit 9: (value 512) PGS_CBP_Sat_CB_Vector() gave PGSTD_E_BAD_INITIAL_TIME; Bit 10: (value 1024) PGS_CBP_Sat_CB_Vector() gave PGSCBP_E_TIME_OUT_OF_RANGE; Bit 11: (value 2048) PGS_CBP_Sat_CB_Vector() gave PGSTD_E_SC_TAG_UNKNOWN; Bit 12: (value 4096) PGS_CBP_Sat_CB_Vector() gave PGSEPH_E_BAD_EPHEM_FILE_HDR; Bit 13: (value 8192) PGS_CBP_Sat_CB_Vector() gave PGSEPH_E_NO_SC_EPHEM_FILE; Bit 14: (value 16384) PGS_CBP_Sat_CB_Vector() gave PGS_E_TOOLKIT; Bit 15: not used

Full Swath Data Fields

These fields appear for every footprint of every scanline in the granule (GeoTrack * GeoXTrack times)

Name	Type	Extra Dimensions	Explanation
Geolocation			
satzen	32-bit floating-point	None	Spacecraft zenith angle (0.0 ... 180.0) degrees from zenith (measured relative to the geodetic vertical on the reference (WGS84) spheroid and including corrections outlined in EOS SDP toolkit for normal accuracy.)
satazi	32-bit floating-point	None	Spacecraft azimuth angle (-180.0 ... 180.0) degrees E of N GEO)
solzen	32-bit floating-point	None	Solar zenith angle (0.0 ... 180.0) degrees from zenith (measured relative to the geodetic vertical on the reference (WGS84) spheroid and including corrections outlined in EOS SDP toolkit for normal accuracy.)
solazi	32-bit floating-point	None	Solar azimuth angle (-180.0 ... 180.0) degrees E of N GEO)
sun_glint_distance	16-bit integer	None	Distance (km) from footprint center to location of the sun glint (-9999 for unknown, 30000 for no glint visible because spacecraft is in Earth's shadow)
Surface ancillary information from geolocation			
topog	32-bit floating-point	None	Mean topography in meters above reference ellipsoid
topog_err	32-bit floating-point	None	Error estimate for topog
landFrac	32-bit floating-point	None	Fraction of spot that is land (0.0 ... 1.0)

landFrac_err	32-bit floating-point	None	Error estimate for landFrac
latAIRS	32-bit floating-point	AIRSTrack (= 3) * AIRSXTrack (= 3)	Geodetic center latitude of AIRS spots in degrees North (-90.0 ... 90.0)
lonAIRS	32-bit floating-point	AIRSTrack (= 3) * AIRSXTrack (= 3)	Geodetic center longitude of AIRS spots in degrees East (-180.0 ... 180.0)
PSurfStd	32-bit floating-point	None	Surface pressure first guess in hPa, interpolated from forecast
PSurfStd_QC	16-bit unsigned integer	None	Quality flag for surface pressure guess input.; 0: Highest Quality -- from timely forecast; 1: Good Quality -- from climatology; 2: Do Not Use
nSurfStd	32-bit integer	None	Index in pressStd array of first pressure level above mean surface (1 ... 15)
Quality Indicator Pressure Boundaries			
PBest	32-bit floating-point	None	Maximum value of pressure for which temperature is Quality = 0 (hPa)
PGood	32-bit floating-point	None	Maximum value of pressure for which temperature is Quality = 0 or 1 (hPa)
nBestStd	16-bit integer	None	Standard level index of highest pressure (i.e. lowest altitude) for which Quality = 0. A value of 29 indicates that no part of the profile passes the test. (1 ... 29)
nGoodStd	16-bit integer	None	Standard level index of highest pressure (i.e. lowest altitude) for which Quality = 0 or 1. A value of 29 indicates that no part of the profile passes the test. (1 ... 29)
Surface Property Retrievals			
TSurfStd	32-bit floating-point	None	Surface skin temperature in Kelvins
TSurfStd_QC	16-bit unsigned integer	None	Quality flag for TSurfStd.; 0: Highest Quality; 1: Good Quality; 2: Do Not Use
TSurfStdErr	32-bit floating-point	None	Error estimate for TSurfStd
numHingeSurf	16-bit integer	None	Number of IR hinge points for surface emissivity and reflectivity
freqEmis	32-bit floating-point	HingeSurf (= 100)	Frequencies for surface emissivity and reflectivity in cm-1 (in order of increasing frequency. Only first numHingeSurf elements are valid)

emisIRStd	32-bit floating-point	HingeSurf (= 100)	Spectral IR Surface Emissivities (in order of increasing frequency. Only first numHingeSurf elements are valid)
emisIRStd_QC	16-bit unsigned integer	HingeSurf (= 100)	Quality Control for emisIRStd.; 0: Highest Quality; 1: Good Quality; 2: Do Not Use
emisIRStdErr	32-bit floating-point	HingeSurf (= 100)	Error estimate for emisIRStd
Air Temperature Retrievals			
TAirStd	32-bit floating-point	StdPressureLev (= 28)	Atmospheric Temperature at StdPressLev in Kelvins.
TAirStd_QC	16-bit unsigned integer	StdPressureLev (= 28)	Quality Control for TAirStd.; 0: Highest Quality; 1: Good Quality; 2: Do Not Use
TAirStdErr	32-bit floating-point	StdPressureLev (= 28)	Error estimate for TAirStd
TSurfAir	32-bit floating-point	None	Surface air temperature in Kelvins
TSurfAir_QC	16-bit unsigned integer	None	Quality Control for TSurfAir.; 0: Highest Quality; 1: Good Quality; 2: Do Not Use
TSurfAirErr	32-bit floating-point	None	Error estimate for TSurfAir
Temp_dof	32-bit floating-point	None	Measure of the amount of information in temperature profile retrieval (deg of freedom).
Water Vapor Saturation Quantities Derived from Temperature			
H2OMMRSat	32-bit floating-point	H2OPressureLay (= 14)	Layer Water vapor saturation mass mixing ratio (gm / kg dry air) over equilibrium phase (set to -9999. when saturation pressure exceeds 1% of ambient pressure.)
H2OMMRSat_QC	16-bit unsigned integer	H2OPressureLay (= 14)	Quality Control for H2OMMRSat.; 0: Highest Quality; 1: Good Quality; 2: Do Not Use
H2OMMRSatLevStd	32-bit floating-point	H2OPressureLev (= 15)	Level Water vapor saturation mass mixing ratio (gm / kg dry air) over equilibrium phase (set to -9999. when saturation pressure exceeds 1% of ambient pressure.)
H2OMMRSatLevStd_QC	16-bit unsigned integer	H2OPressureLev (= 15)	Quality Control for H2OMMRSatLevStd.; 0: Highest Quality; 1: Good Quality; 2: Do Not Use

H2OMMRSatSurf	32-bit floating-point	None	Water Vapor saturation Mass Mixing Ratio at the surface (gm / kg dry air) over equilibrium phase
H2OMMRSatSurf_QC	16-bit unsigned integer	None	Quality Control for H2OMMRSatSurf.; 0: Highest Quality; 1: Good Quality; 2: Do Not Use
H2OMMRSat_liquid	32-bit floating-point	H2OPressure Lay (= 14)	Layer Water vapor saturation mass mixing ratio (gm / kg dry air) over liquid phase (set to -9999. when saturation pressure exceeds 1% of ambient pressure.)
H2OMMRSat_liquid_QC	16-bit unsigned integer	H2OPressure Lay (= 14)	Quality Control for H2OMMRSat_liquid.; 0: Highest Quality; 1: Good Quality; 2: Do Not Use
H2OMMRSatLevStd_liquid	32-bit floating-point	H2OPressure Lev (= 15)	Level Water vapor saturation mass mixing ratio (gm / kg dry air) over liquid phase (set to -9999. when saturation pressure exceeds 1% of ambient pressure.)
H2OMMRSatLevStd_liquid_QC	16-bit unsigned integer	H2OPressure Lev (= 15)	Quality Control for H2OMMRSatLevStd_liquid.; 0: Highest Quality; 1: Good Quality; 2: Do Not Use
H2OMMRSatSurf_liquid	32-bit floating-point	None	Water Vapor saturation Mass Mixing Ratio at the surface (gm / kg dry air) over liquid phase
H2OMMRSatSurf_liquid_QC	16-bit unsigned integer	None	Quality Control for H2OMMRSatSurf_liquid.; 0: Highest Quality; 1: Good Quality; 2: Do Not Use
Tropopause Derived from Temperature			
PTropopause	32-bit floating-point	None	Tropopause height (hPa)
PTropopause_QC	16-bit unsigned integer	None	Quality Control for PTropopause.; 0: Highest Quality; 1: Good Quality; 2: Do Not Use
T_Tropopause	32-bit floating-point	None	Tropopause temperature (K)
T_Tropopause_QC	16-bit unsigned integer	None	Quality Control for T_Tropopause.; 0: Highest Quality; 1: Good Quality; 2: Do Not Use
Water Vapor Retrievals			
totH2OStd	32-bit floating-point	None	Total precipitable water vapor (kg / m**2)

totH2OStd_QC	16-bit unsigned integer	None	Quality Control for totH2OStd.; 0: Highest Quality; 1: Good Quality; 2: Do Not Use
totH2OStdErr	32-bit floating-point	None	Error estimate for totH2OStd
H2OMMRStd	32-bit floating-point	H2OPressure Lay (= 14)	Water Vapor Mass Mixing Ratio (gm / kg dry air)
H2OMMRStd_QC	16-bit unsigned integer	H2OPressure Lay (= 14)	Quality Control for H2OMMRStd.; 0: Highest Quality; 1: Good Quality; 2: Do Not Use
H2OMMRStdErr	32-bit floating-point	H2OPressure Lay (= 14)	Error estimate for H2OMMRStd
H2OMMRLevStd	32-bit floating-point	H2OPressure Lev (= 15)	Water Vapor Mass Mixing Ratio (gm / kg dry air)
H2OMMRLevStd_QC	16-bit unsigned integer	H2OPressure Lev (= 15)	Quality Control for H2OMMRLevStd.; 0: Highest Quality; 1: Good Quality; 2: Do Not Use
H2OMMRLevStdErr	32-bit floating-point	H2OPressure Lev (= 15)	Error estimate for H2OMMRLevStd
H2OMMRSurf	32-bit floating-point	None	Water Vapor Mass Mixing Ratio at the surface (gm / kg dry air)
H2OMMRSurf_QC	16-bit unsigned integer	None	Quality Control for H2OMMRSurf.; 0: Highest Quality; 1: Good Quality; 2: Do Not Use
H2OMMRSurfErr	32-bit floating-point	None	Error estimate for H2OMMRSurf
num_H2O_Func	16-bit integer	None	Number of valid entries in each dimension of H2O_ave_kern_21func.
H2O_verticality_21func	32-bit floating-point	H2OFunc (= 21)	Sum of the rows of H2O_ave_kern_21func.
H2O_dof	32-bit floating-point	None	Measure of the amount of information in H2O retrieval (deg of freedom).
Relative Humidity Derived from Temperature and Water Vapor			
RelHum	32-bit floating-point	H2OPressure Lev (= 15)	Relative humidity over equilibrium phase (%)
RelHum_QC	16-bit unsigned integer	H2OPressure Lev (= 15)	Quality control for RelHum.; 0: Highest Quality; 1: Good Quality; 2: Do Not Use

RelHumSurf	32-bit floating-point	None	Relative humidity at the surface over equilibrium phase (%)
RelHumSurf_QC	16-bit unsigned integer	None	Quality Control for RelHumSurf.; 0: Highest Quality; 1: Good Quality; 2: Do Not Use
RelHum_liquid	32-bit floating-point	H2OPressure Lev (= 15)	Relative humidity over liquid phase (%)
RelHum_liquid_QC	16-bit unsigned integer	H2OPressure Lev (= 15)	Quality control for RelHum_liquid.; 0: Highest Quality; 1: Good Quality; 2: Do Not Use
RelHumSurf_liquid	32-bit floating-point	None	Relative humidity at the surface over liquid phase (%)
RelHumSurf_liquid_QC	16-bit unsigned integer	None	Quality Control for RelHumSurf_liquid.; 0: Highest Quality; 1: Good Quality; 2: Do Not Use
Geopotential Height Derived from Temperature and Water Vapor			
GP_Tropopause	32-bit floating-point	None	Geopotential height at tropopause (m above mean sea level)
GP_Tropopause_QC	16-bit unsigned integer	None	Quality Control for GP_Tropopause.; 0: Highest Quality; 1: Good Quality; 2: Do Not Use
GP_Height	32-bit floating-point	StdPressureLe v (= 28)	Geopotential Heights at StdPressureLev (m above mean sea level)
GP_Height_QC	16-bit unsigned integer	StdPressureLe v (= 28)	Quality Control for GP_Height.; 0: Highest Quality; 1: Good Quality; 2: Do Not Use
GP_Surface	32-bit floating-point	None	Geopotential Height of surface (m above mean sea level)
GP_Surface_QC	16-bit unsigned integer	None	Quality Control for GP_Surface.; 0: Highest Quality; 1: Good Quality; 2: Do Not Use
Cloud Formation Retrievals on 3 by 3 AIRS Fields of View			
CldFrcTot	32-bit floating-point	None	Total cloud fraction over all cloud layers and all 9 spots (0.0 ... 1.0) assuming unit cloud top emissivity.
CldFrcTot_QC	16-bit unsigned integer	None	Quality Control for CldFrcTot.; 0: Highest Quality; 1: Good Quality; 2: Do Not Use
CldFrcStd	32-bit floating-point	AIRSTrack (= 3) * AIRSXTrack	Cloud fraction (0.0 ... 1.0) assuming unit cloud top emissivity (in order of increasing pressure. Only first nCld elements are valid) Caution: For

		(= 3) * Cloud (= 2)	CldFrcStd = 1, only the average cloud fraction over the nine spots is reported (duplicated nine times) for each level.
CldFrcStd_QC	16-bit unsigned integer	AIRSTrack (= 3) * AIRSXTrack (= 3) * Cloud (= 2)	Quality Control for CldFrcStd.; 0: Highest Quality; 1: Good Quality; 2: Do Not Use
CldFrcStdErr	32-bit floating-point	AIRSTrack (= 3) * AIRSXTrack (= 3) * Cloud (= 2)	Error estimate for CldFrcStd
PCldTop	32-bit floating-point	AIRSTrack (= 3) * AIRSXTrack (= 3) * Cloud (= 2)	Cloud top pressure in hPa. (in order of increasing pressure. Only first nCld elements are valid)
PCldTop_QC	16-bit unsigned integer	AIRSTrack (= 3) * AIRSXTrack (= 3) * Cloud (= 2)	Quality Control for PCldTop.; 0: Highest Quality; 1: Good Quality; 2: Do Not Use
PCldTopErr	32-bit floating-point	AIRSTrack (= 3) * AIRSXTrack (= 3) * Cloud (= 2)	Error estimate for PCldTop.
TCldTop	32-bit floating-point	AIRSTrack (= 3) * AIRSXTrack (= 3) * Cloud (= 2)	Cloud top temperature in Kelvins (in order of increasing pressure. Only first nCld elements are valid)
TCldTop_QC	16-bit unsigned integer	AIRSTrack (= 3) * AIRSXTrack (= 3) * Cloud (= 2)	Quality Control for TCldTop.; 0: Highest Quality; 1: Good Quality; 2: Do Not Use
TCldTopErr	32-bit floating-point	AIRSTrack (= 3) * AIRSXTrack (= 3) * Cloud (= 2)	Error estimate for TCldTop.
nCld	32-bit integer	AIRSTrack (= 3) * AIRSXTrack (= 3)	Number of cloud layers in each of the 9 spots
Ozone Retrievals			
totO3Std	32-bit floating-point	None	Total ozone burden (Dobson units)
totO3Std_QC	16-bit unsigned integer	None	Quality Control for totO3Std.; 0: Highest Quality; 1: Good Quality; 2: Do Not Use

totO3StdErr	32-bit floating-point	None	Error estimate for totO3Std
O3VMRStd	32-bit floating-point	StdPressureLay (= 28)	Dry column ozone Volume Mixing Ratio on standard layers (ppv)
O3VMRStd_QC	16-bit unsigned integer	StdPressureLay (= 28)	Quality Control for O3VMRStd.; 0: Highest Quality; 1: Good Quality; 2: Do Not Use
O3VMRStdErr	32-bit floating-point	StdPressureLay (= 28)	Error estimate for O3VMRStd
O3VMRLevStd	32-bit floating-point	StdPressureLev (= 28)	Dry column ozone Volume Mixing Ratio at standard levels (ppv)
O3VMRLevStd_QC	16-bit unsigned integer	StdPressureLev (= 28)	Quality Control for O3VMRLevStd.; 0: Highest Quality; 1: Good Quality; 2: Do Not Use
O3VMRLevStdErr	32-bit floating-point	StdPressureLev (= 28)	Error estimate for O3VMRLevStd
num_O3_Func	16-bit integer	None	Number of valid entries in each dimension of O3_ave_kern_20func.
O3_verticality_20func	32-bit floating-point	O3Func (= 20)	Sum of the rows of O3_ave_kern_20func.
O3_dof	32-bit floating-point	None	Measure of the amount of information in O3 retrieval (deg of freedom).
Carbon Monoxide Retrievals			
CO_total_column	32-bit floating-point	None	Retrieved total column CO (molecules/cm2).
CO_total_column_QC	16-bit unsigned integer	None	Quality Control for CO_total_column.; 0: Highest Quality; 1: Good Quality; 2: Do Not Use
COVMRLevStd	32-bit floating-point	StdPressureLev (= 28)	Dry column CO Volume Mixing Ratio at standard levels (ppv)
COVMRLevStd_QC	16-bit unsigned integer	StdPressureLev (= 28)	Quality Control for COVMRLevStd.; 0: Highest Quality; 1: Good Quality; 2: Do Not Use
COVMRLevStdErr	32-bit floating-point	StdPressureLev (= 28)	Error estimate for COVMRLevStd
num_CO_Func	16-bit integer	None	Number of valid entries in each dimension of CO_ave_kern.
CO_verticality	32-bit floating-point	COFunc (= 9)	Sum of the rows of CO_ave_kern.

CO_dof	32-bit floating-point	None	Measure of the amount of information in CO retrieval (deg of freedom).
Methane Retrievals			
CH4_total_column	32-bit floating-point	None	Retrieved total column CH4 (molecules/cm2).
CH4_total_column_QC	16-bit unsigned integer	None	Quality Control for CH4_total_column.; 0: Highest Quality; 1: Good Quality; 2: Do Not Use
CH4VMRLevStd	32-bit floating-point	StdPressureLev (= 28)	Dry column CH4 Volume Mixing Ratio at standard levels (ppv)
CH4VMRLevStd_QC	16-bit unsigned integer	StdPressureLev (= 28)	Quality Control for CH4VMRLevStd.; 0: Highest Quality; 1: Good Quality; 2: Do Not Use
CH4VMRLevStdErr	32-bit floating-point	StdPressureLev (= 28)	Error estimate for CH4VMRLevStd
num_CH4_Func	16-bit integer	None	Number of valid entries in each dimension of CH4_ave_kern.
CH4_verticality_10func	32-bit floating-point	CH4Func (= 10)	Sum of the rows of CH4_ave_kern.
CH4_dof	32-bit floating-point	None	Measure of the amount of information in CH4 retrieval (deg of freedom).
Outgoing Longwave Radiation Retrievals			
olr	32-bit floating-point	None	Outgoing Longwave Radiation Flux integrated over 100 to 2800 cm**-1 (Watts/m**2)
olr_QC	16-bit unsigned integer	None	Quality Control for olr.; 0: Highest Quality; 1: Good Quality; 2: Do Not Use
olr3x3	32-bit floating-point	AIRSTrack (= 3) * AIRSXTrack (= 3)	Outgoing Longwave Radiation Flux integrated over 100 to 2800 cm**-1 (per 15 km AIRS FOV) (Watts/m**2)
olr3x3_QC	16-bit unsigned integer	AIRSTrack (= 3) * AIRSXTrack (= 3)	Quality Control for olr3x3.; 0: Highest Quality; 1: Good Quality; 2: Do Not Use
olr_err	32-bit floating-point	None	Error estimate for olr (Watts/m**2)
clrolr	32-bit floating-point	None	Clear-sky Outgoing Longwave Radiation Flux integrated over 100 to 2800 cm**-1 (Watts/m**2)
clrolr_QC	16-bit unsigned integer	None	Quality Control for clrolr.; 0: Highest Quality; 1: Good Quality; 2: Do Not Use

clrolr_err	32-bit floating-point	None	Error estimate for clrolr (Watts/m**2)
Geolocation QA			
ftptgeoqa	32-bit unsigned integer	None	Footprint Geolocation QA flags:; Bit 0: (LSB, value 1) bad input value; Bit 1: (value 2) PGS_TD_TAItoUTC() gave PGSTD_E_NO_LEAP_SECS; Bit 2: (value 4) PGS_TD_TAItoUTC() gave PGS_E_TOOLKIT; Bit 3: (value 8) PGS_CSC_GetFOV_Pixel() gave PGSCSC_W_MISS_EARTH; Bit 4: (value 16) PGS_CSC_GetFOV_Pixel() gave PGSTD_E_SC_TAG_UNKNOWN; Bit 5: (value 32) PGS_CSC_GetFOV_Pixel() gave PGSCSC_W_ZERO_PIXEL_VECTOR; Bit 6: (value 64) PGS_CSC_GetFOV_Pixel() gave PGSCSC_W_BAD_EPH_FOR_PIXEL; Bit 7: (value 128) PGS_CSC_GetFOV_Pixel() gave PGSCSC_W_INSTRUMENT_OFF_BOARD; Bit 8: (value 256) PGS_CSC_GetFOV_Pixel() gave PGSCSC_W_BAD_ACCURACY_FLAG; Bit 9: (value 512) PGS_CSC_GetFOV_Pixel() gave PGSCSC_E_BAD_ARRAY_SIZE; Bit 10: (value 1024) PGS_CSC_GetFOV_Pixel() gave PGSCSC_W_DEFAULT_EARTH_MODEL; Bit 11: (value 2048) PGS_CSC_GetFOV_Pixel() gave PGSCSC_W_DATA_FILE_MISSING; Bit 12: (value 4096) PGS_CSC_GetFOV_Pixel() gave PGSCSC_E_NEG_OR_ZERO_RAD; Bit 13: (value 8192) PGS_CSC_GetFOV_Pixel() gave PGSMEM_E_NO_MEMORY; Bit 14: (value 16384) PGS_CSC_GetFOV_Pixel() gave PGSTD_E_NO_LEAP_SECS; Bit 15: (value 32768) PGS_CSC_GetFOV_Pixel() gave PGSTD_E_TIME_FMT_ERROR; Bit 16: (value 65536) PGS_CSC_GetFOV_Pixel() gave PGSTD_E_TIME_VALUE_ERROR; Bit 17: (value 131072)

			PGS_CSC_GetFOV_Pixel() gave PGSCSC_W_PREDICTED_UT1; Bit 18: (value 262144) PGS_CSC_GetFOV_Pixel() gave PGSTD_E_NO_UT1_VALUE; Bit 19: (value 524288) PGS_CSC_GetFOV_Pixel() gave PGS_E_TOOLKIT; Bit 20: (value 1048576) PGS_CSC_GetFOV_Pixel() gave PGSEPH_E_BAD_EPHEM_FILE_HDR; Bit 21: (value 2097152) PGS_CSC_GetFOV_Pixel() gave PGSEPH_E_NO_SC_EPHEM_FILE; Bit 22-31: not used
zengeoqa	16-bit unsigned integer	None	Satellite zenith Geolocation QA flags:; Bit 0: (LSB, value 1) (Spacecraft) bad input value; Bit 1: (value 2) PGS_CSC_ZenithAzimuth(S/C) gave PGSCSC_W_BELOW_HORIZON; Bit 2: (value 4) PGS_CSC_ZenithAzimuth(S/C) gave PGSCSC_W_UNDEFINED_AZIMUTH; Bit 3: (value 8) PGS_CSC_ZenithAzimuth(S/C) gave PGSCSC_W_NO_REFRACTION; Bit 4: (value 16) PGS_CSC_ZenithAzimuth(S/C) gave PGSCSC_E_INVALID_VECTAG; Bit 5: (value 32) PGS_CSC_ZenithAzimuth(S/C) gave PGSCSC_E_LOOK_PT_ALTIT_RANGE; Bit 6: (value 64) PGS_CSC_ZenithAzimuth(S/C) gave PGSCSC_E_ZERO_INPUT_VECTOR; Bit 7: (value 128) PGS_CSC_ZenithAzimuth(S/C) gave PGS_E_TOOLKIT; Bit 8: (value 256) (Sun) bad input value; Bit 9: (value 512) (suppressed) PGS_CSC_ZenithAzimuth(Sun) gave PGSCSC_W_BELOW_HORIZON (This is not an error condition - the sun is below the horizon at night); Bit 10: (value 1024) PGS_CSC_ZenithAzimuth(Sun) gave PGSCSC_W_UNDEFINED_AZIMUTH; Bit 11: (value 2048) PGS_CSC_ZenithAzimuth(Sun) gave PGSCSC_W_NO_REFRACTION; Bit 12: (value 4096)

			PGS_CSC_ZenithAzimuth(Sun) gave PGSCSC_E_INVALID_VECTAG; Bit 13: (value 8192) PGS_CSC_ZenithAzimuth(Sun) gave PGSCSC_E_LOOK_PT_ALTIT_RANGE; Bit 14: (value 16384) PGS_CSC_ZenithAzimuth(Sun) gave PGSCSC_E_ZERO_INPUT_VECTOR; Bit 15: (value 32768) PGS_CSC_ZenithAzimuth(Sun) gave PGS_E_TOOLKIT
demgeoqa	16-bit unsigned integer	None	Digital Elevation Model (DEM) Geolocation QA flags:; Bit 0: (LSB, value 1) bad input value; Bit 1: (value 2) Could not allocate memory; Bit 2: (value 4) Too close to North or South pole. Excluded. (This is not an error condition - a different model is used); Bit 3: (value 8) Layer resolution incompatibility. Excluded; Bit 4: (value 16) Any DEM Routine (elev) gave PGSDEM_E_IMPROPER_TAG; Bit 5: (value 32) Any DEM Routine (elev) gave PGSDEM_E_CANNOT_ACCESS_DATA; Bit 6: (value 64) Any DEM Routine (land/water) gave PGSDEM_E_IMPROPER_TAG; Bit 7: (value 128) Any DEM Routine (land/water) gave PGSDEM_E_CANNOT_ACCESS_DATA; Bit 8: (value 256) Reserved for future layers; Bit 9: (value 512) Reserved for future layers; Bit 10: (value 1024) PGS_DEM_GetRegion(elev) gave PGSDEM_M_FILLVALUE_INCLUDED; Bit 11: (value 2048) PGS_DEM_GetRegion(land/water) gave PGSDEM_M_FILLVALUE_INCLUDED; Bit 12: (value 4096) Reserved for future layers; Bit 13: (value 8192) PGS_DEM_GetRegion(all) gave PGSDEM_M_MULTIPLE_RESOLUTIONS; Bit 14: (value 16384)

			PGS_CSC_GetFOV_Pixel() gave any 'W' class return code except PGSCSC_W_PREDICTED_UT1; Bit 15: (value 32768) PGS_CSC_GetFOV_Pixel() gave any 'E' class return code
Miscellaneous			
dust_flag	16-bit integer	AIRSTrack (= 3) * AIRSXTrack (= 3)	Flag telling whether dust was detected in this scene; 1: Dust detected; 0: Dust not detected; -1: Dust test not valid because of land; -2: Dust test not valid because of high latitude; -3: Dust test not valid because of suspected cloud; -4: Dust test not valid because of bad input data
all_spots_avg	8-bit integer	None	1: the cloud clearing step judged the scene to be clear enough that it averaged all spots' radiances; 0: cloud clearing was applied to the radiances; -1/255: cloud clearing not attempted
retrieval_type	8-bit integer	None	Deprecated -- use Xxx_QC flags. Retrieval type:; 0 for full retrieval; 10 for MW + final succeeded, initial retrieval failed; 20 for MW + initial succeeded, final failed; 30 for only MW stage succeeded, initial + final retrieval failed; 40 for MW + initial succeeded, final cloud-clearing failed; 50 for only MW stage succeeded, initial + final cloud-clearing failed; 100 for no retrieval;
SurfClass	8-bit integer	None	Surface class used in physical retrieval, from microwave (MW) and/or infrared (IR). Identical to MWSurfClass when MW is used:; 0 for coastline (Liquid water covers 50-99% of area); 1 for land (Liquid water covers < 50% of area); 2 for ocean (Liquid water covers > 99% of area); 3 for sea ice (Indicates high MW emissivity when MW information is used); 4 for sea ice (Indicates low MW emissivity. This value is only produced when MW information is used.); 5 for snow (Indicates higher-frequency MW scattering when MW information is

			used); 6 for glacier/snow (Indicates very low-frequency MW scattering. This value is only produced when MW information is used.); 7 for snow (Indicates lower-frequency MW scattering. This value is only produced when MW information is used.); -1 for unknown
Microwave Dependent			
TAirMWOnlyStd	32-bit floating-point	StdPressureLev (= 28)	Atmospheric Temperature retrieved using only MW information (no IR) at StdPressLev in Kelvins.
TAirMWOnlyStd_QC	16-bit unsigned integer	StdPressureLev (= 28)	Quality Control for TAirMWOnlyStd.; 0: Highest Quality; 1: Good Quality; 2: Do Not Use
MWSurfClass	8-bit integer	None	Surface class from microwave (MW) information:; 0 for coastline (Liquid water covers 50-99% of area); 1 for land (Liquid water covers < 50% of area); 2 for ocean (Liquid water covers > 99% of area); 3 for sea ice (High MW emissivity); 4 for sea ice (Low MW emissivity); 5 for snow (Higher-frequency MW scattering); 6 for glacier/snow (Very low-frequency MW scattering); 7 for snow (Lower-frequency MW scattering); -1 for unknown (not attempted)
sfcTbMWStd	32-bit floating-point	MWHingeSurf (= 7)	Microwave surface brightness (Kelvins) (Emitted radiance only, reflected radiance not included. Product of MW only algorithm)
sfcTbMWStd_QC	16-bit unsigned integer	MWHingeSurf (= 7)	Quality Control for sfcTbMWStd.; 0: Highest Quality; 1: Good Quality; 2: Do Not Use
EmisMWStd	32-bit floating-point	MWHingeSurf (= 7)	Spectral MW emissivity at the 7 MW frequencies listed for dimension MWHingeSurf (Product of MW only algorithm)
EmisMWStd_QC	16-bit unsigned integer	MWHingeSurf (= 7)	Quality Control for EmisMWStd.; 0: Highest Quality; 1: Good Quality; 2: Do Not Use
EmisMWStdErr	32-bit floating-point	MWHingeSurf (= 7)	Error estimate for EmisMWStd

totH2OMWOnlyStd	32-bit floating-point	None	Total precipitable water vapor from MW-only retrieval (no IR information used) (kg / m**2)
totH2OMWOnlyStd_QC	16-bit unsigned integer	None	Quality Control for totH2OMWOnlyStd.; 0: Highest Quality; 1: Good Quality; 2: Do Not Use
GP_Height_MWOnly	32-bit floating-point	StdPressureLev (= 28)	Geopotential Heights from MW-Only retrieval (No IR information used) at StdPressureLev (m above mean sea level)
GP_Height_MWOnly_QC	16-bit unsigned integer	StdPressureLev (= 28)	Quality Control for GP_Height_MWOnly.; 0: Highest Quality; 1: Good Quality; 2: Do Not Use
MW_ret_used	8-bit integer	None	MW-only final retrieval used
totCldH2OStd	32-bit floating-point	None	Total cloud liquid water in kg/m**2
totCldH2OStd_QC	16-bit unsigned integer	None	Quality Control for totCldH2OStd; 0: Highest Quality; 1: Good Quality; 2: Do Not Use
totCldH2OStdErr	32-bit floating-point	None	Error estimate for totCldH2OStd

A2: L2 Support Atmospheric/Surface Product Interface Specification

Interface Specification Version 7.0.1.0
2019-12-04

ESDT ShortNames = "AIRX2SUP", “AIRS2SUP”, “AIRH2SUP”

Swath Name = "L2_Support_atmospheric&surface_product"

Level = "Level2"

Footprints = 30

scanlines per scanset = 1

Dimensions

These fields define all dimensions that can be used for HDF-EOS swath fields.

The names "GeoTrack" and "GeoXTrack" have a special meaning for this document: "Cross-Track" data fields have a hidden dimension of "GeoXTrack"; "Along-Track" data fields have a hidden dimension of "GeoTrack"; "Full Swath Data Fields have hidden dimensions of both "GeoTrack" and "GeoXTrack".

Name	Value	Explanation
GeoXTrack	30	Dimension across track for footprint positions. Same as number of footprints per scanline. -- starting at the left and increasing towards the right as you look along the satellite's path
GeoTrack	# of scan lines in swath	Dimension along track for footprint positions. Same as number of scanlines in granule. Parallel to the satellite's path, increasing with time. (Nominally 45)
StdPressureLev	28	Number of standard pressure altitude levels (from bottom of the atmosphere up).
AIRSXTrack	3	The number of AIRS cross-track spots per AMSU-A spot. Direction is the same as GeoXTrack -- starting at the left and increasing towards the right as you look along the satellite's path
AIRSTrack	3	The number of AIRS along-track spots per AMSU-A spot. Direction is the same as GeoTrack -- parallel to the satellite's path, increasing with time
Cloud	2	Cloud layer dimension in order of increasing pressure. Only first nCld or numCloud elements are valid
ChanAMSUA	15	Dimension of AMSU-A Channel array; Channel 1: 23.8 GHz; Ch 2: 31.4 GHz; Ch 3: 50.3 GHz; Ch 4: 52.8 GHz; Ch 5: 53.596 +/- 0.115 GHz; Ch 6: 54.4 GHz; Ch 7: 54.94 GHz; Ch 8: 55.5 GHz; Ch 9: f0; Ch 10: f0 +/- 0.217 GHz Ch 11: f0 +/- df +/- 48 MHz;

		Ch 12: f0 +/- df +/- 22 MHz; Ch 13: f0 +/- df +/- 10 MHz; Ch 14: f0 +/- df +/- 4.5 MHz; Ch 15: 89 GHz; (f0 = 57290.344 MHz; df = 322.4 MHz)
ChanHSB	5	Dimension of HSB Channel array; Channel 1: Deleted 89.0 GHz channel: always invalid; Ch 2: 150.0 GHz; Ch 3: f0 +/- 1.0 GHz; Ch 4: f0 +/- 3.0 GHz; Ch 5: f0 +/- 7.0 GHz; (f0 = 183.31 GHz)
MWHingeSurf	7	Number of standard frequency hinge points in Microwave surface emissivity and surface brightness. Frequencies are 23.8, 31.4, 50.3, 52.8, 89.0, 150.0, 183.31 GHz respectively.Values are also found in field MWHingeSurfFreqGHz.
H2OFunc	21	Functions on which water vapor retrieval is calculated
O3Func	20	Functions on which ozone retrieval is calculated
COFunc	9	Functions on which carbon monoxide retrieval is calculated
CH4Func	10	Functions on which methane retrieval is calculated
HingeSurf	100	Maximum number of frequency hinge points in IR surface emissivity
H2OPressureLev	15	Number of water vapor pressure altitude levels (from bottom of the atmosphere up).
XtraPressureLev	100	Number of pressure altitude layers in high vertical resolution support products (from top of the atmosphere down). nSurfSup is the 1-based index of the last valid level for a given profile. Any levels beyond this are below the surface. Since the actual surface will not be be exactly at this level, it will be necessary to extrapolate or interpolate to get precise surface values. See entries for specific fields for more details.
XtraPressureLay	100	Number of pressure altitude layers in high vertical resolution support products (Always equal to XtraressureLev: first layer goes from the top of the atmosphere to level 1). nSurfSup is the 1-based index of the last valid layer for a given profile. Any layers beyond this are below the surface. Since the actual surface will not be be exactly at the bottom of this layer, it will be necessary to extrapolate or interpolate to get total amounts for surface layers. See entries for specific fields for more details.
HingeCloud	7	Frequency hinge points in cloud emissivity in order of increasing frequency. Only first numHingeCloud elements are valid
HingeSurfInit	50	Maximum number of frequency hinge points in IR surface emissivity from initial regression
ScoresBand	10	The number of IR frequency bands for which Initial_CC_subscores are calculated. Band limits are (in cm^-1): 645., 704., 800., 1000., 1200., 2200., 2304., 2382., 2390., 2400., 2600.
MODISEmisBand	6	MODIS bands for IR emissivity first guess: 833.33, 909.09, 1169.6, 2469.1, 2531.6, and 2666.7 cm**-1.
MODISEmis10Hinge	10	MODIS hinge points for IR emissivity first guess: 699.30, 826.45, 925.93, 1075.27, 1204.82, 1315.79, 1724.14, 2000.0, 2325.58, and 2777.78 cm**-1.
MODISEmisQualLevels	4	MODIS emissivity quality levels:; average emissivity error <= 0.01;

		average emissivity error <= 0.02;
		average emissivity error <= 0.04;
		average emissivity error > 0.04

MODISLSTQualLevels	4	MODIS land surface temperature quality levels:;
		average LST error <= 1 K;
		average LST error <= 2 K;
		average LST error <= 3 K;
		average LST error > 3 K

TempFunc	30	Functions on which temperature retrieval is calculated
Channel	2378	Dimension of channel array (Channels are generally in order of increasing wavenumber, but because frequencies can vary and because all detectors from a physical array of detector elements (a "module") are always grouped together there are sometimes small reversals in frequency order where modules overlap.)
Module	17	Number of modules on the focal plane in which airs channels are grouped. The order is M-01a, M-02a, M-01b, M-02b, M-04d, M-04c, M-03, M-04b, M-04a, M-05, M-06, M-07, M-08, M-09, M-10, M-11, M-12.
OLRBand	16	Spectral bands used in OLR (cm-1):; 1 10 - 350; 2 350 - 500; 3 500 - 630; 4 630 - 700; 5 700 - 820; 6 820 - 980; 7 980 - 1080; 8 1080 - 1180; 9 1180 - 1390; 10 1390 - 1480; 11 1480 - 1800; 12 1800 - 2080; 13 2080 - 2250; 14 2250 - 2380; 15 2380 - 2600; 16 2600 - 3250
SccnnBtCorr	2	Channels reported for the brightness temperature correction in cloud clearing in SCCNN

Geolocation Fields

These fields appear for every footprint (GeoTrack * GeoXTrack times) and correspond to footprint center coordinates and "shutter" time.

Name	Explanation
Latitude	Footprint boresight geodetic Latitude in degrees North (-90.0 ... 90.0)
Longitude	Footprint boresight geodetic Longitude in degrees East (-180.0 ... 180.0)
Time	Footprint "shutter" TAI Time: floating-point elapsed seconds since Jan 1, 1993

Attributes

These fields appear only once per granule and use the HDF-EOS "Attribute" interface

Name	Type	Explanation
processing_level	string of 8-bit characters	Zero-terminated character string denoting processing level ("Level2")

instrument	string of 8-bit characters	Zero-terminated character string denoting instrument ("AIRS")
DayNightFlag	string of 8-bit characters	Zero-terminated character string set to "Night" when the subsatellite points at the beginning and end of a granule are both experiencing night according to the "civil twilight" standard (center of refracted sun is below the horizon). It is set to "Day" when both are experiencing day, and "Both" when one is experiencing day and the other night. "NA" is used when a determination cannot be made.
AutomaticQAFlag	string of 8-bit characters	Zero-terminated character string denoting granule data quality: (Always "Passed", "Failed", or "Suspect")
NumTotalData	32-bit integer	Total number of expected scene footprints
NumProcessData	32-bit integer	Number of scene footprints which are present and can be processed routinely (state = 0)
NumSpecialData	32-bit integer	Number of scene footprints which are present and can be processed only as a special test (state = 1)
NumBadData	32-bit integer	Number of scene footprints which are present but cannot be processed (state = 2)
NumMissingData	32-bit integer	Number of expected scene footprints which are not present (state = 3)
NumLandSurface	32-bit integer	Number of scene footprints for which the surface is more than 90% land
NumOceanSurface	32-bit integer	Number of scene footprints for which the surface is less than 10% land
node_type	string of 8-bit characters	Zero-terminated character string denoting whether granule is ascending, descending, or pole-crossing: ("Ascending" and "Descending" for entirely ascending or entirely descending granules, or "NorthPole" or "SouthPole" for pole-crossing granules. "NA" when determination cannot be made.)
start_year	32-bit integer	Year in which granule started, UTC (e.g. 1999)
start_month	32-bit integer	Month in which granule started, UTC (1 ... 12)
start_day	32-bit integer	Day of month in which granule started, UTC (1 ... 31)
start_hour	32-bit integer	Hour of day in which granule started, UTC (0 ... 23)
start_minute	32-bit integer	Minute of hour in which granule started, UTC (0 ... 59)
start_sec	32-bit floating-point	Second of minute in which granule started, UTC (0.0 ... 59.0)
start_orbit	32-bit integer	Orbit number of mission in which granule started
end_orbit	32-bit integer	Orbit number of mission in which granule ended
orbit_path	32-bit integer	Orbit path of start orbit (1 ... 233 as defined by EOS project)
start_orbit_row	32-bit integer	Orbit row at start of granule (1 ... 248 as defined by EOS project)
end_orbit_row	32-bit integer	Orbit row at end of granule (1 ... 248 as defined by EOS project)

granule_number	32-bit integer	Number of granule within day (1 ... 240)
num_scansets	32-bit integer	Number of scansets in granule (1 ... 45)
num_scanlines	32-bit integer	Number of scanlines in granule (1 * num_scansets)
start_Latitude	64-bit floating-point	Geodetic Latitude of spacecraft at start of granule (subsatellite location at midpoint of first scan) in degrees North (-90.0 ... 90.0)
start_Longitude	64-bit floating-point	Geodetic Longitude of spacecraft at start of granule (subsatellite location at midpoint of first scan) in degrees East (-180.0 ... 180.0)
start_Time	64-bit floating-point	TAI Time at start of granule (floating-point elapsed seconds since start of 1993)
end_Latitude	64-bit floating-point	Geodetic Latitude of spacecraft at end of granule (subsatellite location at midpoint of last scan) in degrees North (-90.0 ... 90.0)
end_Longitude	64-bit floating-point	Geodetic Longitude of spacecraft at end of granule (subsatellite location at midpoint of last scan) in degrees East (-180.0 ... 180.0)
end_Time	64-bit floating-point	TAI Time at end of granule (floating-point elapsed seconds since start of 1993)
eq_x_longitude	32-bit floating-point	Longitude of spacecraft at southward equator crossing nearest granule start in degrees East (-180.0 ... 180.0)
eq_x_tai	64-bit floating-point	Time of eq_x_longitude in TAI units (floating-point elapsed seconds since start of 1993)
LonGranuleCen	16-bit integer	Geodetic Longitude of the center of the granule in degrees East (-180 ... 180)
LatGranuleCen	16-bit integer	Geodetic Latitude of the center of the granule in degrees North (-90 ... 90)
LocTimeGranuleCen	16-bit integer	Local solar time at the center of the granule in minutes past midnight (0 ... 1439)
num_fpe	16-bit integer	Number of floating point errors
orbitgeoqa	32-bit unsigned integer	Orbit Geolocation QA:; Bit 0: (LSB, value 1) bad input value (last scanline); Bit 1: (value 2) bad input value (first scanline); Bit 2: (value 4) PGS_EPH_GetEphMet() gave PGSEPH_E_NO_SC_EPHEM_FILE; Bit 3: (value 8) PGS_EPH_GetEphMet() gave PGSEPH_E_BAD_ARRAY_SIZE; Bit 4: (value 16) PGS_EPH_GetEphMet() gave PGSTD_E_TIME_FMT_ERROR; Bit 5: (value 32) PGS_EPH_GetEphMet() gave PGSTD_E_TIME_VALUE_ERROR; Bit 6: (value 64) PGS_EPH_GetEphMet() gave PGSTD_E_SC_TAG_UNKNOWN; Bit 7: (value 128) PGS_EPH_GetEphMet() gave PGS_E_TOOLKIT; Bit 8: (value 256) PGS_TD_UTCtoTAI() gave PGSTD_E_NO_LEAP_SECS;

		Bit 9: (value 512) PGS_TD_UTCtoTAI() gave PGSTD_E_TIME_FMT_ERROR; Bit 10: (value 1024) PGS_TD_UTCtoTAI() gave PGSTD_E_TIME_VALUE_ERROR; Bit 11: (value 2048) PGS_TD_UTCtoTAI() gave PGS_E_TOOLKIT; Bit 12: (value 4096) PGS_CSC_DayNight() gave PGSTD_E_NO_LEAP_SECS; Bit 13: (value 8192) PGS_CSC_DayNight() gave PGSCSC_E_INVALID_LIMITTAG; Bit 14: (value 16384) PGS_CSC_DayNight() gave PGSCSC_E_BAD_ARRAY_SIZE; Bit 15: (value 32768) PGS_CSC_DayNight() gave PGSCSC_W_ERROR_IN_DAYNIGHT; Bit 16: (value 65536) PGS_CSC_DayNight() gave PGSCSC_W_BAD_TRANSFORM_VALUE; Bit 17: (value 131072) PGS_CSC_DayNight() gave PGSCSC_W_BELOW_HORIZON; Bit 18: (value 262144) PGS_CSC_DayNight() gave PGSCSC_W_PREDICTED_UT1 (This is expected except when reprocessing.); Bit 19: (value 524288) PGS_CSC_DayNight() gave PGSTD_E_NO_UT1_VALUE; Bit 20: (value 1048576) PGS_CSC_DayNight() gave PGSTD_E_BAD_INITIAL_TIME; Bit 21: (value 2097152) PGS_CSC_DayNight() gave PGSCBP_E_TIME_OUT_OF_RANGE; Bit 22: (value 4194304) PGS_CSC_DayNight() gave PGSCBP_E_UNABLE_TO_OPEN_FILE; Bit 23: (value 8388608) PGS_CSC_DayNight() gave PGSMEM_E_NO_MEMORY; Bit 24: (value 16777216) PGS_CSC_DayNight() gave PGS_E_TOOLKIT; Bit 25-31: not used
num_satgeoqa	16-bit integer	Number of scans with problems in satgeoqa
num_glintgeoqa	16-bit integer	Number of scans with problems in glintgeoqa
num_moongeoqa	16-bit integer	Number of scans with problems in moongeoqa
num_ftptgeoqa	16-bit integer	Number of footprints with problems in ftptgeoqa
num_zengeoqa	16-bit integer	Number of footprints with problems in zengeoqa
num_demgeoqa	16-bit integer	Number of footprints with problems in demgeoqa
NumSO2FOVs	16-bit unsigned integer	Number of fields-of-view (out of a nominal 1350) with a signifcant SO2 concentration based on the value of BT_diff_SO2.
CO_first_guess	string of 8-bit characters	Name of CO First Guess source.
CH4_first_guess	string of 8-bit characters	Name of CH4 First Guess source.

numHingeSurfInit	32-bit integer	Number of IR hinge points for surface emissivity and reflectivity from initial regression (not used in retrieval)
nFOV_big_ang_adj	16-bit integer	The number of FOVs with nchan_big_ang_adj over 5
num_retrieval_type_000	16-bit integer	The number of retrievals with retrieval_type equal to 0
num_retrieval_type_010	16-bit integer	The number of retrievals with retrieval_type equal to 10
num_retrieval_type_020	16-bit integer	The number of retrievals with retrieval_type equal to 20
num_retrieval_type_030	16-bit integer	The number of retrievals with retrieval_type equal to 30
num_retrieval_type_040	16-bit integer	The number of retrievals with retrieval_type equal to 40
num_retrieval_type_050	16-bit integer	The number of retrievals with retrieval_type equal to 50
num_retrieval_type_100	16-bit integer	The number of retrievals with retrieval_type equal to 100
NumMWStratIrRetOnly	32-bit integer	Number of profiles in which the final product comes only from MW and stratospheric IR information (retrieval_types 20, 30, 40)
NumNoHSB	32-bit integer	Number of retrieval profiles for which no HSB input data is used
NumNoAMSUA	32-bit integer	Number of retrieval profiles for which no AMSU-A input data is used
NumNoAIRS	32-bit integer	Number of retrieval profiles for which no AIRS-IR input data is used
NumNoVis	32-bit integer	Number of retrieval profiles for which no AIRS-V/NIR input data is used
DCRCount	32-bit integer	Number of times a Direct Current Restore was executed for any module
PopCount	32-bit integer	Number of popcorn events within granule, i.e. number of times than an AIRS channel used in the Level 2 retrieval has suffered a sudden discontinuity in dark current
MoonInViewMWCount	32-bit integer	Number of scanlines in granule with the moon in a Microwave space view (approx)

Per-Granule Data Fields

These fields appear only once per granule and use the HDF-EOS "Field" interface

Name	Type	Extra Dimensions	Explanation
pressSupp	32-bit floating-point	XtraPressureLev (= 100)	Support pressures (lower boundary) in hPa.
pressStd	32-bit floating-point	StdPressureLev (= 28)	Standard pressures in hPa (bottom of the atmosphere first)
Temp_trapezoid_layers_30func	32-bit integer	TempFunc (= 30)	Layers on which the Temperature variables are defined.
H2O_trapezoid_layers_21func	32-bit integer	H2OFunc (= 21)	Layers on which the H2O variables are defined.
O3_trapezoid_layers_20func	32-bit integer	O3Func (= 20)	Layers on which the O3 variables are defined.

CO_trapezoid_layers	32-bit integer	COFunc (= 9)	Layers on which the CO variables are defined.
CH4_trapezoid_layers_10func	32-bit integer	CH4Func (= 10)	Layers on which the CH4 variables are defined.
MWHingeSurfFreqGHz	32-bit floating-point	MWHingeSurf (= 7)	Frequencies in GHz for MW surface parameters (SfcTbMWStd, EmisMWStd,...)
freqEmisInit	32-bit floating-point	HingeSurfInit (= 50)	Frequencies for surface emissivity and reflectivity in cm-1 (in order of increasing frequency. Only first numHingeSurfInit elements are valid)

Along-Track Data Fields

These fields appear once per scanline (GeoTrack times)

Name	Type	Extra Dimensions	Explanation
satheight	32-bit floating-point	None	Satellite altitude at nadirTAI in km above reference ellipsoid (e.g. 725.2)
satroll	32-bit floating-point	None	Satellite attitude roll angle at nadirTAI (-180.0 ... 180.0 angle about the +x (roll) ORB axis, +x axis is positively oriented in the direction of orbital flight completing an orthogonal triad with y and z.)
satpitch	32-bit floating-point	None	Satellite attitude pitch angle at nadirTAI (-180.0 ... 180.0 angle about +y (pitch) ORB axis. +y axis is oriented normal to the orbit plane with the positive sense opposite to that of the orbit's angular momentum vector H.)
satyaw	32-bit floating-point	None	Satellite attitude yaw angle at nadirTAI (-180.0 ... 180.0 angle about +z (yaw) axis. +z axis is positively oriented Earthward parallel to the satellite radius vector R from the spacecraft center of mass to the center of the Earth.)
glintlat	32-bit floating-point	None	Solar glint geodetic latitude in degrees North at nadirTAI (-90.0 ... 90.0)
glintlon	32-bit floating-point	None	Solar glint geodetic longitude in degrees East at nadirTAI (-180.0 ... 180.0)
nadirTAI	64-bit floating-point	None	TAI time at which instrument is nominally looking directly down. (between footprints 15 & 16 for AMSU or between footprints 45 & 46 for AIRS/Vis & HSB) (floating-point elapsed seconds since start of 1993)
sat_lat	64-bit floating-point	None	Satellite geodetic latitude in degrees North (-90.0 ... 90.0)
sat_lon	64-bit floating-point	None	Satellite geodetic longitude in degrees East (-180.0 ... 180.0)
scan_node_type	8-bit integer	None	'A' for ascending, 'D' for descending, 'E' when an error is encountered in trying to determine a value.
satgeoqa	32-bit unsigned integer	None	Satellite Geolocation QA flags:; Bit 0: (LSB, value 1) bad input value; Bit 1: (value 2) PGS_TD_TAItoUTC() gave

			PGSTD_E_NO_LEAP_SECS; Bit 2: (value 4) PGS_TD_TAItoUTC() gave PGS_E_TOOLKIT; Bit 3: (value 8) PGS_EPH_EphemAttit() gave PGSEPH_W_BAD_EPHEM_VALUE; Bit 4: (value 16) PGS_EPH_EphemAttit() gave PGSEPH_E_BAD_EPHEM_FILE_HDR; Bit 5: (value 32) PGS_EPH_EphemAttit() gave PGSEPH_E_NO_SC_EPHEM_FILE; Bit 6: (value 64) PGS_EPH_EphemAttit() gave PGSEPH_E_NO_DATA_REQUESTED; Bit 7: (value 128) PGS_EPH_EphemAttit() gave PGSTD_E_SC_TAG_UNKNOWN; Bit 8: (value 256) PGS_EPH_EphemAttit() gave PGSEPH_E_BAD_ARRAY_SIZE; Bit 9: (value 512) PGS_EPH_EphemAttit() gave PGSTD_E_TIME_FMT_ERROR; Bit 10: (value 1024) PGS_EPH_EphemAttit() gave PGSTD_E_TIME_VALUE_ERROR; Bit 11: (value 2048) PGS_EPH_EphemAttit() gave PGSTD_E_NO_LEAP_SECS; Bit 12: (value 4096) PGS_EPH_EphemAttit() gave PGS_E_TOOLKIT; Bit 13: (value 8192) PGS_CSC_ECItoECR() gave PGSCSC_W_BAD_TRANSFORM_VALUE; Bit 14: (value 16384) PGS_CSC_ECItoECR() gave PGSCSC_E_BAD_ARRAY_SIZE; Bit 15: (value 32768) PGS_CSC_ECItoECR() gave PGSTD_E_NO_LEAP_SECS; Bit 16: (value 65536) PGS_CSC_ECItoECR() gave PGSTD_E_TIME_FMT_ERROR; Bit 17: (value 131072) PGS_CSC_ECItoECR() gave PGSTD_E_TIME_VALUE_ERROR; Bit 18: unused (set to zero); Bit 19: (value 524288) PGS_CSC_ECItoECR() gave PGSTD_E_NO_UT1_VALUE; Bit 20: (value 1048576) PGS_CSC_ECItoECR() gave PGS_E_TOOLKIT; Bit 21: (value 2097152) PGS_CSC_ECRtoGEO() gave PGSCSC_W_TOO_MANY_ITERS; Bit 22: (value 4194304) PGS_CSC_ECRtoGEO() gave PGSCSC_W_INVALID_ALTITUDE; Bit 23: (value 8388608) PGS_CSC_ECRtoGEO() gave PGSCSC_W_SPHERE_BODY; Bit 24: (value 16777216) PGS_CSC_ECRtoGEO() gave PGSCSC_W_LARGE_FLATTENING; Bit 25: (value 33554432) PGS_CSC_ECRtoGEO() gave PGSCSC_W_DEFAULT_EARTH_MODEL; Bit 26: (value 67108864) PGS_CSC_ECRtoGEO() gave PGSCSC_E_BAD_EARTH_MODEL; Bit 27: (value 134217728) PGS_CSC_ECRtoGEO() gave PGS_E_TOOLKIT; Bit 28-31: not used
glintgeoqa	16-bit unsigned integer	None	Glint Geolocation QA flags:; Bit 0: (LSB, value 1) bad input value; Bit 1: (value 2) glint location in Earth's shadow (Normal

			for night FOVs); Bit 2: (value 4) glint calculation not converging; Bit 3: (value 8) glint location sun vs. satellite zenith mismatch; Bit 4: (value 16) glint location sun vs. satellite azimuth mismatch; Bit 5: (value 32) bad glint location; Bit 6: (value 64) PGS_CSC_ZenithAzimuth() gave any 'W' class return code; Bit 7: (value 128) PGS_CSC_ZenithAzimuth() gave any 'E' class return code; Bit 8: (value 256) PGS_CBP_Earth_CB_Vector() gave any 'W' class return code; Bit 9: (value 512) PGS_CBP_Earth_CB_Vector() gave any 'E' class return code; Bit 10: (value 1024) PGS_CSC_ECItoECR() gave any 'W' class return code except PGSCSC_W_PREDICTED_UT1 (for Glint); Bit 11: (value 2048) PGS_CSC_ECItoECR() gave any 'E' class return code (for Glint); Bit 12: (value 4096) PGS_CSC_ECRtoGEO() gave any 'W' class return code (for Glint); Bit 13: (value 8192) PGS_CSC_ECRtoGEO() gave any 'E' class return code (for Glint); Bit 14: (value 16384) PGS_CSC_ECItoECR() gave any 'W' class return code except PGSCSC_W_PREDICTED_UT1 ; Bit 15: (value 32768) PGS_CSC_ECItoECR() gave any 'E' class return code
moongeoqa	16-bit unsigned integer	None	Moon Geolocation QA flags:; Bit 0: (LSB, value 1) bad input value; Bit 1: (value 2) PGS_TD_TAItoUTC() gave PGSTD_E_NO_LEAP_SECS; Bit 2: (value 4) PGS_TD_TAItoUTC() gave PGS_E_TOOLKIT; Bit 3: (value 8) PGS_CBP_Sat_CB_Vector() gave PGSCSC_W_BELOW_SURFACE; Bit 4: (value 16) PGS_CBP_Sat_CB_Vector() gave PGSCBP_W_BAD_CB_VECTOR; Bit 5: (value 32) PGS_CBP_Sat_CB_Vector() gave PGSCBP_E_BAD_ARRAY_SIZE; Bit 6: (value 64) PGS_CBP_Sat_CB_Vector() gave PGSCBP_E_INVALID_CB_ID; Bit 7: (value 128) PGS_CBP_Sat_CB_Vector() gave PGSMEM_E_NO_MEMORY; Bit 8: (value 256) PGS_CBP_Sat_CB_Vector() gave PGSCBP_E_UNABLE_TO_OPEN_FILE; Bit 9: (value 512) PGS_CBP_Sat_CB_Vector() gave PGSTD_E_BAD_INITIAL_TIME; Bit 10: (value 1024) PGS_CBP_Sat_CB_Vector() gave PGSCBP_E_TIME_OUT_OF_RANGE; Bit 11: (value 2048) PGS_CBP_Sat_CB_Vector() gave PGSTD_E_SC_TAG_UNKNOWN; Bit 12: (value 4096) PGS_CBP_Sat_CB_Vector() gave PGSEPH_E_BAD_EPHEM_FILE_HDR; Bit 13: (value 8192) PGS_CBP_Sat_CB_Vector() gave

			PGSEPH_E_NO_SC_EPHEM_FILE; Bit 14: (value 16384) PGS_CBP_Sat_CB_Vector() gave PGS_E_TOOLKIT; Bit 15: not used
orbit_phase_deg	32-bit floating-point	None	Orbit phase in degrees. 0.0 is nighttime equator crossing. 90.0 is near the south pole. 180.0 is near the daytime equator crossing. 270.0 is near the north pole. [0.0, 360.0]
shift_y0	32-bit floating-point	Module (= 17)	Focal plane shift in the y (spectral dispersion) direction relative to prelaunch nominal. (microns)
scan_freq	32-bit floating-point	Channel (= 2378)	Dynamic frequencies (in cm**-1) of each channel for each scan

Full Swath Data Fields

These fields appear for every footprint of every scanline in the granule (GeoTrack * GeoXTrack times)

Name	Type	Extra Dimensions	Explanation
Geolocation			
satzen	32-bit floating-point	None	Spacecraft zenith angle (0.0 ... 180.0) degrees from zenith (measured relative to the geodetic vertical on the reference (WGS84) spheroid and including corrections outlined in EOS SDP toolkit for normal accuracy.)
satazi	32-bit floating-point	None	Spacecraft azimuth angle (-180.0 ... 180.0) degrees E of N GEO)
solzen	32-bit floating-point	None	Solar zenith angle (0.0 ... 180.0) degrees from zenith (measured relative to the geodetic vertical on the reference (WGS84) spheroid and including corrections outlined in EOS SDP toolkit for normal accuracy.)
solazi	32-bit floating-point	None	Solar azimuth angle (-180.0 ... 180.0) degrees E of N GEO)
sun_glint_distance	16-bit integer	None	Distance (km) from footprint center to location of the sun glint (-9999 for unknown, 30000 for no glint visible because spacecraft is in Earth's shadow)
Surface ancillary information from geolocation			
topog	32-bit floating-point	None	Mean topography in meters above reference ellipsoid
topog_err	32-bit floating-point	None	Error estimate for topog
landFrac	32-bit floating-point	None	Fraction of spot that is land (0.0 ... 1.0)

landFrac_err	32-bit floating-point	None	Error estimate for landFrac
latAIRS	32-bit floating-point	AIRSTrack (= 3) * AIRSXTrack (= 3)	Geodetic center latitude of AIRS spots in degrees North (-90.0 ... 90.0)
lonAIRS	32-bit floating-point	AIRSTrack (= 3) * AIRSXTrack (= 3)	Geodetic center longitude of AIRS spots in degrees East (-180.0 ... 180.0)
PSurfStd	32-bit floating-point	None	Surface pressure first guess in hPa, interpolated from forecast
PSurfStd_QC	16-bit unsigned integer	None	Quality flag for surface pressure guess input.; 0: Highest Quality -- from timely forecast; 1: Good Quality -- from climatology; 2: Do Not Use
nSurfSup	32-bit integer	None	Index of last profile pressure layer used in retrieval. (90 ... 100)
nSurfStd	32-bit integer	None	Index in pressStd array of first pressure level above mean surface (1 ... 15)
Dust, SO2, and cloud phase flags from radiances			
dust_flag	16-bit integer	AIRSTrack (= 3) * AIRSXTrack (= 3)	Flag telling whether dust was detected in this scene; 1: Dust detected; 0: Dust not detected; -1: Dust test not valid because of land; -2: Dust test not valid because of high latitude; -3: Dust test not valid because of suspected cloud; -4: Dust test not valid because of bad input data
dust_score	16-bit integer	AIRSTrack (= 3) * AIRSXTrack (= 3)	Dust score. Each bit results from a different test comparing radiances. Higher scores indicate more certainty of dust present. Dust probable when score is over 380. Not valid when dust_flag is negative.
BT_diff_SO2	32-bit floating-point	AIRSTrack (= 3) * AIRSXTrack (= 3)	Brightness temperature difference Tb(1361.44 cm-1) - Tb(1433.06 cm-1) used as an indicator of SO2 release from volcanoes. Values under -6 K have likely volcanic SO2. (Kelvins)
BT_diff_SO2_QC	16-bit unsigned integer	AIRSTrack (= 3) * AIRSXTrack (= 3)	Quality Control for BT_diff_SO2.; 0: Highest Quality; 1: Good Quality; 2: Do Not Use
cloud_phase_3x3	16-bit integer	AIRSTrack (= 3) * AIRSXTrack (= 3)	Flag telling whether clouds are ice or liquid water; -9999: No cloud phase retrieval was possible; -2: Liquid water (high confidence);

			-1: Liquid water (low confidence); 0: Unknown; 1: Ice (low confidence); 2: Ice (higher confidence); 3: Ice (very high confidence); 4: Ice (very high confidence)
cloud_phase_bits	16-bit integer	AIRSTrack (= 3) * AIRSXTrack (= 3)	Internal bit field of individual tests used in cloud phase determination; Bit 15: (MSB, 0x8000, value 32768) unused; Bit 14: (0x4000, value 16384) unused; Bit 13: (0x2000, value 8192) unused; Bit 12: (0x1000, value 4096) unused; Bit 11: (0x0800, value 2048) unused; Bit 10: (0x0400, value 1024) unused; Bit 9: (0x0200, value 512) Warm test; Bit 8: (0x0100, value 256) Liquid water test #2; Bit 7: (0x0080, value 128) Liquid water test #1; Bit 5: (0x0040, value 64) Ice test #4; Bit 4: (0x0020, value 32) Ice test #3; Bit 3: (0x0010, value 16) Ice test #2; Bit 2: (0x0008, value 8) Cold cloud test (ice test #1); Bit 2: (0x0004, value 4) Cloud fraction test; Bit 1: (0x0002, value 2) Desert test; Bit 0: (LSB, 0x0001, value 1) One or more tests could not be performed
Quality Indicator Pressure Boundaries			
PBest	32-bit floating-point	None	Maximum value of pressure for which temperature is Quality = 0 (hPa)
PGood	32-bit floating-point	None	Maximum value of pressure for which temperature is Quality = 0 or 1 (hPa)
nBestSup	16-bit integer	None	Support level index of highest pressure (i.e. lowest altitude) for which Quality = 0. A value of 0 indicates that no part of the profile passes the test. (0 ... 100)
nGoodSup	16-bit integer	None	Support level index of highest pressure (i.e. lowest altitude) for which Quality = 0 or 1. A value of 0 indicates that no part of the profile passes the test. (0 ... 100)
nBestStd	16-bit integer	None	Standard level index of highest pressure (i.e. lowest altitude) for which Quality = 0. A value of 29 indicates that no part of the profile passes the test. (1 ... 29)
nGoodStd	16-bit integer	None	Standard level index of highest pressure (i.e. lowest altitude) for which Quality = 0 or 1. A value of 29

			indicates that no part of the profile passes the test. (1 ... 29)
Surface Property Retrievals			
TSurfStd	32-bit floating-point	None	Surface skin temperature in Kelvins
TSurfStd_QC	16-bit unsigned integer	None	Quality flag for TSurfStd.; 0: Highest Quality; 1: Good Quality; 2: Do Not Use
TSurfStdErr	32-bit floating-point	None	Error estimate for TSurfStd
numHingeSurf	16-bit integer	None	Number of IR hinge points for surface emissivity and reflectivity
freqEmis	32-bit floating-point	HingeSurf (= 100)	Frequencies for surface emissivity and reflectivity in cm-1 (in order of increasing frequency. Only first numHingeSurf elements are valid)
emisIRStd	32-bit floating-point	HingeSurf (= 100)	Spectral IR Surface Emissivities (in order of increasing frequency. Only first numHingeSurf elements are valid)
emisIRStd_QC	16-bit unsigned integer	HingeSurf (= 100)	Quality Control for emisIRStd.; 0: Highest Quality; 1: Good Quality; 2: Do Not Use
emisIRStdErr	32-bit floating-point	HingeSurf (= 100)	Error estimate for emisIRStd
Effective_Solar_Reflectance	32-bit floating-point	HingeSurf (= 100)	Effective spectral IR bidirectional surface solar reflectance, including cloud shadow effects (in order of increasing frequency. Only first numHingeSurf elements are valid)
Effective_Solar_Reflectance_QC	16-bit unsigned integer	HingeSurf (= 100)	Quality Control for Effective_Solar_Reflectance.; 0: Highest Quality; 1: Good Quality; 2: Do Not Use
Air Temperature Retrievals			
TAirSup	32-bit floating-point	XtraPressureLev (= 100)	Atmospheric Temperature at XtraPressLev in Kelvins. Value at 1-based index of nSurfSup may be an unphysical extrapolated value for a pressure level below the surface. Use TSurfAir for the surface air temperature.
TAirSup_QC	16-bit unsigned integer	XtraPressureLev (= 100)	Quality Control for TAirSup.; 0: Highest Quality; 1: Good Quality; 2: Do Not Use
TAirSupErr	32-bit floating-point	XtraPressureLev (= 100)	Error estimate for TAirSup (K)

TSurfAir	32-bit floating-point	None	Surface air temperature in Kelvins
TSurfAir_QC	16-bit unsigned integer	None	Quality Control for TSurfAir.; 0: Highest Quality; 1: Good Quality; 2: Do Not Use
TSurfAirErr	32-bit floating-point	None	Error estimate for TSurfAir
num_Temp_Func	16-bit integer	None	Number of valid entries in each dimension of Temp_ave_kern.
Temp_eff_press_30func	32-bit floating-point	TempFunc (= 30)	Temperature effective pressure for the center of each trapezoid
Temp_ave_kern_30func	32-bit floating-point	TempFunc (= 30) * TempFunc (= 30)	Averaging kernel for temperature retrieval.
Temp_verticality_30func	32-bit floating-point	TempFunc (= 30)	Sum of the rows of Temp_ave_kern_30func.
Temp_dof	32-bit floating-point	None	Measure of the amount of information in temperature profile retrieval (deg of freedom).
Water Vapor Saturation Quantities Derived from Temperature			
H2OMMRSatLevSup	32-bit floating-point	XtraPressureLev (= 100)	Level Water vapor saturation mass mixing ratio (gm / kg dry air) over equilibrium phase (set to -9999. when saturation pressure exceeds 1% of ambient pressure.)
H2OMMRSatLevSup_QC	16-bit unsigned integer	XtraPressureLev (= 100)	Quality Control for H2OMMRSatLevSup.; 0: Highest Quality; 1: Good Quality; 2: Do Not Use
H2OMMRSatSurf	32-bit floating-point	None	Water Vapor saturation Mass Mixing Ratio at the surface (gm / kg dry air) over equilibrium phase
H2OMMRSatSurf_QC	16-bit unsigned integer	None	Quality Control for H2OMMRSatSurf.; 0: Highest Quality; 1: Good Quality; 2: Do Not Use
H2OMMRSatLevSup_liquid	32-bit floating-point	XtraPressureLev (= 100)	Level Water vapor saturation mass mixing ratio (gm / kg dry air) over liquid phase (set to -9999. when saturation pressure exceeds 1% of ambient pressure.)
H2OMMRSatLevSup_liquid_QC	16-bit unsigned integer	XtraPressureLev (= 100)	Quality Control for H2OMMRSatLevSup_liquid.; 0: Highest Quality; 1: Good Quality; 2: Do Not Use

H2OMMRSatSurf_liquid	32-bit floating-point	None	Water Vapor saturation Mass Mixing Ratio at the surface (gm / kg dry air) over liquid phase
H2OMMRSatSurf_liquid_QC	16-bit unsigned integer	None	Quality Control for H2OMMRSatSurf_liquid.; 0: Highest Quality; 1: Good Quality; 2: Do Not Use
surf_dew_point_temp	32-bit floating-point	None	Dew-point temnperature at the surface (K)
surf_dew_point_temp_QC	16-bit unsigned integer	None	Quality Control for surf_dew_point_temp.; 0: Highest Quality; 1: Good Quality; 2: Do Not Use
Tropopause Derived from Temperature			
PTropopause	32-bit floating-point	None	Tropopause height (hPa)
PTropopause_QC	16-bit unsigned integer	None	Quality Control for PTropopause.; 0: Highest Quality; 1: Good Quality; 2: Do Not Use
T_Tropopause	32-bit floating-point	None	Tropopause temperature (K)
T_Tropopause_QC	16-bit unsigned integer	None	Quality Control for T_Tropopause.; 0: Highest Quality; 1: Good Quality; 2: Do Not Use
Water Vapor Retrievals			
totH2OStd	32-bit floating-point	None	Total precipitable water vapor (kg / m**2)
totH2OStd_QC	16-bit unsigned integer	None	Quality Control for totH2OStd.; 0: Highest Quality; 1: Good Quality; 2: Do Not Use
totH2OStdErr	32-bit floating-point	None	Error estimate for totH2OStd
H2OCDSup	32-bit floating-point	XtraPressureLay (= 100)	Layer column water vapor (molecules / cm**2)
H2OCDSup_QC	16-bit unsigned integer	XtraPressureLay (= 100)	Quality Control for H2OCDSup.; 0: Highest Quality; 1: Good Quality; 2: Do Not Use
H2OCDSupErr	32-bit floating-point	XtraPressureLay (= 100)	Error estimate for H2OCDSup
H2OMMRLevSup	32-bit floating-point	XtraPressureLev (= 100)	Water Vapor Mass Mixing Ratio (gm / kg dry air)

H2OMMRLevSup_QC	16-bit unsigned integer	XtraPressureLev (= 100)	Quality Control for H2OMMRLevSup.; 0: Highest Quality; 1: Good Quality; 2: Do Not Use
H2OMMRLevSupErr	32-bit floating-point	XtraPressureLev (= 100)	Error estimate for H2OMMRLevSup
H2OMMRSurf	32-bit floating-point	None	Water Vapor Mass Mixing Ratio at the surface (gm / kg dry air)
H2OMMRSurf_QC	16-bit unsigned integer	None	Quality Control for H2OMMRSurf.; 0: Highest Quality; 1: Good Quality; 2: Do Not Use
H2OMMRSurfErr	32-bit floating-point	None	Error estimate for H2OMMRSurf
num_H2O_Func	16-bit integer	None	Number of valid entries in each dimension of H2O_ave_kern_21func.
H2O_eff_press_21func	32-bit floating-point	H2OFunc (= 21)	H20 effective pressure for the center of each trapezoid
H2O_VMR_eff_21func	32-bit floating-point	H2OFunc (= 21)	Effective H2O volume mixing ratio for each trapezoid.
H2O_VMR_eff_21func_QC	16-bit unsigned integer	H2OFunc (= 21)	Quality Control for H2O_VMR_eff_21func.; 0: Highest Quality; 1: Good Quality; 2: Do Not Use
H2O_VMR_eff_21func_err	32-bit floating-point	H2OFunc (= 21)	Error estimate for H2O_VMR_eff_21func
H2O_verticality_21func	32-bit floating-point	H2OFunc (= 21)	Sum of the rows of H2O_ave_kern_21func.
H2O_dof	32-bit floating-point	None	Measure of the amount of information in H2O retrieval (deg of freedom).
H2O_ave_kern_21func	32-bit floating-point	H2OFunc (= 21) * H2OFunc (= 21)	Averaging kernel for water vapor retrieval.
Relative Humidity, Boundary Layer Top, and Geopotential Height Derived from Temperature and Water Vapor			
RelHum	32-bit floating-point	H2OPressureLev (= 15)	Relative humidity over equilibrium phase (%)
RelHum_QC	16-bit unsigned integer	H2OPressureLev (= 15)	Quality control for RelHum.; 0: Highest Quality; 1: Good Quality; 2: Do Not Use
RelHumSurf	32-bit floating-point	None	Relative humidity at the surface over equilibrium phase (%)

RelHumSurf_QC	16-bit unsigned integer	None	Quality Control for RelHumSurf.; 0: Highest Quality; 1: Good Quality; 2: Do Not Use
RelHum_liquid	32-bit floating-point	H2OPressureLev (= 15)	Relative humidity over liquid phase (%)
RelHum_liquid_QC	16-bit unsigned integer	H2OPressureLev (= 15)	Quality control for RelHum_liquid.; 0: Highest Quality; 1: Good Quality; 2: Do Not Use
RelHumSurf_liquid	32-bit floating-point	None	Relative humidity at the surface over liquid phase (%)
RelHumSurf_liquid_QC	16-bit unsigned integer	None	Quality Control for RelHumSurf_liquid.; 0: Highest Quality; 1: Good Quality; 2: Do Not Use
surf_h2o_vap_pres_deficit	32-bit floating-point	None	Near-surface water vapor saturation pressure deficit (VPD) (Pa)
surf_h2o_vap_pres_deficit_QC	16-bit unsigned integer	None	Quality Control for surf_h2o_vap_pres_deficit.; 0: Highest Quality; 1: Good Quality; 2: Do Not Use
bndry_lyr_top	32-bit floating-point	None	Pressure at top of boundary layer (hPa)
bndry_lyr_top_QC	16-bit unsigned integer	None	Quality Control for bndry_lyr_top.; 0: Highest Quality; 1: Good Quality; 2: Do Not Use
GP_Tropopause	32-bit floating-point	None	Geopotential height at tropopause (m above mean sea level)
GP_Tropopause_QC	16-bit unsigned integer	None	Quality Control for GP_Tropopause.; 0: Highest Quality; 1: Good Quality; 2: Do Not Use
GP_HeightSup	32-bit floating-point	XtraPressureLev (= 100)	Geopotential Heights (m above mean sea level)
GP_HeightSup_QC	16-bit unsigned integer	XtraPressureLev (= 100)	Quality Control for GP_HeightSup.; 0: Highest Quality; 1: Good Quality; 2: Do Not Use
GP_Surface	32-bit floating-point	None	Geopotential Height of surface (m above mean sea level)
GP_Surface_QC	16-bit unsigned integer	None	Quality Control for GP_Surface.; 0: Highest Quality; 1: Good Quality; 2: Do Not Use

Longwave IR Cloud Formation Retrievals on 3 by 3 AIRS Fields of View			
CldFrcTot	32-bit floating-point	None	Total cloud fraction over all cloud layers and all 9 spots (0.0 ... 1.0) assuming unit cloud top emissivity.
CldFrcTot_QC	16-bit unsigned integer	None	Quality Control for CldFrcTot.; 0: Highest Quality; 1: Good Quality; 2: Do Not Use
CldFrcStd	32-bit floating-point	AIRSTrack (= 3) * AIRSXTrack (= 3) * Cloud (= 2)	Cloud fraction (0.0 ... 1.0) assuming unit cloud top emissivity (in order of increasing pressure. Only first nCld elements are valid) Caution: For CldFrcStd = 1, only the average cloud fraction over the nine spots is reported (duplicated nine times) for each level.
CldFrcStd_QC	16-bit unsigned integer	AIRSTrack (= 3) * AIRSXTrack (= 3) * Cloud (= 2)	Quality Control for CldFrcStd.; 0: Highest Quality; 1: Good Quality; 2: Do Not Use
CldFrcStdErr	32-bit floating-point	AIRSTrack (= 3) * AIRSXTrack (= 3) * Cloud (= 2)	Error estimate for CldFrcStd
PCldTop	32-bit floating-point	AIRSTrack (= 3) * AIRSXTrack (= 3) * Cloud (= 2)	Cloud top pressure in hPa. (in order of increasing pressure. Only first nCld elements are valid)
PCldTop_QC	16-bit unsigned integer	AIRSTrack (= 3) * AIRSXTrack (= 3) * Cloud (= 2)	Quality Control for PCldTop.; 0: Highest Quality; 1: Good Quality; 2: Do Not Use
PCldTopErr	32-bit floating-point	AIRSTrack (= 3) * AIRSXTrack (= 3) * Cloud (= 2)	Error estimate for PCldTop.
TCldTop	32-bit floating-point	AIRSTrack (= 3) * AIRSXTrack (= 3) * Cloud (= 2)	Cloud top temperature in Kelvins (in order of increasing pressure. Only first nCld elements are valid)
TCldTop_QC	16-bit unsigned integer	AIRSTrack (= 3) * AIRSXTrack (= 3) * Cloud (= 2)	Quality Control for TCldTop.; 0: Highest Quality; 1: Good Quality; 2: Do Not Use
TCldTopErr	32-bit floating-point	AIRSTrack (= 3) * AIRSXTrack (= 3) * Cloud (= 2)	Error estimate for TCldTop.
nCld	32-bit integer	AIRSTrack (= 3) * AIRSXTrack (= 3)	Number of cloud layers in each of the 9 spots
Longwave IR Cloud Formation Retrievals on Single AMSU Fields of View			
PCldTopStd	32-bit floating-point	Cloud (= 2)	Cloud top pressure in hPa assuming the same two cloud formations over all 9 spots.; DEPRECATED. Newer PCldTop is a more finely resolved version.
PCldTopStd_QC	16-bit unsigned integer	Cloud (= 2)	Quality Control for PCldTopStd.; 0: Highest Quality; 1: Good Quality; 2: Do Not Use

PCldTopStdErr	32-bit floating-point	Cloud (= 2)	Error estimate for PCldTopStd
TCldTopStd	32-bit floating-point	Cloud (= 2)	Cloud top temperature in Kelvins (in order of increasing pressure. Only first numCloud elements are valid) assuming the same two cloud formations over all 9 spots.; DEPRECATED. Newer TCldTop is a more finely resolved version.
TCldTopStd_QC	16-bit unsigned integer	Cloud (= 2)	Quality Control for TCldTopStd.; 0: Highest Quality; 1: Good Quality; 2: Do Not Use
TCldTopStdErr	32-bit floating-point	Cloud (= 2)	Error estimate for TCldTopStd
numCloud	32-bit integer	None	Number of cloud layers (max over the 9 spots). Deprecated. Use only with deprecated fields PCldTopStd and TCldTopStd. Otherwise use nCld.
Cloud Spectral Properties assumed in Longwave IR Cloud Formation Retrievals			
numHingeCloud	16-bit integer	None	Number of hinge points for cloud emissivity and reflectivity
cldFreq	32-bit floating-point	Cloud (= 2) * HingeCloud (= 7)	Frequencies for cloud emissivity and reflectivity (in order of increasing pressure. Only first numCloud elements are valid) (in order of increasing frequency. Only first numHingeCloud elements are valid)
CldEmis	32-bit floating-point	Cloud (= 2) * HingeCloud (= 7)	Ratio of cloud IR emissivity to that at 930 cm-1 (in order of increasing frequency. Only first numHingeCloud elements are valid)
CldEmis_QC	16-bit unsigned integer	Cloud (= 2) * HingeCloud (= 7)	Quality Control for CldEmis.; 0: Highest Quality; 1: Good Quality; 2: Do Not Use; Set to 1 to show the value is assumed, not retrieved
CldEmisErr	32-bit floating-point	Cloud (= 2) * HingeCloud (= 7)	Error estimate for CldEmis
CldRho	32-bit floating-point	Cloud (= 2) * HingeCloud (= 7)	Future Cloud IR reflectivity -- DO NOT USE
CldRho_QC	16-bit unsigned integer	Cloud (= 2) * HingeCloud (= 7)	Quality Control for CldRho.; 0: Highest Quality; 1: Good Quality; 2: Do Not Use; Set to 1 to show the value is assumed, not retrieved
CldRhoErr	32-bit floating-point	Cloud (= 2) * HingeCloud (= 7)	Error estimate for CldRho

Cirrus Cloud Optical Properties Retrievals			
ice_cld_opt_dpth	32-bit floating-point	AIRSTrack (= 3) * AIRSXTrack (= 3)	Ice cloud optical depth
ice_cld_opt_dpth_QC	16-bit unsigned integer	AIRSTrack (= 3) * AIRSXTrack (= 3)	Quality control for ice_cld_opt_dpth.; 0: Highest Quality; 1: Good Quality; 2: Do Not Use
ice_cld_eff_diam	32-bit floating-point	AIRSTrack (= 3) * AIRSXTrack (= 3)	Ice cloud effective diameter (microns)
ice_cld_eff_diam_QC	16-bit unsigned integer	AIRSTrack (= 3) * AIRSXTrack (= 3)	Quality control for ice_cld_eff_diam.; 0: Highest Quality; 1: Good Quality; 2: Do Not Use
ice_cld_temp_eff	32-bit floating-point	AIRSTrack (= 3) * AIRSXTrack (= 3)	Ice cloud effective cloud top temperature (K)
ice_cld_temp_eff_QC	16-bit unsigned integer	AIRSTrack (= 3) * AIRSXTrack (= 3)	Quality control for ice_cld_temp_eff.; 0: Highest Quality; 1: Good Quality; 2: Do Not Use
ice_cld_fit_reduced_chisq	32-bit floating-point	AIRSTrack (= 3) * AIRSXTrack (= 3)	Normalized chi-square of the obs-calc radiance residual in the ice cloud optical properties calculation
ice_cld_opt_dpth_ave_kern	32-bit floating-point	AIRSTrack (= 3) * AIRSXTrack (= 3)	Scalar value of averaging kernel for ice cloud optical depth
ice_cld_eff_diam_ave_kern	32-bit floating-point	AIRSTrack (= 3) * AIRSXTrack (= 3)	Scalar value of averaging kernel for ice cloud effective diameter
ice_cld_temp_eff_ave_kern	32-bit floating-point	AIRSTrack (= 3) * AIRSXTrack (= 3)	Scalar value of averaging kernel for ice cloud effective cloud top temperature
ice_cld_opt_dpth_err	32-bit floating-point	AIRSTrack (= 3) * AIRSXTrack (= 3)	Error estimate for ice cloud optical depth
ice_cld_eff_diam_err	32-bit floating-point	AIRSTrack (= 3) * AIRSXTrack (= 3)	Error estimate for ice cloud effective diameter
ice_cld_temp_eff_err	32-bit floating-point	AIRSTrack (= 3) * AIRSXTrack (= 3)	Error estimate for ice cloud effective cloud top temperature (K)
log_ice_cld_opt_dpth_prior_var	32-bit floating-point	AIRSTrack (= 3) * AIRSXTrack (= 3)	A priori variance for the logarithm of ice cloud optical depth
log_ice_cld_eff_diam_prior_var	32-bit floating-point	AIRSTrack (= 3) * AIRSXTrack (= 3)	A priori variance for the logarithm of ice cloud effective diameter
ice_cld_temp_eff_prior_var	32-bit floating-point	AIRSTrack (= 3) * AIRSXTrack (= 3)	A priori variance for ice cloud effective cloud top temperature (K)
ice_cld_opt_dpth_first_guess	32-bit floating-point	AIRSTrack (= 3) * AIRSXTrack (= 3)	First guess for ice cloud optical depth

ice_cld_eff_diam_first_guess	32-bit floating-point	AIRSTrack (= 3) * AIRSXTrack (= 3)	First guess for ice cloud effective diameter
ice_cld_temp_eff_first_guess	32-bit floating-point	AIRSTrack (= 3) * AIRSXTrack (= 3)	First guess for ice cloud effective cloud top temperature (K)
Ozone Retrievals			
totO3Std	32-bit floating-point	None	Total ozone burden (Dobson units)
totO3Std_QC	16-bit unsigned integer	None	Quality Control for totO3Std.; 0: Highest Quality; 1: Good Quality; 2: Do Not Use
totO3StdErr	32-bit floating-point	None	Error estimate for totO3Std
O3CDSup	32-bit floating-point	XtraPressureLay (= 100)	Layer column ozone in molecules per cm**2
O3CDSup_QC	16-bit unsigned integer	XtraPressureLay (= 100)	Quality Control for O3CDSup.; 0: Highest Quality; 1: Good Quality; 2: Do Not Use
O3CDSupErr	32-bit floating-point	XtraPressureLay (= 100)	Error estimate for O3CDSupErr
O3VMRLevSup	32-bit floating-point	XtraPressureLev (= 100)	Dry column ozone Volume Mixing Ratio on support levels (ppv)
O3VMRLevSup_QC	16-bit unsigned integer	XtraPressureLev (= 100)	Quality Control for O3VMRLevSup.; 0: Highest Quality; 1: Good Quality; 2: Do Not Use
O3VMRLevSupErr	32-bit floating-point	XtraPressureLev (= 100)	Error estimate for O3VMRLevSup
O3VMRSurf	32-bit floating-point	None	Dry column ozone Volume Mixing Ratio at the surface (ppv)
O3VMRSurf_QC	16-bit unsigned integer	None	Quality Control for O3VMRSurf.; 0: Highest Quality; 1: Good Quality; 2: Do Not Use
O3VMRSurfErr	32-bit floating-point	None	Error estimate for O3VMRSurf
num_O3_Func	16-bit integer	None	Number of valid entries in each dimension of O3_ave_kern_20func.
O3_eff_press_20func	32-bit floating-point	O3Func (= 20)	O3 effective pressure for the center of each trapezoid
O3_VMR_eff_20func	32-bit floating-point	O3Func (= 20)	Effective dry column ozone volume mixing ratio for each trapezoid.

O3_VMR_eff_20func_QC	16-bit unsigned integer	O3Func (= 20)	Quality Control for O3_VMR_eff_20func.; 0: Highest Quality; 1: Good Quality; 2: Do Not Use
O3_VMR_eff_20func_err	32-bit floating-point	O3Func (= 20)	Error estimate for O3_VMR_eff_20func
O3_verticality_20func	32-bit floating-point	O3Func (= 20)	Sum of the rows of O3_ave_kern_20func.
O3_dof	32-bit floating-point	None	Measure of the amount of information in O3 retrieval (deg of freedom).
O3_ave_kern_20func	32-bit floating-point	O3Func (= 20) * O3Func (= 20)	Averaging kernel for ozone retrieval.
Carbon Monoxide Retrievals			
CO_total_column	32-bit floating-point	None	Retrieved total column CO (molecules/cm2).
CO_total_column_QC	16-bit unsigned integer	None	Quality Control for CO_total_column.; 0: Highest Quality; 1: Good Quality; 2: Do Not Use
COCDSup	32-bit floating-point	XtraPressureLay (= 100)	Layer column carbon monoxide in molecules per cm**2 (climatology when bad_co is not 0)
COCDSup_QC	16-bit unsigned integer	XtraPressureLay (= 100)	Quality Control for COCDSup.; 0: Highest Quality; 1: Good Quality; 2: Do Not Use
COCDSupErr	32-bit floating-point	XtraPressureLay (= 100)	Error estimate for COCDSup
COVMRLevSup	32-bit floating-point	XtraPressureLev (= 100)	Dry column CO Volume Mixing Ratio at support levels (ppv)
COVMRLevSup_QC	16-bit unsigned integer	XtraPressureLev (= 100)	Quality Control for COVMRLevSup.; 0: Highest Quality; 1: Good Quality; 2: Do Not Use
COVMRLevSupErr	32-bit floating-point	XtraPressureLev (= 100)	Error estimate for COVMRLevSup
COVMRSurf	32-bit floating-point	None	Dry column CO Volume Mixing Ratio at the surface (ppv)
COVMRSurf_QC	16-bit unsigned integer	None	Quality Control for COVMRSurf.; 0: Highest Quality; 1: Good Quality; 2: Do Not Use

COVMRSurfErr	32-bit floating-point	None	Error estimate for COVMRSurf
num_CO_Func	16-bit integer	None	Number of valid entries in each dimension of CO_ave_kern.
CO_eff_press	32-bit floating-point	COFunc (= 9)	CO effective pressure for the center of each trapezoid
CO_VMR_eff	32-bit floating-point	COFunc (= 9)	Effective dry column CO volume mixing ratio for each trapezoid.
CO_VMR_eff_QC	16-bit unsigned integer	COFunc (= 9)	Quality Control for CO_VMR_eff.; 0: Highest Quality; 1: Good Quality; 2: Do Not Use
CO_VMR_eff_err	32-bit floating-point	COFunc (= 9)	Error estimate for CO_VMR_eff
CO_verticality	32-bit floating-point	COFunc (= 9)	Sum of the rows of CO_ave_kern.
CO_dof	32-bit floating-point	None	Measure of the amount of information in CO retrieval (deg of freedom).
CO_ave_kern	32-bit floating-point	COFunc (= 9) * COFunc (= 9)	Averaging kernel for carbon monoxide retrieval.
Methane Retrievals			
CH4_total_column	32-bit floating-point	None	Retrieved total column CH4 (molecules/cm2).
CH4_total_column_QC	16-bit unsigned integer	None	Quality Control for CH4_total_column.; 0: Highest Quality; 1: Good Quality; 2: Do Not Use
CH4CDSup	32-bit floating-point	XtraPressureLay (= 100)	Layer column methane (in molecules per cm**2)
CH4CDSup_QC	16-bit unsigned integer	XtraPressureLay (= 100)	Quality Control for CH4CDSup.; 0: Highest Quality; 1: Good Quality; 2: Do Not Use
CH4CDSupErr	32-bit floating-point	XtraPressureLay (= 100)	Error estimate for CH4CDSup
CH4VMRLevSup	32-bit floating-point	XtraPressureLev (= 100)	Dry column CH4 volume Mixing Ratio at support levels (ppv)
CH4VMRLevSup_QC	16-bit unsigned integer	XtraPressureLev (= 100)	Quality Control for CH4VMRLevSup.; 0: Highest Quality; 1: Good Quality; 2: Do Not Use

CH4VMRLevSupErr	32-bit floating-point	XtraPressureLev (= 100)	Error estimate for CH4VMRLevSup
CH4VMRSurf	32-bit floating-point	None	Dry column CH4 volume Mixing Ratio at the surface (ppv)
CH4VMRSurf_QC	16-bit unsigned integer	None	Quality Control for CH4VMRSurf.; 0: Highest Quality; 1: Good Quality; 2: Do Not Use
CH4VMRSurfErr	32-bit floating-point	None	Error estimate for CH4VMRSurf
num_CH4_Func	16-bit integer	None	Number of valid entries in each dimension of CH4_ave_kern.
CH4_eff_press_10func	32-bit floating-point	CH4Func (= 10)	CH4 effective pressure for the center of each trapezoid
CH4_VMR_eff_10func	32-bit floating-point	CH4Func (= 10)	Effective dry column CH4 volume mixing ratio for each trapezoid.
CH4_VMR_eff_10func_QC	16-bit unsigned integer	CH4Func (= 10)	Quality Control for CH4_VMR_eff_10func.; 0: Highest Quality; 1: Good Quality; 2: Do Not Use
CH4_VMR_eff_10func_err	32-bit floating-point	CH4Func (= 10)	Error estimate for CH4_VMR_eff
CH4_verticality_10func	32-bit floating-point	CH4Func (= 10)	Sum of the rows of CH4_ave_kern.
CH4_dof	32-bit floating-point	None	Measure of the amount of information in CH4 retrieval (deg of freedom).
CH4_ave_kern_10func	32-bit floating-point	CH4Func (= 10) * CH4Func (= 10)	Averaging kernel for methane retrieval.
Outgoing Longwave Radiation Retrievals			
olr	32-bit floating-point	None	Outgoing Longwave Radiation Flux integrated over 2 to 2800 cm**-1 (per 45 km AMSU-A FOV) (Watts/m**2)
olr_QC	16-bit unsigned integer	None	Quality Control for olr.; 0: Highest Quality; 1: Good Quality; 2: Do Not Use
spectralolr	32-bit floating-point	OLRBand (= 16)	Outgoing Longwave Radiation Flux integrated over 16 frequency bands (per 45 km AMSU-A FOV) (Watts/m**2)
spectralolr_QC	16-bit unsigned integer	OLRBand (= 16)	Quality Control for spectralolr.; 0: Highest Quality; 1: Good Quality; 2: Do Not Use

olr3x3	32-bit floating-point	AIRSTrack (= 3) * AIRSXTrack (= 3)	Outgoing Longwave Radiation Flux integrated over 2 to 2800 cm**-1 (per 15 km AIRS FOV) (Watts/m**2)
olr3x3_QC	16-bit unsigned integer	AIRSTrack (= 3) * AIRSXTrack (= 3)	Quality Control for olr3x3.; 0: Highest Quality; 1: Good Quality; 2: Do Not Use
olr_err	32-bit floating-point	None	Error estimate for olr (Watts/m**2)
clrolr	32-bit floating-point	None	Clear-sky Outgoing Longwave Radiation Flux integrated over 2 to 2800 cm**-1 (per 45 km AMSU-A FOV) (Watts/m**2)
clrolr_QC	16-bit unsigned integer	None	Quality Control for clrolr.; 0: Highest Quality; 1: Good Quality; 2: Do Not Use
clrolr_err	32-bit floating-point	None	Error estimate for clrolr (Watts/m**2)
spectralclrolr	32-bit floating-point	OLRBand (= 16)	Clear-sky Outgoing Longwave Radiation Flux integrated over 16 frequency bands (per 45 km AMSU-A FOV) (Watts/m**2)
spectralclrolr_QC	16-bit unsigned integer	OLRBand (= 16)	Quality Control for spectralclrolr.; 0: Highest Quality; 1: Good Quality; 2: Do Not Use
Geolocation QA			
ftptgeoqa	32-bit unsigned integer	None	Footprint Geolocation QA flags:; Bit 0: (LSB, value 1) bad input value; Bit 1: (value 2) PGS_TD_TAItoUTC() gave PGSTD_E_NO_LEAP_SECS; Bit 2: (value 4) PGS_TD_TAItoUTC() gave PGS_E_TOOLKIT; Bit 3: (value 8) PGS_CSC_GetFOV_Pixel() gave PGSCSC_W_MISS_EARTH; Bit 4: (value 16) PGS_CSC_GetFOV_Pixel() gave PGSTD_E_SC_TAG_UNKNOWN; Bit 5: (value 32) PGS_CSC_GetFOV_Pixel() gave PGSCSC_W_ZERO_PIXEL_VECTOR; Bit 6: (value 64) PGS_CSC_GetFOV_Pixel() gave PGSCSC_W_BAD_EPH_FOR_PIXEL; Bit 7: (value 128) PGS_CSC_GetFOV_Pixel() gave PGSCSC_W_INSTRUMENT_OFF_BOARD; Bit 8: (value 256)

			PGS_CSC_GetFOV_Pixel() gave PGSCSC_W_BAD_ACCURACY_FLAG; Bit 9: (value 512) PGS_CSC_GetFOV_Pixel() gave PGSCSC_E_BAD_ARRAY_SIZE; Bit 10: (value 1024) PGS_CSC_GetFOV_Pixel() gave PGSCSC_W_DEFAULT_EARTH_MODEL; Bit 11: (value 2048) PGS_CSC_GetFOV_Pixel() gave PGSCSC_W_DATA_FILE_MISSING; Bit 12: (value 4096) PGS_CSC_GetFOV_Pixel() gave PGSCSC_E_NEG_OR_ZERO_RAD; Bit 13: (value 8192) PGS_CSC_GetFOV_Pixel() gave PGSMEM_E_NO_MEMORY; Bit 14: (value 16384) PGS_CSC_GetFOV_Pixel() gave PGSTD_E_NO_LEAP_SECS; Bit 15: (value 32768) PGS_CSC_GetFOV_Pixel() gave PGSTD_E_TIME_FMT_ERROR; Bit 16: (value 65536) PGS_CSC_GetFOV_Pixel() gave PGSTD_E_TIME_VALUE_ERROR; Bit 17: (value 131072) PGS_CSC_GetFOV_Pixel() gave PGSCSC_W_PREDICTED_UT1; Bit 18: (value 262144) PGS_CSC_GetFOV_Pixel() gave PGSTD_E_NO_UT1_VALUE; Bit 19: (value 524288) PGS_CSC_GetFOV_Pixel() gave PGS_E_TOOLKIT; Bit 20: (value 1048576) PGS_CSC_GetFOV_Pixel() gave PGSEPH_E_BAD_EPHEM_FILE_HDR; Bit 21: (value 2097152) PGS_CSC_GetFOV_Pixel() gave PGSEPH_E_NO_SC_EPHEM_FILE; Bit 22-31: not used
zengeoqa	16-bit unsigned integer	None	Satellite zenith Geolocation QA flags:; Bit 0: (LSB, value 1) (Spacecraft) bad input value; Bit 1: (value 2) PGS_CSC_ZenithAzimuth(S/C) gave PGSCSC_W_BELOW_HORIZON; Bit 2: (value 4) PGS_CSC_ZenithAzimuth(S/C) gave PGSCSC_W_UNDEFINED_AZIMUTH;

			Bit 3: (value 8) PGS_CSC_ZenithAzimuth(S/C) gave PGSCSC_W_NO_REFRACTION; Bit 4: (value 16) PGS_CSC_ZenithAzimuth(S/C) gave PGSCSC_E_INVALID_VECTAG; Bit 5: (value 32) PGS_CSC_ZenithAzimuth(S/C) gave PGSCSC_E_LOOK_PT_ALTIT_RANGE; Bit 6: (value 64) PGS_CSC_ZenithAzimuth(S/C) gave PGSCSC_E_ZERO_INPUT_VECTOR; Bit 7: (value 128) PGS_CSC_ZenithAzimuth(S/C) gave PGS_E_TOOLKIT; Bit 8: (value 256) (Sun) bad input value; Bit 9: (value 512) (suppressed) PGS_CSC_ZenithAzimuth(Sun) gave PGSCSC_W_BELOW_HORIZON (This is not an error condition - the sun is below the horizon at night); Bit 10: (value 1024) PGS_CSC_ZenithAzimuth(Sun) gave PGSCSC_W_UNDEFINED_AZIMUTH; Bit 11: (value 2048) PGS_CSC_ZenithAzimuth(Sun) gave PGSCSC_W_NO_REFRACTION; Bit 12: (value 4096) PGS_CSC_ZenithAzimuth(Sun) gave PGSCSC_E_INVALID_VECTAG; Bit 13: (value 8192) PGS_CSC_ZenithAzimuth(Sun) gave PGSCSC_E_LOOK_PT_ALTIT_RANGE; Bit 14: (value 16384) PGS_CSC_ZenithAzimuth(Sun) gave PGSCSC_E_ZERO_INPUT_VECTOR; Bit 15: (value 32768) PGS_CSC_ZenithAzimuth(Sun) gave PGS_E_TOOLKIT
demgeoqa	16-bit unsigned integer	None	Digital Elevation Model (DEM) Geolocation QA flags:; Bit 0: (LSB, value 1) bad input value; Bit 1: (value 2) Could not allocate memory; Bit 2: (value 4) Too close to North or South pole. Excluded. (This is not an error condition - a different model is used); Bit 3: (value 8) Layer resolution incompatibility. Excluded;

			Bit 4: (value 16) Any DEM Routine (elev) gave PGSDEM_E_IMPROPER_TAG; Bit 5: (value 32) Any DEM Routine (elev) gave PGSDEM_E_CANNOT_ACCESS_DATA; Bit 6: (value 64) Any DEM Routine (land/water) gave PGSDEM_E_IMPROPER_TAG; Bit 7: (value 128) Any DEM Routine (land/water) gave PGSDEM_E_CANNOT_ACCESS_DATA; Bit 8: (value 256) Reserved for future layers; Bit 9: (value 512) Reserved for future layers; Bit 10: (value 1024) PGS_DEM_GetRegion(elev) gave PGSDEM_M_FILLVALUE_INCLUDED; Bit 11: (value 2048) PGS_DEM_GetRegion(land/water) gave PGSDEM_M_FILLVALUE_INCLUDED; Bit 12: (value 4096) Reserved for future layers; Bit 13: (value 8192) PGS_DEM_GetRegion(all) gave PGSDEM_M_MULTIPLE_RESOLUTIONS; Bit 14: (value 16384) PGS_CSC_GetFOV_Pixel() gave any 'W' class return code except PGSCSC_W_PREDICTED_UT1; Bit 15: (value 32768) PGS_CSC_GetFOV_Pixel() gave any 'E' class return code
Miscellaneous			
all_spots_avg	8-bit integer	None	1: the cloud clearing step judged the scene to be clear enough that it averaged all spots' radiances; 0: cloud clearing was applied to the radiances; -1/255: cloud clearing not attempted
retrieval_type	8-bit integer	None	Deprecated -- use Xxx_QC flags. Retrieval type:; 0 for full retrieval; 10 for MW + final succeeded, initial retrieval failed; 20 for MW + initial succeeded, final failed; 30 for only MW stage succeeded, initial + final retrieval failed;

			40 for MW + initial succeeded, final cloud-clearing failed; 50 for only MW stage succeeded, initial + final cloud-clearing failed; 100 for no retrieval;
SurfClass	8-bit integer	None	Surface class used in physical retrieval, from microwave (MW) and/or infrared (IR). Identical to MWSurfClass when MW is used:; 0 for coastline (Liquid water covers 50-99% of area); 1 for land (Liquid water covers < 50% of area); 2 for ocean (Liquid water covers > 99% of area); 3 for sea ice (Indicates high MW emissivity when MW information is used); 4 for sea ice (Indicates low MW emissivity. This value is only produced when MW information is used.); 5 for snow (Indicates higher-frequency MW scattering when MW information is used); 6 for glacier/snow (Indicates very low-frequency MW scattering. This value is only produced when MW information is used.); 7 for snow (Indicates lower-frequency MW scattering. This value is only produced when MW information is used.); -1 for unknown
IR_Precip_Est	32-bit floating-point	None	Regression-based estimate of daily precipitation based on clouds and relative humidity from Level 2 IR/MW retrieval. Analogous to and forms a continuous record when used with TOVS precipitation index. (per 45 km AMSU-A FOV) (mm/day)
IR_Precip_Est_QC	16-bit unsigned integer	None	Quality Control for IR_Precip_Est.; 0: Highest Quality; 1: Good Quality; 2: Do Not Use
IR_Precip_Est3x3	32-bit floating-point	AIRSTrack (= 3) * AIRSXTrack (= 3)	Regression-based estimate of daily precipitation based on clouds and relative humidity from Level 2 IR/MW retrieval. Analogous to and forms a continuous record when used with TOVS precipitation index. (per 15 km AIRS FOV) (mm/day)
IR_Precip_Est3x3_QC	16-bit unsigned integer	AIRSTrack (= 3) * AIRSXTrack (= 3)	Quality Control for IR_Precip_Est3x3.; 0: Highest Quality;

			1: Good Quality; 2: Do Not Use
IR_Precip_Est_Err	32-bit floating-point	None	Error estimate for IR_Precip_Est
Microwave Dependent			
TAirMWOnly	32-bit floating-point	XtraPressureLev (= 100)	Air temperature in Kelvins from startup microwave-only retrieval.
TAirMWOnly_QC	16-bit unsigned integer	XtraPressureLev (= 100)	Quality Control for TAirMWOnly.; 0: Highest Quality; 1: Good Quality; 2: Do Not Use
TAirMWOnlyErr	32-bit floating-point	StdPressureLev (= 28)	Error estimate for TAirMWOnly (Note that error estimate only made at StdPressureLev points even though TAirMWOnly is estimated at XtraPressureLev points)
MWSurfClass	8-bit integer	None	Surface class from microwave (MW) information:; 0 for coastline (Liquid water covers 50-99% of area); 1 for land (Liquid water covers < 50% of area); 2 for ocean (Liquid water covers > 99% of area); 3 for sea ice (High MW emissivity); 4 for sea ice (Low MW emissivity); 5 for snow (Higher-frequency MW scattering); 6 for glacier/snow (Very low-frequency MW scattering); 7 for snow (Lower-frequency MW scattering); -1 for unknown (not attempted)
sfcTbMWStd	32-bit floating-point	MWHingeSurf (= 7)	Microwave surface brightness (Kelvins) (Emitted radiance only, reflected radiance not included. Product of MW only algorithm)
sfcTbMWStd_QC	16-bit unsigned integer	MWHingeSurf (= 7)	Quality Control for sfcTbMWStd.; 0: Highest Quality; 1: Good Quality; 2: Do Not Use
EmisMWStd	32-bit floating-point	MWHingeSurf (= 7)	Spectral MW emissivity at the 7 MW frequencies listed for dimension MWHingeSurf (Product of MW only algorithm)
EmisMWStd_QC	16-bit unsigned integer	MWHingeSurf (= 7)	Quality Control for EmisMWStd.; 0: Highest Quality; 1: Good Quality; 2: Do Not Use
EmisMWStdErr	32-bit floating-point	MWHingeSurf (= 7)	Error estimate for EmisMWStd

Emis50GHz	32-bit floating-point	None	Microwave emissivity at 50.3 GHz (This is from combined IR/MW retrieval. The shape of MW spectral emissivity stays the same as MW only algorithm.)
Emis50GHz_QC	16-bit unsigned integer	None	Quality Control for Emis50GHz.; 0: Highest Quality; 1: Good Quality; 2: Do Not Use
totH2OMWOnlyStd	32-bit floating-point	None	Total precipitable water vapor from MW-only retrieval (no IR information used) (kg / m**2)
totH2OMWOnlyStd_QC	16-bit unsigned integer	None	Quality Control for totH2OMWOnlyStd.; 0: Highest Quality; 1: Good Quality; 2: Do Not Use
H2OCDMWOnly	32-bit floating-point	XtraPressureLay (= 100)	Layer column water vapor from microwave-only retrieval. (molecules / cm**2)
H2OCDMWOnly_QC	16-bit unsigned integer	XtraPressureLay (= 100)	Quality Control for H2OCDMWOnly.; 0: Highest Quality; 1: Good Quality; 2: Do Not Use
totCldH2OStd	32-bit floating-point	None	Total cloud liquid water in kg/m**2
totCldH2OStd_QC	16-bit unsigned integer	None	Quality Control for totCldH2OStd; 0: Highest Quality; 1: Good Quality; 2: Do Not Use
totCldH2OStdErr	32-bit floating-point	None	Error estimate for totCldH2OStd
satzen_amsu	32-bit floating-point	None	Satellite zenith angle (0.0 ... 180.0) degrees from zenith (measured relative to the geodetic vertical on the reference (WGS84) spheroid and including corrections outlined in EOS SDP toolkit for normal accuracy.) (AMSU-A FOV center)
satazi_amsu	32-bit floating-point	None	Spacecraft azimuth angle (-180.0 ... 180.0) degrees E of N GEO (AMSU-A FOV center)
HSB Dependent			
PrecipAA4_50km	8-bit unsigned integer	None	Relative interference (0-2) of precipitation on AMSU-A channel 4 (-1/255 for unknown)
PrecipAA5_50km	8-bit unsigned integer	None	Relative interference (0-2) of precipitation on AMSU-A channel 5 (-1/255 for unknown)

PrecipAA6_50km	8-bit unsigned integer	None	Relative interference (0-2) of precipitation on AMSU-A channel 6 (-1/255 for unknown)
PrecipAA7_50km	8-bit unsigned integer	None	Relative interference (0-2, 3=indeterminate) of precipitation on AMSU-A channel 7 (-1/255 for unknown)
PrecipAA8_50km	8-bit unsigned integer	None	Relative interference (0-2) of precipitation on AMSU-A channel 8 (-1/255 for unknown)
PrecipAA9_50km	8-bit unsigned integer	None	Relative interference (0-2) of precipitation on AMSU-A channel 9 (-1/255 for unknown)
PrecipAA4_15km	8-bit unsigned integer	AIRSTrack (= 3) * AIRSXTrack (= 3)	Relative interference (0-2) of precipitation on AMSU-A channel 4 for HSB 15-km spots (-1/255 for unknown)
PrecipAA5_15km	8-bit unsigned integer	AIRSTrack (= 3) * AIRSXTrack (= 3)	Relative interference (0-2) of precipitation on AMSU-A channel 5 for HSB 15-km spots (-1/255 for unknown)
PrecipAA6_15km	8-bit unsigned integer	AIRSTrack (= 3) * AIRSXTrack (= 3)	Relative interference (0-2) of precipitation on AMSU-A channel 6 for HSB 15-km spots (-1/255 for unknown)
PrecipAA7_15km	8-bit unsigned integer	AIRSTrack (= 3) * AIRSXTrack (= 3)	Relative interference (0-2, 3=indeterminate) of precipitation on AMSU-A channel 7 for HSB 15-km spots (-1/255 for unknown)
PrecipAA8_15km	8-bit unsigned integer	AIRSTrack (= 3) * AIRSXTrack (= 3)	Relative interference (0-2) of precipitation on AMSU-A channel 8 for HSB 15-km spots (-1/255 for unknown)
PrecipAA9_15km	8-bit unsigned integer	AIRSTrack (= 3) * AIRSXTrack (= 3)	Relative interference (0-2) of precipitation on AMSU-A channel 9 for HSB 15-km spots (-1/255 for unknown)
AMSU_A_4_Precip_Corr_50km	32-bit floating-point	None	Correction to AMSU-A channel 4 for precipitation effects (Kelvins)
AMSU_A_5_Precip_Corr_50km	32-bit floating-point	None	Correction to AMSU-A channel 5 for precipitation effects (Kelvins)
AMSU_A_6_Precip_Corr_50km	32-bit floating-point	None	Correction to AMSU-A channel 6 for precipitation effects (Kelvins)
AMSU_A_7_Precip_Corr_50km	32-bit floating-point	None	Correction to AMSU-A channel 7 for precipitation effects (Kelvins)
AMSU_A_8_Precip_Corr_50km	32-bit floating-point	None	Correction to AMSU-A channel 8 for precipitation effects (Kelvins)

AMSU_A_9_Precip_Corr_50km	32-bit floating-point	None	Correction to AMSU-A channel 9 for precipitation effects (Kelvins)
AMSU_A_4_Precip_Corr_15km	32-bit floating-point	AIRSTrack (= 3) * AIRSXTrack (= 3)	Correction to AMSU-A channel 4 for precipitation effects for HSB 15-km spots (Kelvins)
AMSU_A_5_Precip_Corr_15km	32-bit floating-point	AIRSTrack (= 3) * AIRSXTrack (= 3)	Correction to AMSU-A channel 5 for precipitation effects for HSB 15-km spots (Kelvins)
AMSU_A_6_Precip_Corr_15km	32-bit floating-point	AIRSTrack (= 3) * AIRSXTrack (= 3)	Correction to AMSU-A channel 6 for precipitation effects for HSB 15-km spots (Kelvins)
AMSU_A_7_Precip_Corr_15km	32-bit floating-point	AIRSTrack (= 3) * AIRSXTrack (= 3)	Correction to AMSU-A channel 7 for precipitation effects for HSB 15-km spots (Kelvins)
AMSU_A_8_Precip_Corr_15km	32-bit floating-point	AIRSTrack (= 3) * AIRSXTrack (= 3)	Correction to AMSU-A channel 8 for precipitation effects for HSB 15-km spots (Kelvins)
AMSU_A_9_Precip_Corr_15km	32-bit floating-point	AIRSTrack (= 3) * AIRSXTrack (= 3)	Correction to AMSU-A channel 9 for precipitation effects for HSB 15-km spots (Kelvins)
rain_rate_50km	32-bit floating-point	None	Rain rate (mm/hr)
rain_rate_15km	32-bit floating-point	AIRSTrack (= 3) * AIRSXTrack (= 3)	Rain rate for HSB 15-km spots (mm/hr)
lwCDSup	32-bit floating-point	XtraPressureLay (= 100)	Layer molecular column density (molecules / cm**2) of cloud liquid water
lwCDSup_QC	16-bit unsigned integer	XtraPressureLay (= 100)	Quality Control for lwCDSup.; 0: Highest Quality; 1: Good Quality; 2: Do Not Use
lwCDSupErr	32-bit floating-point	XtraPressureLay (= 100)	Error estimate for lwCDSup
cIWSup	32-bit integer	XtraPressureLay (= 100)	Cloud Ice/Water flag (liquid = 0 / Ice = 1)
satzen_hsb	32-bit floating-point	None	Satellite zenith angle (0.0 ... 180.0) degrees from zenith (measured relative to the geodetic vertical on the reference (WGS84) spheroid and including corrections outlined in EOS SDP toolkit for normal accuracy.) (HSB center FOV)
satazi_hsb	32-bit floating-point	None	Spacecraft azimuth angle (-180.0 ... 180.0) degrees E of N GEO (HSB center FOV)
Forecast Quantities			
tsurf_forecast	32-bit floating-point	None	Predicted surface temperature interpolated from NOAA NCEP GFS forecast (K)

Forecast_Wind_U	32-bit floating-point	None	10 meter above surface zonal wind (+ toward east) in meters per second, interpolated from NOAA NCEP GFS forecast.
Forecast_Wind_V	32-bit floating-point	None	10 meter above surface meridional wind (+ toward north) in meters per second, interpolated from NOAA NCEP GFS forecast.
fcast_surf_snow_amnt	32-bit floating-point	None	Predicted surface snow amount interpolated from NOAA NCEP GFS forecast (WEASD) (kg/m^2)
fcast_sea_ice_frac	32-bit floating-point	None	Predicted sea ice fraction interpolated from NOAA NCEP GFS forecast (ICEC) [0.0, 1.0]
Climatology Quantities			
MODIS_emis	32-bit floating-point	MODISEmisBand (= 6)	First guess climatology emissivity from MODIS averaged over MYD11C3 0.05 degree (~5 km) pixels covering an area roughly corresponding to an AMSU FOV or 3x3 of AIRS FOVs.
MODIS_emis_dev	32-bit floating-point	MODISEmisBand (= 6)	Standard Deviation among the MYD11C3 elements used to determine MODIS_emis
MODIS_emis_qct	16-bit integer	MODISEmisQualLevels (= 4)	Count of MODIS emissivity pixels used in each quality category
MODIS_emis_spots	32-bit floating-point	MODISEmisBand (= 6) * AIRSTrack (= 3) * AIRSXTrack (= 3)	First guess emissivity from MODIS averaged over MYD11C3 0.05 degree (~5 km) pixels covering an area roughly corresponding to an AIRS FOV.
MODIS_emis_spots_dev	32-bit floating-point	MODISEmisBand (= 6) * AIRSTrack (= 3) * AIRSXTrack (= 3)	Standard Deviation among the MYD11C3 elements used to determine MODIS_emis
MODIS_emis_10_hinge	32-bit floating-point	MODISEmis10Hinge (= 10)	First guess emissivity from MODIS (MODIS_emis) expanded to 10 hinge points
MODIS_LST	32-bit floating-point	None	First guess climatology land surface temperature from MODIS averaged over MYD11C3 0.05 degree (~5 km) pixels covering an area roughly corresponding to an AMSU FOV or 3x3 of AIRS FOVs.
MODIS_LST_dev	32-bit floating-point	None	Standard Deviation among the MYD11C3 elements used to determine MODIS_LST
MODIS_LST_qct	16-bit integer	MODISLSTQualLevels (= 4)	Count of MODIS land surface temperature pixels used in each quality category
MODIS_LST_spots	32-bit floating-point	AIRSTrack (= 3) * AIRSXTrack (= 3)	First guess land surface temperature from MODIS averaged over MYD11C3 0.05 degree (~5 km) pixels covering an area roughly corresponding to an AIRS FOV.

MODIS_LST_spots_dev	32-bit floating-point	AIRSTrack (= 3) * AIRSXTrack (= 3)	Standard Deviation among the MYD11C3 elements used to determine MODIS_LST_spots
CO2ppmv	32-bit floating-point	None	Column averaged dry carbon dioxide volumetric mixing ratio (ppmv)
CO2ppmv_QC	16-bit unsigned integer	None	Quality Control for CO2ppmv.; 0: Highest Quality; 1: Good Quality; 2: Do Not Use; Set to 2 because the current value is from a model instead of a retrieved value.
CO2ppmvErr	32-bit floating-point	None	Error estimate for CO2ppmv
TSurfClim	32-bit floating-point	None	Surface temperature guess from climatology in Kelvins
TSurfAirClim	32-bit floating-point	None	Surface air temperature guess from climatology in Kelvins
TAirClim	32-bit floating-point	XtraPressureLev (= 100)	Air temperature guess from climatology in Kelvins
H2OCDClim	32-bit floating-point	XtraPressureLay (= 100)	Layer column water vapor guess from climatology (molecules / cm**2)
Tropo_CCI	32-bit floating-point	None	A Tropospheric Coarse Climate Indicator representing the weighted average of retrieved temperatures over the lower troposphere (maximum weight near 700 hPa). The weighting is done in such a manner as to make the weighted temperatures roughly correspond to those given by the MSU2R products in the Spencer and Christy temperature data set, as well as in the TOVS Pathfinder Path A data set (K)
Tropo_CCI_QC	16-bit unsigned integer	None	Quality Control for Tropo_CCI.; 0: Highest Quality; 1: Good Quality; 2: Do Not Use
Tropo_CCI_Est_Err	32-bit floating-point	None	Error estimate for Tropo_CCI
Strato_CCI	32-bit floating-point	None	A Stratospheric Coarse Climate Indicator representing the weighted average of retrieved temperatures over the lower stratosphere (maximum weight near 70 hPa). The weighting is done in such a manner as to make the weighted temperatures roughly correspond to those given by the

			MSU4 products in the Spencer and Christy temperature data set, as well as in the TOVS Pathfinder Path A data set (K)
Strato_CCI_QC	16-bit unsigned integer	None	Quality Control for Strato_CCI.; 0: Highest Quality; 1: Good Quality; 2: Do Not Use
Strato_CCI_Est_Err	32-bit floating-point	None	Error estimate for Strato_CCI
Quality Indicators for internal use in algorithm evaluation			
MoonInViewIR	16-bit integer	None	Flag if moon was in the spaceview for IR calibration. IR calibration will handle this case, but there may be a small degradation in radiance quality. (1: moon in spaceview, 0: moon not in spaceview, -9999: unknown)
pseudo_lapse_rate	32-bit floating-point	AIRSTrack (= 3) * AIRSXTrack (= 3)	Pseudo lapse rate is BT diff of channels 2109 and 2108 (K). Their frequencies are 2388 and 2387 cm-1, respectively. Low values within +/-45 degrees of equator usually indicate existence of cloud. Use with caution at higher latitudes.
TAirSCCNN	32-bit floating-point	XtraPressureLev (= 100)	Air temperature in Kelvins from SCCNN processing.
TAirCldyReg	32-bit floating-point	XtraPressureLev (= 100)	Air temperature in Kelvins from startup cloudy regression retrieval. (not used in retrieval)
H2OCDSCCNN	32-bit floating-point	XtraPressureLay (= 100)	Layer column water vapor from SCCNN processing. (molecules / cm**2)
H2OCDCldyReg	32-bit floating-point	XtraPressureLay (= 100)	Layer column water vapor from cloudy regression retrieval. (not used in retrieval) (molecules / cm**2)
TSurfSCCNN	32-bit floating-point	None	Surface temperature from SCCNN in Kelvins
TSurf1Ret	32-bit floating-point	None	Surface temperature after regression retrieval in Kelvins (not used in retrieval)
TSurfAir1Ret	32-bit floating-point	None	Surface air temperature after regression retrieval in Kelvins (not used in retrieval)
TAir1Ret	32-bit floating-point	XtraPressureLev (= 100)	Air temperature after regression retrieval in Kelvins (not used in retrieval)
H2OCD1Ret	32-bit floating-point	XtraPressureLay (= 100)	Layer column water vapor after regression retrieval (molecules / cm**2) (not used in retrieval)
O3CDInit	32-bit floating-point	XtraPressureLay (= 100)	preliminary Layer column ozone in molecules per cm**2 from initial regression step (not used in retrieval)

numHingeSurfFG	16-bit integer	None	Number of IR hinge points for first guess surface emissivity
freqEmisFG	32-bit floating-point	HingeSurf (= 100)	Frequencies for first guess surface emissivity in cm-1 (in order of increasing frequency. Only first numHingeSurfFG elements are valid)
emisIRFG	32-bit floating-point	HingeSurf (= 100)	First guess Spectral IR Surface Emissivities (in order of increasing frequency. Only first numHingeSurfFG elements are valid)
emisIRInit	32-bit floating-point	HingeSurfInit (= 50)	IR Surface Emissivities from initial regression (in order of increasing frequency. Only first numHingeSurfInit elements are valid) (not used in retrieval)
rhoIRInit	32-bit floating-point	HingeSurfInit (= 50)	IR Surface Reflectivities from initial regression (in order of increasing frequency. Only first numHingeSurfInit elements are valid) (not used in retrieval)
FracLandPlusIce	32-bit floating-point	None	Fraction of scene assumed by physical retrieval to be covered by land or ice
CldClearParam	32-bit floating-point	AIRSTrack (= 3) * AIRSXTrack (= 3)	Cloud clearing parameter Eta. Positive values are cloudier than average for the FOR, negative values are clearer.
CC1_Noise_Amp	32-bit floating-point	None	Internal retrieval quality indicator -- noise amplification factor from first cloud clearing because of extrapolation, dimensionless
Tsurf_4_CC1	32-bit floating-point	None	Internal retrieval quality indicator -- surface temperature used in first cloud clearing
TotCld_4_CC1	32-bit floating-point	None	Internal retrieval quality indicator -- total cloud fraction estimate before the first cloud clearing
CC1_RCode	32-bit integer	None	Internal retrieval quality indicator -- return code from first cloud clearing. Nonzero when code did not execute to completion due to internal computational checks. Most commonly due to ill-conditioned matrices resulting from inadequate information content in observations
CC2_RCode	32-bit integer	None	Internal retrieval quality indicator -- return code from second cloud clearing. Nonzero when code did not execute to completion due to internal computational checks. Most commonly due to ill-conditioned matrices resulting from inadequate information content in observations
Phys_RCode	32-bit integer	None	Internal retrieval quality indicator -- return code from physical retrieval. Nonzero when code did not execute to

			completion due to internal computational checks. Most commonly due to ill-conditioned matrices resulting from inadequate information content in observations
TotCld_below_500mb	32-bit floating-point	None	Internal retrieval quality indicator -- estimated final cloud fraction due only to clouds below 500 hPa (as seen from above), dimensionless between zero and one
Phys_resid_AMSUA	32-bit floating-point	ChanAMSUA (= 15)	Residual for AMSU-A channels after final retrieval (K)
Phys_resid_IR_window_790	32-bit floating-point	None	Residual for IR window channel near 790 cm**-1 after final retrieval (K) (No tuning applied because it is a surface channel)
Phys_resid_IR_window_844	32-bit floating-point	None	Residual for IR window channel near 844 cm**-1 after final retrieval (K) (No tuning applied because it is a surface channel)
Phys_resid_IR_window_917	32-bit floating-point	None	Residual for IR window channel near 917 cm**-1 after final retrieval (K) (No tuning applied because it is a surface channel)
Phys_resid_IR_window_1231	32-bit floating-point	None	Residual for IR window channel near 1231 cm**-1 after final retrieval (K) (No tuning applied because it is a surface channel)
Phys_resid_IR_window_2513	32-bit floating-point	None	Residual for IR window channel near 2513 cm**-1 after final retrieval (K) (No tuning applied because it is a surface channel)
Phys_resid_IR_window_2616	32-bit floating-point	None	Residual for IR window channel near 2616 cm**-1 after final retrieval (K) (No tuning applied because it is a surface channel)
CBTmOBT1231	32-bit floating-point	AIRSTrack (= 3) * AIRSXTrack (= 3)	End-to-end residual for window channel 1231.3 cm-1: computed cloudy brightness temperature for the retrieved atmospheric + cloud state minus angle-corrected observed L1B brightness temperature. (K)
CBTmOBT1231s	32-bit floating-point	AIRSTrack (= 3) * AIRSXTrack (= 3)	Variant of CBTmOBT1231 but using substitute surface properties if those were used in cloud retrieval (i.e. cases where cld_surf_fallback = 1) (K)
CC_noise_eff_amp_factor	32-bit floating-point	None	Effective amplification of noise in IR window channels due to extrapolation in cloud clearing and uncertainty of clear state. (< 1.0 for noise reduction, >1.0 for noise amplification, -9999.0 for unknown)

CC1_noise_eff_amp_factor	32-bit floating-point	None	Equivalent of CC_noise_eff_amp_factor but from the first attempt at cloud clearing
CC1_Resid	32-bit floating-point	None	Internal retrieval quality indicator -- residual between the first cloud cleared radiances for channels used in the determination and the radiances calculated from the best estimate of clear, in K
CCfinal_Resid	32-bit floating-point	None	Internal retrieval quality indicator -- residual between the final cloud cleared radiances for channels used in the determination and the radiances calculated from the best estimate of clear, in K
CCfinal_Noise_Amp	32-bit floating-point	None	Internal retrieval quality indicator -- noise amplification factor from cloud clearing because of extrapolation, dimensionless. Note: the name is misleading: this is the value after the second cloud clearing iteration, not the last.
Tdiff_IR_MW_ret	32-bit floating-point	None	Internal retrieval quality indicator -- layer mean difference in lower atmosphere between final IR temperature retrieval and the last internal MW-only temperature determination. High values suggest problems with MW or problems with cloud clearing.
Tdiff_IR_4CC1	32-bit floating-point	None	Internal retrieval quality indicator -- layer mean difference in lower atmosphere between final IR temperature retrieval and the temperature used in the first cloud clearing.
TSurfdiff_IR_4CC1	32-bit floating-point	None	Internal retrieval quality indicator -- absolute value of surface temperature difference between final IR retrieval and the surface temperature used as input in the first cloud clearing.
TSurfdiff_IR_4CC2	32-bit floating-point	None	Internal retrieval quality indicator -- absolute value of surface temperature difference between final IR retrieval and the surface temperature used as input in the second cloud clearing.
AMSU_Chans_Resid	32-bit floating-point	None	Internal retrieval quality indicator -- residual of selected AMSU channels (currently channel 5 only) against that calculated from the final IR retrieval state, K. High values suggest lower atmosphere retrieval disagrees with MW due to problems with MW or cloud clearing.

TotCld_4_CCfinal	32-bit floating-point	None	Internal retrieval quality indicator -- total cloud fraction estimated before final cloud clearing (as seen from above), dimensionless between zero and one
Surf_Resid_Ratio	32-bit floating-point	None	Internal retrieval quality indicator -- residuals of surface channels as compared to predicted uncertainty (dimensionless factor)
Temp_Resid_Ratio	32-bit floating-point	None	Internal retrieval quality indicator -- residuals of temperature channels as compared to predicted uncertainty (dimensionless factor)
Water_Resid_Ratio	32-bit floating-point	None	Internal retrieval quality indicator -- residuals of water channels as compared to predicted uncertainty (dimensionless factor)
Cloud_Resid_Ratio3x3	32-bit floating-point	AIRSTrack (= 3) * AIRSXTrack (= 3)	Internal retrieval quality indicator -- residuals of cloud channels as compared to predicted uncertainty (dimensionless factor)
Cloud_Resid_Ratio	32-bit floating-point	None	Internal retrieval quality indicator -- residuals of cloud channels as compared to predicted uncertainty (mean of 9 values in Cloud_Resid_Ratio3x3) (dimensionless factor)
O3_Resid_Ratio	32-bit floating-point	None	Internal retrieval quality indicator -- residuals of ozone channels as compared to predicted uncertainty (dimensionless factor)
CO_Resid_Ratio	32-bit floating-point	None	Internal retrieval quality indicator -- residuals of carbon monoxide channels as compared to predicted uncertainty (dimensionless factor)
CH4_Resid_Ratio	32-bit floating-point	None	Internal retrieval quality indicator -- residuals of methane channels as compared to predicted uncertainty (dimensionless factor)
MWCheck_Resid_Ratio	32-bit floating-point	None	Internal retrieval quality indicator -- residuals of channels used in MW check as compared to predicted uncertainty (dimensionless factor)
O3_Chan_Resid	32-bit floating-point	None	Internal retrieval quality indicator -- actual RMS brightness temperature residual for ozone channels used
Emis_Diagnostic_for_Ozone	32-bit floating-point	None	Internal retrieval quality indicator -- difference in emissivity at 1020 cm-1 hinge point from first guess to final retrieval minus average difference at 877 and 1204 cm-1 hinge points.
MaxOzoFcnChange	32-bit floating-point	None	Internal retrieval quality indicator -- largest desired ozone change in function in first iteration in second

			pass ozone retrieval, too large indicates incorrect initial state.
invalid	8-bit integer	None	No valid output (1: True, 0: False, 255/-1: Unknown)
MW_ret_used	8-bit integer	None	MW-only final retrieval used
bad_clouds	8-bit integer	None	invalid cloud parameters
Start_Clim	8-bit integer	None	Source of climatology used as initial state; 0: for None; 1: for NCEP/UARS; 2: for ECMWF land only; 3: for ECMWF sea only; 4: for ECMWF land + sea; 5: for ECMWF mixed surface fallback
Startup	8-bit integer	None	Source of startup input atmospheric state used in first cloud clearing step.; 0: MW-only retrieval; 1: IR-Only cloudy regression; 2: IR+MW cloudy regression, with some info from MW-only physical retrieval; 3: Climatology; 4: Neural Network
cld_surf_fallback	8-bit integer	None	cloud retrieval used a surface state from an earlier retrieval step
nchan_big_ang_adj	16-bit integer	None	The number of good chans with an angle adjustment over 20 * noise level in at least one of the 6 angle-adjusted IR FOVs.
bad_l1b	8-bit integer	None	Level 2 process not allowed due to bad level 1b data
bad_l1b_amsu	8-bit integer	None	Bad AMSU-A level 1b data
bad_l1b_hsb	8-bit integer	None	Bad HSB level 1b data
bad_l1b_airs	8-bit integer	None	Bad AIRS level 1b data
bad_l1b_vis	8-bit integer	None	Bad VIS level 1b data
forecast	8-bit integer	None	Complete forecast guess was used
no_psurf_guess	8-bit integer	None	No surface pressure was available. Topography was used for surf press
bad_temps	8-bit integer	None	invalid temp and surface skin temp
bad_h2o	8-bit integer	None	invalid water vapor profile
bad_o3	8-bit integer	None	invalid ozone profile
bad_co	8-bit integer	None	Invalid CO profile (profiles with bad_co = 1 had successful physical retrieval of CO but unsuccessful physical retrieval overall. These had

			climatology COCDSup. This value is no longer used. Profiles with bad_co = 2 have failed or not attempted physical CO retrieval and also have climatology in COCDSup)
no_tuning	8-bit integer	None	Standard br temp tuning NOT applied
no_ang_corr	8-bit integer	None	Standard angle correction NOT applied
no_mw	8-bit integer	None	MW only retrieval not attempted
no_initial	8-bit integer	None	First retrieval not attempted
no_final	8-bit integer	None	Final retrieval not attempted
mw_fpe	8-bit integer	None	floating-point exception in MW-Only retrieval step
cloudy_reg_fpe	8-bit integer	None	floating-point exception in cloudy regression retrieval step
initial_fpe	8-bit integer	None	floating-point exception in Initial retrieval step
final_fpe	8-bit integer	None	floating-point exception in Final retrieval step
MWPrecip	8-bit integer	None	Precipitation was detected over 0.5 mm/hr
MWsurf_T0	32-bit floating-point	None	low-frequency surface adjustment parameter -- T0
MWsurf_Tinf	32-bit floating-point	None	high-frequency surface adjustment parameter -- Tinfinity
MWsecant_ratio	32-bit floating-point	None	ratio of reflected to direct path length (only valid for mostly-water scenes)
MWseaice_conc	32-bit floating-point	None	Fraction of field-of-view with frozen covering. For predominately water areas (landFrac < 0.5, MWSurfClass = 3,4) MWseaice_conc refers to sea ice and MWseaice_conc range is [0.05 ... (1.0 - landFrac)]. For predominately land areas (landFrac >= 0.5, MWSurfClass = 5,6,7) MWseaice_conc refers to snow/glacier and MWseaice_conc range is [0.0 ... 1.0]. Frozen surface of the minority element of a coastal field-of-view is not accounted for. Other surface classes have MWseaice_conc=0.0
MWresidual_temp	32-bit floating-point	None	sum of squares of temperature residuals normalized by channel sensitivities
MWresidual_mois	32-bit floating-point	None	sum of squares of moisture residuals normalized by channel sensitivities

MWresidual_AMSUA	32-bit floating-point	ChanAMSUA (= 15)	Brightness temperature residual for each AMSU-A channel (Kelvin)
MWresidual_HSB	32-bit floating-point	ChanHSB (= 5)	brightness temperature residual for each HSB channel (Kelvin)
MWiter_temp	8-bit integer	None	# of iterations of the temperature profile
MWiter_mois	8-bit integer	None	# of iterations of the moisture profile
mw_ret_code	8-bit integer	None	Return code status of MW retrieval: values can be summed if more than one applies:; 0 All OK; 1 Moisture variables rejected by residual test; 2 Troposphere temperature profile rejected by residual test; 4 Excessive liquid water; 8 Insufficient valid channels; 16 Numerical error; 32 Emissivity > 1 for any AMSU-A channel; 64 Stratosphere temperature profile rejected by residual test; 128/-128 MW retrieval not attempted
sccnn_ret_code	8-bit integer	None	Return code status of startup neural net retrieval:; 0 All OK; 1 Problem encountered;
cloudy_reg_ret_code	8-bit integer	None	Return code status of startup cloudy regression retrieval: values can be summed if more than one applies:; 0 All OK; 1 Problem encountered; 16 Numerical error; 128/-128 Cloudy regression not attempted
Cloudy_Reg_FOV_chan	16-bit integer	None	Channel number (1-2378) of channel used to select from among the 9 IR FOVs the one to be used in cloudy regression (-9999 for N/A)
Cloudy_Reg_FOV	16-bit integer	None	FOV number of IR FOV used in cloudy regression (1-9, -9999 for N/A)
Cloudy_Reg_FOV_BT	32-bit floating-point	None	Brightness temperature for channel Cloudy_Reg_FOV_chan at FOV Cloudy_Reg_FOV (K, -9999 for N/A)
Cloudy_Reg_Score	32-bit floating-point	None	Indicator of how well the initial cloudy radiances match radiances reconstructed from cloudy eigenvectors. (Unitless ratio. should be ~1.0. >10.0 indicates a major problem)
cloud_ice	8-bit integer	None	Scattering by cloud ice present in FOV

icc_too_cloudy	8-bit integer	None	Initial cloud clearing pass too cloudy
icc_low_contrast	8-bit integer	None	Initial cloud clearing pass contrast too low
icc_bad_rad	8-bit integer	None	Initial cloud clearing pass cloud cleared radiances do not match clear guess - reject the IR retrieval
icc_contrast	32-bit floating-point	None	Initial cloud clearing contrast (units?)
bad_1st	8-bit integer	None	The initial retrieval failed
bad_1st_surf	8-bit integer	None	The initial surface retrieval failed
bad_1st_cc	8-bit integer	None	The first cloud clearing failed
bad_1st_regres	8-bit integer	None	The regression guess failed
bad_1st_phys	8-bit integer	None	The first physical retrieval failed
fcc_too_cloudy	8-bit integer	None	Final cloud clearing pass too cloudy
fcc_low_contrast	8-bit integer	None	Final cloud clearing pass contrast too low
fcc_bad_rad	8-bit integer	None	Final cloud clearing pass cloud cleared radiances do not match clear guess - reject the IR retrieval
fcc_contrast1	32-bit floating-point	None	Final cloud clearing contrast (units?) pass 1
fcc_contrast2	32-bit floating-point	None	Final cloud clearing contrast (units?) pass 2
bad_final	8-bit integer	None	Final retrieval failed
bad_final_cc	8-bit integer	None	final cloud clearing failed
bad_final_ir	8-bit integer	None	final IR retrieval failed
bad_final_surf	8-bit integer	None	final surface ret failed
bad_final_temp	8-bit integer	None	final temp ret failed
bad_final_h2o	8-bit integer	None	final water vapor ret failed
bad_final_o3	8-bit integer	None	final ozone ret failed
bad_final_cloud	8-bit integer	None	final cloud ret failed
bad_cc_cld_ret	8-bit integer	None	Cloud clearing and cloud ret are inconsistent
MW_IR_ret_differ	8-bit integer	None	Microwave and IR temperature retrieval differ too much - reject final IR retrieval

bad_MW_low_resid	8-bit integer	None	Microwave residuals in lower atmosphere too large - reject final IR retrieval
MW_low_atm_resid	32-bit floating-point	None	MW residual for lower atmosphere after final retrieval
final_AMSU_ret	8-bit integer	None	0 for success; 1 for did not converge; 2 for residual too large; 3 for retrieval step not attempted
final_HSB_ret	8-bit integer	None	0 for success; 1 for did not converge; 2 for residual too large; 3 for retrieval step not attempted
final_cloud_ret	8-bit integer	None	0 for success; 1 for did not converge; 2 for matrix inversion residual too large; 3 for retrieval step not attempted; 4 for singular matrix (unobservable quantity)
final_cloud_spot_ret3x3	8-bit integer	AIRSTrack (= 3) * AIRSXTrack (= 3)	0 for success; 1 for did not converge; 2 for matrix inversion residual too large; 3 for retrieval step not attempted; 4 for singular matrix (unobservable quantity)
final_surf_ret	8-bit integer	None	0 for success; 1 for did not converge; 2 for residual too large; 3 for retrieval step not attempted
final_temp_ret	8-bit integer	None	0 for success; 1 for did not converge; 2 for residual too large; 3 for retrieval step not attempted
final_h2o_ret	8-bit integer	None	0 for success; 1 for did not converge; 2 for residual too large; 3 for retrieval step not attempted
final_o3_ret	8-bit integer	None	0 for success; 1 for did not converge; 2 for residual too large; 3 for retrieval step not attempted
final_ch4_ret	8-bit integer	None	0 for success; 1 for did not converge; 2 for residual too large; 3 for retrieval step not attempted
final_co_ret	8-bit integer	None	0 for success; 1 for did not converge; 2 for residual too large; 3 for retrieval step not attempted
final_co2_ret	8-bit integer	None	0 for success; 1 for did not converge;

			2 for residual too large; 3 for retrieval step not attempted
bad_vis_rad	8-bit integer	None	Vis/NIR radiance out of range
bad_vis_cal	8-bit integer	None	Vis/NIR calibration data old or invalid
bad_vis_det_temp	8-bit integer	None	Vis/NIR Detector temperature out of range
bad_scan_hd_temp	8-bit integer	None	Scan Head Assembly temperature out of range
Initial_CC_score	32-bit floating-point	None	Indicator of how well the initial cloud-cleared radiances match radiances reconstructed from clear eigenvectors. (Unitless ratio); 0.33 is best possible, a 3X noise reduction; <0.8 for a very good match; <3.0 for a pretty good match; >10.0 indicates a major problem
Initial_CC_subscores	32-bit floating-point	ScoresBand (= 10)	Sub-scores contributing to Initial_CC_score, by frequency band
sccnn_bt_corr	32-bit floating-point	SccnnBtCorr (= 2)	Quality indicator based on amount of cloud clearing in the internal CC of the SCCNN algorithm. Lower absolute values are better. (K)
sccnn_bt_corr_freq	32-bit floating-point	SccnnBtCorr (= 2)	Frequencies of channels used to compute sccnn_bt_corr (cm-1)
relayer_num_nonpos_coef_h2o	32-bit integer	None	Internal indicator from relayering of water vapor: # of spline coefficients <= 0.0 -1 if LSQ problem fails.
relayer_num_nonpos_coef_o3	32-bit integer	None	Internal indicator from relayering of ozone vapor: # of spline coefficients <= 0.0 -1 if LSQ problem fails.
relayer_num_nonpos_coef_co	32-bit integer	None	Internal indicator from relayering of carbon monoxide: # of spline coefficients <= 0.0 -1 if LSQ problem fails.
relayer_num_nonpos_coef_ch4	32-bit integer	None	Internal indicator from relayering of methane: # of spline coefficients <= 0.0 -1 if LSQ problem fails.
relayer_num_knots	32-bit integer	None	Internal indicator from relayering of gases: # of knots in spline
relayer_degree	32-bit integer	None	Internal indicator from relayering of gases: Degree of spline. Nominally 4 for cubic.
relayer_runge_kutta_bits	32-bit integer	None	Internal indicator from relayering of gases: for temperature mass layer integrator, bit-mapped diagnostics of Runge-Kutta integrator; 0 - successful return; 2nd bit - Soft Error: This is being used inefficiently because the step size has been reduced drastically many times

			to get answers at many points.; 3rd bit - Soft Error: A considerable amount of work has been expended in the (primary) integration.; 4th bit - Soft Error: It appears that this problem is "stiff". ; 5th bit - Hard Error: It does not appear possible to achieve the accuracy specified by TOL and THRES; 6th bit - Hard Error: The global error assessment may not be reliable beyond the current integration point.
Num_Fill_Chan_Cloudy_Reg	16-bit integer	None	Number of channels the cloudy regression processing step determined to be of low quality and calculated substitute values for before proceeding.
Num_Fill_Chan_SCCNN	16-bit integer	None	Number of channels the SCCNN processing step determined to be of low quality and calculated substitute values for before proceeding.
Num_Fill_Chan_Ang_Adj	16-bit integer	None	Number of channels the local angle adjustment processing step determined to be of low quality and calculated substitute values for before proceeding.
Doppler_shift_ppm	32-bit floating-point	None	Doppler shift for this footprint in parts per million.
spectral_clear_indicator	16-bit integer	AIRSTrack (= 3) * AIRSXTrack (= 3)	Flag telling whether scene was flagged as clear by a spectral filter. Only ocean filter is validated; 2: Ocean test applied and scene identified as clear; 1: Ocean test applied and scene not identified as clear; 0: Calculation could not be completed. Possibly some inputs were missing or FOV is on coast or on the edge of a scan or granule; -1: Unvalidated land test applied and scene not identified as clear; -2: Unvalidated land test applied and scene identified as clear
num_clear_spectral_indicator	16-bit integer	None	Number of 9 IR FOVs which are clear according to spectral_clear_indicator. -1 when the spectral clear indicator could not be applied to any of the spots. Note that the spectral clear indicator is not validated for land scenes.

A3: L2 Standard Cloud Cleared Radiance Product Interface Specification

Interface Specification Version 7.0.1.0
2019-12-04

ESDT ShortNames = "AIRI2CCF"", “AIRS2CCF”, “AIRH2CCF”

Swath Name = "L2_Standard_cloud-cleared_radiance_product"

Level = "Level2"

Footprints = 30

scanlines per scanset = 1

Dimensions

These fields define all dimensions that can be used for HDF-EOS swath fields.

The names "GeoTrack" and "GeoXTrack" have a special meaning for this document: "Cross-Track" data fields have a hidden dimension of "GeoXTrack"; "Along-Track" data fields have a hidden dimension of "GeoTrack"; "Full Swath Data Fields have hidden dimensions of both "GeoTrack" and "GeoXTrack".

Name	Value	Explanation
GeoXTrack	30	Dimension across track for footprint positions. Same as number of footprints per scanline. -- starting at the left and increasing towards the right as you look along the satellite's path
GeoTrack	# of scan lines in swath	Dimension along track for footprint positions. Same as number of scanlines in granule. Parallel to the satellite's path, increasing with time. (Nominally 45)
Channel	2378	Dimension of channel array (Channels are generally in order of increasing wavenumber, but because frequencies can vary and because all detectors from a physical array of detector elements (a "module") are always grouped together there are sometimes small reversals in frequency order where modules overlap.)
AIRSXTrack	3	The number of AIRS cross-track spots per AMSU-A spot. Direction is the same as GeoXTrack -- starting at the left and increasing towards the right as you look along the satellite's path
AIRSTrack	3	The number of AIRS along-track spots per AMSU-A spot. Direction is the same as GeoTrack -- parallel to the satellite's path, increasing with time
Module	17	Number of modules on the focal plane in which airs channels are grouped. The order is M-01a, M-02a, M-01b, M-02b, M-04d, M-04c, M-03, M-04b, M-04a, M-05, M-06, M-07, M-08, M-09, M-10, M-11, M-12.

Geolocation Fields

These fields appear for every footprint (GeoTrack * GeoXTrack times) and correspond to footprint center coordinates and "shutter" time.

Name	Explanation
Latitude	Footprint boresight geodetic Latitude in degrees North (-90.0 ... 90.0)
Longitude	Footprint boresight geodetic Longitude in degrees East (-180.0 ... 180.0)

Time	Footprint "shutter" TAI Time: floating-point elapsed seconds since Jan 1, 1993

Attributes

These fields appear only once per granule and use the HDF-EOS "Attribute" interface

Name	Type	Explanation
processing_level	string of 8-bit characters	Zero-terminated character string denoting processing level ("Level2")
instrument	string of 8-bit characters	Zero-terminated character string denoting instrument ("AIRS")
DayNightFlag	string of 8-bit characters	Zero-terminated character string set to "Night" when the subsatellite points at the beginning and end of a granule are both experiencing night according to the "civil twilight" standard (center of refracted sun is below the horizon). It is set to "Day" when both are experiencing day, and "Both" when one is experiencing day and the other night. "NA" is used when a determination cannot be made.
AutomaticQAFlag	string of 8-bit characters	Zero-terminated character string denoting granule data quality: (Always "Passed", "Failed", or "Suspect")
NumTotalData	32-bit integer	Total number of expected scene footprints
NumProcessData	32-bit integer	Number of scene footprints which are present and can be processed routinely (state = 0)
NumSpecialData	32-bit integer	Number of scene footprints which are present and can be processed only as a special test (state = 1)
NumBadData	32-bit integer	Number of scene footprints which are present but cannot be processed (state = 2)
NumMissingData	32-bit integer	Number of expected scene footprints which are not present (state = 3)
NumLandSurface	32-bit integer	Number of scene footprints for which the surface is more than 90% land
NumOceanSurface	32-bit integer	Number of scene footprints for which the surface is less than 10% land
node_type	string of 8-bit characters	Zero-terminated character string denoting whether granule is ascending, descending, or pole-crossing: ("Ascending" and "Descending" for entirely ascending or entirely descending granules, or "NorthPole" or "SouthPole" for pole-crossing granules. "NA" when determination cannot be made.)
start_year	32-bit integer	Year in which granule started, UTC (e.g. 1999)
start_month	32-bit integer	Month in which granule started, UTC (1 ... 12)
start_day	32-bit integer	Day of month in which granule started, UTC (1 ... 31)
start_hour	32-bit integer	Hour of day in which granule started, UTC (0 ... 23)
start_minute	32-bit integer	Minute of hour in which granule started, UTC (0 ... 59)
start_sec	32-bit floating-point	Second of minute in which granule started, UTC (0.0 ... 59.0)

start_orbit	32-bit integer	Orbit number of mission in which granule started
end_orbit	32-bit integer	Orbit number of mission in which granule ended
orbit_path	32-bit integer	Orbit path of start orbit (1 ... 233 as defined by EOS project)
start_orbit_row	32-bit integer	Orbit row at start of granule (1 ... 248 as defined by EOS project)
end_orbit_row	32-bit integer	Orbit row at end of granule (1 ... 248 as defined by EOS project)
granule_number	32-bit integer	Number of granule within day (1 ... 240)
num_scansets	32-bit integer	Number of scansets in granule (1 ... 45)
num_scanlines	32-bit integer	Number of scanlines in granule (3 * num_scansets)
start_Latitude	64-bit floating-point	Geodetic Latitude of spacecraft at start of granule (subsatellite location at midpoint of first scan) in degrees North (-90.0 ... 90.0)
start_Longitude	64-bit floating-point	Geodetic Longitude of spacecraft at start of granule (subsatellite location at midpoint of first scan) in degrees East (-180.0 ... 180.0)
start_Time	64-bit floating-point	TAI Time at start of granule (floating-point elapsed seconds since start of 1993)
end_Latitude	64-bit floating-point	Geodetic Latitude of spacecraft at end of granule (subsatellite location at midpoint of last scan) in degrees North (-90.0 ... 90.0)
end_Longitude	64-bit floating-point	Geodetic Longitude of spacecraft at end of granule (subsatellite location at midpoint of last scan) in degrees East (-180.0 ... 180.0)
end_Time	64-bit floating-point	TAI Time at end of granule (floating-point elapsed seconds since start of 1993)
eq_x_longitude	32-bit floating-point	Longitude of spacecraft at southward equator crossing nearest granule start in degrees East (-180.0 ... 180.0)
eq_x_tai	64-bit floating-point	Time of eq_x_longitude in TAI units (floating-point elapsed seconds since start of 1993)
LonGranuleCen	16-bit integer	Geodetic Longitude of the center of the granule in degrees East (-180 ... 180)
LatGranuleCen	16-bit integer	Geodetic Latitude of the center of the granule in degrees North (-90 ... 90)
LocTimeGranuleCen	16-bit integer	Local solar time at the center of the granule in minutes past midnight (0 ... 1439)
num_fpe	16-bit integer	Number of floating point errors
orbitgeoqa	32-bit unsigned integer	Orbit Geolocation QA:; Bit 0: (LSB, value 1) bad input value (last scanline); Bit 1: (value 2) bad input value (first scanline); Bit 2: (value 4) PGS_EPH_GetEphMet() gave PGSEPH_E_NO_SC_EPHEM_FILE; Bit 3: (value 8) PGS_EPH_GetEphMet() gave PGSEPH_E_BAD_ARRAY_SIZE;

		Bit 4: (value 16) PGS_EPH_GetEphMet() gave PGSTD_E_TIME_FMT_ERROR; Bit 5: (value 32) PGS_EPH_GetEphMet() gave PGSTD_E_TIME_VALUE_ERROR; Bit 6: (value 64) PGS_EPH_GetEphMet() gave PGSTD_E_SC_TAG_UNKNOWN; Bit 7: (value 128) PGS_EPH_GetEphMet() gave PGS_E_TOOLKIT; Bit 8: (value 256) PGS_TD_UTCtoTAI() gave PGSTD_E_NO_LEAP_SECS; Bit 9: (value 512) PGS_TD_UTCtoTAI() gave PGSTD_E_TIME_FMT_ERROR; Bit 10: (value 1024) PGS_TD_UTCtoTAI() gave PGSTD_E_TIME_VALUE_ERROR; Bit 11: (value 2048) PGS_TD_UTCtoTAI() gave PGS_E_TOOLKIT; Bit 12: (value 4096) PGS_CSC_DayNight() gave PGSTD_E_NO_LEAP_SECS; Bit 13: (value 8192) PGS_CSC_DayNight() gave PGSCSC_E_INVALID_LIMITTAG; Bit 14: (value 16384) PGS_CSC_DayNight() gave PGSCSC_E_BAD_ARRAY_SIZE; Bit 15: (value 32768) PGS_CSC_DayNight() gave PGSCSC_W_ERROR_IN_DAYNIGHT; Bit 16: (value 65536) PGS_CSC_DayNight() gave PGSCSC_W_BAD_TRANSFORM_VALUE; Bit 17: (value 131072) PGS_CSC_DayNight() gave PGSCSC_W_BELOW_HORIZON; Bit 18: (value 262144) PGS_CSC_DayNight() gave PGSCSC_W_PREDICTED_UT1 (This is expected except when reprocessing.); Bit 19: (value 524288) PGS_CSC_DayNight() gave PGSTD_E_NO_UT1_VALUE; Bit 20: (value 1048576) PGS_CSC_DayNight() gave PGSTD_E_BAD_INITIAL_TIME; Bit 21: (value 2097152) PGS_CSC_DayNight() gave PGSCBP_E_TIME_OUT_OF_RANGE; Bit 22: (value 4194304) PGS_CSC_DayNight() gave PGSCBP_E_UNABLE_TO_OPEN_FILE; Bit 23: (value 8388608) PGS_CSC_DayNight() gave PGSMEM_E_NO_MEMORY; Bit 24: (value 16777216) PGS_CSC_DayNight() gave PGS_E_TOOLKIT; Bit 25-31: not used
num_satgeoqa	16-bit integer	Number of scans with problems in satgeoqa
num_glintgeoqa	16-bit integer	Number of scans with problems in glintgeoqa
num_moongeoqa	16-bit integer	Number of scans with problems in moongeoqa
num_ftptgeoqa	16-bit integer	Number of footprints with problems in ftptgeoqa
num_zengeoqa	16-bit integer	Number of footprints with problems in zengeoqa
num_demgeoqa	16-bit integer	Number of footprints with problems in demgeoqa

CalGranSummary	8-bit unsigned integer	Bit field. Bitwise OR of CalChanSummary, over all channels with ExcludedChans < 3.; Zero means all these channels were well calibrated, for all scanlines.; Bit 7: (MSB, value 128) scene over/underflow; Bit 6: (value 64) anomaly in offset calculation; Bit 5: (value 32) anomaly in gain calculation; Bit 4: (value 16) pop detected with no offset anomaly; Bit 3: (value 8) noise out of bounds; Bit 2: (value 4) anomaly in spectral calibration; Bit 1: (value 2) Telemetry; Bit 0: (LSB, value 1) unused (reserved);
DCR_scan	16-bit integer	Level-1B scanline number following (first) DC-Restore. 0 for no DC-Restore. DCR_scan refers to Level-1 8/3-second scans, not Level-2 8-second scansets. DCR_scan = 1 refers to an event before the first scan of the first scanset. DCR_scan = 2 or 3 refer to events within the first scanset, DCR_scan = 4 to events between the first and second scansets.
granules_present_L1B	string of 8-bit characters	Zero-terminated character string denoting which adjacent granules were available for smoothing during Level-1B calibration processing. ("All" for both previous & next, "Prev" for previous but not next, "Next" for next but not previous, "None" for neither previous nor next)

Per-Granule Data Fields

These fields appear only once per granule and use the HDF-EOS "Field" interface

Name	Type	Extra Dimensions	Explanation
nominal_freq	32-bit floating-point	Channel (= 2378)	Nominal frequencies (in cm**-1) of each channel
CalChanSummary	8-bit unsigned integer	Channel (= 2378)	Bit field. Bitwise OR of CalFlag, by channel, over all scanlines. Noise threshold and spectral quality added.; Zero means the channel was well calibrated for all scanlines; Bit 7 (MSB): scene over/underflow; Bit 6: (value 64) anomaly in offset calculation; Bit 5: (value 32) anomaly in gain calculation; Bit 4: (value 16) pop detected with no offset anomaly; Bit 3: (value 8) noise out of bounds; Bit 2: (value 4) anomaly in spectral calibration; Bit 1: (value 2) Telemetry; Bit 0: (LSB, value 1) unused (reserved);
ExcludedChans	8-bit unsigned integer	Channel (= 2378)	An integer 0-6, indicating A/B detector weights. Used in L1B processing.; 0 - A weight = B weight. Probably better that channels with state > 2; 1 - A-side only. Probably better that channels with state > 2; 2 - B-side only. Probably better that channels with state > 2; 3 - A weight = B weight. Probably better than channels with state = 6;

			4 - A-side only. Probably better than channels with state = 6; 5 - B-side only. Probably better than channels with state = 6; 6 - Has anomalous gain performance. Probably not usable.
NeN_L1B	32-bit floating-point	Channel (= 2378)	Level-1B Noise-equivalent Radiance (radiance units) for an assumed 250K scene. Note that effective noise on cloud-cleared radiances will be modified.
NeN_L1B_Static	32-bit floating-point	Channel (= 2378)	Expected Noise-equivalent Radiance (radiance units) for an assumed 250K scene. This static estimate comes from a channel properties file and reflects nominal conditions for an epoch of months. It is a more stable value than NeN_L1B but does not reflect recent or transient changes to noise levels.

Along-Track Data Fields

These fields appear once per scanline (GeoTrack times)

Name	Type	Extra Dimensions	Explanation
satheight	32-bit floating-point	None	Satellite altitude at nadirTAI in km above reference ellipsoid (e.g. 725.2)
satroll	32-bit floating-point	None	Satellite attitude roll angle at nadirTAI (-180.0 ... 180.0 angle about the +x (roll) ORB axis, +x axis is positively oriented in the direction of orbital flight completing an orthogonal triad with y and z.)
satpitch	32-bit floating-point	None	Satellite attitude pitch angle at nadirTAI (-180.0 ... 180.0 angle about +y (pitch) ORB axis. +y axis is oriented normal to the orbit plane with the positive sense opposite to that of the orbit's angular momentum vector H.)
satyaw	32-bit floating-point	None	Satellite attitude yaw angle at nadirTAI (-180.0 ... 180.0 angle about +z (yaw) axis. +z axis is positively oriented Earthward parallel to the satellite radius vector R from the spacecraft center of mass to the center of the Earth.)
glintlat	32-bit floating-point	None	Solar glint geodetic latitude in degrees North at nadirTAI (-90.0 ... 90.0)
glintlon	32-bit floating-point	None	Solar glint geodetic longitude in degrees East at nadirTAI (-180.0 ... 180.0)
nadirTAI	64-bit floating-point	None	TAI time at which instrument is nominally looking directly down. (between footprints 15 & 16 for AMSU or between footprints 45 & 46 for AIRS/Vis & HSB) (floating-point elapsed seconds since start of 1993)
sat_lat	64-bit floating-point	None	Satellite geodetic latitude in degrees North (-90.0 ... 90.0)
sat_lon	64-bit floating-point	None	Satellite geodetic longitude in degrees East (-180.0 ... 180.0)

scan_node_type	8-bit integer	None	'A' for ascending, 'D' for descending, 'E' when an error is encountered in trying to determine a value.
satgeoqa	32-bit unsigned integer	None	Satellite Geolocation QA flags:; Bit 0: (LSB, value 1) bad input value; Bit 1: (value 2) PGS_TD_TAItoUTC() gave PGSTD_E_NO_LEAP_SECS; Bit 2: (value 4) PGS_TD_TAItoUTC() gave PGS_E_TOOLKIT; Bit 3: (value 8) PGS_EPH_EphemAttit() gave PGSEPH_W_BAD_EPHEM_VALUE; Bit 4: (value 16) PGS_EPH_EphemAttit() gave PGSEPH_E_BAD_EPHEM_FILE_HDR; Bit 5: (value 32) PGS_EPH_EphemAttit() gave PGSEPH_E_NO_SC_EPHEM_FILE; Bit 6: (value 64) PGS_EPH_EphemAttit() gave PGSEPH_E_NO_DATA_REQUESTED; Bit 7: (value 128) PGS_EPH_EphemAttit() gave PGSTD_E_SC_TAG_UNKNOWN; Bit 8: (value 256) PGS_EPH_EphemAttit() gave PGSEPH_E_BAD_ARRAY_SIZE; Bit 9: (value 512) PGS_EPH_EphemAttit() gave PGSTD_E_TIME_FMT_ERROR; Bit 10: (value 1024) PGS_EPH_EphemAttit() gave PGSTD_E_TIME_VALUE_ERROR; Bit 11: (value 2048) PGS_EPH_EphemAttit() gave PGSTD_E_NO_LEAP_SECS; Bit 12: (value 4096) PGS_EPH_EphemAttit() gave PGS_E_TOOLKIT; Bit 13: (value 8192) PGS_CSC_ECItoECR() gave PGSCSC_W_BAD_TRANSFORM_VALUE; Bit 14: (value 16384) PGS_CSC_ECItoECR() gave PGSCSC_E_BAD_ARRAY_SIZE; Bit 15: (value 32768) PGS_CSC_ECItoECR() gave PGSTD_E_NO_LEAP_SECS; Bit 16: (value 65536) PGS_CSC_ECItoECR() gave PGSTD_E_TIME_FMT_ERROR; Bit 17: (value 131072) PGS_CSC_ECItoECR() gave PGSTD_E_TIME_VALUE_ERROR; Bit 18: unused (set to zero); Bit 19: (value 524288) PGS_CSC_ECItoECR() gave PGSTD_E_NO_UT1_VALUE; Bit 20: (value 1048576) PGS_CSC_ECItoECR() gave PGS_E_TOOLKIT; Bit 21: (value 2097152) PGS_CSC_ECRtoGEO() gave PGSCSC_W_TOO_MANY_ITERS; Bit 22: (value 4194304) PGS_CSC_ECRtoGEO() gave PGSCSC_W_INVALID_ALTITUDE; Bit 23: (value 8388608) PGS_CSC_ECRtoGEO() gave PGSCSC_W_SPHERE_BODY; Bit 24: (value 16777216) PGS_CSC_ECRtoGEO() gave PGSCSC_W_LARGE_FLATTENING; Bit 25: (value 33554432) PGS_CSC_ECRtoGEO() gave PGSCSC_W_DEFAULT_EARTH_MODEL; Bit 26: (value 67108864) PGS_CSC_ECRtoGEO() gave PGSCSC_E_BAD_EARTH_MODEL; Bit 27: (value 134217728) PGS_CSC_ECRtoGEO()

			gave PGS_E_TOOLKIT; Bit 28-31: not used
glintgeoqa	16-bit unsigned integer	None	Glint Geolocation QA flags:; Bit 0: (LSB, value 1) bad input value; Bit 1: (value 2) glint location in Earth's shadow (Normal for night FOVs); Bit 2: (value 4) glint calculation not converging; Bit 3: (value 8) glint location sun vs. satellite zenith mismatch; Bit 4: (value 16) glint location sun vs. satellite azimuth mismatch; Bit 5: (value 32) bad glint location; Bit 6: (value 64) PGS_CSC_ZenithAzimuth() gave any 'W' class return code; Bit 7: (value 128) PGS_CSC_ZenithAzimuth() gave any 'E' class return code; Bit 8: (value 256) PGS_CBP_Earth_CB_Vector() gave any 'W' class return code; Bit 9: (value 512) PGS_CBP_Earth_CB_Vector() gave any 'E' class return code; Bit 10: (value 1024) PGS_CSC_ECItoECR() gave any 'W' class return code except PGSCSC_W_PREDICTED_UT1 (for Glint); Bit 11: (value 2048) PGS_CSC_ECItoECR() gave any 'E' class return code (for Glint); Bit 12: (value 4096) PGS_CSC_ECRtoGEO() gave any 'W' class return code (for Glint); Bit 13: (value 8192) PGS_CSC_ECRtoGEO() gave any 'E' class return code (for Glint); Bit 14: (value 16384) PGS_CSC_ECItoECR() gave any 'W' class return code except PGSCSC_W_PREDICTED_UT1 ; Bit 15: (value 32768) PGS_CSC_ECItoECR() gave any 'E' class return code
moongeoqa	16-bit unsigned integer	None	Moon Geolocation QA flags:; Bit 0: (LSB, value 1) bad input value; Bit 1: (value 2) PGS_TD_TAItoUTC() gave PGSTD_E_NO_LEAP_SECS; Bit 2: (value 4) PGS_TD_TAItoUTC() gave PGS_E_TOOLKIT; Bit 3: (value 8) PGS_CBP_Sat_CB_Vector() gave PGSCSC_W_BELOW_SURFACE; Bit 4: (value 16) PGS_CBP_Sat_CB_Vector() gave PGSCBP_W_BAD_CB_VECTOR; Bit 5: (value 32) PGS_CBP_Sat_CB_Vector() gave PGSCBP_E_BAD_ARRAY_SIZE; Bit 6: (value 64) PGS_CBP_Sat_CB_Vector() gave PGSCBP_E_INVALID_CB_ID; Bit 7: (value 128) PGS_CBP_Sat_CB_Vector() gave PGSMEM_E_NO_MEMORY; Bit 8: (value 256) PGS_CBP_Sat_CB_Vector() gave PGSCBP_E_UNABLE_TO_OPEN_FILE; Bit 9: (value 512) PGS_CBP_Sat_CB_Vector() gave PGSTD_E_BAD_INITIAL_TIME; Bit 10: (value 1024) PGS_CBP_Sat_CB_Vector() gave PGSCBP_E_TIME_OUT_OF_RANGE;

			Bit 11: (value 2048) PGS_CBP_Sat_CB_Vector() gave PGSTD_E_SC_TAG_UNKNOWN; Bit 12: (value 4096) PGS_CBP_Sat_CB_Vector() gave PGSEPH_E_BAD_EPHEM_FILE_HDR; Bit 13: (value 8192) PGS_CBP_Sat_CB_Vector() gave PGSEPH_E_NO_SC_EPHEM_FILE; Bit 14: (value 16384) PGS_CBP_Sat_CB_Vector() gave PGS_E_TOOLKIT; Bit 15: not used
CalFlag	8-bit unsigned integer	Channel (= 2378)	Bit field, by channel, for calibration the current scanset.; Zero means the channel was well calibrated, for this scanset.; Bit 7: (MSB, value 128) scene over/underflow; Bit 6: (value 64) anomaly in offset calculation; Bit 5: (value 32) anomaly in gain calculation; Bit 4: (value 16) pop detected; Bit 3: (value 8) DCR Occurred; Bit 2: (value 4) Moon in View; Bit 1: (value 2) telemetry out of limit condition; Bit 0: (LSB, value 1) cold scene noise
CalScanSummary	8-bit unsigned integer	None	Bit field. Bitwise OR of CalFlag over the good channel list (see ExcludedChans).; Zero means all "good" channels were well calibrated for this scanset; Bit 7: (MSB, value 128) scene over/underflow; Bit 6: (value 64) anomaly in offset calculation; Bit 5: (value 32) anomaly in gain calculation; Bit 4: (value 16) pop detected; Bit 3: (value 8) DCR Occurred; Bit 2: (value 4) Moon in View; Bit 1: (value 2) telemetry out of limit condition; Bit 0: (LSB, value 1) cold_scene noise
orbit_phase_deg	32-bit floating-point	None	Orbit phase in degrees. 0.0 is nighttime equator crossing. 90.0 is near the south pole. 180.0 is near the daytime equator crossing. 270.0 is near the north pole. [0.0, 360.0]
shift_y0	32-bit floating-point	Module (= 17)	Focal plane shift in the y (spectral dispersion) direction relative to prelaunch nominal. (microns)
scan_freq	32-bit floating-point	Channel (= 2378)	Dynamic frequencies (in cm**-1) of each channel for each scan

Full Swath Data Fields

These fields appear for every footprint of every scanline in the granule (GeoTrack * GeoXTrack times)

Name	Type	Extra Dimensions	Explanation
radiances	32-bit floating-point	Channel (= 2378)	Cloud-cleared radiances for each channel in milliWatts/m**2/cm**-1/steradian
radiances_QC	16-bit unsigned integer	Channel (= 2378)	Quality Control for radiances.; 0: Highest Quality; 1: Good Quality; 2: Do Not Use

radiance_err	32-bit floating-point	Channel (= 2378)	Error estimate for radiances (milliWatts/m**2/cm**-1/steradian)
CldClearParam	32-bit floating-point	AIRSTrack (= 3) * AIRSXTrack (= 3)	Cloud clearing parameter Eta. Positive values are cloudier than average for the FOR, negative values are clearer.
scanang	32-bit floating-point	None	Scanning angle of the central AIRS instrument field-of-view with respect to the spacecraft (-180.0 ... 180.0, negative at start of scan, 0 at nadir)
satzen	32-bit floating-point	None	Spacecraft zenith angle (0.0 ... 180.0) degrees from zenith (measured relative to the geodetic vertical on the reference (WGS84) spheroid and including corrections outlined in EOS SDP toolkit for normal accuracy.)
satazi	32-bit floating-point	None	Spacecraft azimuth angle (-180.0 ... 180.0) degrees E of N GEO)
solzen	32-bit floating-point	None	Solar zenith angle (0.0 ... 180.0) degrees from zenith (measured relative to the geodetic vertical on the reference (WGS84) spheroid and including corrections outlined in EOS SDP toolkit for normal accuracy.)
solazi	32-bit floating-point	None	Solar azimuth angle (-180.0 ... 180.0) degrees E of N GEO)
sun_glint_distance	16-bit integer	None	Distance (km) from footprint center to location of the sun glint (-9999 for unknown, 30000 for no glint visible because spacecraft is in Earth's shadow)
topog	32-bit floating-point	None	Mean topography in meters above reference ellipsoid
topog_err	32-bit floating-point	None	Error estimate for topog
landFrac	32-bit floating-point	None	Fraction of spot that is land (0.0 ... 1.0)
landFrac_err	32-bit floating-point	None	Error estimate for landFrac
ftptgeoqa	32-bit unsigned integer	None	Footprint Geolocation QA flags:; Bit 0: (LSB, value 1) bad input value; Bit 1: (value 2) PGS_TD_TAItoUTC() gave PGSTD_E_NO_LEAP_SECS; Bit 2: (value 4) PGS_TD_TAItoUTC() gave PGS_E_TOOLKIT; Bit 3: (value 8) PGS_CSC_GetFOV_Pixel() gave PGSCSC_W_MISS_EARTH; Bit 4: (value 16) PGS_CSC_GetFOV_Pixel() gave PGSTD_E_SC_TAG_UNKNOWN; Bit 5: (value 32) PGS_CSC_GetFOV_Pixel() gave

			PGSCSC_W_ZERO_PIXEL_VECTOR; Bit 6: (value 64) PGS_CSC_GetFOV_Pixel() gave PGSCSC_W_BAD_EPH_FOR_PIXEL; Bit 7: (value 128) PGS_CSC_GetFOV_Pixel() gave PGSCSC_W_INSTRUMENT_OFF_BOARD; Bit 8: (value 256) PGS_CSC_GetFOV_Pixel() gave PGSCSC_W_BAD_ACCURACY_FLAG; Bit 9: (value 512) PGS_CSC_GetFOV_Pixel() gave PGSCSC_E_BAD_ARRAY_SIZE; Bit 10: (value 1024) PGS_CSC_GetFOV_Pixel() gave PGSCSC_W_DEFAULT_EARTH_MODEL; Bit 11: (value 2048) PGS_CSC_GetFOV_Pixel() gave PGSCSC_W_DATA_FILE_MISSING; Bit 12: (value 4096) PGS_CSC_GetFOV_Pixel() gave PGSCSC_E_NEG_OR_ZERO_RAD; Bit 13: (value 8192) PGS_CSC_GetFOV_Pixel() gave PGSMEM_E_NO_MEMORY; Bit 14: (value 16384) PGS_CSC_GetFOV_Pixel() gave PGSTD_E_NO_LEAP_SECS; Bit 15: (value 32768) PGS_CSC_GetFOV_Pixel() gave PGSTD_E_TIME_FMT_ERROR; Bit 16: (value 65536) PGS_CSC_GetFOV_Pixel() gave PGSTD_E_TIME_VALUE_ERROR; Bit 17: (value 131072) PGS_CSC_GetFOV_Pixel() gave PGSCSC_W_PREDICTED_UT1; Bit 18: (value 262144) PGS_CSC_GetFOV_Pixel() gave PGSTD_E_NO_UT1_VALUE; Bit 19: (value 524288) PGS_CSC_GetFOV_Pixel() gave PGS_E_TOOLKIT; Bit 20: (value 1048576) PGS_CSC_GetFOV_Pixel() gave PGSEPH_E_BAD_EPHEM_FILE_HDR; Bit 21: (value 2097152) PGS_CSC_GetFOV_Pixel() gave PGSEPH_E_NO_SC_EPHEM_FILE; Bit 22-31: not used
zengeoqa	16-bit unsigned integer	None	Satellite zenith Geolocation QA flags:; Bit 0: (LSB, value 1) (Spacecraft) bad input value; Bit 1: (value 2) PGS_CSC_ZenithAzimuth(S/C) gave PGSCSC_W_BELOW_HORIZON;

			Bit 2: (value 4) PGS_CSC_ZenithAzimuth(S/C) gave PGSCSC_W_UNDEFINED_AZIMUTH; Bit 3: (value 8) PGS_CSC_ZenithAzimuth(S/C) gave PGSCSC_W_NO_REFRACTION; Bit 4: (value 16) PGS_CSC_ZenithAzimuth(S/C) gave PGSCSC_E_INVALID_VECTAG; Bit 5: (value 32) PGS_CSC_ZenithAzimuth(S/C) gave PGSCSC_E_LOOK_PT_ALTIT_RANGE; Bit 6: (value 64) PGS_CSC_ZenithAzimuth(S/C) gave PGSCSC_E_ZERO_INPUT_VECTOR; Bit 7: (value 128) PGS_CSC_ZenithAzimuth(S/C) gave PGS_E_TOOLKIT; Bit 8: (value 256) (Sun) bad input value; Bit 9: (value 512) (suppressed) PGS_CSC_ZenithAzimuth(Sun) gave PGSCSC_W_BELOW_HORIZON (This is not an error condition - the sun is below the horizon at night); Bit 10: (value 1024) PGS_CSC_ZenithAzimuth(Sun) gave PGSCSC_W_UNDEFINED_AZIMUTH; Bit 11: (value 2048) PGS_CSC_ZenithAzimuth(Sun) gave PGSCSC_W_NO_REFRACTION; Bit 12: (value 4096) PGS_CSC_ZenithAzimuth(Sun) gave PGSCSC_E_INVALID_VECTAG; Bit 13: (value 8192) PGS_CSC_ZenithAzimuth(Sun) gave PGSCSC_E_LOOK_PT_ALTIT_RANGE; Bit 14: (value 16384) PGS_CSC_ZenithAzimuth(Sun) gave PGSCSC_E_ZERO_INPUT_VECTOR; Bit 15: (value 32768) PGS_CSC_ZenithAzimuth(Sun) gave PGS_E_TOOLKIT
demgeoqa	16-bit unsigned integer	None	Digital Elevation Model (DEM) Geolocation QA flags:; Bit 0: (LSB, value 1) bad input value; Bit 1: (value 2) Could not allocate memory; Bit 2: (value 4) Too close to North or South pole. Excluded. (This is not an error condition - a different model is used); Bit 3: (value 8) Layer resolution incompatibility. Excluded; Bit 4: (value 16) Any DEM Routine (elev) gave PGSDEM_E_IMPROPER_TAG; Bit 5: (value 32) Any DEM Routine (elev) gave PGSDEM_E_CANNOT_ACCESS_DATA;

			Bit 6: (value 64) Any DEM Routine (land/water) gave PGSDEM_E_IMPROPER_TAG; Bit 7: (value 128) Any DEM Routine (land/water) gave PGSDEM_E_CANNOT_ACCESS_DATA; Bit 8: (value 256) Reserved for future layers; Bit 9: (value 512) Reserved for future layers; Bit 10: (value 1024) PGS_DEM_GetRegion(elev) gave PGSDEM_M_FILLVALUE_INCLUDED; Bit 11: (value 2048) PGS_DEM_GetRegion(land/water) gave PGSDEM_M_FILLVALUE_INCLUDED; Bit 12: (value 4096) Reserved for future layers; Bit 13: (value 8192) PGS_DEM_GetRegion(all) gave PGSDEM_M_MULTIPLE_RESOLUTIONS; Bit 14: (value 16384) PGS_CSC_GetFOV_Pixel() gave any 'W' class return code except PGSCSC_W_PREDICTED_UT1; Bit 15: (value 32768) PGS_CSC_GetFOV_Pixel() gave any 'E' class return code
Doppler_shift_ppm	32-bit floating-point	None	Doppler shift for this footprint in parts per million.
dust_flag	16-bit integer	None	Flag telling whether dust was detected in any of the 9 Level-1B IR fields of view that make up this scene; 1: Dust detected in at least one contributing FOV; 0: Dust test valid in at least one contributing IR FOV but dust not detected in any of the valid contributing IR FOVs; -1: Dust test not valid for any contributing IR FOV (land, poles, cloud, problem with inputs)
CC_noise_eff_amp_factor	32-bit floating-point	None	Effective amplification of noise in IR window channels due to extrapolation in cloud clearing and uncertainty of clear state. (< 1.0 for noise reduction, >1.0 for noise amplification, -9999.0 for unknown)
CC1_noise_eff_amp_factor	32-bit floating-point	None	Equivalent of CC_noise_eff_amp_factor but from the first attempt at cloud clearing
CC1_Resid	32-bit floating-point	None	Internal retrieval quality indicator -- residual between the first cloud cleared radiances for channels used in the determination and the radiances calculated from the best estimate of clear, in K

CCfinal_Resid	32-bit floating-point	None	Internal retrieval quality indicator -- residual between the final cloud cleared radiances for channels used in the determination and the radiances calculated from the best estimate of clear, in K
TotCld_4_CCfinal	32-bit floating-point	None	Internal retrieval quality indicator -- total cloud fraction estimated before final cloud clearing (as seen from above), dimensionless between zero and one
CCfinal_Noise_Amp	32-bit floating-point	None	Internal retrieval quality indicator -- noise amplification factor from cloud clearing because of extrapolation, dimensionless. Note: the name is misleading: this is the value after the second cloud clearing iteration, not the last.
invalid	8-bit integer	None	Profile is not valid
all_spots_avg	8-bit integer	None	1: the cloud clearing step judged the scene to be clear enough that it averaged all spots' radiances; 0: cloud clearing was applied to the radiances; -1/255: cloud clearing not attempted
MW_ret_used	8-bit integer	None	MW-only final retrieval used
bad_clouds	8-bit integer	None	invalid cloud parameters
retrieval_type	8-bit integer	None	Deprecated -- use Xxx_QC flags. Retrieval type:; 0 for full retrieval; 10 for MW + final succeeded, initial retrieval failed; 20 for MW + initial succeeded, final failed; 30 for only MW stage succeeded, initial + final retrieval failed; 40 for MW + initial succeeded, final cloud-clearing failed; 50 for only MW stage succeeded, initial + final cloud-clearing failed; 100 for no retrieval;